

**UNIVERSITY OF HERTFORDSHIRE**

**School of Life and Medical Sciences**

**&**

**WESTERN SYDNEY UNIVERSITY**

**Hawkesbury Institute for the Environment**

**Bioprospecting for fungal-based biocontrol agents**

**A thesis submitted to the University of Hertfordshire and Western**

**Sydney University for the degree of Doctor of Philosophy**

**Charalampos Filippou, BSc., MSc.**

Supervisors: Dr. Robert Coutts, Dr. Avice Hall, Dr. Alexie Papanicolaou & Dr. Uffe Nielsen

May 2021

## **Declaration of Originality**

I hereby declare that this thesis entitled “Bioprospecting for fungal-based biocontrol agents” is the product of my own research work unless otherwise acknowledged in the text or by references. The thesis has not been accepted for any degree and is not concurrently submitted in candidature of any other degree.

Signature:

A handwritten signature in blue ink, consisting of a stylized, cursive letter 'B' with a long horizontal stroke extending to the right.

Date: May, 2021

## **Copyright Declaration**

The copyright of this thesis rests with the author and is made available under a Creative Commons Attribution Non-Commercial No Derivatives license. Researchers are free to copy, distribute or transmit the thesis on the condition that they attribute it, that they do not use it for commercial purposes and that they do not alter, transform, or build upon it. For any reuse or redistribution, researchers must make clear to others the license terms of this work.

## Abstract

The research objective of this project was to investigate how a virus infecting the fungus can improve its effectiveness as a pesticide. This mycovirus-induced hypervirulence was investigated using microbiological and genomic techniques to characterise the molecular interactions between the virus and the fungus host so that an improved mycopesticide can be deployed commercially. Prior to this work, it was reported that a newly proposed virus family called the *Polymycoviridae* can confer mild hypervirulence to their fungal host. In this work, attempts to cure a *B. bassiana* isolate (ATHUM 4946) which harbours a polymycovirus-3 (BbPmV-3) were successful and I built and confirmed two isogenic lines of virus-free and virus-infected. Furthermore, BbPmV-3 has six genomic dsRNA segments and its complete sequence is reported here. Phylogenetic analysis of RNA-dependent RNA polymerase (RdRP) protein sequences revealed that BbPmV-3 is closely related to BbPmV-2 but not BbPmV-1. Consequently, examining the effects of BbPmV-3 and BbPmV-1 on their respective hosts revealed similar phenotypic effects including increased pigmentation, sporulation, and radial growth. However, this polymycovirus-mediated effect on growth is dependent on the carbon and nitrogen sources available to the host fungus. When sucrose is replaced by lactose, trehalose, glucose, or glycerol both BbPmV-3 and BbPmV-1 increase growth of ATHUM 4946 and EABb 92/11-Dm respectively, whereas these effects were reversed on maltose and fructose. Similarly, both BbPmV-3 and BbPmV-1 decrease growth of ATHUM and EABb 92/11-Dm when sodium nitrate is replaced by sodium nitrite, potassium nitrate, or ammonium nitrate. To this extent, this hypervirulent effect was tested on *Tenebrio molitor*, where a virus-infected EABb 92/11-Dm line demonstrated increased mortality rate when compared to the commercial *B. bassiana* ATCC 74040, *B. bassiana* GHA, and the virus-free isogenic line. Furthermore, gene expression data from five timepoints of the two isogenic lines were used in a candidate pathway approach, investigating key pathways known to affect resistance to stresses and carbon uptake. Secretion of organic acid during growth can change the pH of the growth medium creating a toxic environment causing stress and death. Consequently, genes involved in stress tolerance such as heat shock proteins, trehalose and mannitol biosynthesis, and calcium homeostasis were upregulated in virus-infected isolate. Likewise, genes involved in carbon uptake such as BbAGT1 and BbJen1 transporters were upregulated in virus-infected isolate. Equally, here we demonstrate that BbPmV-1 drives the up-regulation of *nirA* gene which is linked to nitrate uptake and/or assimilation and secondary metabolites such as Tenellin, Beauvericin and Bassianolide. These results reveal a symbiotic relationship between BbPmV-1 and its fungal host. To conclude, these data present a crucial first step in characterising how mycopesticides can be improved to deliver better and safer pest management.

## **Acknowledgements**

I would like to express my honest appreciation to my supervisors Dr. Robert Coutts and Dr. Avic Hall, who gave me the opportunity to follow this project as well as their guidance and inspiration. Likewise, I would like to express my gratitude to my supervisor Dr Alexie Papanicolaou for his help during my work at the Hawkesbury Institute for the Environment in Australia and during the NGS analysis.

I would like to express my deepest gratitude to God Almighty as well as to my family and especially my wife for their support and encouragement. I also want to thank the staff of the Hawkesbury Institute for the Environment and the University of Hertfordshire for their support. A warm appreciation goes to Dr. Yagiz Alagoz and Sam El-Kamand for their assistance and laboratory guidance.

Last but not least I cannot thank Dr Ioly Kotta-Loizou enough for her help since she has taught me so much during my first year's research and has been a constant source of encouragement to me in my studies.

## Abbreviations

BbPmV-1	<i>Beauveria bassiana</i> Polymycovirus -1
BbPmV-3	<i>Beauveria bassiana</i> Polymycovirus - 3
cDNA	complementary deoxyribonucleic acid
DMSO	Dimethyl sulfoxide
DNA	Deoxyribonucleic acid
dNTP	Deoxynucleotide phosphate
dsRNA	double stranded ribonucleic acid
DTT	Dithiothreitol
EDTA	Ethylenediaminetetraacetic acid
g	gram
GFP	Green Fluorescent Protein
Kb	Kilobase
LB	Luria broth
LmV-1	<i>Lecanicillium muscarium</i> Virus-1
LmV-1.F	<i>Lecanicillium muscarium</i> Virus-1.Free (LmV-1.F)
LmV-1.I	<i>Lecanicillium muscarium</i> Virus-1.Infected (LmV-1.I)
mg	Milligram
mL	millilitre
mRNA	messenger ribonucleic acid
NGS	Next Generation Sequencing
PCR	polymerase chain reaction
PDA	Potato Dextrose Agar
PEG	Polyethylene glycol
PmV-1.F	Polymycovirus-1 Free
PmV-1.I	Polymycovirus-1 Infected
PmV-3.F	Polymycovirus-3 Free
PmV-3.I	Polymycovirus-3 Infected
QC	Quality Control
qRT-PCR	Real-Time Quantitative reverse transcription PCR

RdRP	RNA dependent RNA Polymerase
RLM-Race	RNA Ligase-Mediated-Rapid Amplification of cDNA Ends
RNA	Ribonucleic acid
rPCR	random-Polymerase Chain Reaction
RPM	Revolutions per minute
RT - PCR	Reverse - Transcription Polymerase Chain Reaction
μl	microlitre
3'-UTR	3 prime untranslated region
5'-UTR	5 prime untranslated region

# Table of contents

<b>Abstract.</b>	<b>I</b>
<b>Acknowledgements.</b>	<b>II</b>
<b>List of Figures.</b>	<b>XI</b>
<b>List of Tables.</b>	<b>XVI</b>
<b>Chapter 1. General Introduction.</b>	<b>1</b>
1.1 Entomopathogenic fungi as biological control agents.	2
1.1.1 <i>Beauveria bassiana</i> .	3
1.1.1.1 Production of toxic metabolites.	7
1.1.1.2 Effect of environmental factors.	7
1.1.2 <i>Metarhizium</i> spp.	8
1.1.3 <i>Lecanicillium</i> spp.	10
1.2 Mycoviruses.	11
1.3 Origins of mycoviruses.	15
1.4 Mycovirus effects on host phenotypes.	15
1.4.1 Asymptomatic infections (cryptic).	15
1.4.2 Hypovirulence.	16
1.4.3 Hypervirulence.	16
1.5 Transmission of fungal viruses.	17
1.6 Modes of dsRNA virus replication.	20
1.7 Mycoviruses as biocontrol agents.	20
1.8 Polymycoviruses discovered in the entomopathogenic fungi <i>Beauveria bassiana</i>	21
1.9 Aims and objectives.	25
<b>CHAPTER 2. General Materials and Methods.</b>	<b>26</b>
2.1. Inoculation and growth of isolates.	27
2.2 Nucleic acid manipulation.	27
2.2.1. Phenol and chloroform extraction.	27
2.2.2. Nucleic acid precipitation.	27
2.2.3. DNase 1 treatment.	28
2.2.4. S1 nuclease treatment.	28

2.2.5. Gel electrophoresis.	28
2.2.6. Gel purification for recovery of dsRNA.	29
2.3 Genome walking.	29
2.4 Ligation of PCR products with vector.	30
2.5 Transformation of XL10 Gold competent <i>Escherichia coli</i> cells with DNA.	30
2.6 Plasmid extraction from XL10 Gold competent cells using the alkaline lysis method.	31
2.7 Construction of cDNA library from dsRNA by random-PCR (rPCR).	32
2.8 RNA linker-mediated rapid amplification of cDNA ends (RLM-RACE).	32
2.8.1 cDNA Synthesis.	36
2.9 Northern blot hybridization.	37
2.9.1 <i>In vitro</i> transcription-labelling of RNA with digoxigenin.	37
2.9.2 DNA template preparation.	37
2.9.3 <i>In vitro</i> transcription using the MAXI Script®T7 kit.	38
2.9.4 DIG-RNA labelling.	39
2.9.5 DIG northern blot hybridization.	39
2.9.5.1 Separation of dsRNA samples on agarose gels.	39
2.9.5.2 Transferring dsRNA to a membrane and fixation.	40
2.9.5.3 Hybridisation with RNA probes.	40
2.9.5.4 Immunological detection.	41
2.10 Fungal genomic DNA extraction.	42
2.11 Total RNA extraction using E.Z.N.A Fungal RNA kit (OMEGA).	43
2.11.1 On column DNase I digestion and RNA elution.	43
2.12 Sequencing.	44
2.12.1 Sanger DNA sequencing.	44
2.12.2 RNA sequencing.	45
2.12.2.1 3'mRNA-Seq Library Prep.	45
2.12.2.2 Detailed Protocol for library preparation using the 3'mRNA-Seq kit.	46
2.12.2.3 RNA removal.	47
2.12.2.4 Second strand synthesis.	47
2.12.2.5 Purification.	47

2.12.2.6 Library amplification.	48
2.12.2.7 quantitative (q) PCR.	49
2.12.2.8 Single Indexing (i7 only).	51
2.12.3 Whole genome sequencing of EABb 92/11-Dm.	52
2.13 Generation of RNA standards curves representative for positive and negative strands of Lecanicillium virus-1 (LmV-1) genomic dsRNA.	53
2.14 Fungal spore counting.	54
2.15 Fungal spore germination assessment.	54
2.15.1 Preparation of mycelia-free conidia suspension.	54
2.15.2 Spore germination.	55
2.16 Inoculation of <i>T. molitor</i> with <i>B. bassiana</i> by direct injection or spraying.	55
2.17 Transfection assay.	56
2.17.1 Protoplast isolation.	56
2.17.2 Protoplast transfection.	57
2.18 Sequencing analysis.	57
2.18.1 RNA-Seq.	58
2.18.1.1 Quality control of sequencing reads.	58
2.18.1.2 Adapter trimming and low-quality bases from FastQ files.	58
2.18.1.3 Second FastQC run on the processed reads from the above steps.	58
2.18.1.4 TRINITY, GeneMark and Augustus for genome assembly and gene prediction.	59
2.19 Hygromycin B susceptibility of <i>B. bassiana</i> isolates Naturalis and BotaniGard.	59
<b>Chapter 3. Identification and characterization of mycoviruses in fungi.</b>	<b>61</b>
3.1 Completion of the sequence of the Aspergillus fumigatus partitivirus 1 genome.	63
3.2 Screening of fungal isolates for dsRNA mycoviruses and population studies.	68
3.2.1 Mixed infections of <i>Beauveria bassiana</i> isolates with up to three different mycoviruses.	70
3.2.2 Evidence of vertical and horizontal transmission of mycoviruses.	70
3.3 A novel mycovirus discovered in the entomopathogenic fungus <i>L. muscarium</i> contains one unique dsRNA.	71
3.3.1 Northern blot analysis of LmV-1 dsRNA from <i>Lecanicillium muscarium</i> isolates 143.62 and 102071.	74
3.3.2 Sensitivity of LmV-1 dsRNA to DNase, RNase A and RNase III.	76

3.3.3 Sequencing of LmV-1 dsRNA using an RLM-RACE protocol.	76
3.3.4 The genomic sequence of LmV-1 dsRNA1.	78
3.3.5 Quantitative polymerase chain reaction (qRT-PCR).	80
3.3.6 Generation of RNA standards representing positive and negative strands of genomic RNA.	80
3.3.7 Time course study of viral dsRNA levels relative to fungal growth.	83
3.4 Characterisation of <i>Beauveria bassiana</i> polymycovirus-3.	85
3.4.1 Construction of a cDNA library of BbPmV-3 dsRNA5 by rPCR to obtain the full sequence of the RNAs.	85
3.4.2 Determination of the 5'-and 3'- terminal sequences of BbPmV-3 dsRNA5.	88
3.4.3 The genomic sequence of BbPmV-3 dsRNA5.	88
3.4.4 Construction of cDNA clones of BbPmV-3 dsRNA6 using rPCR amplification.	90
3.4.5 Determination of the 5'- and 3'-terminal sequences of BbPmV-3 dsRNA6 using RLM -RACE.	91
3.4.6 The genomic sequence of BbPmV-3 dsRNA6.	93
3.4.7 Sequence analysis of the remaining 4 dsRNAs of BbPmV-3.	95
3.4.8 Multiple sequence alignment of Polymycovirus-3 dsRNAs.	96
3.4.9 Phylogenetic analysis of the putative BbPmV-3 RdRP gene.	101
<b>Chapter 4. Eradication of mycoviral infection exhibits symptomatic and asymptomatic effects.</b>	<b>105</b>
4.1 Curing of mycoviral infection and confirmation of isogenic lines.	107
4.1.2 Cycloheximide curing of BbPmV-3 in <i>B. bassiana</i> ATHUM 4946 isolates.	109
4.1.3 Ribavirin curing of LmV-1 in <i>L. muscarium</i> 143.62.	112
4.1.4 Phenotypic differences between VI and VF isogenic lines (symptomatic & asymptomatic).	114
4.1.5 Vegetative growth of <i>B. bassiana</i> EABb 92/11-Dm and ATHUM 4946 virus-free and EABb 92/11-Dm and ATHUM 4946 virus-infected isogenic lines on media containing different carbon and nitrogen sources.	119
4.2 Investigation of <i>B. bassiana</i> isolates pathogenicity against live insects.	124
4.2.1 <i>Tenebrio molitor</i> (army mealworm beetle) larvae.	124
4.2.2 Injection and spray inoculation of <i>T. molitor</i> .	125
4.2.3 Survival assay.	127
4.3 Evaluation of fungicides used as selection markers.	133
4.3.1 Hygromycin B susceptibility of <i>B. bassiana</i> strains.	133

4.3.2 Sulfonylurea and Benomyl susceptibility of <i>B. bassiana</i> strains.	137
4.3.3 GFP expression in <i>B. bassiana</i> to study mycovirus replication and localization.	140
4.3.4 GFP expression in transformed <i>B. bassiana</i> .	140
4.3.5 Isolation of protoplasts for virus transfection and GFP expression.	145
<b>Chapter 5. Comparative transcriptomic analysis of the PmV-1.F and the PmV-1.I <i>B. bassiana</i> EABb 92/11-Dm isolate.</b>	<b>149</b>
5.1 Harvesting mycelia from PmV-1.F and PmV-1.I isogenic lines at different time points.	151
5.1.2 Analysis of NGS of RNA isolated from <i>B. bassiana</i> infected <i>T. molitor</i> .	151
5.2 Genome structural annotation of EABb 92/11-Dm.	151
5.2.1 Counting, normalisation and differential expression.	153
5.2.2 Manual curation of structural annotation.	155
5.2.3 Program to assemble spliced alignments (PASA).	161
5.3 Using gene expression box plots to derive functional annotations for key genes.	171
5.3.1 <i>B. bassiana</i> virulence factors.	172
5.3.2 Transcriptomic analysis of genes involved in <i>Beauveria bassiana</i> virulence.	173
5.3.2.1 Host adherence.	173
5.3.2.2 Cuticle penetration.	178
5.3.2.3 Carbohydrate transporters in <i>B. bassiana</i> .	182
5.3.2.4 Calcium signalling and transport.	189
5.3.2.5 <i>Beauveria bassiana</i> secondary metabolites (mycotoxin).	196
5.3.2.5.1 Tenellin.	196
5.3.2.5.2 Beauvericin.	197
5.3.2.5.3 Bassianolide.	198
5.3.2.6 Metabolic pathways and other genes examined.	201
5.3.2.7 Heat shock proteins (Hsp30, Hsp70, Hsp90).	207
5.3.2.8 Thaumatin-like proteins.	211
<b>Chapter 6. General Discussion.</b>	<b>214</b>
6.1 General Aims	215
6.1.2 Brief outline of thesis	215
6.2 General Discussion	216

6.3 Conclusion, Overall impact, limitations, and future work	226
<b>References.</b>	<b>230</b>
<b>Appendices.</b>	<b>257</b>
<b>Part A.</b>	<b>257</b>
<b>Antibiotics.</b>	<b>257</b>
<b>Buffers, Media and Solutions.</b>	<b>257</b>
<b>Part B.</b>	<b>264</b>
<b>Publications.</b>	<b>309</b>

# List of Figures

<b>Figure 1.1a</b> Insect host range of <i>Beauveria bassiana</i> .	4
<b>Figure 1.1b</b> Overview of the basic infection cycle of <i>Beauveria bassiana</i> in invertebrates.	6
<b>Figure 1.1c</b> Demonstration of the anamorphic life cycle of <i>Beauveria bassiana</i> and <i>Metarhizium anisopliae</i> in northern temperate regions.	9
<b>Figure 1.2a</b> dsRNA mycovirus families and their general properties examined in this study.	14
<b>Figure 1.4a</b> Methods of mycovirus transmission.	19
<b>Figure 1.8a</b> Electrophoretic profiles of polymycoviruses in <i>Beauveria bassiana</i> .	24
<b>Figure 2.12.2.7</b> Calculation of the number of cycles for endpoint PCR.	50
<b>Figure 3.1a</b> Genomic organisation of AfuPV-1A and comparisons of the amino acid sequences of putative proteins encoded by dsRNA3 elements of representative partitiviruses.	66
<b>Figure 3.2a</b> A) 1% (w/v) agarose gel electrophoresis of dsRNA elements isolated from four <i>Beauveria bassiana</i> isolates, representative of the four different electrophoretic profiles.	69
<b>Figure 3.3a</b> Agarose gel electrophoresis of dsRNA elements present in both <i>Lecanicillium muscarium</i> 143.62 and 102071 isolates (Circled in Red).	73
<b>Figure 3.3b</b> Northern hybridisation of LmV-1 dsRNA.	75
<b>Figure 3.3c</b> Agarose gel electrophoresis showing the PCR products generated by RLM-RACE.	77
<b>Figure 3.3d</b> Diagrammatic representation of the genome organisation of LmV-1 dsRNA 1.	79
<b>Figure 3.3e</b> Relative RNA levels of the positive and negative strands of LmV-1 as shown by RT-qPCR amplification.	82
<b>Figure 3.3f</b> Time course of biomass production of <i>Lecanicillium muscarium</i> isolate 143.62 grown in liquid Czapek-Dox CM over a 7-day incubation period coupled with LmV-1 dsRNA accumulation.	84
<b>Figure 3.4a</b> 1.5% (w/v) Agarose gel electrophoresis (left) and schematic representation (right) of the BbPmV-3 dsRNA genome.	87
<b>Figure 3.4b</b> Diagrammatic representation of genome organisation of BbPmV-3 dsRNA5.	89
<b>Figure 3.4c</b> 1% (w/v) agarose gel electrophoresis of RLM-RACE amplicons generated from BbPmV-3 dsRNA6 5'- (lane 2) and 3'- (lane 4) -termini.	92
<b>Figure 3.4d</b> Diagrammatic representation of the genome organisation of BbPmV-3 dsRNA6.	94
<b>Figure 3.4e</b> Multiple sequence alignment of the 5'-UTRs (A) and 3'-UTRs (B and C) of BbPmV-3 dsRNAs using ClustalW2 program.	99

- Figure 3.4f** Predicted secondary structures of respectively the 5'- (A) and 3'-UTRs (B) of BbPmV-3 dsRNA5 and the 5'- (C) and 3'-UTRs (D) of BbPmV-3 dsRNA6. 100
- Figure 3.4g** Schematic representation of BbPmV-3 dsRNA1, encoding an RdRP whose ORF (dark red coloured box) is flanked by 5'- and 3'-UTRs (black boxes). 102
- Figure 3.4h:** ML phylogenetic tree comparing polymycovirus RdRP sequences. Sequences were aligned with MUSCLE as implemented by MEGA 6. 103
- Figure 4.1a** (A) RT-PCR amplification using sequence specific oligonucleotide primers designed to generate amplicons (699 bp) representing a fragment of the coding region of the BbPmV-3 RdRP present in *B. bassiana* ATHUM 4946 (lane 2) but absent from a cured, virus-free isogenic line (lane 4). 111
- Figure 4.1b:** (A) Cultures of BbPmV-3-infected (left) and BbPmV-3-free (right) isogenic lines of *B. bassiana* ATHUM 4649 grown on PDA at 25°C for 2 weeks, showing significant differences in pigmentation. (B) Spore suspensions from BbPmV-3-infected (left) and BbPmV-3-free (right) isogenic lines of *Beauveria bassiana* ATHUM 4946, demonstrating increased sporulation in the BbPmV-3-infected isogenic line as compared to the BbPmV-3-free line. (C) Difference in sporulation between virus-infected and virus-free isogenic lines. Student's t test: \*\*indicates P-value < 0.01. 115
- Figure 4.1c:** A) Agarose gel electrophoresis showing eradication of virus from isolate *Lecanicillium muscarium* 143.62; lane 2 143.62VI, lane 3 143.62 VF, lane 4 102071 untreated, lane 5 102071 treated, lane 6 negative control as shown by RT-PCR amplification assay of a virus-specific 441 bp amplicon. B) Difference in sporulation between virus-infected and virus-free isogenic lines. C) Average spore count of virus-free and virus-infected isogenic lines (P – value < 0.005). 117
- Figure 4.1d:** Radial growth of LmV-1.I and LmV-1.F *Lecanicillium muscarium* isolate 143.62 after 18 days growth on (A) Czapek-Dox MM; and (B) Czapek-Dox CM (P – value < 0.005). 118
- Figure 4.1e** Growth of *Beauveria bassiana* isolates EABb 92/11-Dm PmV-1.I (BBI) and PmV-1.F (BBII) and ATHUM 4946 PmV-3.F (V-) and PmV-3.I (V+) isogenic lines after 18 days culture on Czapek-Dox media containing different carbohydrates. 2-way ANOVA; indicates P-value < 0.0001. 122
- Figure 4.1f** Growth of *Beauveria bassiana* isolates EABb 92/11-Dm PmV-1.I (BBI) and PmV-1.F (BBII) and ATHUM 4946 PmV-3.F (V-) and PmV-3.I (V+) isogenic lines after 18 days of incubation on Czapek Dox media containing different Nitrogen-based source. 2-way ANOVA; indicates P-value < 0.0001. 123
- Figure 4.2a** Lifecycle of the beetle *Tenebrio molitor*: (A) larval stage, (B) pupal stage, and (C) adult stage. Taken from de Souza *et al.* (2015). 125

<b>Figure 4.2b</b> <i>Tenebrio molitor</i> infection model system.	126
<b>Figure 4.2c</b> Mycosis was observed on the majority of the infected insects 72 h post-mortem.	130
<b>Figure 4.2d</b> Survival curves of <i>Tenebrio molitor</i> larvae infected with four isolates of <i>Beauveria bassiana</i> following spray inoculation with $10^7$ spores/larvae (A) or direct injection with $10^5$ spores /larva (B).	132
<b>Figure 4.3a</b> HmB susceptibility test of <i>Beauveria bassiana</i> Naturalis and Botanigard isolates spore suspension ( $1 \times 10^7$ ) in liquid Czapek-Dox CM containing different concentrations of the HmB antibiotic.	135
<b>Figure 4.3b</b> Overlay method; <b>(A)</b> A sparse growth of Naturalis in 1 mg/mL concentration of HmB; <b>(B)</b> No effect on the growth and sporulation of Botanigard.	136
<b>Figure 4.3c</b> Benomyl sensitivity of <i>Beauveria bassiana</i> isolates ATCC 704040 Naturalis and GHA; A and B respectively (first panels) grown in liquid Czapek-Dox media.	138
<b>Figure 4.3d</b> Sulfonyleurea sensitivity of <i>Beauveria bassiana</i> isolate ATCC 704040 (Naturalis; A and C) and GHA (Botanigard; B and D).	139
<b>Figure 4.3e A)</b> Fluorescence micrographs of <i>Beauveria bassiana</i> ATCC 704040 showing GFP labelled mycelia and hyphae following transfection of protoplasts with a plasmid carrying GFP and fungus regeneration. <b>B)</b> Fluorescence micrographs of <i>Beauveria bassiana</i> GHA showing GFP labelled mycelia and hyphae following transfection of protoplasts with plasmid carrying GFP and fungus regeneration.	142
<b>Figure 4.3f</b> Fluorescence micrographs of <i>Beauveria bassiana</i> ATCC 704040 showing GFP labelled conidiospores following transfection of protoplasts plasmid carrying GFP and fungus regeneration (400x magnification).	143
<b>Figure 4.3g</b> Protoplasts freshly isolated from <i>Beauveria bassiana</i> Naturalis (A) and Botanigard (B) viewed in a haemocytometer with a light microscope using 400x magnification.	144
<b>Figure 4.3h</b> RT-PCR amplification of a ca. 180 bp amplicon from the LbQV-1 RNA genome using extracts of cultured mycelia recovered from <i>Leptosphaeria biglobosa</i> protoplasts transfected with LbQV-1 (lane 2); Lane 1, 1 kb Hyperladder marker; Lane 3, amplicon generated from a positive control of purified LbQV-1; Lane 4 water control.	146
<b>Figure 5.2a</b> TPS2 gene, white regions are the UTRs that were allocated using evidence such as “Public RNA coverage” and “intron/exon junction reads”.	156
<b>Figure 5.2b</b> Curation of an alternative spliced isoform in the ATG1 gene. The Apollo editing window shows a “User-created annotation” at top, followed by incorrect atg1_CDS_translation.mRNA (“Virulence Factors”). Public RNASeq coverage shows the RNA coverage, which was used to allocate the UTRs, followed by other gene	

prediction software such as GeneMark, Augustus, and PASA and interestingly none of these managed to suggest the alternative spliced isoform. 158

**Figure 5.2c** The CDEP1 gene first appeared as a single exon (“Virulence factors”) before manual curation (black arrow). Following the evidence provided from “Public RNA coverage”, and Intron/Exon Junction Reads it was possible to create the correct final annotation indicated as (“User created annotations”). Then this was cross referenced with “PASA Golden”, and “Gene Mark”, demonstrating that manual curation is more accurate than gene prediction software. 160

**Figure 5.2d** Examples of updated curation in *Beauveria bassiana* isolate Naturalis. Panels A-E compare the curated genemodel (A) to Ascomycota Proteins (B), PASA Golden refinement (C), Public RNA-seq coverage (D), and pile- up of aligned RNA-seq reads (E). Intronic regions are shown by lines and white boxes represent UTRs. 162

**Figure 5.2e** Cytochrome P450 subfamily CYP52X1 gene translated from the right to the left Graphical representation of start (ATG; Methionine; red arrow) and stop (TAG; black arrow) codons exhibiting start point and stop point of translation. 163

**Figure 5.2f** Black arrow indicates incorrect coverage of the 3’ UTR after final curation. Grey arrow indicates spurious alignments (the reads are outside the predicted 3’ UTR coverage). 164

**Figure 5.2g** Spurious alignments before Burrows-Wheeler Aligner (BWA) mapping-alignment. 166

**Figure 5.2h** The black arrow indicates the correct coverage of the 3’ UTR after the final curation. 167

**Figure 5.2i** A) Library “BBI\_Day\_10\_2” repeat showing spurious alignments with no reads aligned to the 3’UTR. B) Library “BBI\_Day\_10\_1” repeat demonstrating read alignments covering the entire 3’UTR. 169

**Figure 5.2j** Libraries “BBI\_Day\_10\_1” and BBI\_Day\_10\_3” repeats demonstrating three overexpressed genes. 170

**Figure 5.3a** Boxplots demonstrating the expression profiles of adhesion proteins. 177

**Figure 5.3b** Boxplots demonstrating the expression profiles of cuticle degrading proteins. 181

**Figure 5.3c** Overview of select *Beauveria bassiana* transporters. Jen1 (light blue), carboxylic acid transporter, Agt1 (light green), carbohydrate transporter, Mdr1, Mrp1, Pdr1, Pdr2, and Pdr5 (gray), ABC-type (multidrug) transporters. (Modified from Ortiz-Urquiza *et al.*, 2016). 183

**Figure 5.3d** Boxplots demonstrating the expression profiles of carbohydrate transport proteins. 182

<b>Figure 5.3e</b> Summary of <i>B. bassiana</i> genes involved in calcium signalling and transport. Csa1, calcium sensor acidification; CnA/B, calcineurin catalytic and regulatory subunits; Vcx1, vacuolar; Pmr1, are analysed in detail. (Modified from Ortiz-Urquiza et al., 2016).	191
<b>Figure 5.3f</b> Boxplots demonstrating the expression profiles of calcium binding and transport proteins.	194
<b>Figure 5.3g</b> Boxplots demonstrating the expression profiles of secondary metabolites.	200
<b>Figure 5.3h</b> Boxplots demonstrating the expression profiles of genes involved in metabolic pathways.	206
<b>Figure 5.3i</b> Boxplots demonstrating the expression profile of heat shock protein genes.	210
<b>Figure 5.3j</b> Boxplots demonstrating the expression profile of thaumatin-like protein.	212

## List of Tables

**Table 4.1a** (A) Sequence specific oligonucleotide primers used to amplify the coding region of the BbPmV-3 RdRP gene (699bp), (B) the universal primers ITS1F were used for both *Lecanicillium muscarium* and *Beauveria bassiana* ATHUM4946 isogenic lines, and C) primers for amplifying a region of the LmV-1 RdRP sequence (471bp). 113

**Table 4.3a** Spore suspensions of *Beauveria bassiana* Naturalis and Botanigard were plated on solid CM media containing 0-1 mg/mL<sup>-1</sup> HmB: The (+) sign specifies significant growth and sporulation of the fungus isolate, while (±) sign specifies sparse fungal growth. 136

**Table 4.3b:** Primer pair used for detecting the LbQV-1 in *Leptosphaeria biglobosa* transfected protoplasts. 146

# **Chapter 1**

## **General Introduction**

## 1.1 Entomopathogenic fungi as biological control agents

Arthropod pests are a threat for human health as well as the global production of crops used as biofuels, fibres and most importantly food. Additionally, many insects act as vectors transmitting deadly diseases to humans, including malaria, yellow fever, and dengue. Likewise, insect pests cause damage to crop and this threat is growing each year worldwide. It has been reported that a decade ago the reduction of the annual crop yield caused by insect pests was approximately 18%, not including losses of stored gains (Bergvinson & García-Lara, 2004). Furthermore, it has been reported that an approximate reduction of 8% of the major crops in Brazil was observed due to pests despite control measures being taken (Oliveira *et al.* 2014). Increased resistance to chemical pesticides was observed due to their extensive use in agriculture for many years. Additionally, the broad application of these pesticides has potential consequences of pesticide poisoning as well as environmental pollution. For these reasons it is imperative to use or develop alternative pesticides. Biopesticides such as entomopathogenic fungi currently used as biological control agents are very promising (de Faria *et al.*, 2007). Large numbers of entomopathogenic fungi have been discovered and several are marketed as biocontrol agents. At least twelve fungal species or subspecies have been used as mycoinsecticides and mycoacaricides. Products based on *Beauveria bassiana* (33.9%), *Metarhizium anisopliae* (33.9%), *Isaria fumosorosea* (5.8%), and *B. brongniartii* (4.1%) are the most common amongst >200 commercial products available (Kotta-Loizou *et al.*, 2017). Entomopathogenic fungi are found in a wide range of habitats including agricultural, pastoral, aquatic forest, desert and urban habitats (Chandler *et al.*, 1997). Their ability to attack and regulate insect populations raised interest and has been studied in both tropical and temperate habitats (Evans, 1982). Soil is an excellent shelter for entomopathogenic fungi due to the fact that it provides a natural protection against UV radiation and other unfavorable abiotic and biotic influences (Evans, 1982).

### 1.1.1 *Beauveria bassiana*

Two major entomopathogenic fungal species belong to *Beauveria* spp., *B. bassiana* (Balsamo-Crivelli) Vuillemin and *B. brongniartii* (Saccardo) Petch and were first reported 170 and 110 years ago, respectively. The cosmopolitan entomopathogenic fungus *B. bassiana* belongs to the order *Hypocreales*, class *Sordariomycetes*, phylum *Ascomycota* and is capable of exploiting a wide range of environments such as plants, soil and insects. This fungus has the ability to live as an endophyte in plants, as a saprophyte in soil and as an entomopathogen affecting a wide range of arthropods (Boomsma *et al.*, 2014; Claudio *et al.*, 2016). Furthermore, *B. bassiana* exhibits a dimorphic life cycle when infecting insects. *B. bassiana* infection starts with the attachment of conidia on a compatible host, then colonization of the host and eventually death of the insect. *B. bassiana* insect hosts include crop pests (e.g., whiteflies), ecologically hazardous pests (e.g., termites), and insect disease vectors such as mosquitos and ticks (Blanford *et al.*, 2005; Brownbridge *et al.*, 2001; Claudio *et al.*, 2016). This ability to infect a wide host range makes it a suitable organism to control different pests as long as it targets only the pest species rather than useful friendly insects. In Europe, *B. brongniartii* mainly attacks the field and the forest cockchafer, *Melolontha melolontha* and *M. hippocastani* (Gisbert, 2007).

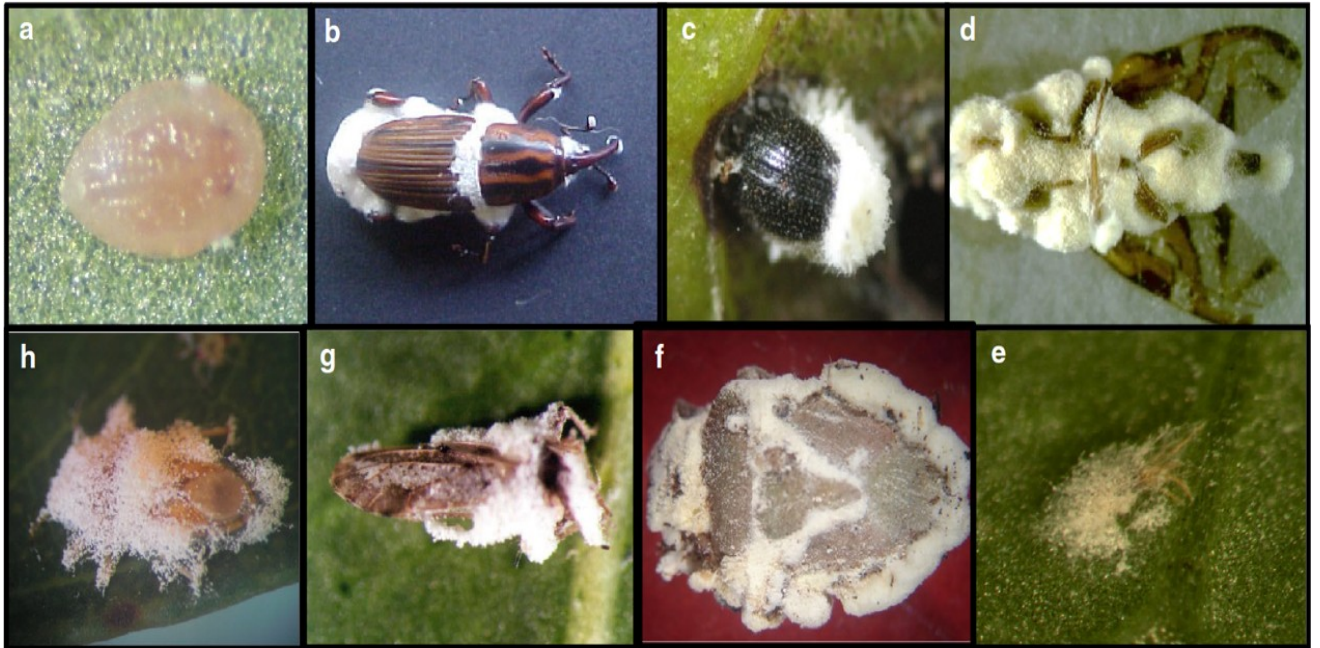


**Figure 1.1a** Insect host range of *Beauveria bassiana*; **(a)** Nymph of the silver leaf whitefly *Bemisia tabaci* biotype B; **(b)** Banana weevil *Metamasius hemipterus*; **(c)** Coffee berry borer *Hypotenemus hampei*; **(d)** Fruit fly *Anastrepha fraterculus*; **(e)** Spider mite *Tetranychus urticae*; **(f)** Soybean stinkbug *Nezara viridula*; **(g)** Citrus psyllid *Diaphorina citri*; **(h)** Eucalyptus bronze bug *Thaumastocoris peregrinus*. Taken from Mascarín *et al.* (2016).

The infection pathway of *Beauveria* spp. includes (1) attachment of the conidia to the cuticle; (2) germination; (3) penetration through the cuticle; (4) evading the host immune response; (5) proliferation within the host *via* the formation of hyphal blastospores; (6) saprophytic outgrowth from the dead host and production of new conidia (See Figure 1.1b). Germination and successful infection depends on a number of factors including susceptible host and host stage and certain environmental factors, such as optimal temperature and humidity. Naturally, germination of *B. bassiana* conidia starts after *ca.* 10 h and is largely completed in 20 h at 20 - 25°C (Gisbert, 2007).

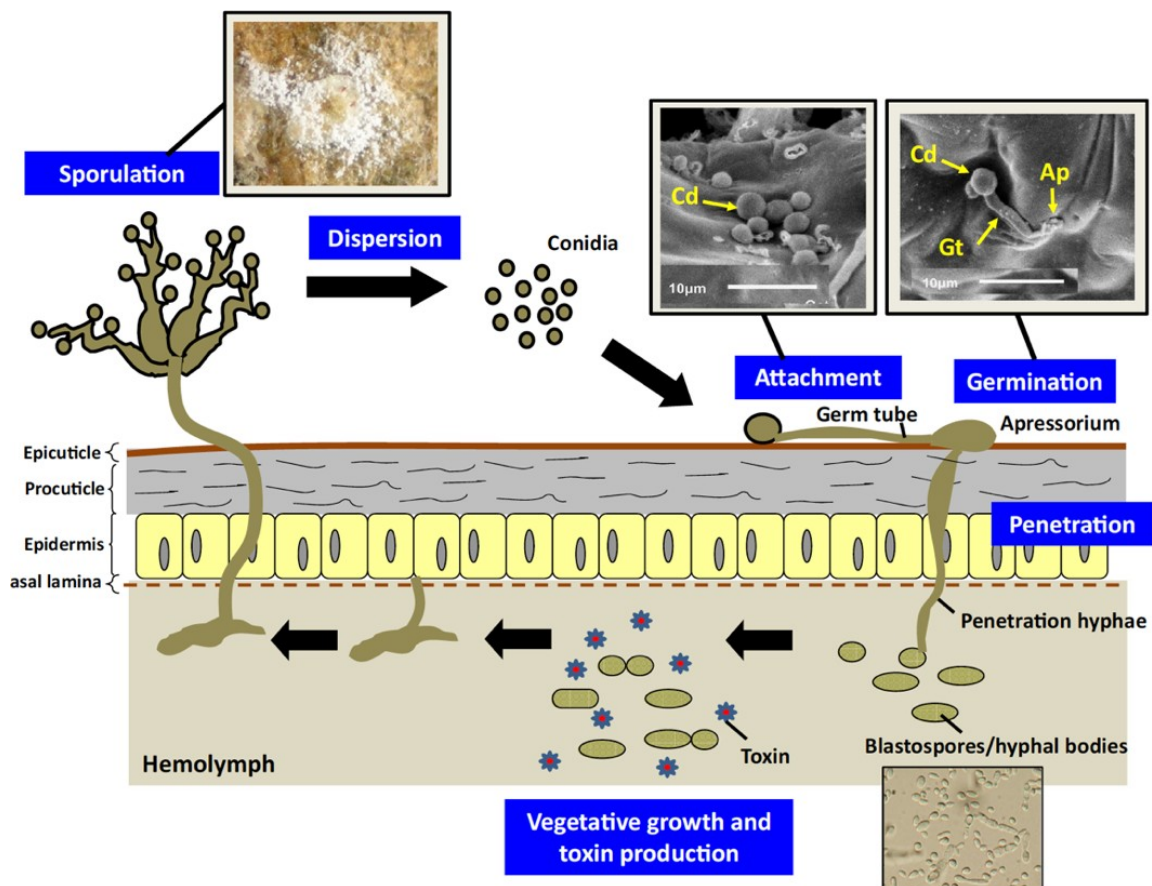


**Figure 1.1b** Overview of the basic infection cycle of *Beauveria bassiana* in invertebrates; Conidia are spread by wind, rain splash or by arthropod vectors that assist the fungus to establish infection in susceptible hosts. During infection, the fungus can secrete toxic metabolites to suppress the host immune response, thus supporting successful colonization of the host. Taken from Mascarin *et al.* (2016).

#### **1.1.1.1 Production of toxic metabolites**

Microorganisms, especially fungi, produce a wide variety of compounds or metabolites, mostly within their secondary metabolism, which generally have diverse activities and functions. Beauvericin is a toxic cyclic hexadepsipeptide and is the most important compound reported from *B. bassiana*. Experiments done to investigate this compound have demonstrated that it has insecticidal, antibiotic, cytotoxic and ionophoric properties. Beauvericin is a cholesterol acetyltransferase inhibitor, which can induce programmed cell death and is toxic against *Artemia salina* larvae, insect, murine and human cell lines (Macdonald & Fulbright 1991; Varga *et al.*, 2003; Pearson *et. al* 2009; Gisbert 2007).

#### **1.1.1.2 Effect of environmental factors**

The survival and propagation of any microorganism found in the environment is affected by various biotic and abiotic factors. The major abiotic environmental factors affecting fungi in general are humidity or moisture, temperature and solar radiation. These factors play an important role in the efficiency of commercial entomopathogenic fungi (Gisbert 2007; Clerk & Madelin 1965). For instance, temperature can affect an entomopathogen in several ways such as influencing germination, growth and viability of the fungus. The entomopathogen can be inactivated before contact with the pest in high temperatures. On the other hand, low temperatures may decrease or even stop germination and growth therefore a successful infection might be prolonged or impaired. Additionally, growth within an insect can be reduced or accelerated depending on the temperature requirements of the entomopathogen and the host pest (Gisbert, 2007). Muller-Kogler (1965), described the optimum temperature of *B. bassiana* as *ca.* 23-28°C, the minimum 5-10°C and the maximum *ca.* 30-38°C, depending on the isolate (Gisbert, 2007).

Another important environmental factor is humidity, which is especially important for the efficacy and survival of entomopathogens. High moisture levels are important for germination and sporulation after outgrowth from dead host insects. On the other hand, high or low humidity in combination with high temperature may influence the viability and persistence of fungal spores. Normally, the range for relative humidity for germination of *B. bassiana* conidia is 92-100 % (Gisbert, 2007; Hallsworth & Magan 1999).

Solar radiation is also an important environmental factor for the survival and propagation of the entomopathogens. UV-B (290–330 nm) and UV-A (330-400 nm) sunlight is the most harmful environmental factor influencing field persistence of fungal insecticides. Gardner *et al.* (1977), demonstrated that entomopathogens are inactivated within hours or days after exposure to sunlight (Gardner *et al.*, 1977). Likewise, Krieg *et al.* (1981), demonstrated that under simulated sunlight almost all conidia from *B. bassiana* were inactivated by UV-C after 16 min, and after 31 min exposure to UV-A and UV-B (Gardner *et al.*, 1977; Gisbert, 2007). Ignoffo & Garcia (1992) demonstrated that the half-life of *B. bassiana* conidia after irradiation with simulated sunlight is *ca.* 2 h (Gisbert, 2007).

### **1.1.2 *Metarhizium* spp**

*Metarhizium anisopliae* was the first fungus worldwide to be produced in large quantity and be exploited for insect-pest control of the beet weevil *Cleonus punctiventris* (Roberts & St Leger, 2004; Suzaki *et al.*, 2005). However, in terms of field application importance for insect control *Metarhizium* spp., also members of the order *Hypocreales*, phylum *Ascomycota*, followed by *Beauveria* spp represent the ranking order. Soil is considered to be an excellent environmental shelter for entomopathogenic fungi and provides the ideal environment for *Metarhizium* spp. where they are protected from UV radiation and colonise and control susceptible insects. Even within a small geographical area significant genetic variability of

*Metarhizium* spp. can be found (Figure 1.1c; Kim *et al.*, 2007; Jaronski & Jacksonki 2008). Additionally, these anamorphic entomopathogens are natural enemies of a broad range of insects and have a cosmopolitan distribution (Sharzei *et al.*, 2007).

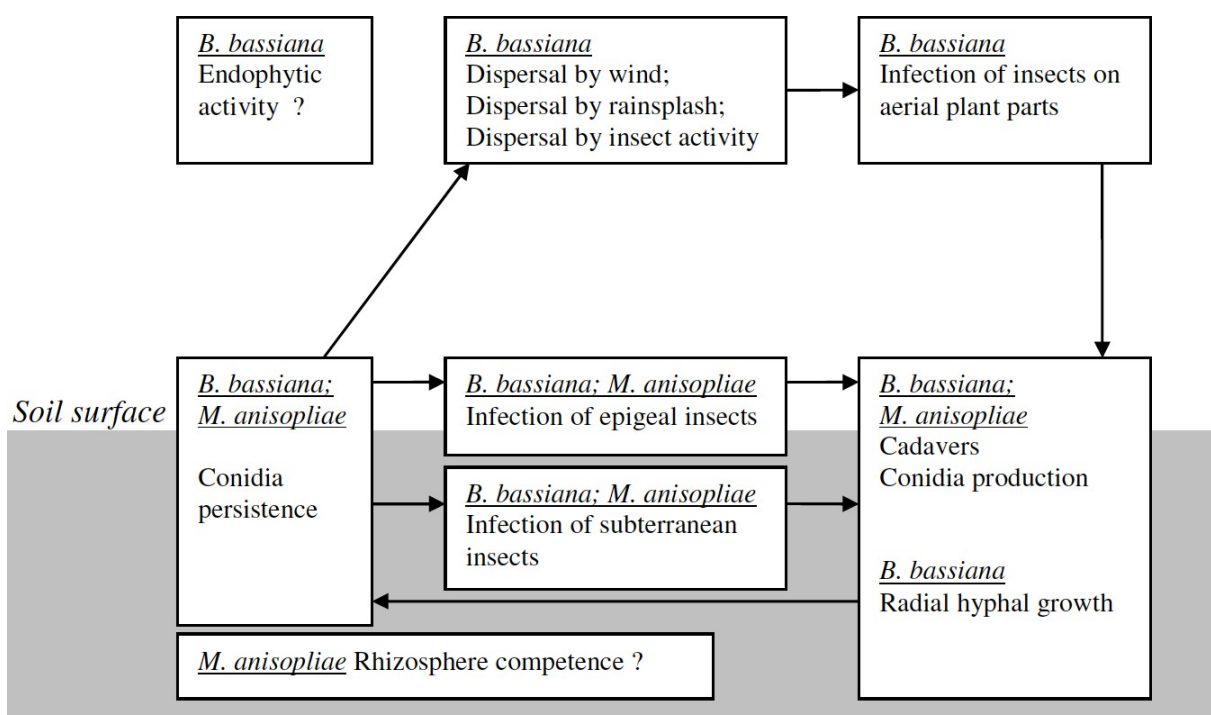


**Figure 1.1c** Demonstration of the anamorphic life cycle of *Beauveria bassiana* and *Metarhizium anisopliae* in northern temperate regions. The grey area represents the soil while the white background represents the area above ground. Significant dispersal and infection pathways are indicated by arrows. Taken from Meyling & Eilenberg (2007).

Entomopathogenic fungi rely on arthropod hosts to build up population levels of infective stages (mitosporic conidia). Both *M. anisopliae* and *B. bassiana* require resources from their hosts in order to grow and build up substantial fungal biomass. It appears that these fungi persist as conidia in the soil in anticipation of infecting new hosts (Oliveira *et al.*, 2014).

### **1.1.3 *Lecanicillium* spp**

Fungal entomopathogens in the genera of *Lecanicillium* spp., previously known and classified as *Verticillium lecanii*, are important tools against pests and some have been developed as commercial biopesticides. These fungal species have a wide host ranges including arthropods, nematodes, fungi and plants, which suggests that they have the potential to be developed as biopesticides with multiple roles.

*Lecanicillium* spp. follow the same pathway of pathogenesis of the other two mitosporic fungal species *Beauveria* and *Metarhizium*. Additionally, some *Lecanicillium* spp. are able to produce toxic metabolites *in vitro* to assist the fungus to overcome the hosts' response (Nuss, 2005).

At least eleven products based on *Lecanicillium* spp. are commercialised for use against a series of pests in several countries throughout the world (Reddy, 2020). Zare & Gams (2001) reported that *L. attenuatum* was isolated from caterpillars in Poland, also Kim *et al.* (2007) reported that the same isolate has been found in aphids in South Korea (King *et al.*, 2011; Zare & Gams 2001). *L. lecanii* infects largely soft scale insects, while *L. nodulosum* substrates include various insects, mites and decaying wood (Zare & Gams 2001). Furthermore, *L. muscarium* has been isolated from insects and fungi indicating its broad host range. Additionally, *L. muscarium* isolates have been commercialised as the biopesticides e.g., Mycotal<sup>®</sup> which is active against whiteflies and thrips and Verticillin<sup>®</sup> active against whiteflies, aphids and mites (de Faria & Wraight, 2007). It is clear that the potential of *Lecanicillium* spp. for its development as biopesticide and bioinsecticide is very promising. Development of a single microbial control

agent based on *Lecanicillium* spp. which could potentially be effective against numerous pest insects, plant diseases and parasitic nematodes is an ultimate goal.

## 1.2 Mycoviruses

As designated by their name mycoviruses are viruses that infect and replicate in fungi (Buck, 1986; Van Diepeningen *et al.*, 2000). Mycoviruses are widespread in yeasts, filamentous fungi, mushrooms and oomycetes (Yamada *et al.*, 1991). Mycoviruses were first discovered in the economically important mushroom *Agaricus bisporus* and found to cause what was later named La France disease in 1948 (Ghabrial *et al.*, 2009). However, in 1962 viruses were reported for the first time in cultivated mushroom. The presence of three types of viral particles as shown by electron microscopy represented the first experimental evidence for the existence of mycoviruses (Ghabrial, 1980; Hollings, 1962). This finding led to the study of more fungal isolates resulting in the discovery of double-stranded RNA (dsRNA) elements in *Penicillium* spp. and *Aspergillus* spp. (Border *et al.*, 1972; Buck, 1986; Ghabrial, 1980). These findings triggered mycovirus research in fungi that are economically important because of their potential antifungal properties.

Mycoviruses generally possess single-stranded (ss) or dsRNA as their genetic material. Additionally, mycoviruses have diverse genome structures: for example, *Endornaviridae*, *Partitiviridae*, *Totiviridae*, *Quadriviridae*, *Reoviridae*, *Chrysoviridae* and *Megabirnaviridae* have dsRNA genomes, whereas *Narnaviridae*, *Barnaviridae*, *Gammaflexiviridae*, *Hypoviridae* and *Alphaflexiviridae* have ssRNA genomes (Ghabrial *et al.*, 2015). Furthermore, *Pseudoviridae* and *Metaviridae* do not encode an RNA-dependent RNA polymerase (RdRP) for their replication; instead they use a reverse transcriptase (Yamada *et al.*, 1991). It is worth mentioning that full molecular characterisation of many mycoviruses is yet to be accomplished (Pearson *et al.*, 2009).

Members of the family of *Partitiviridae* have bisegmented genomes 1.4-2.4 kbp in length, which are able to encompass open reading frames (ORFs). The viral RdRP is encoded by the larger ORF, while the smaller ORF encodes a coat protein (CP). Two separate virus particles are produced at the end of the packaging process of two genome segments. Furthermore, there are four different genera in this family as shown by Ghabrial *et al.* (2015): *Alpha-*, *Beta-*, *Gamma-* and *Deltapartitivirus*. It has been noted that *Alpha-* and *Beta-partitiviruses* infect filamentous fungi and plants, *Gammapartitiviruses* only infect filamentous fungi and *Deltapartitiviruses* only infect plants (Ghabrial *et al.*, 2015).

On the other hand, *chrysovirus*, which belongs to the family *Chrysoviridae*, is the only genus of this family and *Penicillium chrysogenum* virus (PcV) is the prototype. Its genome comprises of four dsRNA segments, 2.4-3.6 kbp in size that are separately encapsidated in virions. Viral RdRP is encoded by dsRNA1 segment, while dsRNA2 encodes for CP. The function of proteins P4 and P3 encoded by dsRNA3 and dsRNA4 remains unclear. The 5'- and 3'- terminal untranslated sequences (UTRs) of these four dsRNAs are highly conserved (Jiang *et al.*, 2004). Members of the family of *Totiviridae* usually encompass two overlapping ORFs on one strand ranging in size between 4.6-7.0 kbp. These two ORFs encode the CP and the RdRP. Moreover, members on this family are divided into two genera depending on the host they infect. For example, viruses infecting smut fungi and yeasts have been placed in the genus *Totivirus*, while those infecting filamentous fungi are placed in the *Victorivirus* genus (Ghabrial & Suzuki 2009; King *et al.*, 2009)

Furthermore, based on recent reports members of this family use three different strategies for RdRP expression: (1) fusion protein (CP/RdRP) resulting in ribosomal frameshifting, an example is the parasitic protozoan viruses and *Saccharomyces cerevisiae* virus L-A (ScV-L-A; Dinman *et al.*, 1991). (2) fusion protein following fusion with the CP gene without ribosomal frameshifting, as in *Ustilago maydis* virus H1 (Keller *et al.*, 1989); and (3) non-fused

protein by a termination re-initiation mechanism, as shown for victoriviruses and *Helminthosporium victoriae* virus 190S (HvV190S; Huang *et al.*, 1996; Lin *et al.*, 1987). Finally, a novel virus family designated as the *Polymycoviridae* has recently been recognised. Polymycoviruses have a genome comprise of four to eleven dsRNA segments ranging in size from 0.8 – 3.1 Kb. DsRNA 1 encodes for viral RdRP, dsRNA 2 encodes for an ORF containing a cysteine-rich, zinc finger-like motif and all proteins encoded by this segment appear to be rich in arginine repeats. Moreover, dsRNA 3 encodes for a methyl transferase and dsRNA 4 encodes proteins that are rich in proline-alanine-serine (PAS) repeats (Kanhayuwa *et al.*, 2015; Kotta-Loizou & Coutts, 2017). Polymycoviruses are non-conventionally encapsidated, infectious as dsRNA and the GDD catalytic site for RdRP has been replaced with a CDNQ motif (Kanhayuwa *et al.*, 2015; Kotta-Loizou & Coutts, 2017).



**\*Polymycoviridae**

- Unencapsidated
- 1.2 – 2.4 kbp
- 4 linear segments
- *Aspergillus fumigatus* tetramycovirus 1 (AfuTmV-1)

Kanhayuwa *et al.* 2015

**Figure 1.2a** dsRNA mycovirus families and their general properties examined in this study.

Modified from King *et al.* (2012).

\* *Polymycoviridae* belong to realm *Riboviria* (ICTV 2019;

<https://talk.ictvonline.org/taxonomy/>).

### **1.3 Origins of Mycoviruses**

Most of the mycoviruses discovered so far possess RNA genomes. Naturally, these viruses are prone to errors during replication and the calculated mutation rate is found to be  $10^{-3}$ - $10^{-5}$  errors per nucleotide per replication cycle (Delarue *et al.*, 1990; Pearson *et al.*, 2009). Therefore, RNA viruses encompass a complex and dynamic group of sequences referred as ‘quasi species’ (Delarue *et al.*, 1990; Pearson *et al.*, 2009; Varga *et al.*, 2003). This may be an advantage in terms of evolution in order to adapt to new environments, however there is usually a tendency towards genetic stability particularly within homogenous populations.

In order to explain the origins and evolutionary history of mycoviruses two hypotheses have been suggested. The first hypothesis is based on the ancient co-evolution hypothesis, which suggests that infections are ancient originating from an unknown source and coevolving with their hosts. The second hypothesis, which is based on the plant virus hypothesis, suggests that for plant pathogenic fungi, the viruses have moved from the host plant to the fungus (Pearson *et al.*, 2009).

### **1.4 Mycovirus effects on host phenotypes**

#### **1.4.1 Asymptomatic infections (cryptic)**

The word “cryptic” comes from the Greek word “kryptos” which means hidden, like the symptoms of some of the mycoviruses can be described as cryptic (asymptomatic) and stay hidden and only be expressed under specific conditions. Usually when expressed they do not lead to any obvious effects (Ghabrial *et al.*, 2009; Punt *et al.*, 1987). It has been observed that mycoviruses in general are considered to be associated with asymptomatic infection, however small effects such as the reduction or enhancement of host pathogenicity (e. g., effects on spore production and growth rate) have been observed in isogenic lines of *Aspergillus* spp. (Bhatti *et al.*, 2012; Elias *et al.*, 1996).

### 1.4.2 Hypovirulence

Hypovirulence, a reduction of fungal pathogenicity, is characterised by the reduction of host growth rate, sporulation and pigmentation (Dawe *et al.*, 2001). The reduction of fungal pathogenicity caused by the presence of viral dsRNA has been reported in several fungi such as *Botrytis cinerea* (Castro *et al.*, 2003; Wu *et al.*, 2012), *Sclerotinia sclerotiorum* (Boland, 1992), while the best example and the most widely studied is *Cryphonectria parasitica* hypovirus 1 (CHV-1) which causes hypovirulence in *Cryphonectria parasitica* (Choi *et al.*, 1992; Nuss, 2005).

Likewise, another group of viruses called mitoviruses have been reported to cause hypovirulence (Nuss, 2005). Some examples are *Ophiostoma novo-ulmi* (responsible for Dutch elm disease) and *Botrytis cinerea* were both found to possess a mitovirus causing hypovirulence along with reduced sporulation and laccase activity (Castro *et al.*, 2003). Consequently, wide interest has been expressed in mycovirus-mediated hypovirulence as a potential biocontrol agent for fungal diseases such as invasive pulmonary Aspergillosis (Nuss, 2005).

### 1.4.3 Hypervirulence

Whilst some mycoviruses can cause hypovirulence, such as CHV-1, others can cause hypervirulence meaning the enhancement of fungal virulence providing advantages to their hosts (Choi *et al.*, 1992). Some beneficial effects of mycoviruses to their hosts have been reported including tolerance to high temperature of both the pathogen and the host plant allowing them to survive at high temperatures (Choi *et al.*, 1992). McCabe *et al.*, (1999) has demonstrated the killer phenomenon of dsRNA genomes encoding a proteinaceous toxin that while the host fungus is immune to it for other strains of the same fungus that do not produce

the toxin and it is lethal. This phenomenon is naturally observed when host strains use it to eliminate competitor strains occupying the same host niche (McCabe *et al.*, 1999).

Hypervirulence was first observed in a root pathogen *Nectria radicicola*, when a dsRNA with a size of approximate 6 kbp was found to interfere with the signal transduction pathways resulting in an increase of host pathogen virulence (Ahn *et al.*, 2001). Similar to hypovirulence, mycovirus-mediated hypervirulence is also of a great interest as a prospective biocontrol agent for the use against insects.

### **1.5 Transmission of fungal viruses**

Mycoviruses are not capable of natural extracellular transmission, like bacteriophages, however for intracellular transmission they depend on their fungal hosts (Buck, 1998). Additionally, mycoviruses can be transmitted using two methods: either (1) horizontally by heterokaryosis or (2) vertically by sporulation.

Lhoas (1971) first confirmed the transmission of viruses in fungi through heterokaryosis. He demonstrated the transmission of the virus from a virus-infected strain to a non-infected strain using genetically marked strains of *Aspergillus niger* and *P. stoloniferum* as models. Horizontal transmission through protoplasmic fusion is a successful method of transmission of mycoviruses between different fungal strains (Souza *et al.*, 2000, Xie *et al.*, 2006, Dalzoto *et al.*, 2006). The exchange of cytoplasm and genetic material including mycoviruses is undergone during anastomosis. This is a result of the hyphal fusion that occurs between different fungal strains. However, for this method to be successful the two fungal strains have to be vegetatively compatible. For example, in ascomycetes vegetative incompatibility (*vic*) and heterokaryon incompatibility genes control this process making it extremely difficult to exchange genetic material through anastomosis if the two fungal strains are not vegetatively compatible (Glass *et al.*, 2006; Schnell *et al.*, 1995). Consequently, virus transmission between

incompatible fungi through heterokaryosis is restricted, which has an effect on the host range of a mycovirus. However, successful horizontal transmission of CHV1 was observed in several species of *Cryphonectria* and similar phenomena have been described in different taxa of basidiomycetes and ascomycetes (Ikeda *et al.*, 2005). Additionally, mycoviruses are capable of interspecies transmission and an example is the transmission of mycoviruses between black *Aspergillus* spp. and *Fusarium poae* via protoplast fusion. This has been successfully demonstrated (Van Diepeningen *et al.*, 2006) and the mycovirus was found to be stable even after numerous rounds of subculture.

Another primary mode of mycovirus spread is *via* vertical transmission through spores; yet the fungus/virus combination as well as the spore type (i.e., sexual, or asexual) plays an important role in the rate of transmission. It has been reported that for fungi with a prolonged sexual stage in their life cycle the transmission rate of mycoviruses *via* sexual spores is very low (Vey *et al.*, 2001), whereas it is much easier for a mycovirus to be transmitted to asexual spores produced from modified hyphae (Buck, 1998).

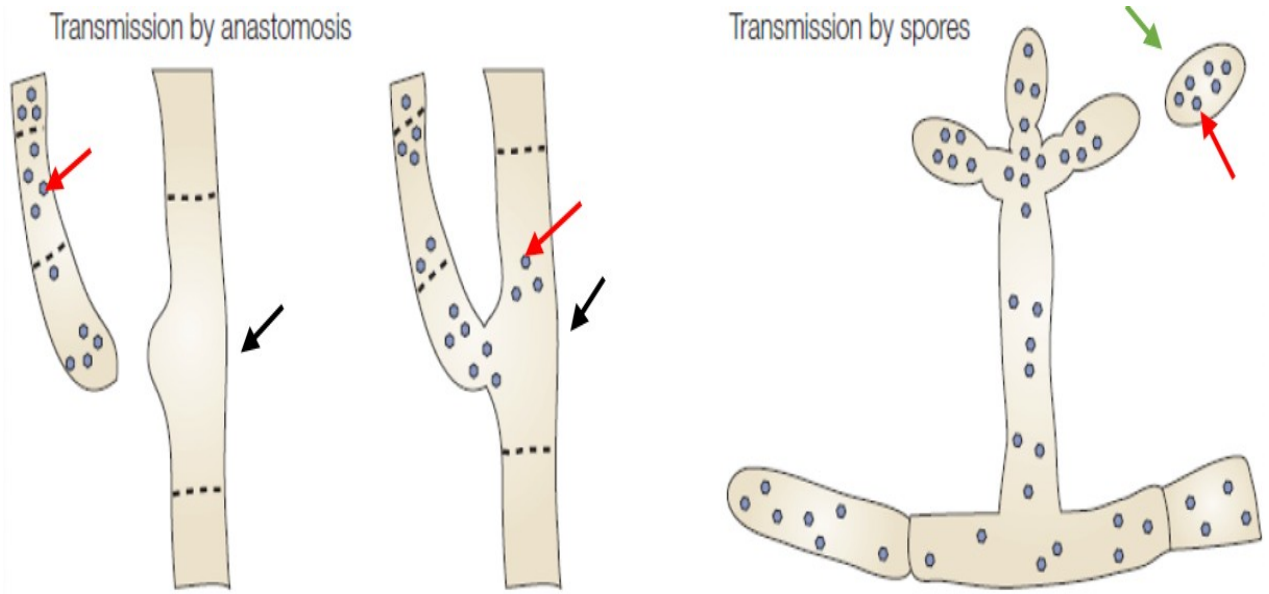


**Figure 1.4a** Methods of mycovirus transmission; Mycoviruses are transmitted vertical (by spores) or horizontally (by hyphal anastomosis). Black arrows indicate fungal hypha, green arrow indicate fungal spores, and red arrows indicate mycoviruses. Taken from Nuss (2005).

## **1.6 Modes of dsRNA virus replication**

The replication mode of mycoviruses depends on the species and differs considerably for each fungus. Due to the complexity of host mycoviruses replication has not been studied extensively (Lhoas, 1975). There are two mechanisms that mycoviruses use to replicate by a conservative or by a semi-conservative mechanism (Buck, 1978; Wickner, 1996). Despite genetic and structural complexity there are some basic similarities in viral replication between dsRNA viruses and these are described below.

In contrast to ssRNA viruses, dsRNA does not operate as mRNA and RdRP transcribes dsRNA into mRNA following amplification. These mRNA transcripts are translated into regulatory and structural viral proteins. Additionally, positive (+) strands are able to be encapsidated in order to form immature virions. The mRNA transcripts serve as a template for the synthesis of complementary negative (-) strands therefore the complete mature virions are produced by encapsidated dsRNA (Castón *et al.*, 1997).

## **1.7 Mycoviruses as biocontrol agents**

One of the best examples of viruses successfully used as biocontrol agents are the hypoviruses of the chestnut blight fungus. Hypoviruses have been used to control *C. parasitica* which is the main causative agent of chestnut blight in chestnut trees (*Castanea* spp.). Usually, the trunk and the branches of the tree are the main parts affected by the fungus leading to swollen or sunken cankers (Soldevila *et al.*, 2000).

Originally, the Italian plant pathologist, Antonio Biraghi, discovered spontaneous recovery of European chestnut trees from cankers. Likewise, Jeane Grente, a renowned French mycologist, discovered some unusual isolates of *C. parasitica* that were responsible for this recovery phenomenon (Macdonald & Fulbright, 1991). The recovered cankers had reduced pigmentation as compared to the bright orange pigmentation found with wild-type strains.

Interestingly, these isolates rarely cause fatal infection in European chestnuts (Malpartida *et al.*, 1983). This observation confirmed that these effects were caused by mycovirus infection resulting in hypovirulence. Furthermore, the cytoplasmic genetic factors responsible for the hypovirulent phenotype were shown to be transmissible through *in vivo* and *in vitro* studies. Finally, these elements were identified as dsRNAs, ranging in size from 8 to 12 kb and have been successfully used as biocontrol agents ever since (Malpartida *et al.*, 1983).

### **1.8 Polymycoviruses discovered in the entomopathogenic fungi *Beauveria bassiana***

This project is a continuation of the study based on polymycoviruses discovered in the entomopathogenic fungi *B. bassiana* and their potential use as biocontrol agents that was published by my supervisory team Dr Ioly Kotta-Loizou and Dr. Robert Coutts at PLOS pathogens in 2017.

This study examines members of the newly proposed family *Polymycoviridae* that were discovered in some *B. bassiana* isolates (Figure 1.8a). Following partial analysis of the genomic sequence of the four large dsRNA elements from ATHUM 4946 and IMI 391043 displayed a homologous relationship to the ones found in EABb 92/11-Dm. However, after phylogenetic analysis the authors concluded that BbPmV-2 and BbPmV-3 are closely related together, while they are distantly related to BbPmV-1.

Viruses that belong in the family *Polymycoviridae* possess proteins known to be conserved, such as dsRNA-1 which encodes for the RdRP necessary for viral replication, dsRNA-2 which act as a scaffold protein, dsRNA-3 encoding for a methyl transferase, and dsRNA-4 which coats the viral RNA genome instead of a capsid. Subsequently, BLAST searches of the viral proteins confirmed that the genome of these viruses belongs to the *Tetramycoviridae*, the prototype member of which is *Aspergillus fumigatus* tetramycovirus-1 (AfuTmV-1). However, considering that two of the viruses originated from ATHUM 4946 and IMI 391043, have six

and seven segments, respectively, along with mycoviruses from *Cladosporium cladosporioides* and *Botryosphaeria dothidea* (Zhai et al., 2016) belonging to the same family and each with five segments, this family was then renamed by the authors as *Polymycoviridae* (poly = 'many' in Greek, in contrast to tetra = 'four'; Kotta-Loizou & Coutts, 2017). Therefore, the viruses originated from EABb 92/11-Dm, IMI 391043 and ATHUM 4946 isolates were termed as *Beauveria bassiana* polymycovirus (BbPmV)-1, -2 and -3 respectively. Additionally, EABb 92/11-Dm supports the replication of one larger dsRNA segment which was then designated as *Beauveria bassiana* non-segmented virus (BbNV)-1. This virus belongs to the newly proposed viral family *Unirnaviridae* and it has two overlapping ORFs encoding an RdRP and a protein of unknown function. BbNV-1 is uncapped compared to polymycoviruses which are capped, indicating differences in translation initiation methods between the two viruses facilitating their co-existence in the same fungal host.

Polymycoviruses generally possess high GC content genome, ranging from 57% to 63%, and their RdRPs contain three partially conserved motifs that are normally found in RNA eukaryotic viruses such as picornaviruses. Furthermore, a close evolutionary relationship between the polymycovirus RdRP and members of the families *Caliciviridae* and *Astroviridae* was confirmed after a phylogenetic analysis.

Isogenic lines of virus-free and virus-infected EABb 92/11-Dm isolate were generated using cycloheximide with the aim of evaluating the effects of mycoviruses on the growth and virulence of their fungal host. After the absence of BbPmV-1 and BbNV-1 was confirmed by RT-PCR amplification an increase in both solid and liquid Czapek-Dox complete medium was observed in virus-infected when compared to virus-free isogenic lines. Similar results were also observed when the virulence of the isogenic lines were compared using the greater wax moth *Galleria mellonella*.

Consequently, the authors attempted to reintroduce by transfection purified BbPmV-1 and

BbNV-1 into EABb 92/11-Dm virus-free and in parallel into *B. bassiana* ATCC 704040 protoplasts. *B. bassiana* ATCC 704040 is a virus-free commercially available strain used as biocontrol agent against a variety of arthropod pests and was unable to support replication of either BbPmV-1 or BbNV-1, indicating a possible incompatibility between specific mycoviruses and different fungal strains. Unlike ATCC 704040, EABb 92/11-Dm virus-free isogenic line was able to support the replication of both viruses, as expected, and the virus-transfected isolate was named EABb 92/11-DmT. Similarly, the radial growth, biomass and virulence of the isolates EABb 92/11-DmT was increased when compared to the virus-free isogenic line.

To conclude this was the first report of a hypervirulent agent found in an entomopathogenic fungus and their potential use in the biological control of arthropod pests highlighting the ecological and economic implications in the future.

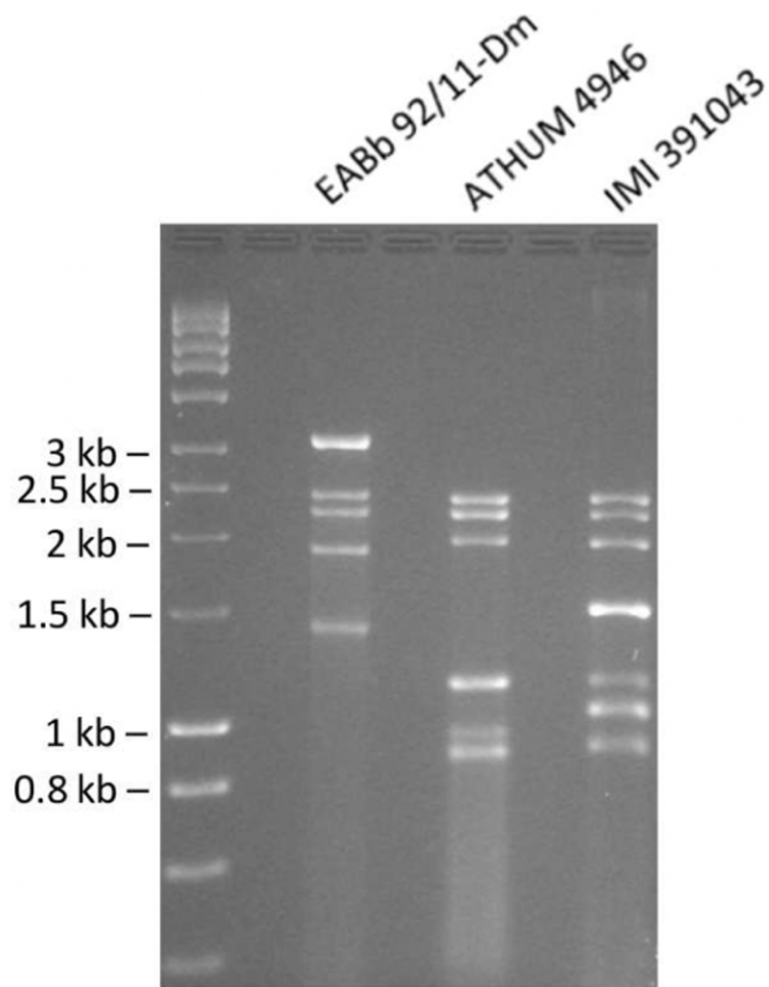


**Figure 1.8a** Electrophoretic profiles of polymycoviruses in *Beauveria bassiana*. DsRNA extracted from *Beauveria bassiana* isolates EABb 92/11-Dm, IMI 391043 and ATHUM 4946 harbouring BbPmV-1, BbPmV-2 and BbPmV-3 respectively. Taken from Kotta-Loizou & Coutts (2017).

## 1.9 Thesis Aims and Objectives

The main objective of this project is to evaluate the occurrence of mycoviruses in entomopathogenic fungi and to investigate their effects on growth and pathogenicity of their fungal hosts. The investigation focused on *Beauveria bassiana* but incorporated other entomopathogenic fungi including *Lecanicillium* spp. and *Metarhizium* spp. This study aims to use mycovirus-mediated hypervirulence to enhance commercially available mycopesticides.

### Objectives:

1. To isolate entomopathogenic fungal strains and identify which ones carry mycoviruses (Chapter 3).
2. To obtain the full genomic sequence of dsRNA 5 and 6 of a known mycovirus infecting *B. bassiana* polymycovirus-3 (BbPmV-3) ATHUM 4946 (Chapter 3).
3. To analyse a novel virus discovered in two *Lecanicillium muscarium* isolates (Chapter 3).
4. To cure PmV-3 and LmV-1 infections on *B. bassiana* isolate ATHUM 4649 and *L. muscarium* 143.62 and 102071 respectively, and examine phenotypic changes for isogenic lines (Chapter 4).
5. To use *Tenebrio molitor* insects to study the survival rates against EABb 92/11-Dm virus- free (PmV-1.F) and virus-infected (PmV-1.I) isogenic lines, Naturalis and BotaniGard (Chapter 4).
6. To transfect Naturalis and BotaniGard protoplasts with polymycoviruses- BbPmV-1 and -3 (Chapter 4).
7. To perform RNA sequencing to analyse the transcriptome of PmV-1.F and PmV-1.I isogenic lines (Chapter 5).
8. To perform RNA sequencing of the infection model to compare pathogenicity of PmV-1.F, PmV-1.I, Naturalis and BotaniGard, against *T. molitor* infection model (Transcriptomics and comparative genomics; Chapter 5).

# **Chapter 2**

## **General materials and methods**

## **2.1 Inoculation and growth of isolates**

Fungal isolates for screening were grown on Czapek-Dox, Sabouraud dextrose agar, Potato dextrose agar and Malt extract agar containing a cocktail of antibiotics including kanamycin A, ampicillin, and streptomycin to prevent bacterial contamination. On occasion media were covered with autoclaved cellulose discs prior to inoculation. All fungal cultures were grown at 25°C in complete darkness.

## **2.2 Nucleic acid manipulation**

### **2.2.1. Phenol and Chloroform extraction**

For nucleic acid extraction and protein denaturation phenol and chloroform were added in equal volumes (25:25 v/v) to an equivalent volume of solution containing nucleic acids. The mixture was then mixed by vortexing and centrifuged at 13,000 rpm for 5 min to separate aqueous and organic phases. The upper aqueous solution was transferred into new sterile Eppendorf tubes and equal amounts of chloroform were added, vortexed and centrifuged to remove any residual phenol from the mixture.

### **2.2.2. Nucleic acid precipitation**

Precipitation of nucleic acid was achieved following the addition of 1/10 the volume of 3 M sodium acetate (pH 5.5) and 2.5 volumes of absolute ethanol (100%). The mixture was inverted 6 times and kept for 16 h at -20°C for nucleic acid precipitation. Nucleic acids were collected by centrifugation at 13,000 rpm for 10 min. Supernatants were discarded after centrifugation and pellets were air dried for 30 min and then resuspended in sterile water.

### **2.2.3. DNase 1 treatment**

Nucleic acid preparations were subjected to DNase 1 treatment to remove any residual fungal DNA. Here pellets were resuspended in 90  $\mu\text{L}$  of RNase free water followed by the addition of 10  $\mu\text{L}$  of DNase 1 buffer (10x) and 1  $\mu\text{L}$  of DNase enzyme (1 U/  $\mu\text{L}$ ; Promega) and the mixture incubated for  $> 1$  h at  $37^\circ\text{C}$ . After incubation, 250  $\mu\text{L}$  of RNase Free water was added and nucleic acids were extracted with an equal volume of phenol and chloroform to remove DNase.

### **2.2.4. S1 nuclease treatment**

After DNase 1 treatment and overnight  $-20^\circ\text{C}$  ethanol precipitation of dsRNA nucleic acids were collected by centrifugation and the supernatant was discarded prior to air drying the pellets for 30 min at room temperature. In order to obtain pure dsRNA, S1 nuclease was added to the mixture to remove any fungal RNA. The pellet was resuspended in 90  $\mu\text{L}$  of RNase free water followed by the addition of 10  $\mu\text{L}$  of S1 nuclease buffer (10x) and 1  $\mu\text{L}$  of S1 nuclease enzyme (1 U/  $\mu\text{L}$ : Promega). The mixture was then incubated at  $37^\circ\text{C}$  for  $>1$  h. Then the phenol and chloroform extraction method was used to remove the S1 enzyme. The dsRNAs were precipitated as described above and resuspended in Millipore water prior to further manipulation.

### **2.2.5. Gel electrophoresis**

Nucleic acids were separated and visualised by agarose gel electrophoresis. 1% agarose gel was prepared by dissolving agarose powder, 0.75g in 50mL of 1x TBE buffer, by boiling in a microwave oven for 2 min. When the temperature was *ca.*  $35\text{-}40^\circ\text{C}$  5  $\mu\text{L}$  (1:100) of ethidium bromide staining dye (ThermoFisher Scientific) was added to the gel. Next, the gel was poured into a casting tray and left to solidify for 30 min before loading the samples. The samples

contained 6x loading buffer. The gel was electrophoresed in 1x TBE buffer for 2 h at 50 V and observed under UV light.

### **2.2.6 Gel purification for recovery of dsRNA**

DsRNA bands of interest were excised from gels using a sterile scalpel blade transferred into 2mL sterile microcentrifuge tubes and weighed. Gel purification was performed using the QIA MinElute gel extraction kit (Qiagen). The gel purification process was followed as described in the manufacturers protocol. Three volumes of buffer QG were added to each volume of gel. The solution was incubated at 55°C for 10 min until the gel slice melted completely. This process was facilitated by the inversion of the tube every 2 min during incubation. One gel volume of isopropanol was then added to the sample and mixed. The solution was then transferred to a silica membrane based MinElute spin column and centrifuged for 1 min to assist RNA binding to the membrane. Next the flow through was discarded and 500 µL of QG buffer was added to the column, which was then centrifuged for 1 min. The resulting flow through was again discarded. The same method was repeated after the addition of 750 µL of buffer PE (containing ethanol). For complete removal of any residual buffer the column was centrifuged again for 1 min. After the removal of impurities, the column was placed in a 1.5 mL tube and 20 µL of RNase free water was added in the middle of the column and left to stand for 1 min. Next the tube was centrifuged for 1 min at 13,000 rpm and pure dsRNA was collected in a tube and stored at -20°C until further use.

### **2.3 Genome walking**

The genome walking procedure was used to characterize and sequence mycovirus dsRNA from *B. bassiana*. In this procedure, primers were designed on the basis of known sequence and PCR

was performed as described in Section 2.7. Schematic representation of this technique is illustrated in Appendix Part B Figures S3.4.2 and S3.4.4.

#### **2.4 Ligation of PCR amplicons**

For this method 3  $\mu\text{L}$  of PCR amplicons were ligated with 1  $\mu\text{L}$  of pGEM-T Easy (Promega; 3:1 ratio) vector in 5  $\mu\text{L}$  of 2x ligation buffer and 1  $\mu\text{L}$  of T4 DNA ligase enzyme. The ligation mixtures were kept at 4°C for a minimum of 16 h.

#### **2.5 Transformation of XL10 Gold competent *Escherichia coli* cells with DNA**

Transformation was used with competent cells to generate recombinant plasmids. Competent *E. coli* cells (10-50  $\mu\text{L}$ ) previously stored at -80°C were thawed on ice and mixed with 5  $\mu\text{L}$  of ligation mix from above in an Eppendorf tube and kept on ice for 30 min prior to heat-shock for 45 sec at 42°C in a heat block. Then the tube was placed on ice for 2 min. Next 950  $\mu\text{L}$  of LB broth was added to the mixture and the tube incubated at 37°C on a shaker for 2-3 h. The solution was then centrifuged at 13,000 rpm for 2 min and 850  $\mu\text{L}$  of the supernatant was discarded and the pellet was resuspended by pipetting the remaining solution. While the mixture was incubating at 37°C 20 mL of LB agar plates containing 20  $\mu\text{L}$  ampicillin, 20  $\mu\text{L}$  IPTG and 40  $\mu\text{L}$  of X-Gal were prepared. The transformation mixture was then spread on the LB plates and incubated overnight at 37°C. Successful transformants with recombinant plasmids were screened using blue-white selection. White colonies were distinguished from wild type blue colonies, were picked and transferred into 5 mL LB medium containing ampicillin or kanamycin and incubated at 37°C overnight with shaking at 180 rpm.

## **2.6 Plasmid extraction from XL10 Gold competent cells using the alkaline lysis method**

For the isolation of the plasmid DNA from transformed *E. coli* cells the QIA Miniprep kit (Qiagen) was used. Overnight cultures were centrifuged at 4,000 rpm for 10 min to pellet the cells. The supernatants were removed by decanting the tubes and the pelleted cells were resuspended in 250  $\mu$ L of P1 buffer. The pelleted cells were again resuspended by vortexing, transferred into a 1.5 mL microcentrifuge tubes and 250  $\mu$ L P2 buffer (0.2 N NaOH and 1% SDS) was added. Then the tubes were inverted 4 to 6 times to ensure efficient bacterial cell lysis. When the mixtures became transparent, 350  $\mu$ L of N buffer was added for neutralization and the tubes were again inverted 4 to 6 times. The extracts were then centrifuged at 13,300 rpm for 10 min and the supernatants transferred into a QIA Miniprep columns. The columns were then centrifuged for 1 min at 13,300 rpm to allow the plasmid DNA to bind to the columns while the flow-through was discarded. Then, 500  $\mu$ L of PE buffer was added to wash the DNA which was removed by centrifugation for 1 min at 13,300 rpm. Columns were re-washed with 750  $\mu$ L of PE buffer and re-centrifuged for 1 min at 13,300 rpm. The flow through was discarded followed by a final centrifugation to remove any residual washing buffer. Finally, the tubes were placed into 1.5 mL Eppendorf tubes and 20  $\mu$ L of RNase free water was added and left to stand for 1 to 5 min for the efficient elution of plasmid DNA followed by 1 min centrifugation to collect the DNA.

## 2.7 Construction of cDNA library from dsRNA by random-PCR (rPCR)

The procedure described by Froussard (1992) was adapted to construct a library of cDNA clones from the small uncharacterised dsRNA present in the fungal isolates examined in this study (Appendix Part B Table S6.1a). This method allows the production of a cDNA library from small amounts of dsRNA. The procedure involves the use of a 26-nucleotide primer containing a random hexamer at its 3'-terminus for cDNA synthesis (Froussard-FOR) and a PCR amplification step using the same primer in combination with a complementary reverse primer (Froussard REV).

Froussard-FOR	5'- GCCGGAGCTGTGCAGAATTCNNNNNN
Froussard-REV	5'- GCCGGAGCTGTGCAGAATTC

Viral dsRNA (8  $\mu$ l, 0.5  $\mu$ g) was mixed with 2  $\mu$ l of Froussard-FOR primer (100  $\mu$ M) and the mixture was denatured by the addition of 2  $\mu$ l methyl mercuric hydroxide (CH<sub>3</sub>HgOH; 100 mM SERVA), following incubation at room temperature for 20 min and snap cooling on ice for 1 min. First strand cDNA and PCR amplification of cDNAs was performed as described in Section 2.8.1 below.

## 2.8 RNA linker-mediated rapid amplification of cDNA ends (RLM-RACE)

RLM-RACE is a PCR-based technique modified from Coutts and Livieratos (2003) which facilitates the cloning of full length cDNAs and is often used to specifically amplify 5'- or 3'-termini of dsRNAs. An oligonucleotide primer nominated LIG-Rev ([5'-kinated-PO<sub>4</sub>; 3'-OH-blocked]; 5'GATCCAAGTCTAGAGCGG]) was ligated to the 3' end of dsRNA using T4 RNA ligase (NEB). The dsRNA (7  $\mu$ L, 0.5  $\mu$ g) was denatured together with the LIG-Rev primer (1  $\mu$ L: 100 pmol) by heating the mixture at 90°C for 2 min and then snap-cooling on

ice. The ligation reaction mixture was prepared by adding 10  $\mu$ L T4 RNA buffer (NEB), 1  $\mu$ L ATP (10 mM; Promega) and 62.5  $\mu$ L H<sub>2</sub>O (If the buffer contains ATP, add 63.5  $\mu$ L distilled H<sub>2</sub>O). This mixture was incubated at 37°C for 10 min and then cooled at room temperature for 2 min prior to the addition of 10  $\mu$ L DMSO, 2.5  $\mu$ L RNase Inhibitor (Promega), 1  $\mu$ L T4 DNA ligase (Promega; 1-3U/  $\mu$ L) and 5.0  $\mu$ L T4 RNA ligase (NEB; 10U/  $\mu$ L). The reactants were then pelleted to the base of the Eppendorf reaction tube and the denatured dsRNA from above added prior to incubation at 17°C for 15 h.

Following incubation, 250  $\mu$ L distilled H<sub>2</sub>O was added to the reaction to give a final volume of 350  $\mu$ L from which nucleic acids were precipitated following the addition of 0.1 volume of 3 M sodium acetate and 2.5 volumes of cold absolute ethanol and incubated at -20°C for overnight precipitation. The mixture was then centrifuged at 15,000 rpm for 25 min and the resultant pellet left to air-dry for 15-30 min prior to resuspension in 100  $\mu$ L water. To ensure completed molecules had been assembled correctly the 100  $\mu$ L of ligated-dsRNA was added to 40  $\mu$ L of 5x GoTaq® Reaction Buffer, followed by the addition of 4.8  $\mu$ L of 10 mM dNTPs mix, 1  $\mu$ L of GoTaq® DNA polymerase and 54.2  $\mu$ L distilled H<sub>2</sub>O to make a total volume of 200  $\mu$ L. The mixture was incubated at 68°C for 3 h and the ligated dsRNA precipitated overnight (at -20°C) following addition of 0.1 volume 3 M sodium acetate and 2.5 volumes cold absolute ethanol. The ligated dsRNA was recovered by centrifugation at 13,000 rpm for 25 min at 4°C. The supernatant was discarded, and the pellet was washed by adding iced-chilled 70% ethanol followed by centrifugation at 13,000 rpm for 25 min. The supernatant was discarded, and the pellet was dried under a lamp for 30 min prior to resuspension in 8  $\mu$ L sterile DEPC-treated water on ice for 30 min.

The ligated dsRNA (8  $\mu$ L) was denatured by adding 2  $\mu$ L CH<sub>3</sub>HgOH (100 mM) together with 2  $\mu$ L of a LIG-For oligonucleotide primer (5'- CCGCTCTAGAACTAGTTGGATC-3'; 100

$\mu\text{M}$ ). The mixture was incubated at room temperature for 20 min and then rapidly cooled on ice for 1 min.

First strand cDNA was then synthesised using 12  $\mu\text{L}$  of denatured dsRNA as template which was added to the reaction mixture below which was pre-heated at 50-55  $^{\circ}\text{C}$  for 1 min. The reaction mixture was prepared by mixing the following components:

10 $\mu\text{L}$	5x First-strand buffer (Invitrogen)
4 $\mu\text{L}$	0.1 M DTT (Invitrogen)
1.25 $\mu\text{L}$	RNasin® Ribonuclease Inhibitor (Promega)
2.4 $\mu\text{L}$	10 mM dNTPs (10 mM each dATP, dGTP, dCTP and dTTP; Promega)
19.35 $\mu\text{L}$	DEPC-H <sub>2</sub> O

SuperScript™ III reverse transcriptase (1  $\mu\text{L}$  of 200 U/  $\mu\text{L}$ ) was added to the mixture containing denatured dsRNA and the whole reaction was incubated at 50 $^{\circ}\text{C}$  for random hexamer or degenerate primers, or 55 $^{\circ}\text{C}$  for sequence specific primers for 1 h and then 70 $^{\circ}\text{C}$  for 15 min to inactivate the enzyme. First strand cDNA reaction mixture was size fractionated using a Nanosep 30K column as before prior to PCR amplification.

PCR was performed in 100  $\mu$ L reaction mixtures in thin walled 0.5 ml PCR Eppendorf tubes and contained the following components:

50 $\mu$ L	cDNA (from first-strand reaction)
25.1 $\mu$ L	DEPC-H <sub>2</sub> O
20 $\mu$ L	5x GoTaq® Reaction Buffer (Promega)
2.4 $\mu$ L	10 mM dNTPs mix (Promega)
1 $\mu$ L	Lig-For primer (100 $\mu$ M)
1 $\mu$ L	Sequence specific primer (100 $\mu$ M)
1 $\mu$ L	RNase H (NEB)
0.5 $\mu$ L	GoTaq® DNA polymerase (5 units/ $\mu$ l; Promega)

The samples were then subjected to thermal cycling using PCR amplification specifically for GoTaq® DNA polymerase as described below.

Initial denaturation	95 °C	2 min		1 cycle
Denaturation	95 °C	1 min	}	30 cycles
Annealing	60 °C	1 min		
Extension	72 °C	3 min		
Final extension	72 °C	5 min		1 cycle
Hold	4 °C	forever		1 cycle

### 2.8.1 cDNA Synthesis

DsRNA (11  $\mu\text{L}$ ) that were previously extracted from different isolates were denatured by the addition of 1  $\mu\text{L}$  of 100 mM methyl mercury. Next 1  $\mu\text{L}$  of the forward sequence specific oligonucleotide primer (100  $\mu\text{M}$ ) was added to the denatured template in order to facilitate annealing. Afterwards, the mixture was incubated for 20 min at room temperature and then for 2 min on ice.

#### Reaction mixture for the first strand cDNA synthesis:

1. 5x RT buffer	4 $\mu\text{L}$
2. DTT (100 mM)	1 $\mu\text{L}$
3. dNTPs (10 mM)	1 $\mu\text{L}$
4. RNasin (40 units/ $\mu\text{L}$ - Promega)	0.5 $\mu\text{L}$
5. ssRTIII (200 units/ $\mu\text{L}$ - Invitrogen)	0.5 $\mu\text{L}$
<hr/>	
6. Ds RNA, methyl mercury and H <sub>2</sub> O to a total volume of 20 $\mu\text{L}$	

The mixture was then incubated at 50°C for 60 min and then at 70°C for 15 min to synthesize cDNA. After incubation 10  $\mu\text{L}$  of the solution containing cDNA was moved into another sterile PCR tube and was mixed with 10  $\mu\text{L}$  of PCR Green mix containing GoTaq DNA polymerase and 1  $\mu\text{L}$  of the Reverse sequence specific primer (100 $\mu\text{M}$ ).

PCR amplification was performed in a PCR thermocycler with specific conditions according to the oligonucleotide primers and the DNA polymerase used.

## Thermocycling conditions for PCR amplification using GoTaq DNA polymerase

94°C	2 min (denaturation)		(1 cycle)
94°C	1 min (denaturation)		(30cycles)
60°C	1 min (annealing)		
72°C	1min/kb (extension)		
72°C	5 min (final extension)		(1 cycle)
Hold forever	4°C		(1 cycle)

One tenth of each reaction mixture was used to analyse the amplicons following 1% agarose gel electrophoresis.

## **2.9 Northern blot hybridisation**

### **2.9.1 *In vitro* transcription-labelling of RNA with digoxigenin**

The DIG Northern Starter Kit (Roche) was used to generate DIG labelled, single stranded RNA probes of defined length by *in vitro* transcription of template DNA in the presence of digoxigenin-UTP, using SP6, T7 RNA polymerases.

### **2.9.2 DNA template preparation**

Representative plasmids of each dsRNA under investigation were retransformed into pGEM-T Easy vector and recombinant DNA isolated. Plasmid DNA was linearised using a restriction site in the poly-linker sequence downstream of the cloned insert to be transcribed (multiple cloning sites of the SP6 or T7 promoter region) and the length of the sequence to be transcribed adjusted to 200-1000 bp. A restriction enzyme which leaves a 5' overhang was selected using the NEB cutter V2.0 program (<http://tools.neb.com/NEBcutter2>) to avoid transcription of undesirable sequences.

### 2.9.3 *In vitro* transcription using the MAXI Script®T7 Kit

The MAXIScript®T7 Kit (Ambion®) was used for the *in vitro* synthesis of unlabelled RNA probes. The transcription reaction was assembled at room temperature with all components being added in the order shown below:

To 20 $\mu$ L	Nuclease-free water
1 $\mu$ g	Linearised plasmid DNA template
2 $\mu$ L	10x Transcription buffer
1 $\mu$ L	10 mM ATP
1 $\mu$ L	10 mM CTP
1 $\mu$ L	10 mM GTP
1 $\mu$ L	10 mM UTP
2 $\mu$ L	T7/SP6 Enzyme mix
20 $\mu$ L	total volume

The mixture was pipetted gently, centrifuged briefly to collect the reaction mixture at the bottom of the tube and then incubated at 37°C for 1 h. To remove template DNA, TURBO DNase (1  $\mu$ L) was added to the reaction, incubated at 37°C for 15 min and then 0.1  $\mu$ L of 0.5 M EDTA was added to stop the reaction. The transcript was then examined by Nanodrop and agarose gel electrophoresis as above.

## 2.9.4 DIG-RNA labelling

The labelling procedure is designed for 1 µg of DNA template. RNA transcripts were labelled by *in vitro* transcription reaction with digoxigenin-11-UTP using a labelling mixture and an optimised transcription buffer shown below:

10 µL	1 µg linearised plasmid DNA
4 µL	5x labeling mix (vial 1a)
4 µL	5x transcription buffer (vial 1b)
2 µL	T7/SP6 RNA polymerase
20 µL	total volume

The reaction tube was centrifuged briefly and then incubated at 42°C for 1 h. DNase I was then added to the reaction to digest the template DNA following incubation for 15 min at 37°C. The reaction was stopped by the addition of 2 µL 0.2 M EDTA (pH 8.0). The labelled transcript was divided into 5 µL aliquots and concentration checked using a Nanodrop counter.

## 2.9.5 DIG northern blot hybridisation

### 2.9.5.1 Separation of dsRNA samples on agarose gels

The standard protocol for gel electrophoresis was used for dsRNA separation as described (Section 2.2.5). A 1% agarose gel was prepared in 1x TAE buffer containing ethidium bromide at a final concentration of 50 µg/100 ml. The agarose was poured into a casting tray and left to set for 45 min. Before loading, samples were mixed with 5x gel loading buffer, alongside a DNA size marker (GeneRuler 1 kb, Promega). Electrophoresis was performed in 1 X TAE buffer at a voltage of 60 V for 3 h until the dsRNAs were well-separated following visualisation under a blue-light transilluminator (Syngene).

### **2.9.5.2 Transferring dsRNA to a membrane and fixation**

Nucleic acids separated in agarose gels were fixed by soaking in 0.25 N HCl for 20 min. To denature nucleic acids gels were placed on a new tray and then immersed in 100 mM NaOH for 30 min, followed by neutralization twice in 100 mM Tris-HCl (pH 8.0) for 20 min.

A blot transfer sandwich was set up by placing a fibre pad, which had been soaked with 1x TAE buffer, onto a blot cassette with the grey side down. A piece of pre-wetted chromatography paper (3 MM CHR, Whatman) was then placed on the fibre pad, followed by the gel. A sterile pipette was used to roll over the gel to remove all air bubbles that formed between the gel and paper. A piece of positively charged Amersham Hybond TM-N membrane (GE Healthcare) was carefully placed directly on top of the gel and then the blot assembly was completed by adding a soaked sheet of Whatman paper and fibre pad on the top of the blot stack. The cassette was closed firmly and placed in a Trans-Blot® electrophoresis transfer tank (BIO-RAD) filled with 1xTAE transfer buffer. A stir bar was added to maintain even buffer temperature and buffer distribution in the tank. A power supply (BIO-RAD) was connected to the tank and the transfer achieved following overnight electrophoresis at 15 V at 4 °C.

Upon completion of electrophoresis the blotting sandwich was disassembled. The membrane was placed on Whatman 3MM paper soaked with 2xSSC and then the RNA was fixed to the membrane by UV-cross linking for 25 min at the energy level of 2000 x 100 µL/cm<sup>3</sup> (UVP CL-1000 Ultraviolet Crosslinker).

### **2.9.5.3 Hybridisation with RNA probes**

DIG Easy Hyb (10 mL) was prewarmed to hybridization temperature at 68°C for 20 min in a UVP HC-3000 HybriCycler™ hybridization oven. The membrane was placed in a Falcon tube containing pre-warmed DIG Easy Hyb and pre-hybridised at 68°C for 30 min with gentle agitation in a rotisserie. DIG-labeled RNA probe (5 µL) was denatured by boiling at 95°C for

5 min and rapidly cooled in ice. The denatured probe (100 ng/ml) was then added to a prewarmed DIG Easy Hyb (4 mL) and mixed well but avoiding foaming. The pre-hybridisation solution was removed, and the probe/hybridisation mixture added to the membrane. The hybridisation tube was incubated overnight at 68°C with gentle agitation. After hybridisation, the solution was removed, and the membrane washed in an RNase-free plastic container. Low stringency buffer (2xSSC, 0.1% SDS) was used to wash the membrane twice for 5 min at room temperature in the HybriCycler, followed by a high stringency wash with a prewarmed 0.1xSSC, 0.1% SDS solution at 68°C for 15 min, twice in the HybriCycler.

#### **2.9.5.4 Immunological detection**

After hybridization and high stringency washing, the membrane was rinsed briefly for 5 min in a 50 ml washing buffer on a rotary shaker at room temperature. The buffer was removed, and the membrane was incubated in 100 ml blocking solution for 30 min, followed by incubating in 50 mL antibody solution for 30 min on a rotary shaker. The membrane was washed twice in 100 mL washing buffer for 15 min, equilibrated for 5 min in 100 mL detection buffer on a rotary shaker and then placed on a development folder with the RNA transfer side facing up. Approximately 1 mL of CDP-Star solution was evenly applied rapidly to the membrane until it was soaked. The second sheet of the folder was rapidly folded to cover the membrane and spread the substrate evenly without air bubbles prior to sealing the edge of the folder. Membranes were not allowed to dry at any stage since this would ruin the exposure and the image. The membrane was exposed to an imaging device and developed by phosphor imaging (Fuji Film LAS-3000 Imaging System) for 2-10 min at -25 °C.

## 2.10 Fungal genomic DNA extraction

Fungal mycelia were harvested from Malt Extract Agar (MEA) plates and ground to a fine powder using liquid nitrogen and a sterile mortar and pestle. The homogenate was then transferred into a 1.5 mL Eppendorf tube using a sterile scoop pre-dipped in liquid nitrogen. Then, 500  $\mu$ L of the fungal DNA extraction buffer (0.2M Tris-HCl (pH 7.5), 0.5M NaCl, 10 mM EDTA (pH 8.0) plus 1% (w/v) SDS) was immediately added to the sample before the homogenate thawed. Next, 500  $\mu$ L of phenol chloroform isoamyl alcohol mixture in a ratio of 25:24:1 was added, followed by 5 min moderate vortex mixing. The sample was then centrifuged at 10,000 rpm for 8 min at room temperature. The aqueous top layer was immediately transferred into a new 1.5 mL Eppendorf tube avoiding transfer of the middle pellet layer. Next, 500  $\mu$ L of chloroform-isoamyl alcohol in a ratio of 24:1 was added, and the mixture was mixed well, followed by centrifugation at 10,000 rpm for 8 min at room temperature. Then the aqueous top layer was transferred into a new Eppendorf tube, 10  $\mu$ L of RNase solution was added and mixed well in order to degrade RNA present in the sample. The mixture was incubated at 37°C for 1 h.

A phenol-chloroform-isoamyl alcohol extraction step was performed followed by centrifugation for 10 min at 12,000 rpm as before. The top aqueous layer was transferred into a new Eppendorf tube and a final chloroform-isoamyl alcohol wash performed followed by centrifugation as above. The top aqueous layer was transferred into a new Eppendorf tube and 2.5 volumes of 100% ethanol was added and mixed gently by inverting the tube 5-6 times. The mixture was then incubated at room temperature for 2 min and then centrifuged as above. The tube was then decanted to remove the ethanol and 200  $\mu$ L of ice-cold 70 % ethanol was added. The sample was then centrifuged at 1200 rpm for 2 min, the ethanol was then discarded, and the pellet was left to air dry for 30 min. The pellets were then dissolved in 50  $\mu$ L of nuclease free H<sub>2</sub>O and stored at -20°C.

Fungal gDNA was then used for ITS amplification using the universal primers ITS1F (Gardes & Bruns 1993) and ITS4 (White *et al.* 1990) to amplify the complete sequence of internal transcribed spacer (ITS) 1, the 5.8S ribosomal RNA gene, and the internal transcribed spacer 2, flanked by the partial sequence of the 18S and 28S ribosomal RNA genes

### **2.11 Total RNA extraction using E.Z.N.A Fungal RNA kit (OMEGA)**

Total RNA extracts from fungal mycelia were produced using the E.Z.N.A Fungal RNA kit (OMEGA). Here fungal mycelia (50-100 mg) was homogenised using a mortar and pestle with liquid nitrogen to break the cells. The powder was quickly mixed, with 500 µL of RB Buffer lysis buffer plus 20 µL of β- mercaptoethanol before it was allowed to thaw and the extract vortexed vigorously to ensure that all clumps were dispersed. Then the lysate was transferred to the homogenizer mini column and centrifuged for 5 min at 13,000 rpm to remove cell-debris. Carefully and without disrupting the pellet the supernatant of the flow-through was transferred to a microcentrifuge tube. Depending on the volume of the cleared lysate half volume of absolute ethanol was added to it. Next the mixture was transferred to the HiBind® RNA Mini column and centrifuged for 30 sec at  $\geq 10,000$  rpm.

#### **2.11.1 On column DNase I digestion and RNA elution**

Since the HiBind® matrix of the RNA Mini Column eliminates most DNA, DNase I digestion was not necessary for most downstream applications. However, because library preparation is a sensitive application and any genomic DNA present in the sample will affect the results, further DNA removal is crucial for this extraction.

HiBind® RNA Mini Column RNA Wash Buffer I (250 µL) was added to the mixture and the tube centrifuged for 1 min at 10,000 x g. The filtrate was then discarded and 75 µL DNase I digestion mixture was added directly onto the surface of the membrane of the HiBind® RNA



Sequence data were analysed using the bioinformatics tools and programs below.

<http://blast.ncbi.nlm.nih.gov/Blast.cgi>

<http://mafft.cbrc.jp/alignment/server/>

<http://bio.lundberg.gu.se/edu/translat.html>

<http://web.expasy.org/translate/>

<http://www.ebi.ac.uk/Tools/msa/clustalw2/>

## **2.12.2 RNA sequencing**

### **2.12.2.1 3'mRNA-Seq Library Prep**

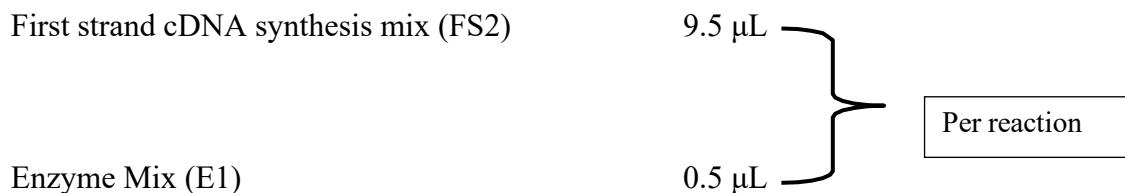
Lexogen's QuantSeq kit FWD HT provides a high-throughput library preparation designed to generate Illumina-compatible libraries from polyadenylated RNA within 4.5 h. The QuantSeq only generates one fragment per transcript, resulting in extremely accurate gene expression values. The sequences obtained are close to the 3' termini of the transcripts. QuantSeq FWD HT is a high-throughput version with optional dual indexing to prevent sample mix-ups and to increase the number of available indices. The Read 1 linker sequence is located at the second strand synthesis primer, hence NGS reads are generated towards the poly(A) tail and directly correspond to the mRNA sequence. Read 2 would start with the poly(T) stretch, and as a result of sequencing through the homopolymer stretch the quality of Read 2 would be extremely low. It maintains strand-specificity and allows mapping of reads to their corresponding strand on the genome, enabling the discovery and quantification of antisense transcripts and overlapping genes. Additionally, it uses total RNA as input, hence no prior poly(A) enrichment or rRNA depletion is required. Library generation is initiated by oligo(dT) priming. The primer already contains an Illumina-compatible linker sequences. After first strand cDNA synthesis the RNA is removed, and second strand synthesis is initiated by random priming and DNA polymerase. The random primer also contains an Illumina-compatible linker

sequences. No purification is required between first and second strand synthesis. Second strand synthesis is followed by a magnetic bead-based purification step. The library is then amplified, introducing the sequences required for cluster generation.

Normally, high RNA quality is required in order to construct a good library for RNA-seq, the Lexogen kit, however, can construct libraries with lower RNA integrity as long as the 3' poly-A end is present.

### 2.12.2.2 Detailed Protocol for library preparation using the 3'mRNA-Seq kit

Initially 1  $\mu\text{g}$  of total RNA in a volume of 5  $\mu\text{L}$  was mixed with 5  $\mu\text{L}$  First Strand cDNA Synthesis Mix 1 (FS1) in a PCR tube. The mixture was mixed well by pipetting. Next, the RNA/FS1 mixture was denatured by heating it at 85°C for 3 min and then was cooled to 40°C where it was left to sit until the mastermix for the next step was prepared. The mastermix was prepared as follows.



The mastermix was pre-warmed for 3 min at 42°C.

The PCR tubes were next briefly centrifuged to collect all liquid at the bottom of the tubes and put back in the thermocycler and 10 $\mu\text{L}$  of the mastermix was added to each tube. The tubes then were incubated for 15 min.

### **2.12.2.3 RNA removal**

RNA removal was achieved by degrading the remaining RNA which was essential for efficient second strand synthesis. To do this 5  $\mu$ L of the RNA Removal Solution (RS) was added directly to the first strand cDNA synthesis reaction, mixed well by pipetting and incubated for 10 min at 95°C and then cooled to 25°C.

### **2.12.2.4 Second strand synthesis**

Second strand synthesis is performed to convert the cDNA library to dsDNA and is initiated by a random primer containing an Illumina-compatible linker at its 5'end. A reverse complementary sequence prevents the linker sequence from taking part in the hybridization. To the reaction 10  $\mu$ L of Second Strand Synthesis Mix 1 (SS1) was added and mixed well by pipetting. The reaction was then incubated for 1 min at 98 °C in the thermocycler and slowly cooled to 25 °C. Then the reaction was incubated for 30 min at 25 °C. A mastermix containing 4  $\mu$ L Second Strand Synthesis Mix 2 (SS2) and 1  $\mu$ L Enzyme Mix 2 (E2) was prepared and mixed well. Next 5  $\mu$ L of the mastermix was added per reaction mixed well and briefly centrifuged to collect all liquid at the tubes bottom. The libraries were incubated for 15 min at 25 °C.

### **2.12.2.5 Purification**

The double-stranded library was purified using magnetic beads to remove all reaction components. The Purification Module (PB, PS, EB) was equilibrated for 30 min at room temperature before use. For this step low-bind Eppendorf tubes were used instead to optimize the purification of the libraries and prevent any primer-dimer-artificial contamination. Per reaction 16  $\mu$ L of properly resuspended Purification Beads (PB) was added, mixed well, and incubated for 5 min at room temperature. The tubes were placed onto a magnetic plate, and the

beads were collected for 2 - 5 min or until the supernatant is completely clear. The supernatant was then discarded without disturbing the beads and removing the tubes from the magnetic plate. To each reaction 40  $\mu$ L of the Elution Buffer (EB) was added and the tubes were removed from the magnet and beads were properly resuspended and incubated for 2 min at room temperature. To the mixture 56  $\mu$ L of Purification Solution (PS) was added to reprecipitate the library, mixed thoroughly, and incubated for 5 min at room temperature. The plate was again placed onto a magnetic plate, and the beads were collected for 2-5 min or until the supernatant was completely clear. The supernatant was then discarded without disturbing the beads and removing the tubes from the magnetic plate. Next, 120  $\mu$ L of 80 % EtOH was added per reaction tube and incubated for 30 sec. The tubes were left in contact with the magnet as beads should not be resuspended during this washing step. The supernatant was removed and discarded, and this wash step was repeated twice. The tubes were then left on the magnet to air-dry for 5-10 min at room temperature. Then, 20  $\mu$ L of EB was added per reaction tube and incubated at room temperature for 2 min, next they were placed on the magnetic plate to let the beads collect for 2-5 min. Finally, 17  $\mu$ L of the clear supernatant was transferred into a fresh PCR tube carefully without transferring any beads.

#### **2.12.2.6 Library amplification**

The library is amplified to add the complete adapter sequences required for cluster generation and to generate sufficient material for quality control and sequencing. For single indexing i7 index was used only. At this point it is important to perform a quantitative (q) PCR assay to determine the optimal PCR cycle number for the RNA sample type used because this varies.

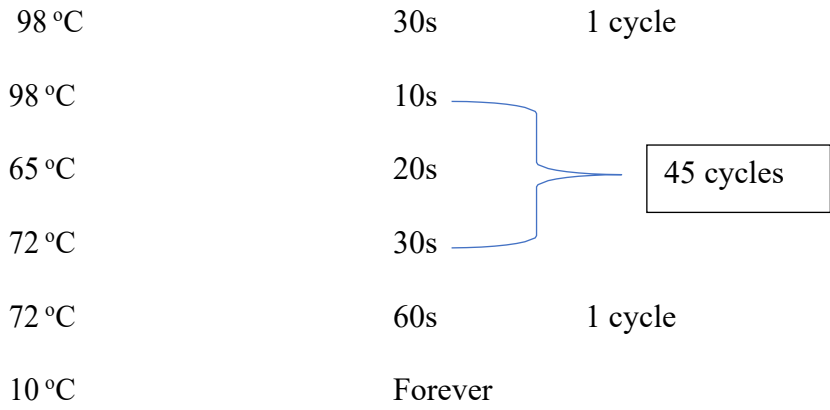
### 2.12.2.7 quantitative (q) PCR

The mRNA content and quality of total RNA affects the number of PCR cycles needed for the final library amplification step. It is crucial to perform a qPCR assay in order to determine the number of PCR cycles. Over- or under cycling may introduce bias in sequencing results (transcript abundance estimation and library quantification) and can only be avoided by optimising the PCR cycle number.

The PCR Add-on Kit from Illumina was used to perform the qPCR assays. The dsDNA library from the previous step was diluted by adding 2  $\mu\text{L}$  of EB to 17  $\mu\text{L}$  of library reactants. A qPCR mastermix was prepared as follows.

cDNA library	1.7 $\mu\text{L}$
PCR Mix (PCR)	7 $\mu\text{L}$
P7 Primer (7000)	5 $\mu\text{L}$
Enzyme Mix (E)	1 $\mu\text{L}$
2.5 x SYBR Green I	1.2 $\mu\text{L}$
<u>Elution Buffer</u>	<u>14.1 <math>\mu\text{L}</math></u>
Total	30 $\mu\text{L}$

Next, 28.3  $\mu\text{L}$  of the mastermix was added per reaction into 96-well PCR plates and 1.7  $\mu\text{L}$  of the library was added and mixed well by pipetting. A no-template control was included in the experiment. The PCR plate was then placed in the qPCR machine and 45 cycles of PCR with the following program was performed.



Using the amplification curves in linear scale, the value at which the fluorescence reaches the plateau was determined. Calculation of 50 % of this maximum fluorescence value was performed and determining at which cycle this value was reached. As the endpoint PCR will contain 10x more cDNA as compared to the qPCR, three cycles numbers were subtracted. This is then the final cycle number used for the endpoint PCR with the remaining 17  $\mu$ L of the template.

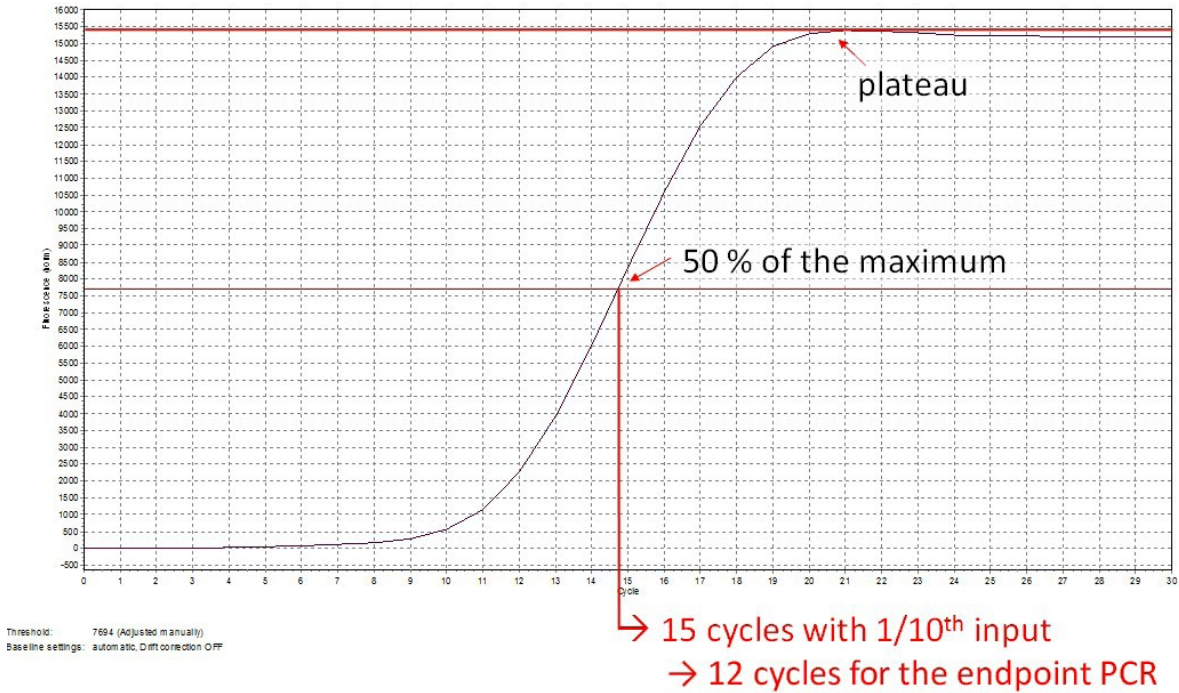


**Figure 2.12.2.7** Calculation of the number of cycles for endpoint PCR. Taken from Lexogen Quantseq user guide.

### 2.12.2.8 Single Indexing (i7 only)

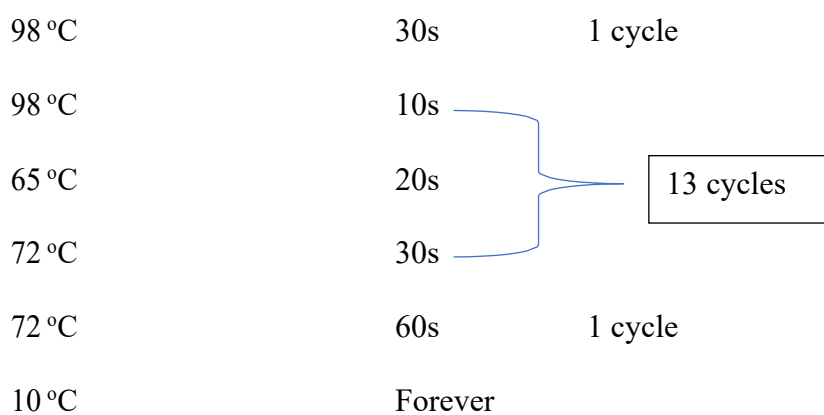
Single indexing PCR (i7 indices only) enables multiplexing and unique indexing of 96 libraries.

A PCR mastermix was prepared as follows.

PCR Mix (PCR)	7 $\mu$ L
Enzyme Mix (E3)	<u>1 <math>\mu</math>L</u>
	8 $\mu$ L

In 17  $\mu$ L of the eluted library 8  $\mu$ L of the mastermix was added followed by 5  $\mu$ L of the respective i7 index code. The reaction was mixed well by pipetting and briefly centrifuged to collect all liquid at the bottom of the PCR tube.

PCR cycles that were determined by qPCR were used to enrich the libraries as follows.



A second purification step is carried out as described above to remove PCR components that can interfere with the sequencing. Libraries are now finished and ready for quality control

(using 2100 Bioanalyzer, or QIAxcel), Qubit to measure the concentration and finally pooling libraries in an Eppendorf tube.

### **2.12.3 Whole genome sequencing of *Beauveria bassiana* strain EABb 92/11-Dm**

Extraction of high molecular weight DNA from fungal mycelia for long read sequencing was performed as follows. Lysis buffer was prepared by mixing buffer components A + B + C (2.5:2.5:1 + 0.1% PVP final concentration) which were heated to 64 °C for 30 min. Each extract was left at room temperature to cool and 17.5 mL was transferred into a 50 mL Falcon tube. Mycelia (500 mg) were crushed using a mortar and pestle in the presence of liquid nitrogen and resuspended in the lysis buffer. RNase T1 (10 µL; 10 Ku; OMEGA) was added to the mixture and left to incubate at room temperature for 30-50 min. Next, 200 µL of Proteinase K was added and left to incubate at room temperature for 30-50 min. The lysate was then cooled on ice for 5 min and 3.5 mL of 5M potassium acetate was added and incubated on ice for 5 min. The mixture was then centrifuged at 5000 x g for 12 min at 4 °C and the supernatant transferred to a fresh 50 mL Falcon tube containing 17.5 mL of phenol : chloroform : isoamyl alcohol (P/C/I) and mixed by inversion for 2 min. The mixture was centrifuged at 6000 x g for 10 min at 4 °C and the supernatant was again transferred to a fresh 50 mL Falcon tube containing 17.5 mL of P/C/I and mixed by inversion for 2 min. The mixture was then centrifuged at 5000 x g for 12 min at 4 °C and the supernatant was transferred to a fresh 50 mL Falcon tube containing 5 µL of RNase added before incubation for 30 min. After incubation 1.8 mL of 3 M sodium acetate was added and mixed by inversion, 18 mL of isopropanol was added next and mixed by inversion and left to incubate at room temperature for 10 min. The mixture was then centrifuged at 10,000 x g for 30 min at 4 °C. The supernatant was carefully discarded not to disturb the pellet, which contains the DNA and any precipitated material. Using a 1 mL cut pipette tip the pellet the remaining supernatant were transferred into a fresh

1.7 mL Eppendorf tube. The Eppendorf tube was then centrifuged at 13,000 x g for 5 min. The supernatant was removed with a pipette tip and the dislodged pellets washed by inversion in 1.5 mL 70% ethanol. This step was repeated four times. The pellet was air-dried for 7-10 min and 200  $\mu$ L of 10 mM Tris-HCl (pH 9) was added and left at room temperature for 3 h to dissolve the DNA. After 3 h the tube was gently flicked to mix and 200  $\mu$ L of TE buffer was added and left overnight at room temperature. Tubes were then transferred to a rotary shaker and incubated for 1 h at 28°C and shaken at 1400 rpm. The DNA was then cleaned using 1.8 vol of room temperature AMPure beads and quantified using NanoDrop and Qubit.

### **2.13 Generation of RNA standards curves representative for positive and negative strands of Lecanicillium virus-1 (LmV-1) genomic dsRNA**

To determine the coding strand of LmV-1 forward primers were used to transcribe cDNA from (-) strand RNA, while reverse primers were used to transcribe cDNA from (+) strand RNA. To ensure there was no contamination in the qPCR reactions negative controls containing no template RNA (NTC) and no reverse transcriptase enzyme (-RT) were included in the assays. Three biological replicates were investigated in MicroAmp 96-well plates (Applied Biosystems, USA). Real-Time qPCR assays were performed in the OneStepPlus Real-Time qPCR System (Applied Biosystems) using non-probe Power SYBR Green PCR Master Mix (Applied Biosystems) and the relative standard curve quantitation. To construct the standard curve and assess amplification efficiency serial dilutions of a pGEM-T Easy vector (Promega) based recombinant plasmid cDNA clone of LmV-1 dsRNA containing a fragment of the ORF predicted from the sequence of the virus ranging from 0.5-0.0000005 ng/ $\mu$ L were amplified by qPCR and Ct values were plotted against the logarithm value for each concentration of template.

## 2.14 Fungal spore counting

Spores of all isolates of *B. bassiana* were collected by first pouring 10 mL of PBS onto agar cultures in Petri dishes and resuspending the mycelia with a sterile scalpel blade. Spores from individual isolates were then diluted in water (1:100) prior to counting 7 $\mu$ L aliquots in two separate chambers of a FastRead 102 disposable plastic counting slide (Immune systems). These slides are disposable and consist of 10 chambers per slide each one containing 4x4 counting grids. Spore counting was performed under x400 microscope magnification and the average of 5/10 counting grids was taken.

The volume above each 4x4 grid was 10<sup>-4</sup> mL (0.1 $\mu$ l) and concentrations (counts/ml) were calculated using the equation:

$$\text{counts/ml} = \frac{\text{total counts} \times 10^4 \times \text{sample dilution (if any)}}{\text{number of complete 4x4 grids counted}}$$

## 2.15 Fungal spore germination assessment

### 2.15.1 Preparation of mycelia-free conidia suspension

Fourteen-day-old spores were harvested by adding 10 mL of PBS buffer and using a sterilised scalpel to liberate the spores from the surface of the media. The spores were filtered through two-layers of sterilised MiraCloth® and the flow-through was collected in a sterile 50mL Falcon tube. Next the spore concentrations were calculated using a haemocytometer as above and adjusted to the desired concentration by serial dilution.

### 2.15.2 Spore germination

The appropriate spore load was plated onto Petri dishes containing PDA and the spore suspension evenly distributed across the plate using a sterile glass rod. The plate was then incubated for 24 h at 25<sup>0</sup>C in complete darkness. Finally, the germlings were observed and counted. The percentage of the germlings and spore viability was determined as follows and compared to the haemocytometer count.

$$\left( X \text{ germlings}/100 \text{ spores per plate} \right)$$

### 2.16 Inoculation of *Tenebrio molitor* with *Beauveria bassiana* by direct injection or spraying

*T. molitor* larvae were injected with 5 $\mu$ L of a fungal spore suspension at a concentration of 1x10<sup>5</sup> spores/mL into the hemocoel, at the second visible sternite above the legs, using a Hamilton syringe with a 22s-gauge needle (Hamilton, USA). For each infection method different spore suspensions were used. For example, for direct injection the amount of the spores used for each isolate was 1x10<sup>5</sup> (total of 500 spores in 5  $\mu$ L), while for spray inoculation 1x10<sup>7</sup> spores were used.

Prior to injection the syringe was disinfected with three washes of absolute ethanol and finally with sterile distilled water. These washing steps were repeated between all the isolates injections but not for replicates, between replicates the syringe was washed with sterile distilled water only. Prior to injection larvae were anaesthetised by placing them on ice for 5 min. The syringe was inserted with caution so as not to kill the larvae. Using this procedure spore suspensions were directly injected into the hemocoel. Any damaged larvae, characterised by not responding to touch, were not used for further experiments and prior to autoclaving them,

they were euthanised by freezing at -20°C for 1 h. Control experiments included: (i) untouched larvae, and (ii) PBS injected larvae. Following injection, larvae were put into appropriately labelled Petri dishes. Furthermore, a piece of carrot was added in each petri dish (changed every 2 days) to keep the moisture levels normal and habitable for the larvae.

## **2.17 Transfection Assays**

### **2.17.1 Protoplast isolation**

Following harvest of a fresh fungal culture using liquid Czapek-Dox medium a suspension of conidiospores ( $1 \times 10^8$ ) was prepared and quantified using a haemocytometer. The spores were then inoculated into 50 mL of liquid Czapek-Dox medium and incubated for 32 to 48 h at 25°C with shaking (150 rpm).

Following incubation fungal mycelia were harvested on sterile Miracloth and washed thoroughly with sterile water. The mycelia were then resuspended in 10 mL of protoplasting solution (prepared just before use) in a sterile 50 mL flask loosely covered with aluminium foil. This solution was obtained by adding 0.32 g of *Trichoderma harzianum* lysing enzyme (Glucanex®, Sigma) and 0.1 g of *Trichoderma* sp. cellulase (Onozuka RS, Sigma) to 10 mL of 0.6 M KCl/citric acid solution and sterilised by filtration (0.2 µm Nalgene™, Thermo Scientific). The protoplasting solution was warmed for 10 min at 55°C in a water bath before being mixed with the mycelia in order to inactivate proteases. The mixture was incubated with shaking (100 rpm) at 30°C for 1.5-2 h. A small quantity was viewed under the microscope to check the state and number of protoplasts. When it was considered sufficient, the protoplast mixture was filtered through Miracloth and centrifuged in a swing out rotor (1,800 x g for 10 min at 4°C) to pellet the protoplasts.

The supernatant was removed, and the protoplast pellet was resuspended in 1 ml of 0.6 M KCl and transferred into a 1.5 mL Eppendorf tube. Protoplasts were then pelleted by centrifugation

(2,400 x g, 3 min). This step was repeated 3 times. The protoplasts were then resuspended in 1 ml of a 0.6 M KCl, 50 mM CaCl<sub>2</sub> solution and centrifuged again at 2,400 x g for 3 min. This step was repeated 2 times. After these steps, the protoplasts were counted under the microscope and their concentration was adjusted to 10<sup>7</sup>/mL in 0.6 M KCl, 50 mM CaCl<sub>2</sub> solution. At this stage, 0.5 mL of 25% polyethylene glycol (PEG), 100 mM CaCl<sub>2</sub>, 0.6M KCl, 10 mM Tris-HCl pH 7.5 and 15 µL of DMSO were added to 1 mL of protoplasts. The solution was then aliquoted (100 µL aliquots) and stored for 1h at -20°C before being transferred to -80°C.

### **2.17.2 Protoplast transfection**

Approximately 30 µg (10 µl) of dsRNA or VLPs were added to 100 µl of protoplasts and vortexed for 1 sec at maximum speed. Next, 50 µL of freshly shaken and filter sterilised 60% PEG 4000 solution held at room temperature was added to the mixture and the mixture was vortexed 4-5 times for 1 sec at maximum speed. It was then incubated on ice for 25 min before being transferred into a 2 mL microcentrifuge tube. After that, 1 mL of 60% PEG 4000 solution was added and the solution was mixed well by pipetting up and down 10 times prior to incubation at room temperature for 25 min. Transfection mixtures were finally spread onto solid Czapek-Dox media plus 10 g/L D-glucose plates. Plates were sealed using parafilm and incubated right-side up overnight at 25°C and then inverted the next day and kept at 25°C for 1-2 days.

### **2.18 Sequencing analysis**

There has been a continual increase in the accessibility of tools and well-known pipelines for building *de novo* transcriptome assemblies. Here, I used a *de novo* transcriptome assembler (TRINITY) which makes use of a greedy k-mer extension algorithm, De Bruijn graph and allele reconstruction. While this makes the assembly process computationally manageable, it

can lead to fragmented assemblies of a large number of contigs that are a subsequence of the original transcripts. Some of the reasons that lead to this fragmentation are sequencing errors, and sequence repeats that leads to gaps in coverage (Grabherr *et al.*, 2013).

## **2.18.1 RNA-Seq**

### **2.18.1.1 Quality control (QC) of sequencing reads**

An important first step before running TRINITY is to examine the base quality distribution, k-mer frequencies and adapter contamination by position in the read in order to understand the underlying quality of our data that are derived from high throughput sequencing pipelines.

Quality metrics were examined using FastQC.

### **2.18.1.2 Adapter trimming and low-quality bases from FastQ files**

The Illumina demultiplexing pipeline may incompletely remove adapter sequences, and when the insert sizes for a given read pair lead to overlaps between the sequenced bases, sequencing for one read can extend into the adapter of the other. These bases, as well as low quality bases should be trimmed prior to running Trinity. Trimmomatic is a flexible read trimming tool for Illumina NGS data and currently is one of the most commonly used for adapter and quality trimming.

### **2.18.1.3 Second FastQC run on the processed reads from the above steps**

A second FastQC step is important prior to running TRINITY. Ideally, there will be no trend in adapter contamination by cycle, and there will be consistency in k-mer distributions, GC content and no over-represented sequences.

#### **2.18.1.4 TRINITY, GeneMark and Augustus for genome assembly and gene prediction**

After trimming and QC the reads were aligned against the fungal public genome *Beauveria bassiana* ARSEF 2860 (ASM28067v1) using TRINITY. The resulting data were assembled into putative transcripts using PASA. The next step involved GeneMark, a gene prediction tool, that was used to refine parameters according to spliced read information. Subsequently, it produced a set of predicted genes which were *ca.* 6718 in number with no alternative splicing. So, in general we predicted genes based on public models then chose the best genes from the assembly and run them on the data. A second run of gene prediction was performed using Augustus.

Augustus is a tool for finding protein-coding genes and their exon-intron structure in genomic sequences. However, external (“extrinsic”) evidence from different sources such as transcriptome sequencing or the annotations of closely related genomes can be integrated in order to improve the accuracy and completeness of the annotation.

Transcriptome data in general can provide evidence about the location of introns and exons. Short read RNA-Seq was aligned individually to the target genome to obtain spliced read and junction gaps information using GSNAP. This information was provided to GeneMark and Augustus to assist with intron prediction. In the case of Augustus, a mild penalty was applied for intron predictions that were not supported by transcriptome data.

#### **2.19 Hygromycin B susceptibility of *Beauveria bassiana* isolates Naturalis and BotaniGard**

In order to develop a selection method based on hygromycin (HygB) for screening potential transformants of *B. bassiana* it is necessary to have knowledge of the sensitivity of the fungus to the antibiotic. To this end two commercial *B. bassiana* isolates (Naturalis and BotaniGard) were directly screened for sensitivity to HygB using a range of concentrations of the antibiotic. Conidial suspensions of the two *B. bassiana* isolates were spread on Czapek-Dox agar medium

containing HygB (0.001-150 mM) Fungal growth was observed at 3, 5 and 7 days after spreading. The same protocol was used for the rest of the antibiotics (Benomyl, sulfonyleurea). In a second HygB screening procedure an overlay technique was used. Here 20 mL of Czapek-Dox agar medium containing HygB of different concentrations was poured into the plates. Conidial suspensions of the two isolates were spread on the plates and left to grow at 25°C overnight. The next day the plates were overlaid with an equal volume of Czapek-Dox agar medium containing HygB. Again, fungal growth was observed at 3, 5 and 7 days post inoculation.

# **Chapter 3:**

## **Identification and characterization of mycoviruses in fungi**

Mycoviruses infect fungi and are found in all major fungal families. They are highly host specific due to their incapability of extracellular transmission; however, phylogenetic analysis supports the occasional occurrence of horizontal transmission between species (Ghabrial & Suzuki 2009; Filippou *et al.*, 2018). Therefore, to investigate the presence and diversity of mycoviruses in large panels of entomopathogenic and human pathogenic fungi, mostly from Spain, Denmark, The Netherlands and Portugal a total of 216 isolates belonging to the genera *Beauveria*, *Metarhizium*, *Lecanicillium*, *Purpureocillium*, *Isaria*, *Paecilomyces*, and *Aspergillus* were screened for the presence of dsRNA elements. Twelve Spanish *B. bassiana*, one Portuguese *A. fumigatus* and two Dutch *L. muscarium* isolates were found to harbour mycoviruses. All identified mycoviruses in Spanish isolates belong to three previously characterised species, the officially recognised *Beauveria bassiana* victorivirus 1 (BbVV-1) and the proposed *Beauveria bassiana* partitivirus 2 (BbPV-2) and *Beauveria bassiana* polymycovirus 1 (BbPmV-1). The mycovirus discovered in the Portuguese *A. fumigatus* isolate was found to contain three dsRNA elements, comprising the genome of a strain of *Aspergillus fumigatus* partitivirus 1 (AfuPV-1) previously thought to contain only the two largest dsRNA elements. Furthermore, the mycovirus discovered in the two Dutch *L. muscarium* isolates has one unique dsRNA segment and sequence analysis of the element revealed an open reading frame encoding a protein of 158 aa. Therefore, in this Chapter I have documented the sporadic appearance of mycoviruses after screening 216 isolates which revealed a total of fourteen putative mycoviruses. Furthermore, the chapter describes the recombination of viral genomes leading to population diversity in mycoviruses found in the Spanish isolates. Also, phylogenetic analysis of the six dsRNA segments of *Beauveria bassiana* Polymycovirus - 3 (BbPmV-3) revealed the close relationship to *Beauveria bassiana* Polymycovirus - 2 (BbPmV-2) and the distant relationship of both to *Beauveria bassiana* Polymycovirus - 1 (BbPmV-1) suggesting a common ancestor between BbPmV-2 and

BbPmV-3 emerged *via* the formation of new and distinct species during evolution.

### **Aims and scope**

The aim of Chapter 3 is to document the assessment of the presence and diversity of mycoviruses in entomopathogenic and human pathogenic fungi *Beauveria*, *Purpureocillium*, *Metarhizium*, *Isaria*, *Lecanicillium*, *Aspergillus* and *Paecilomyces*, isolated in Portugal, Spain, and Denmark. The chapter also describes completing the full sequences of the viral genomes of three viruses discovered in: 1) *B. bassiana* Polymycovirus -3 (BbPmV-3), 2) *L. muscarium* virus -1 (LmV-1) and, 3) *A. fumigatus* partitivirus-1A (AfuPV-1A). Data analysis and sequencing of the mycoviruses provided us with useful information about population structure and dynamics, transmission and pathogenicity. The sections of this chapter concerning *Aspergillus fumigatus* and *Lecanicillium muscarium* were undertaken as developmental technology in the PhD and were performed prior to extended investigations with *Beauveria bassiana*. It is important to clearly state that the entire genome of BbPmV-1 was sequenced by Dr Ioly Kotta-Loizou (Kotta-Loizou & Coutts, 2017), and equally important to highlight that the four largest dsRNA segments (dsRNA1 to 4) of BbPmV-3 have been sequenced by Dr. Ioly Kotta-Loizou and John Daudu, while I have sequenced the remaining two smaller dsRNA segments (dsRNA 5 and 6) to obtain the full viral genome.

### **3.1 Completion of the sequence of the *Aspergillus fumigatus* partitivirus 1 genome**

The increase in number of immunocompromised patients suffering with severe invasive fungal infections such as invasive aspergillosis (IA) has led to the necessity of new antifungal agents (Doffman *et al.*, 2005). The morbidity numbers of IA patients are increasing globally despite the use of antifungals such as azoles. Resistance to azoles is alarmingly increasing against the common agent of IA *Aspergillus fumigatus* (Fukuda *et al.*, 2003; Snelders *et al.*, 2008).

Likewise, antibacterial resistance is alarmingly increasing forcing scientists around the world to find alternative methods. Bacteriophages are viruses that selectively infect bacteria and replication can either be lytic (causing cell lysis) or lysogenic. Furthermore, they are able to induce cell lysis were successfully used in pre-clinical studies against *Pseudomonas aeruginosa*, *Escherichia coli*, and *Klebsiella pneumoniae* (Bodier-Montagutelli *et al.*, 2017; Waters *et al.*, 2017).

Similar to bacteriophages, mycoviruses can selectively infect fungi resulting in different phenotypic changes such as hypovirulence which has been used to control chestnut blight. However, mycoviruses are incapable of extracellular transmission which is an essential feature for them to be used as therapeutic agents. Though, recently a ssDNA mycovirus capable of extracellular mode of transmission was isolated from *Sclerotinia sclerotiorum* and termed (Sclerotinia sclerotiorum hypovirulence-associated DNA virus 1 ;SsHADV-1; Yu *et al.*, 2013). Many mycoviruses were discovered in *Aspergillus* spp. and one of them *Aspergillus fumigatus* partitivirus -1 (AfuPV-1) was found to cause visible phenotypic alteration such as reduced growth and pigmentation (Elias *et al.*, 1996). Sadly, this virus is incapable of extracellular transmission. A Portuguese isolate of *A. fumigatus* was found to contain three dsRNA elements ranging in size from 1.1 to 1.8 kbp and comprising the genome of a strain of *Aspergillus fumigatus* partitivirus 1 (AfuPV-1A; Filippou *et al.*, 2020) previously thought to contain only the two largest dsRNA elements. The strain of AfuPV-1 was isolated, cloned, and sequenced and termed AfuPV-1A. The sequences of the two larger dsRNA were 98-99% identical to that of AfuPV-1. These results confirmed that AfuPV-1A is a strain of AfuPV-1 which can support the replication of a third genomic component termed dsRNA3 and that smaller dsRNAs components can be apparently lost and recovered during partitivirus infections.

Normally partitiviruses possess two dsRNA genome segments (1.3-2.5 kbp in length)

containing respectively a single open reading frame (ORF; Vainio *et al.*, 2018). DsRNA 1 encodes the RdRP and dsRNA 2 encodes the capsid protein (CP; Vainio *et al.*, 2018). The sequence of the smallest dsRNA element revealed an open reading frame encoding a protein of unknown function similar in size and distantly related to elements previously identified in other members of the family *Partitiviridae* (Figure 3.1a).

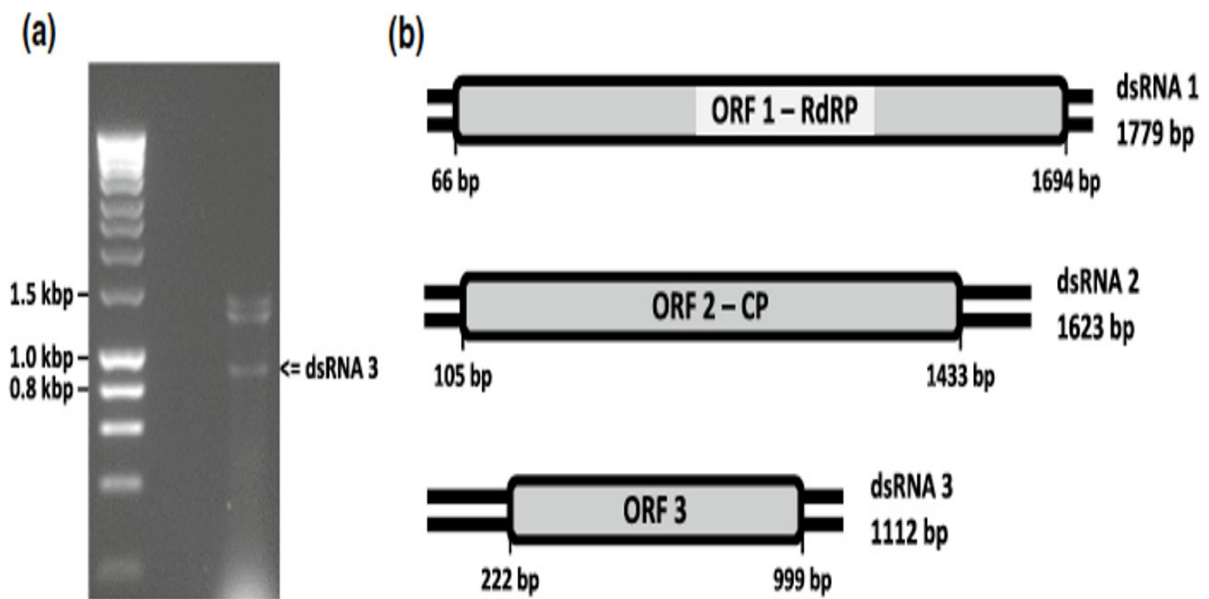


**Figure 3.1a** Genomic organisation of AfuPV-1A and comparisons of the amino acid sequences of putative proteins encoded by dsRNA3 elements of representative partitiviruses. (a) Agarosegel electrophoresis of dsRNA elements extracted from *Aspergillus fumigatus* isolate 12/43. Molecular sizes are indicated on the left with numbers. (b) Schematic representation of the genomic organisation of AfuPV-1A. Taken from Filippou *et al.* (2020).

*A. fumigatus* 12/43 was originally isolated from bronchial secretions of a hospitalised patient in Portugal (Sabino *et al.*, 2014). This was the only *A. fumigatus* isolate found to harbour dsRNA elements following screening of 48 isolates in total: 12 environmental, 12 avian, 12 from cystic fibrosis patients and 12 including 12/43 from non-cystic fibrosis patients (Sabino *et al.*, 2014; 2015; 2019). These isolates were courtesy of the National Institute of Health Dr. Ricardo Jorge, Lisbon, Portugal provided by Dr. Raquel Sabino, in the form of spores and were re-grown at 25°C for 6 to 7 days in liquid Czapek-Dox complete medium with shaking. Cultivation and screening of the isolates (sections 2.1 and 2.2) was carried out in a biosafety level -2 (BSL-2) laboratory at Imperial College under the supervision of Dr Ioly Kotta-Loizou. Genome organisation of AfuPV-1A dsRNAs 1, 2 and 3 revealed a single ORF (Figure 3.1a; grey boxes) flanked by 5'- and 3'-UTRs (Figure 3.1a; black lines). The dsRNA1 is 1779 bp long and contains an ORF that encodes a putative RdRP with a molecular mass (*Mr*) of 63 kDa, while dsRNA2 is 1623 bp long and contains an ORF that encodes a putative CP with a (*Mr*) of 48 kDa. Both were 99% and 98% identical to the sequence of AfuPV-1 dsRNA1 and dsRNA2 respectively. Finally, dsRNA3 is 1112 bp long and contains an ORF that encodes a protein of unknown function with a (*Mr*) of 29 kDa.

The sequence of dsRNA3 was completed by the use of sequence specific primers, genome walking, and RLM-RACE (Sections 2.3 and 2.8; Coutts & Livieratos, 2003). To further investigate AfuPV-1A dsRNA3 role in virus replication, reverse genetic methods could be applied in the future.

With the recent interest in the use of bacteriophages as an alternative to antibiotics increasing everyday mycoviruses against resistant strains of *A. fumigatus* seems to be the logical next step. A case study of recurrent candidemia, resistance to azole, described by Posteraro *et al.* (2006) illustrates the necessity of new alternative antifungal agents.

### 3.2 Screening of fungal isolates for dsRNA mycoviruses and population studies

Initially eight *Metarhizium* spp. isolates and three *B. bassiana* isolates were screened for the presence of mycoviral dsRNA using a small-scale isolation procedure (Section 2.2) but none were infected with mycoviruses. Subsequently a larger panel of entomopathogenic isolates including 61 isolates of *Metarhizium brunneum*, two isolates of *Metarhizium majus* and nine isolates of *Metarhizium robertsii* were screened for dsRNA elements but again none of the 72 isolates were infected. All of these isolates were collected in Denmark and were provided by Dr Nicolai Vitt Meyling, University of Copenhagen. A third screen was performed and investigated 78 Spanish isolates including representative species from genera *B. amorpha*, *B. bassiana*, *B. varroae*, *Metarhizium brunneum*, *Metarhizium guizhouense*, *Metarhizium robertsii*, *Paecilomyces marquandii* and *Purpureocillium lilacinum* provided by Dr. Inmaculada Garrido-Jurado and Prof. Enrique Quesada-Moraga from the University of Cordoba in Spain. Twelve *Beauveria bassiana* isolates and one *Lecanicillium muscarium* isolate were found to contain dsRNA elements (Appendix Part B Table S6.1a). Surprisingly, none of the *Metarhizium* spp., *Purpureocillium lilacinum* or *Paecilomyces marquandii* isolates appeared to contain dsRNA elements. The geographical location of the virus-positive isolates along with the types of mycoviruses infecting them is shown below.

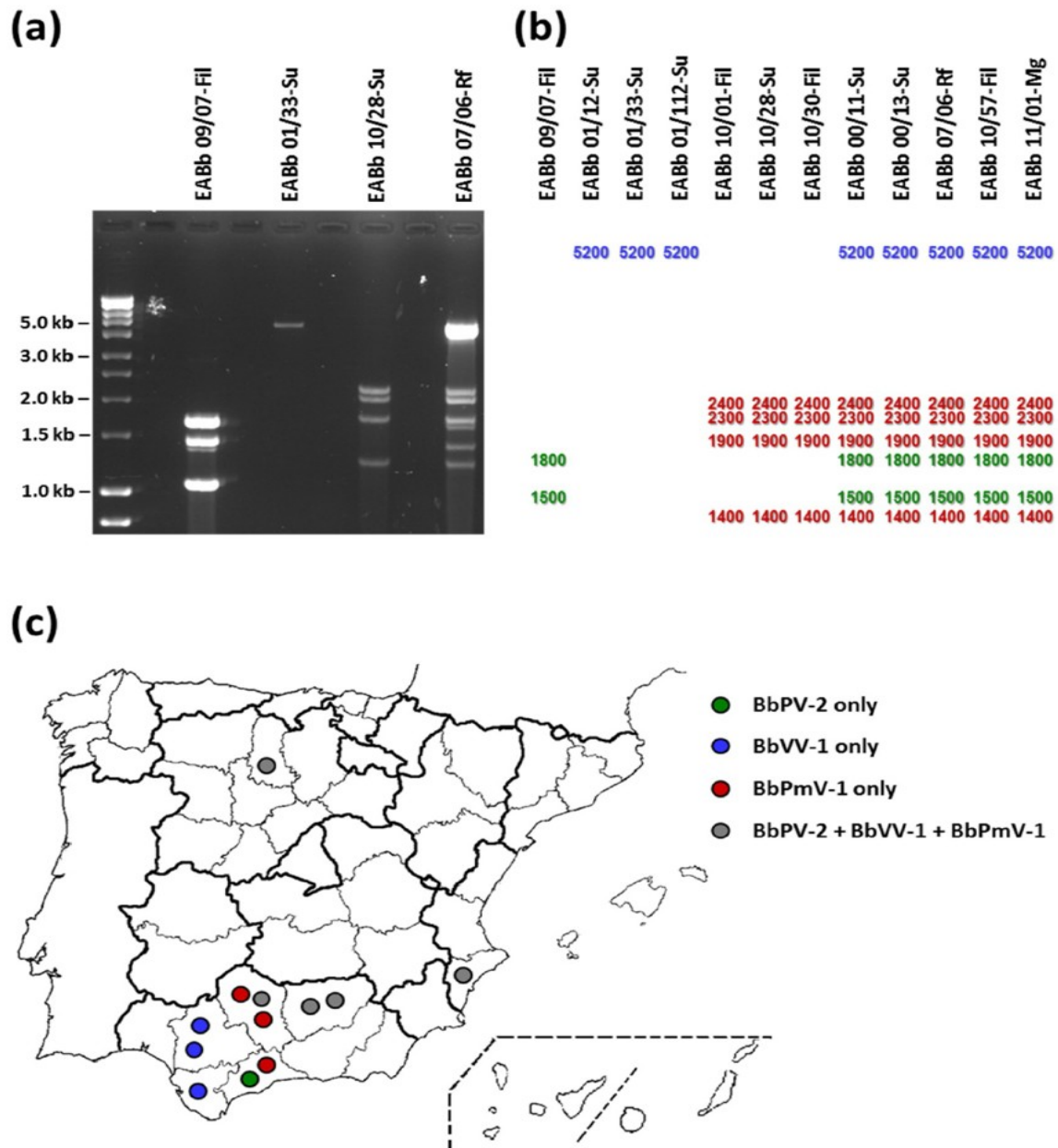


**Figure 3.2a** A) 1% (w/v) agarose gel electrophoresis of dsRNA elements isolated from four *Beauveria bassiana* isolates, representative of the four different electrophoretic profiles. B) Schematic representation of the electrophoretic profiles of dsRNA elements isolated from 12 *Beauveria bassiana* isolates and their relative sizes, green for members of the family *Partitiviridae*, blue for members of the family *Totiviridae* and red for members of the proposed family *Polymycoviridae*. C) Geographical distribution of mycoviruses found in Spanish *Beauveria bassiana* isolates. Taken from Filippou *et al.* (2018).

### **3.2.1 Mixed infections of *Beauveria* isolates with up to three different mycoviruses**

Following agarose electrophoresis of the purified dsRNA elements from all *Beauveria* isolates, four distinct electrophoretic profiles were noted (Figure 3.2a). It was observed that one isolate harbour a member of the family *Partitiviridae* which consists of two dsRNAs 1-2 kbp in size; three isolates found to harbour a sole dsRNA *ca.* 5 kbp in size, possibly belongs to the family of *Totiviridae*, while a banding pattern similar to the one of the proposed family *Polymycoviridae* was observed in three isolates. The rest of the isolates harbour a combination of the mycoviruses above suggesting the presence of multiple mycovirus infection (Appendix Part B Table S3.2.1). Molecular characterisation experiments revealed the presence of quasispecies, highly similar but not necessarily identical (Figure 3.2a; Appendix Part B Table S3.2.2) strains of mycoviruses mentioned before. According to Andino & Domingo (2015), “viral quasispecies are defined as collections of closely related viral genomes subjected to a continuous process of genetic variation, competition among the variants generated, and selection of the most fit distributions in a given environment”. Viral RdRPs are prone to errors, this is evident in all RNA viruses, and can cause significant mutations resulting in a population of mutants instead of identical viral genomes also known as quasispecies (Domingo & Perales, 2018). This is the first report of viral quasispecies in mycoviruses (Filippou *et al.* 2018).

### **3.2.2 Evidence of vertical and horizontal transmission of mycoviruses**

Phylogenetic analysis was performed to determine the evolutionary relationships for BbVV-1-like, BbPV-2-like and BbPmV-1-like strains, due to the similarity of their viral sequences three phylogenetic trees were constructed (Appendix Part B Figure S3.2.1). It has been observed that mycoviruses in the fungal isolates with triple infections form clusters and are closely related to each other than to any of the other quasispecies investigated. To confirm this observation p-distance matrices were used (Appendix Part B Figure S3.2.2). Subsequently,

their genomes are extremely similar, this demonstrates that these three mycoviruses are transmitted simultaneously as a complex, either vertically or horizontally. To understand the mode of transmission, the evolutionary relationships among the *Beauveria* isolates was examined and a phylogenetic tree was constructed using the ITS sequences (Section 2.10; Appendix Part B Figure S3.2.3). ITS sequences revealed very few substitutions between nucleotides demonstrating a very close evolutionary relationship between the *Beauveria* isolates. Interestingly, isolates harbouring triple infections no longer clustered together. This is realistic in the case of one horizontal transmission event for the three viruses between more distantly related isolates, whereas in the case of closely related isolates vertical transmission is the plausible explanation (Filippou *et al.* 2018).

### **3.3 A novel mycovirus discovered in the entomopathogenic fungus *Lecanicillium muscarium* contains a single, unique double-stranded RNA**

Mitosporic fungi such as *Beauveria bassiana*, *Lecanicillium* spp. (previously classified as the single species *Verticillium lecanii*), *Metarhizium anisopliae* and *Isaria fumosorosea* (previously classified as *Paecilomyces fumosoroseus*) are ubiquitous entomopathogens that have been commercially developed as biopesticides (Kabaluk *et al.*, 2005; de Faria & Wraight, 2007). Fungi in the genus *Lecanicillium* are important entomopathogens and some isolates are also active against phytoparasitic nematodes or fungi, suggesting that they have the potential to be developed as multipurpose microbial control agents of pest arthropods, plant parasitic nematodes and plant pathogens (Benhamou & Brodeur, 2000, 2001; Miller *et al.*, 2004).

*Lecanicillium* spp. have a broad host range and have been successfully isolated from a range of insect hosts (Zare & Gams, 2001). Furthermore, *Lecanicillium* spp. follow the usual pathogenesis pathway of entomopathogenic mitosporic fungi; conidia adherence on the host cuticle then conidial germination; insect cuticle penetration; blastospore production within the

hemocoel; mycelial growth and invasion of tissues causing host death; and finally, production of conidia on the surface of the cadaver (mycosis) (Askary *et al.*, 1999). Moreover, some *Lecanicillium* isolates are capable of producing toxic metabolites *in vitro*, which may be connected to the ability of the fungus to overcome its host (Claydon & Grove, 1982; Gindin *et al.*, 1994).

Eleven isolates of *Lecanicillium muscarium* obtained from the Westerdijk Fungal Biodiversity Institute, The Netherlands were screened for the presence of dsRNA elements using a small-scale dsRNA extraction protocol (Section 2.2). Two isolates, 143.62 and 102071, were both found to possess an identically sized single dsRNA element (Fig. 3.3a) which was nominated *Lecanicillium muscarium* virus-1 (LmV-1) and was characterised further.

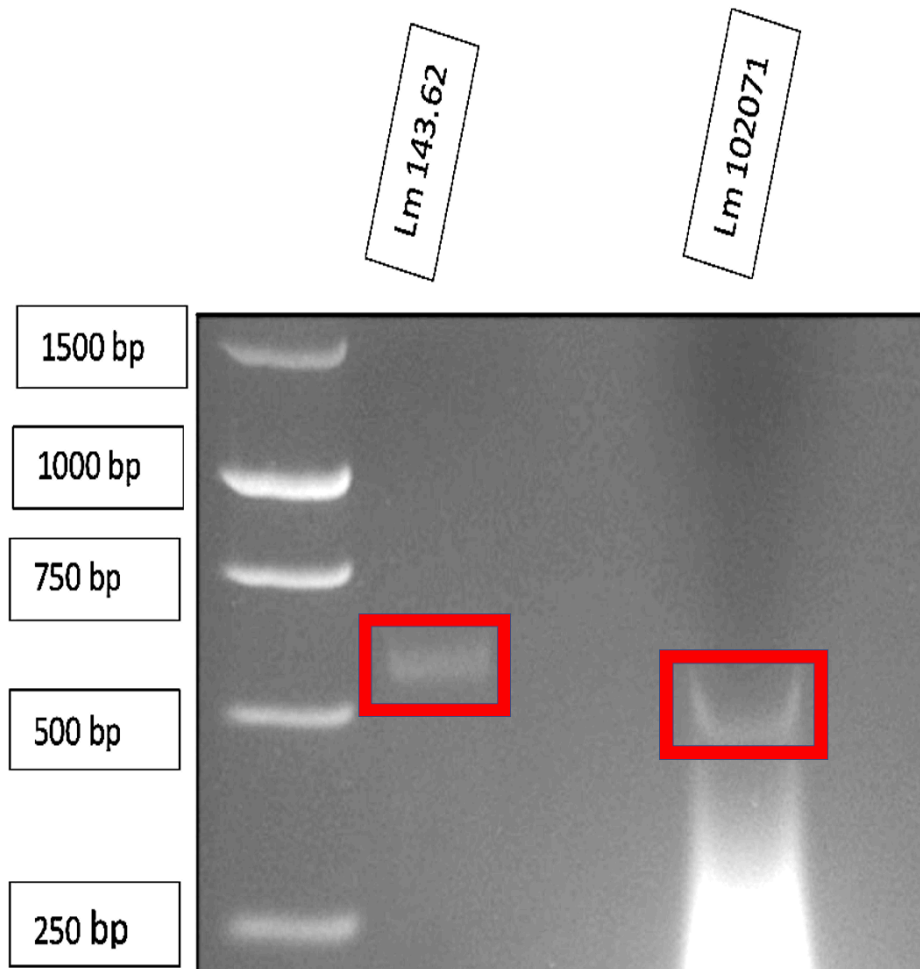


**Figure 3.3a** Agarose gel electrophoresis of dsRNA elements present in both *Lecanicillium muscarium* 143.62 and 102071 isolates (circle in RED). The GeneRuler 1 kbp DNA Ladder (Promega) used as a marker is shown to the left.

### **3.3.1 Northern blot analysis of LmV-1 dsRNA isolated from *Lecanicillium muscarium***

Northern hybridisation analysis (Section 2.9) was performed to verify the authenticity of the cDNA clones generated from purified LmV-1 dsRNA. RNA transcripts were produced from representative LmV-1 cDNA clones using transcription labelling of RNA with digoxigenin (DIG)-11-dUTP (Roche Applied Science, Germany), enabling the detection of dsRNA (Section 2.9.5). Hybridisation analysis showed strong signals for a single dsRNA with individual specific probes confirming that all the cDNA clones were generated from LmV-1 dsRNA (Figure 3.3b).

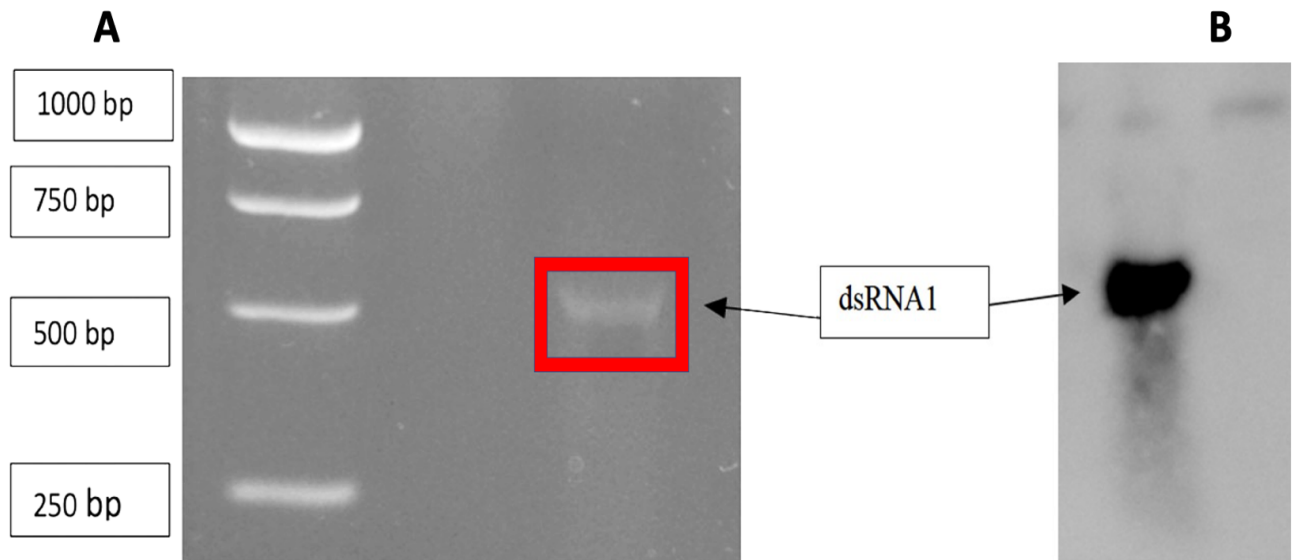


**Figure 3.3b** Northern hybridisation of LmV-1 dsRNA; (a) Purified dsRNA (circled in RED) was separated in a 1% agarose gel in 1xTAE alongside a GeneRuler 1 kbp DNA Ladder (Promega) as a marker. (b) The gel was denatured, blotted onto nylon membrane, and probed with a labelled cDNA clone of LmV-1 dsRNA.

### **3.3.2 Sensitivity of LmV-1 dsRNA to DNase, RNase A and RNase III**

The dsRNA nature of LmV-1 isolated from two isolates of the fungus was confirmed by its resistance to DNase 1 (Section 2.2.3) and to RNase A (Section 2.2.4) treatment in high salt reaction buffer and its sensitivity to RNase III and RNase A in low salt reaction buffer.

Phenol/chloroform-treated dsRNA extracts were subsequently digested with DNase I (digests ssDNA and dsDNA) and S1 nuclease (digests ssDNA and ssRNA). The digests were analysed by 1% agarose gel electrophoresis (Section 2.2.5) showed that the elements were resistant to DNase I and S1 nuclease, suggesting that these elements are dsRNA molecules (Figure 3.3b).

### **3.3.3 Sequencing of LmV-1 dsRNA using an RLM-RACE protocol**

Efforts were made to generate cDNA clones of LmV-1 dsRNA using random-primed PCR (rPCR; Section 2.7) amplification but these proved unsuccessful probably because of the size of the dsRNA under investigation. So, in order to obtain the complete sequence of LmV-1 dsRNA RLM-RACE was conducted using modified Lig primers (Section 2.8). The RLM-RACE amplicons generated from the dsRNA of both isolates were ~ 600 bp in size (Figure 3.3c). All amplicons were cloned into the pGEM-T Easy vector (Section 2.4). At least 3 RLM-RACE clones of each amplicon were sequenced. Analysis of the sequencing results was performed as indicated in Chapter 3 section 3.3.4.

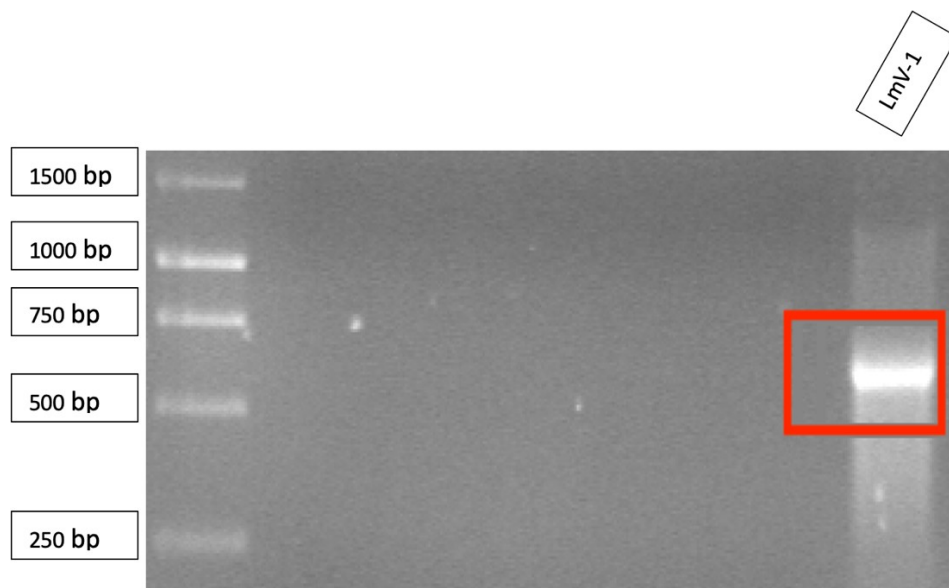
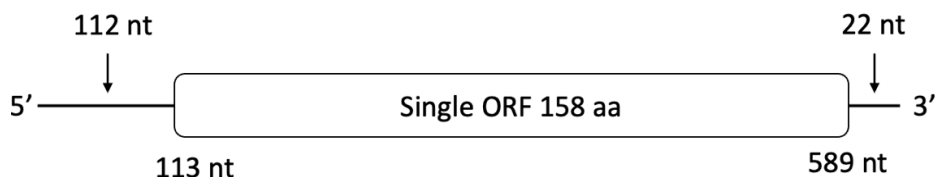


**Figure 3.3c** Agarose gel electrophoresis showing the PCR products generated by RLM-RACE. RLM-RACE of LmV-1 dsRNA; Lane 1, the amplicon produced from RLM-RACE amplification of *Lecanicillium muscarium* 143.62 dsRNA. GeneRuler 1kbp DNA Ladder (Promega) was used as marker.

### **3.3.4 The genomic sequence of LmV-1 dsRNA1**

The complete sequence of LmV-1 dsRNA 1 revealed that the genome comprised 611 bp with 5' and 3' untranslated regions (UTRs) 112 and 22 bp in length respectively (Figure 3.3d) with a GC content of 48.93%. The UTRs flank a single ORF1 which encodes a putative protein of 158 amino acid residues with a molecular mass of 17.42 kDa. Furthermore, searches using public databases including PROSITE, the Pfam protein database and the Conserved Domain database revealed no match to any accessed protein, a BLASTX search revealed no match to any protein available on the database. Also, no signal peptide or trans-membrane helix were predicted using SignalP 4.0 (Petersen *et al.*, 2011) and TMHMM (Krogh *et al.*, 2001). Further examination of LmV-1 dsRNA 1 would be interesting to confirm its function.

**A) Genome organisation of LmV-1 dsRNA1**



**B) Complete sequence of LmV-1 dsRNA1 (611 nt)**

AAGAAATATAGAGAGAACAGAAAACAACGCCCTCTTTATATATCTACAACCTAACTCAAC  
AAACTGAAACCAGTTCGCACTGAGAACGATCACCGTCACCCCTAAAGGCAAGATGATGAT  
CCGTATAAGTGTTCTGGCTGCTTTGGCGTCTGTATGTATAGTCAGCTCTGCAGCCGAGAC  
ATTAAGTGAAGTGCCTCACTACAACCTGTACCCAAACGGTACACTATTGTATAGGCAGAC  
ACTCAAGGTTAAGATGCCACACACGGCTCGCGGCAGTAACCGCAGATCAGGGTGCTTCTA  
CAACACCTATACCGACGAAGGCAAAGATTACTGCCCCAGCGAGGGATATAGGCACTTCTC  
GGGCGATGCCGGTGAATGCATACCGTATGGCACTTACGGCGTCCGGTAGTGCAATGTTTGT  
CCCGGATGGCGACAATTGTAACACAAACAATGACGCGTACTACCAGGACACATACTCAAG  
TGGTGATGGGCAATGTTTCGAGGGGACCTTTCACGCGAAATTTGACGGTCCGACGTGCAT  
AACCACACATCACCACACTGGTGCAGTGAAGCTCTTCAACTTCAATTGAAGATAAAGGGC  
AGGCGGGGAGC

**C) Amino acid sequence encoded from ORF1 (17.42 kDa)**

MMIRISVLAALASVCIVSSAAETLTEVPHYNLYPNGTLLYRQTLKVKMPHTARGSNRRSGCFYNTYT  
DEGKDYCPSEGYRHFSGDAGECIPYGTYGVSAMFVPDGDNCNTNNDAYYQDTYSSGDGQCFEGTFH  
AKFDGPTCITTHHHTGAVKLFNFN

**Figure 3.3d** Diagrammatic representation of the genome organisation of LmV-1 dsRNA 1 (a); (b) nucleotide sequence and (c) amino acid sequence of LmV-1 dsRNA. Start and stop codons are shaded in red.

### **3.3.5 Quantitative polymerase chain reaction (qRT-PCR)**

Real-time quantitative (qRT-PCR) is essential for the detection and quantification of RNA targets. This method is straightforward following the reverse transcription of RNA to cDNA. Since RNA virus genomes must be efficiently copied in the cell that they infect, qPCR assays are important tools for the detection and quantification of replicating virus. This method is based on the detection of sequenced-specific DNA probes, consisting of oligonucleotides that are labelled with a fluorescent reporter, by a machine that monitors the amplification in real time and a suitable software for analysis (Lee & Connell 1993). The principle of qRT-PCR is that the higher the level of target RNA present at the beginning of the experiment the sooner a significant increase in fluorescence is observed. Most of the dsRNA viruses have a segmented genome along with an RdRP that transcribes each dsRNA molecule into an mRNA. Consequently, the amount of cDNA quantified during qPCR must accurately reflect amounts of a specific viral RNA strand in the reverse transcription reaction (Plaskon *et al.*, 2009; Section 2.13).

### **3.3.6 Generation of RNA standards representing positive and negative strands of genomic RNA**

Standard curve analysis was carried out to demonstrate the decreasing levels of expression according to the serial dilutions of the template which gives a good estimate of the PCR amplification efficiency (Section 2.13). Serial dilutions between 0.5 ng/ $\mu$ L to 0.0000005 ng/ $\mu$ L were prepared using a plasmid containing a segment of the LmV-1 dsRNA genome. Ct values were plotted against the logarithm of the starting quantity of template for each dilution and the efficiency of the amplifications was calculated (Kubista *et al.*, 2006; Appendix Part B Table S3.3.7). Furthermore, *ca.* 100 ng of cDNA for each replicate was used in each qPCR reaction.

Also, appropriate negative controls containing no template (NTC) and no reverse transcriptase enzyme (-RT) were subjected to the same procedure to detect any possible contamination.

Three biological replicates were used in MicroAmp 96-well plates (Applied Biosystems, USA). To generate strand-specific standard curves for qPCR, (+) and (-) strand RNA was transcribed *in vitro* from a plasmid containing a portion of LmV-1 dsRNA. The plasmid was produced by ligating a fragment of the viral ORF into the pGEM-T Easy vector (Promega; Section 2.4). The Real-Time qPCR assays were performed in the OneStepPlus Real-Time qPCR System (Applied Biosystems) using non-probe Power SYBR Green PCR Master Mix (Applied Biosystems) and the relative standard curve quantitation (Section 2.13).

Finally, forward primers were used to transcribe cDNA from (-) strand RNA, while reverse primers were used to transcribe cDNA from (+) strand RNA (Appendix Part B Table S3.3.7). The amount of LmV-1 (+) strand RNA in the sample was calculated from standard curves. The standard curve generated for the assay using LV-F and LV-R primers had a slope of -3.374, and amplification efficiency (Eff%) of 97.872% (Appendix Part B Table S3.3.7). The qPCR results indicate higher relative levels of (+) strand rather than (-) strand indicating that the virus is naturally (+) stranded (Figure 3.3c).

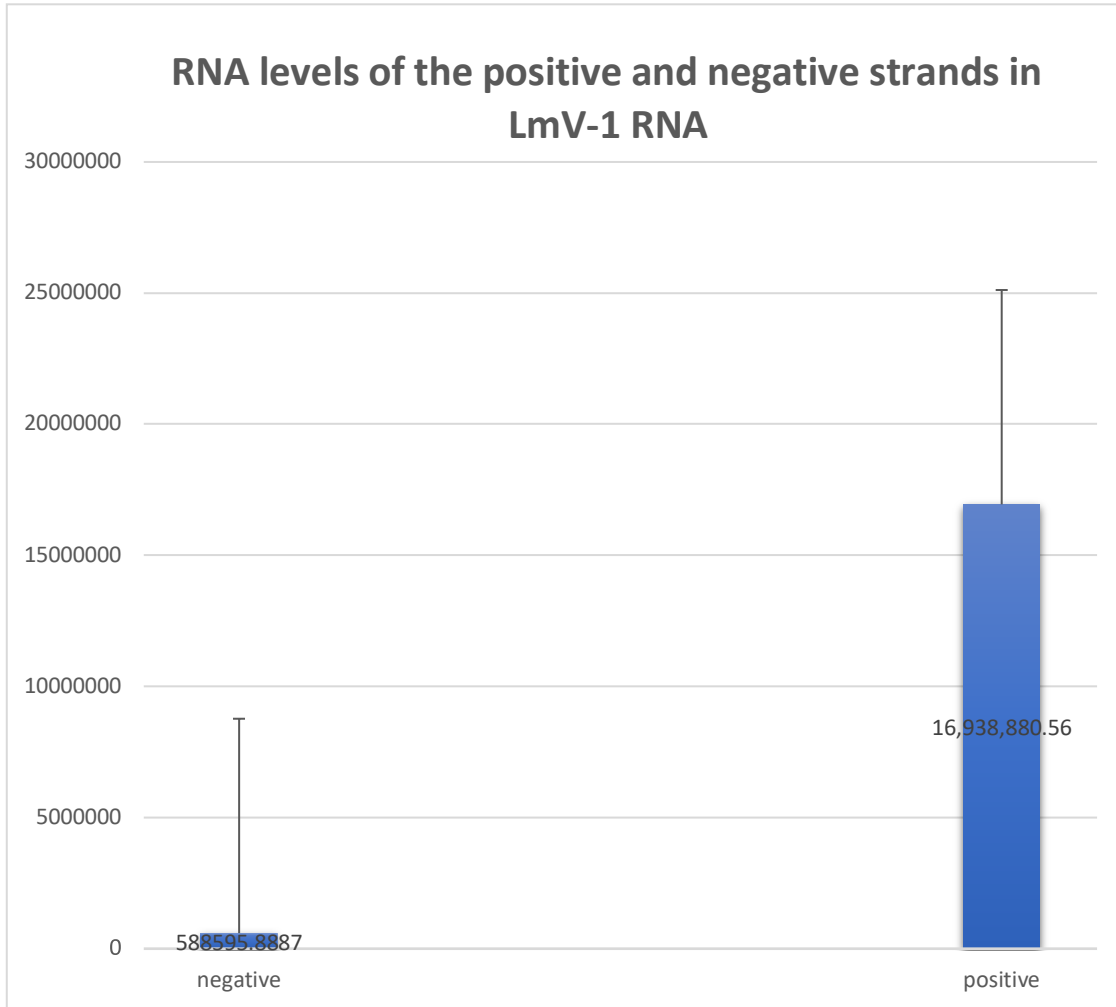


**Figure 3.3e** Relative RNA levels of the positive and negative strands of LmV-1 as shown by RT-qPCR amplification. At least three independent replicates were performed in triplicate and error bars represent standard deviation.

Conclusively, in order to understand the molecular mechanism of RNA replication as well as the role of viral and host factors during virus replication, it is necessary to determine whether the virus is positive or negative stranded (Bustin & Mueller, 2005).

### **3.3.7 Time course study of viral dsRNA levels related with fungal growth**

The biomass of isolate *L. muscarium* 143.62 grown in liquid Czapek-Dox CM was measured daily over 7 days in order to investigate the quantity of LmV-1 dsRNA synthesised with respect to fungal development. Here the LmV-1 dsRNA copy number appears to increase during the early time points of fungal growth in comparison to later time points (Figure 3.3f). As demonstrated by Kotta-Loizou *et al.* (2017) this observation may indicate differences in the replication cycles of encapsidated mycoviruses such as partitiviruses as compared to unencapsidated viruses, which LmV-1 appears to be.

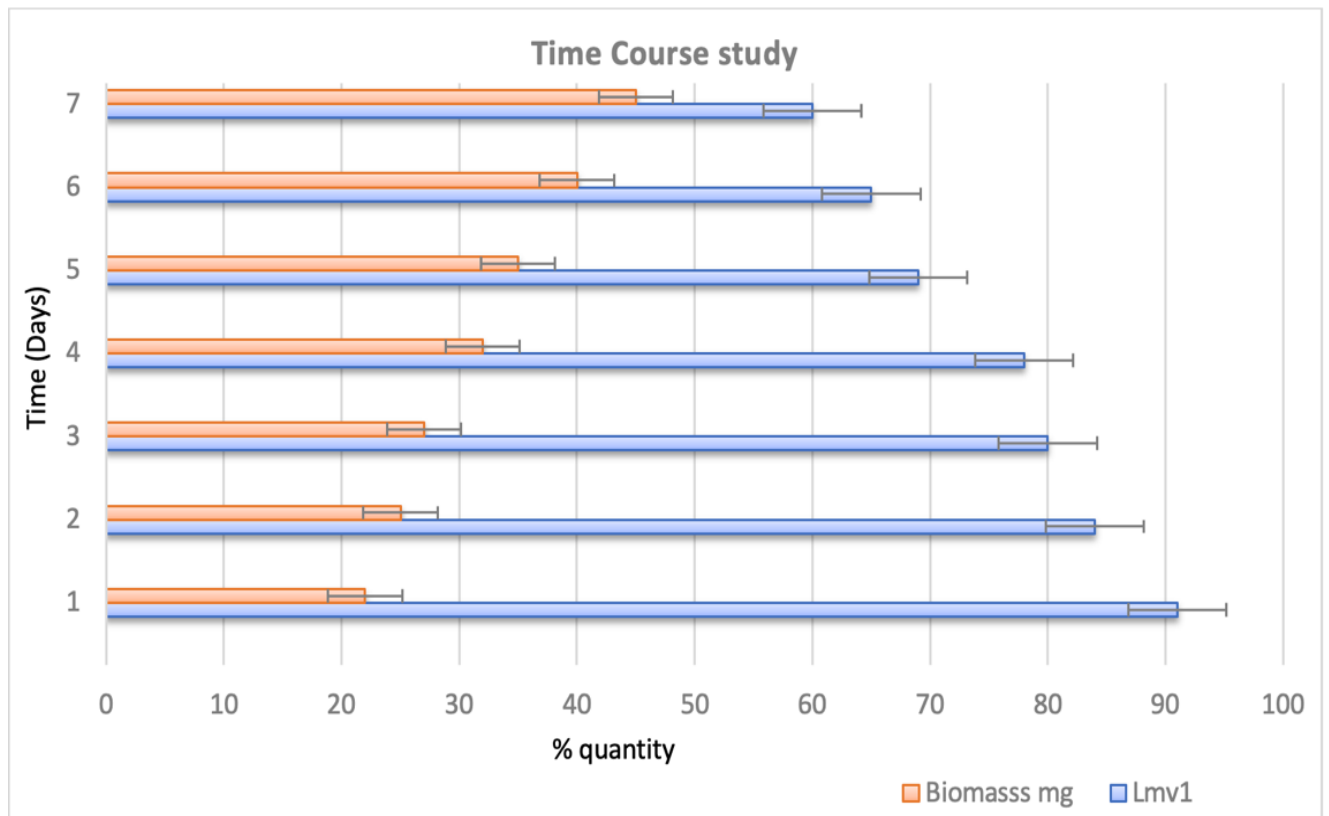


**Figure 3.3f** Time course of biomass production of *Lecanicillium muscarium* isolate 143.62 grown in liquid Czapek-Dox CM over a 7-day incubation period coupled with LmV-1 dsRNA accumulation. LmV-1 dsRNA was extracted from equal amounts of mycelia (blue shading) and biomass were measured using dried mycelia (orange shading). At least three independent replicates were performed in duplicate and error bars represent standard deviation.

### **3.4 Characterisation of *Beauveria bassiana* polymycovirus-3**

*Polymycoviridae* is a recently established family exclusively accommodating viruses infecting fungi in its sole genus *Polymycovirus*. The first member of the family, *Aspergillus fumigatus* tetramycovirus 1, was reported in 2015 (Kanhayuwa *et al.*, 2015) and since then over twenty related mycoviruses have been fully or partially sequenced. Polymycoviruses have a variable number of dsRNA genomic segments, ranging from three (Mu *et al.*, 2018) to eight (Jia *et al.*, 2017; Mahillon *et al.*, 2019), while a closely related, single-stranded (ss) RNA virus with eleven genomic segments named Hadaka virus was recently discovered (Sato *et al.*, 2020). Polymycoviruses are the first dsRNA viruses found to be infectious not only as purified entities but also as naked dsRNA (Kanhayuwa *et al.*, 2015; Jia *et al.*, 2017).

#### **3.4.1 Construction of a cDNA library of BbPmV-3 dsRNA5 by rPCR to obtain the full sequence of the RNA**

Various methods and priming strategies were employed to obtain the full sequence of BbPmV-3 dsRNA5 (Fig. 3.4a). Initially random-primed PCR (rPCR) was used with gel-purified BbPmV-3 dsRNA5 as source material as described (Section 2.7). Following PCR amplification step, amplicons of 336 bp in length appeared as a smear on agarose gels. These amplicons were cloned into the pGem-T Easy vector and recombinants were sequenced.

Following analysis of the sequence data, sequence specific oligonucleotide primers (PmV-3.F5 GTGCGCGTTGGTCGCGATGC, PmV3.R5 CCGGCCAAAGACGGGACCAC and PmV3.1.R5 GTGGTCCCGTCTTTGGCCGG) were designed and used to generate clones to close the gap between the existing clones using the genome-walking RT-PCR protocol. The reaction yielded several amplicons which were gel purified, cloned and sequenced (Appendix Part B Figure S3.4.2).

BLAST analysis of the assembled sequence confirmed that BbPmV-3 dsRNA5 was a component of the genome of a polynucleocystivirus and was similar in sequence to the sequence of BbPmV-2 dsRNA6 present in the *B. bassiana* IMI 391043 isolate.

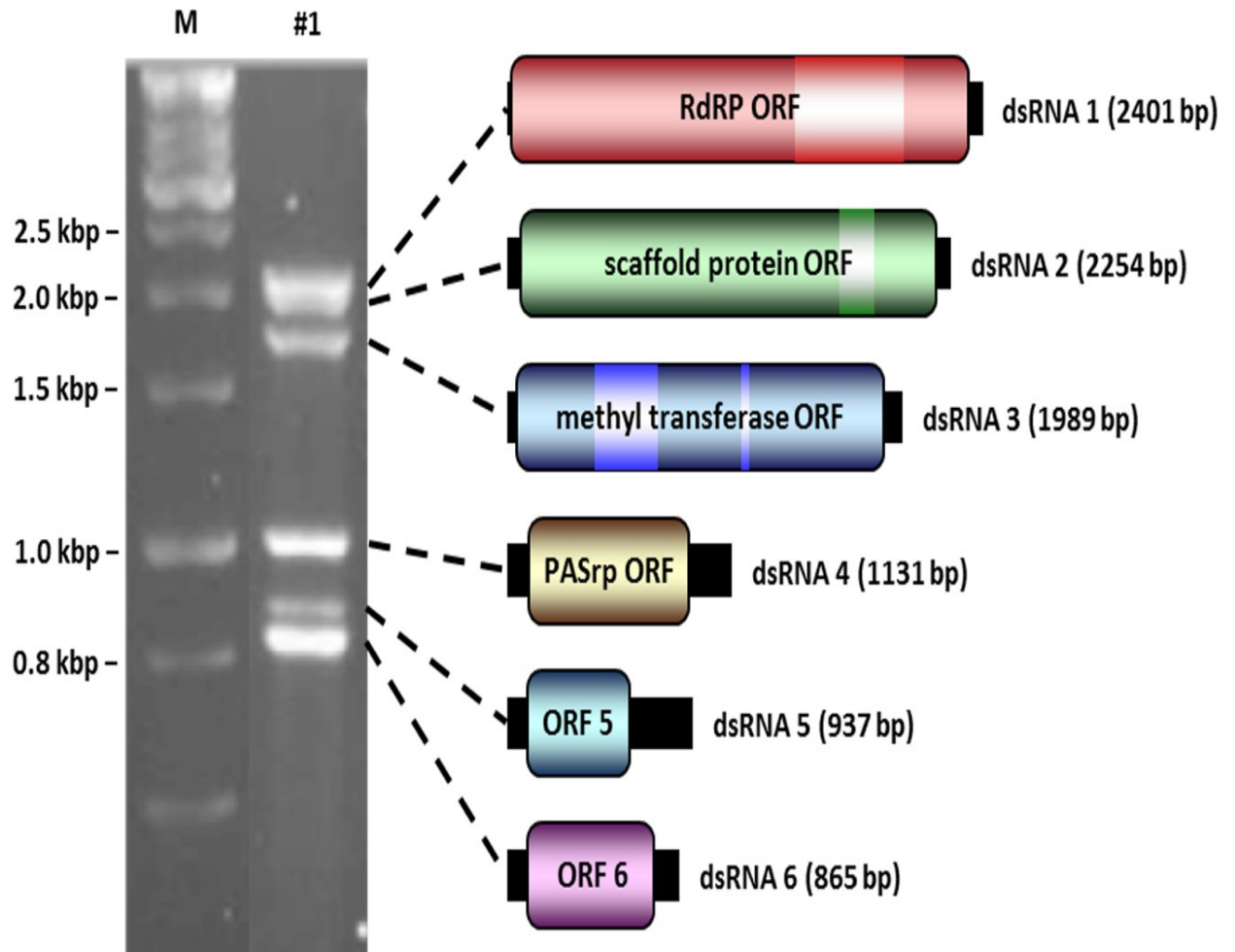


**Figure 3.4a** 1.5% (w/v) Agarose gel electrophoresis (left) and schematic representation (right) of the BbPmV-3 dsRNA genome. The ORFs (dark-coloured boxes) are flanked by 5'- and 3'-UTRs (black boxes). The light-coloured box represents known motifs. Taken from Filippou *et al.* (2021).

### **3.4.2 Determination of the 5'-and 3'- terminal sequences of BbPmV-3 dsRNA5**

RLM RACE was used to obtain the 5'-and 3'-terminal sequences of BbPmV-3 dsRNA5. To achieve this sequence specific oligonucleotide primers were designed (Appendix Part B Table S3.4.2a) based on the sequenced obtained from rPCR step and used for RLM RACE. Using the 5'- terminal specific primer one amplicon *ca.* 162 bp in size was obtained, while the 3'-terminal specific primer gave a prominent band of *ca.* 346 bp (Appendix Part B Table S3.4.2b). Both products were gel purified, cloned, and sequenced.

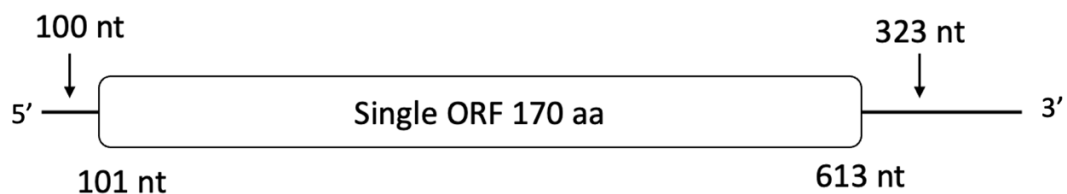
### **3.4.3 The genomic sequence of BbPmV-3 dsRNA5**

All clones were aligned and assembled to obtain the complete sequence of BbPmV-3 dsRNA5, whose genetic organization is shown in Figure 3.4b. BbPmV-3 dsRNA5 comprises 936 bp with 5'- and 3'- UTRs being 100 bp and 323 bp in length, respectively (Figure 3.4b). The UTRs flank a single ORF which encodes a putative protein of 531 amino acid (aa) residues (*Mr*) 21.75 kDa (Fig. 3.4b).

**a) Complete sequence of BbPmV-3 dsRNA5 (936 nt)**

GAACTCAAGCGTTTTTCTTCACAAGCCGGCCCGTACGACCCGGGCTTTACGCATTAGTTACCAAC  
 GTGTCATAAAAATCAAACGACGTGCACTGATTGCGATGCGATGCGATGCTCTTGCCCTTACCGTTTCGTCCCAATCCAGTGAGT  
 TCACTGGTGCGAACGGCGTACCCCGGGAGTGGGTCGTGCGGCTTGTCCCGCCTGACGGTCCGTGG  
 CCGGACCCGCAATTTAACCTGCGTTTTTCGGCTTACGGATTGGGCAGTCGAGCAGCTGCCTGCCGA  
 GCAGAGAGAGATAGCGTGCGATGTTGACGTGGTTTATTACCCCGTCTTCTTGCCGCTCGGGTCAT  
 ACTCTGCCCTCGATCCTGGGCCCCGGCTTGTACTGGCTGTTTATTGACGGCCTTGACCCCTGGTTAT  
 CCATCCGCGTGATCGACGTCATTGACGCCGGTCTCGGCGCGGGTGCCGTTCTGTCTTCATTGACC  
 GGGTGTCAAGTTCGAACTGGCCCCGACCCTTACTTCTCGCTGTTGAGGCAGCTGAGTTGGGGTTCG  
 CGTGGTCCCGTCTTTGGCCGGTAACTTGAAGTTCCAGCCCCCTTTGTTTTGTGTTGTTTTGAGGCGTG  
 TAACACCCCCGAGGGTGGTCCGTGCTTATGTTGGCTATCGAGGGCTGTCTGCCCGGGTTC  
 CCAGTAGTGCATAACCCGGCTCTCAGTCTACGCCAACCCAGTTACGGTTTTGATCGCGCGTGGTTG  
 ATGTCCTGAGTGGTTGCTCCTCGTGTGTTGCCCCGCTGCCTAACCCGCAAGTATGGGATAAGCGT  
 CACGGGCCATGAGACCGCGAAGGTGGCGTTGGTTTGGCGCCAGAAGCGGGGGCTCAATTTTGTTC  
 CCCCCCGTCCATGACTTT

**b) BbPmV-3 dsRNA5**



**c) Amino acid sequence encoded from ORF5 (18.47 kDa)**

MPFLGTHLPPAVANVRVGRDALALHRSSQSSEFTGANGVPREWVVRLVPPDGP  
 WDPQFNLRFRLLTDWAVEQLPAEQREIACDVDVVYYPVFLPLGSYSALDPGPGL  
 YWLFIDGLDPWLSIRVIDVIDAGLGAGAVPVFIDRVSGRTGPDPLLLAVEAAELGS  
 RGPVFGR

**Figure 3.4b** Diagrammatic representation of genome organisation of BbPmV-3 dsRNA5 (a); (b) its complete sequence and (c) amino acid sequence. Start and stop codons were shaded in red.

The predicted amino acid (aa) sequence of the BbPmV-3 dsRNA5 ORF was used to interrogate several public databases including PROSITE, the Pfam protein database, the conserved domain database and SUPERFAMILY1.75. However, whilst no matches to any accessed protein were discovered, BLASTX searches revealed that BbPmV-3 dsRNA5 shared 73% aa sequence identity to the ORF sequence predicted from the nucleotide sequence of BbPmV-2 dsRNA6 isolated from *B. bassiana* IMI 391043. The GC content of BbPmV-3 dsRNA5 was 58.76%. The aa sequence of the protein predicted from the BbPmV-3 dsRNA5 sequence was used to interrogate the MEROPS protease database (Rawlings *et al.*, 2012) and revealed significant similarity to the sequence of ORF 6 predicted from the BbPmV-2 dsRNA6 sequence (A0A292QAQ3, Identity = 73,8%, E value =  $4.5 \times 10^{-64}$ ) confirming the previous BLASTX result. Additional analysis of the ORF sequence predicted from BbPmV-3 dsRNA5 was also performed using SignalP 4.0 (Petersen *et al.*, 2011) and TMHMM (Krogh *et al.*, 2001), however no signal peptide and trans-membrane helix domains were discovered. Currently no function for the protein putatively encoded by BbPmV-3 dsRNA5 can be ascribed.

#### **3.4.4 Construction of cDNA clones of BbPmV-3 dsRNA6 using rPCR amplification**

Unfractionated BbPmV-3 dsRNA6 was used as a template for rPCR amplification using the Froussard primers as described (Section 2.7). The PCR amplicons generated were displayed on agarose gels stained with SYBR Safe (Appendix Part B; Figure S3.4.4) and were shown to be 500 bp in size. PCR amplicons were ligated into the pGEM-T Easy vector and the ligations transformed into *E. coli*. Putative recombinants were screened and those containing inserts were sequenced. Following analysis of the sequence data two sequence specific primers (PmV-3.F6            CCATGACACGCACGAGGCG            and            PmV3.R6  
GTTGCCACTGCCTCATCCAC) were designed and used to synthesize additional cDNAs and obtain the missing sequence using the genome-walking RT-PCR protocol (Appendix Part

B Figure S3.4.4). Insert sequences were analysed using BLASTX to identify homology with reference protein sequences in the GenBank database. BLAST confirmed that dsRNA6 was a genomic component of a polomyovirus. The incomplete sequence of BbPmV-3 dsRNA6 shares significant homology with the sequence of BbPmV-2 dsRNA7 isolated from *B. bassiana* IMI 391043.

### **3.4.5 Determination of the 5'- and 3'-terminal sequences of BbPmV-3 dsRNA6 using RLM-RACE**

Two sequence specific 5'- and 3'- oligonucleotide primers were designed from the known sequence of BbPmV-3 dsRNA6 for RLM-RACE amplification (Appendix Part B Table S3.4.5a and Table S3.4.5b) using 205 ng/ $\mu$ L of dsRNA in each reaction. The RLM-RACE amplicons generated from both reactions were *ca.* 308 in size for the 3' terminal and *ca.* 285 in size for the 5' terminal (Figure 3.4c; Appendix Part B Figure S3.4.4) and were cloned into the pGEM-T Easy vector. Recombinants were sequenced and the insert sequences analysed as before.

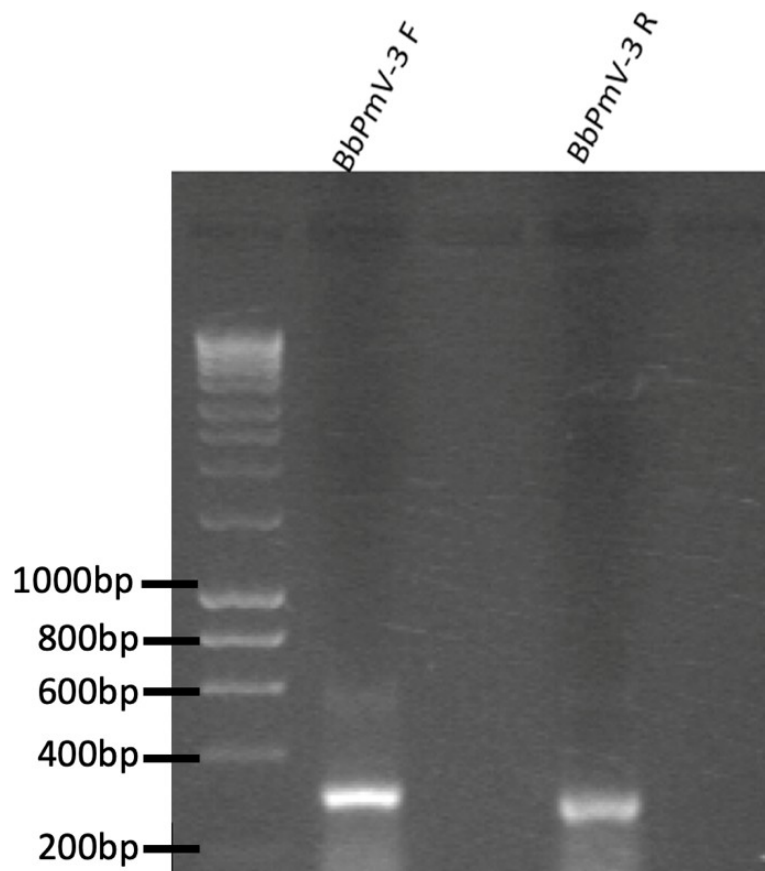


**Figure 3.4c** 1% (w/v) agarose gel electrophoresis of RLM RACE amplicons generated from BbPmV-3 dsRNA6 5'- (lane 2) and 3'- (lane 4) -termini. The HyperLadder 1 kb DNA ladder (Bioline) used as marker is shown in lane 1.

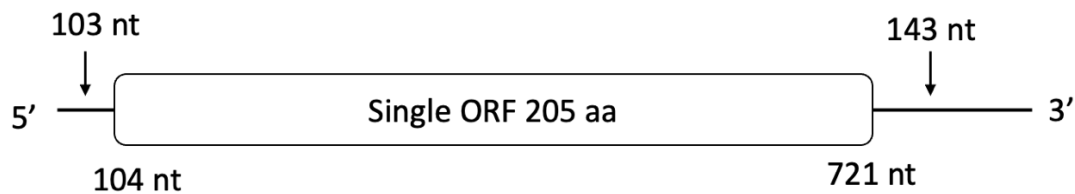
#### **3.4.6 The genomic sequence of BbPmV-3 dsRNA6**

The sequence obtained from amplicons generated by rPCR, RT-PCR and RLM-RACE were assembled and aligned to obtain the complete sequence of BbPmV-3 dsRNA6. The sequence of BbPmV-3 dsRNA6 comprises 864 bp with 5' and 3' UTRs of 103 and 143 bp in length, respectively. The UTRs flank a single ORF which encodes a putative protein of 618 aa residues (*Mr*) 21.75 kDa. The genome of BbPmV-3 dsRNA6 is shown in detail in Figure 3.4d.

**a. Complete Sequence of BbPmV-3 dsRNA6 (864 nt)**

GAAATCAAGAGTTCTTCTACGCAAGCACTGCCTTGCAGTAGGTATCTGGTACTTATTGAC  
 CTTTTTCTCATTTCGCAAGACCTTCTAAGCTCGCTAGTACTG**ATG**TCGGAGGCATCCTCTTT  
 TGTCATGACCGGAGCAGCAGCCGCCAGTCCAAGGGTTGCAGAGTGGGCCGCTGACGCACG  
 CCGTGCCTCGGGGCCGGTCGATCGTAGTGGTATTGGTCGGCCGGTGTGTACCCACCCAG  
 CACCGTGGCGTCTGCTGTTCCGTCCATGACACGCACGAGGCGACGCCAGTCTCCTCCTGCG  
 ACCGTCGTTGACGGTAGTGATGGTGAGGAAAGTGTTTCCCCTGAAGACGCCGATCCC GTT  
 CCCCCGTACGTTTCTCGGCAGGCGCTCGCGCCTGGTGATAGCGTATCTCTCAACGGCAATA  
 GCGGATGGGGTCCGCTGGGACGACCGGTTCTACAGTGAGTCTCACCGACTCGACCGTAG  
 ACCGTTGGCCGTGCGGATCGCTGACCTAACGTTGGTTCGCGGAAAACCGTCGCCGGT  
 TGGTCCCCTGTGGATGAGGCAGTGGCAACTACCGCGGCCACAGGCGCCCTCGTCTGA  
 GCTCAATCAGCGAGAGGCCGGCTGTTGGCGTGTGGCGGCTTTGGTTTTCGGGACCAAGG  
 AGATAGTCTACGACAACAACGCCACGTA**CTG**CGAGCAAGACGACGCGGGCATT**AG**CCC  
 GCCTTGCCTTCCCCTGGATGTGGGGGCCTTTGATGCCGCCATCCTAGCCATGAAGATAGTC  
 CAACCCGGGTTTTCCC CGGCCGCGGAATTTTTCTCGCTTCGGATCATGATTCTTAGTCCCC  
 TTCCAGTTGGAATTTT

**b. BbPmV-3 dsRNA6**



**c. Amino acid sequence encoded from ORF6 (21.75kda)**

MSEASSFVMTGAAAASPRVAEWAADARRASGPVDRSGIGRPVVYPPSTVASAVPS  
 MTRTRRRQSPPATVVDGSDGEESVSPEDADPVPPYVSRQALAPGDSVSLNGNRRM  
 GSAGTTGSTVSLTDSTVDRLAVRIADLNVGSRENRRRLVPTVDEAVATTARHRRPR  
 LSSISERPAVGVLAAALVFGTKEIVYDNKRHVLRARRRGH

**Figure 3.4d** Diagrammatic representation of the genome organisation of BbPmV-3 dsRNA6 (a); (b) the complete sequence and (c) the amino acid sequence. Start and stop codons are shaded in red.

Following a search of the public databases the deduced aa sequence of the BbPmV-3 dsRNA6 ORF using PROSITE, Pfam protein database, conserved domain database and SUPERFAMILY 1.75 revealed no match to any accessed protein. However, the BLASTX and the MEROPS protease database searches revealed that BbPmV-3 dsRNA6 shares significant aa sequence identity to the aa encoded by PmV-2 dsRNA7 (A0A292Q903, Identity = 82.9%, E value =  $2.3 \times 10^{-115}$ ) isolated from *B. bassiana* IMI 391043. Further analysis of the ORF aa sequence predicted from BbPmV-3 dsRNA6 was performed using SignalP 4.0 and TMHMM however no signal peptide or trans-membrane helix domains were discovered.

#### **3.4.7 Sequence analysis of the remaining 4 dsRNAs of BbPmV-3**

As described in detail above BbPmV-3 has a classic genomic organization of other members of the *Polymyoviridae* family (Appendix Part B Table S3.4.7). Six dsRNAs ranging from 2.5 to 0.9 kbp in length comprise the genome of BbPmV-3 (Figure 3.4a). Each one of these dsRNAs carrying an ORF flanked by 5' and 3' untranslated regions. The first larger segment, dsRNA1, encodes the RdRP necessary for viral replication. The second larger segment, dsRNA 2, contains a protein assumed to act as a scaffold protein (Kotta-Loizou & Coutts, 2017). It has been observed that dsRNA2 includes a conserved N-terminus and a cysteine-rich, zinc finger-like motif (Appendix Part B Figure S3.4.7a). Moreover, it is rich in arginine repeats (R-R, R-X-R), associated with endoplasmic reticulum (ER) retention signals. The third largest element, dsRNA3, encodes a methyl transferase (Appendix Part B Figure S3.4.7b), responsible for adding a capping structure at the 5'-termini of the positive-sense strands of the viral dsRNAs (Kanhayuwa *et al.*, 2015; Kotta-Loizou & Coutts, 2017). Like all redox enzymes this one is comprised of two-domain proteins. These two domain proteins contain a methyltransferase catalytic motif and an N-terminal Rossmann-fold domain belonging to the protein family methyltransf\_25 (PF13649) and the protein clan FAD/NAD(P)-binding Rossmann fold

(NADP\_Rossmann; CL0063). The fourth largest element, dsRNA4, encodes a proline-alanine-serine rich protein (PASrp). All PASrp have a high pI, ranging from 8.37 for *Fusarium redolens* polmycovirus 1 to 9.61 for *Aspergillus spelaesus* tetramycovirus 1, while BbPmV-3 PASrp has a pI of 8.94. It is assumed that PASrp is responsible for coating the viral RNA genome *in lieu* of a capsid (Kanhayuwa *et al.*, 2015; Zhai *et al.*, 2016; Kotta-Loizou & Coutts, 2017) and its aa composition, whereas high pI and intrinsic disorder facilitate protein-RNA interactions.

### **3.4.8 Multiple sequence alignment of polmycovirus-3 dsRNAs**

The sequences of the 5'- and 3'-UTRs of the six genomic dsRNA components of *B. bassiana* Polmycovirus-3 were aligned using ClustalW2 multiple alignment online software. The alignment showed that the sequences share extensive similarities in the 5'-UTRs and fewer similarities in the 3'-UTRs. The 5' UTRs of BbPmV-3 dsRNA1-6 were similar in length and sequence, whereas the dsRNA 1 and 3 3'-UTRs shared similarities in both sequence and length, however dsRNAs 2, 4, 5 and 6 are more similar when compared together (Figure 3.4e). Furthermore, CAA repeats were identified within the 5'-UTRs of all six PmV-3 dsRNAs. It has been suggested that CAA repeats upstream of the initiation codon found in mycoviruses belonging to the families *Chrysoviridae* and *Partitiviridae* might serve as translational enhancers (Jiang and Ghabrial, 2004; Tavantzis, 2008).

The 3'-terminal sequences of BbPmV-3 dsRNAs 1 and 3 were similar in length and sequence whereas the remaining 4 dsRNA segments were also similar in length and sequence to each other but aligned in a separate group. Conserved terminal sequences of ds and ss viral RNAs with multipartite genomes are common because of their importance in viral RNA replication, transcription and packaging (Wei *et al.*, 2004).







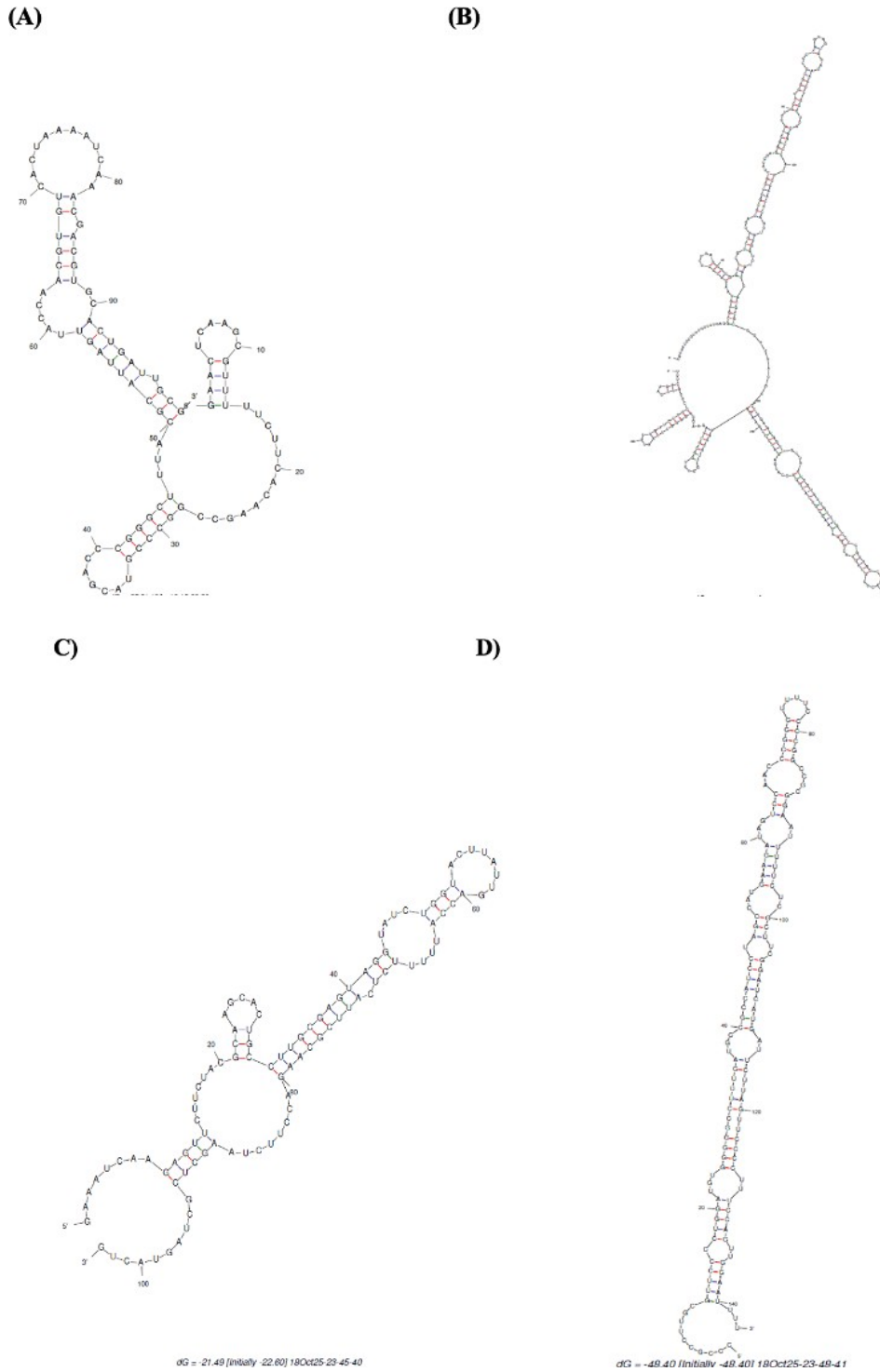


**Figure 3.4f** Predicted secondary structures of respectively the 5'- (A) and 3'-UTRs (B) of BbPmV-3 dsRNA5 and the 5'- (C) and 3'-UTRs (D) of BbPmV-3 dsRNA6. Structures were predicted using the Mfold programme.

### 3.4.9 Phylogenetic analysis of the putative BbPmV-3 RdRP gene

In order to investigate phylogenetic relationships between BbPmV-3 and other RNA mycoviruses an alignment of the RdRP genes from 21 mycoviruses belonging to the families *Partitiviridae*, *Totiviridae*, *Polymycoviridae* and *Chrysoviridae* was made (Appendix Part B Table S3.4.9). As described previously mycoviruses share a common GDD motif when aligned (Kotta-Loizou & Coutts, 2017). However, when the BbPmV-3 RdRP gene was aligned with other mycoviral RdRP genes the highly conserved GDD motif, which is normally invariant for positive-stranded RNA and dsRNA viruses, was replaced by a GDN triplet followed by a Q residue in polymycoviruses. A GDN triplet followed by a Q residue is a common sequence motif naturally found in the L genes of non-segmented, negative-stranded (-) ssRNA animal viruses such as the rabies rhabdovirus (Delarue *et al.*, 1990, Schnell *et al.*, 1995; Jablonski & Morrow, 1995).

As shown in Figure 3.4g the GDNQ motif is an invariant motif in polymycovirus RdRP genes whereas a GDD motif (Appendix Part B Figure S3.4.9) is present in all other mycoviruses described thus far in entomopathogenic fungi.



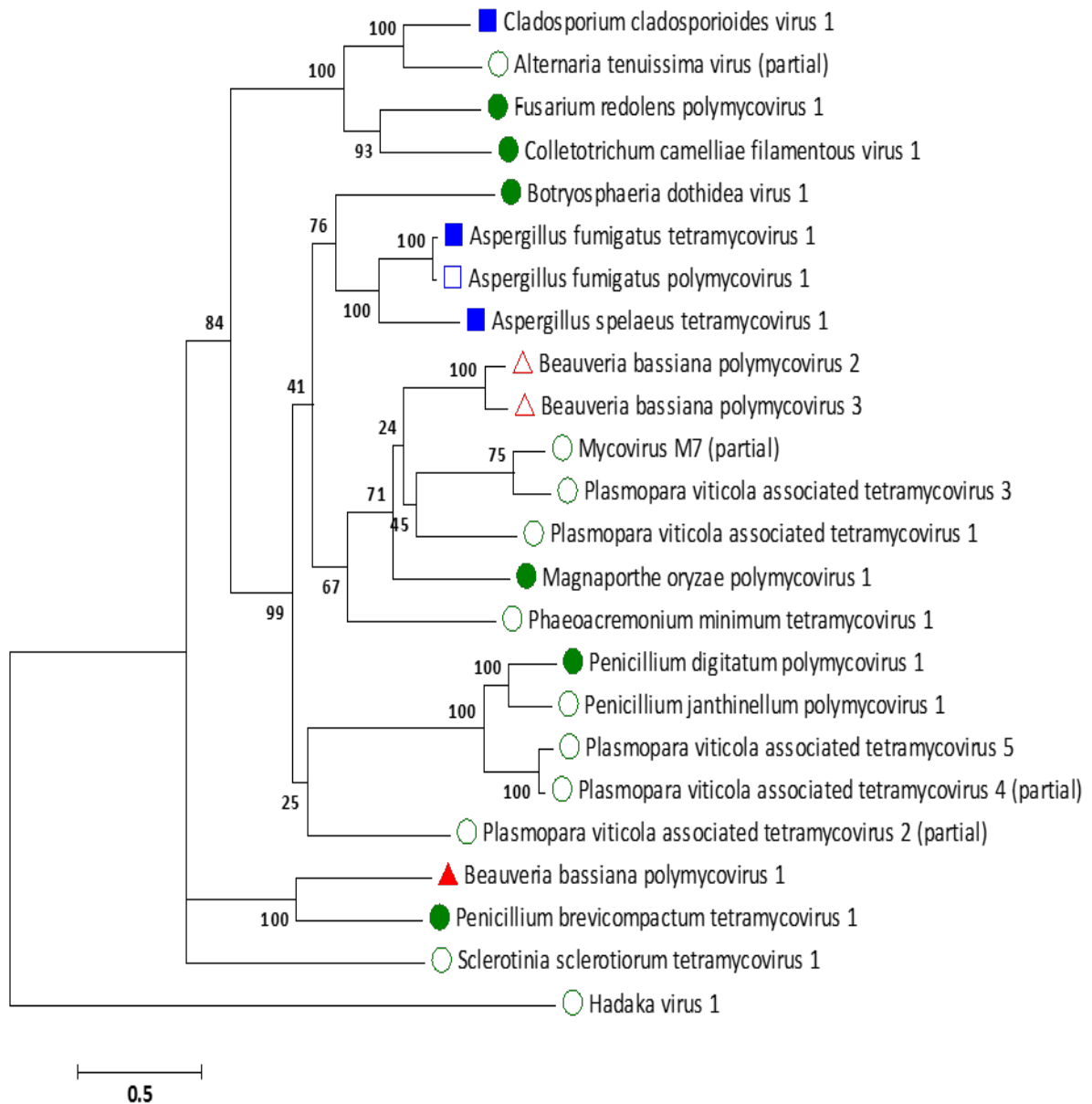


**Figure 3.4h:** ML phylogenetic tree comparing polmycovirus RdRP sequences. Sequences were aligned with MUSCLE as implemented by MEGA 6. At the end of the branches, established members of the family *Polmycoviridae* have shapes filled with dark colours; other polmycoviruses and related viruses have shape outlines. Blue squares indicate pathogenic viruses that infect mammal's; green circles indicate viruses that infect plants and red triangle indicate viruses that infect arthropods. Taken from Filippou *et al.* (2021).

Phylogenetic analysis was performed for all proteins known to be conserved in the family *Polymycoviridae*, the RdRP, the scaffold protein, the methyl transferase and the PASrp. Based on the sequence analysis, BbPmV-3 RdRP is the closest taxon to the BbPmV-2 RdRP, while the BbPmV-1 RdRP appears to be phylogenetically distant (Figure 3.4h). The distance between BbPmV-3 and BbPmV-1 is supported by the phylogenetic analysis of the scaffold protein, the methyl transferase and the PASrp. Geographically, ATHUM 4946 harbouring BbPmV-3 originated from Athens, Greece; BbPmV-2 has been reported in Syria, Russia, and Uzbekistan (Kotta-Loizou & Coutts, 2017); BbPmV-1 has been found predominantly in Spanish populations (Kotta-Loizou & Coutts, 2017; Filippou *et al.*, 2018).

To conclude, between the three polymycoviruses (BbPmV-1, 2 & 3) we have decided to select BbPmV-1 and BbPmV-3 to study and compare their effects on their respective fungal hosts, since, BbPmV-3 supports the replication of two smaller dsRNA segments as well as the distant relationship between BbPmV-1 and 3. Furthermore, in order to confirm the location of viruses within host cells, it would be useful to experimentally determine protein function, protein targeting and localization to enable an understanding of how polymycoviruses infect and replicate.

# **Chapter 4**

**Eradication of mycoviral infection results in  
symptomatic and asymptomatic effects.**

When mycoviruses infect fungi, they can either persist asymptotically or have a marked effect on their fungal hosts influencing them either positively or negatively. To control insect pest attacks against crops the use of mycoviruses to manipulate the virulence of entomopathogenic fungi, such as *Beauveria bassiana*, a popular biocontrol agent, could lead to the development of novel methods. Existing agrochemicals are being withdrawn from the market due to environmental and health concerns, hence, environmental and human friendly alternatives are urgently required. Among the fungal-based biopesticides, entomopathogenic fungi within the Ascomycota and order Hypocreales are represented in over 150 commercially available products (de Faria & Wraight, 2007). Although they constitute an environmentally friendly alternative to chemical pesticides, it is crucial to optimise their application to ensure maximum efficiency and reliability (St. Leger & Wang, 2010). However, to study the possible effects of mycoviruses on their fungal hosts is of great importance to cure mycoviral infection and establish virus-free and virus-infected isogenic lines. In this Chapter I present the curing of the isolate ATHUM 4946 of BbPmV-3 and *L. muscarium* 143.62 of LmV-1. Finally, a comparison of ATHUM 4946 PmV-3 free (PmV-3.F) and ATHUM 4946 PmV-3 infected (PmV-3.I) isogenic lines revealed a mild hypervirulent effect of mycoviruses on growth, sporulation and pigmentation of their host. Whereas no apparent symptoms were observed when a comparison between *L. muscarium* 143.62 LmV-1 free (LmV-1.F) and *L. muscarium* 143.62 LmV-1 infected (LmV-1.I) was performed. Moreover, a comparison of EABb 92/11 – Dm PmV-1 free (PmV-1.F) and EABb 92/11 – Dm PmV-1 infected (PmV-1.I) isogenic lines obtained by Dr. Ioly Kotta-Loizou (Kotta-Loizou & Coutts, 2017) revealed a significant increase on growth, sporulation and pathogenicity against the army mealworm beetle *Tenebrio molitor*, highlighting the potential of polymycoviruses as enhancers of biocontrol agents. As mentioned earlier, mycoviruses are transmitted intercellularly through hyphal anastomosis or spores, therefore, lacking an extracellular phase. Transfection methods using

purified virus particles or full-length viral cDNA clones are one way to expand the host ranges of some mycoviruses. Consequently, in this Chapter I also present the use of Benomyl as a potential fungicide suitable for use as selective marker for viral transfection and localization experiments.

### **Aims and scope**

The aim of Chapter 4 is to describe the effects of eradicating mycoviral infections from *B. bassiana* ATHUM 4946 and *L. muscarium* 143.62 using cycloheximide and Ribavirin respectively with specific reference to fungal growth, germination, pigmentation and insect pathogenicity. The chapter also investigates which fungicides might be suitable for use as selective markers for viral transfection and localization.

### **4.1 Curing of mycoviral infection and confirmation of isogenic lines**

Since most infections caused by mycoviruses are cryptic or latent and do not cause any phenotypic changes in their hosts, at least no obvious ones, this has resulted in limited studies on the replication of mycoviruses. Nevertheless, studies have shown that some mycoviruses can indeed cause considerable physiological and morphological changes, including alterations to virulence, morphology and pigmentation (Castro *et al.*, 2003; Dawe *et al.*, 2001). For investigations on the interactions between fungi and mycoviruses it is desirable to compare isolates with identical genetic backgrounds. Likewise, in order to explore in depth these interactions it is necessary to establish Polymycovirus-3 free (PmV-3.F) and Polymycovirus-3 infected (PmV-3.I) isogenic lines. The process of creating isogenic lines can be challenging due to the fact that sometimes virus infections can be unstable. This is because the fungus can be recalcitrant to curing making the procedure difficult to investigate (Aoki *et al.*, 2009; Carroll *et al.*, 1995; Herrero *et al.*, 2012; Salaipeh *et al.*, 2014).

Another method of creating isogenic lines is through direct transfection of wild type, virus free fungi with purified virions, which being the most direct and simple way of studying horizontal virus transmission. However, this method is yet to be optimised for most mycovirus/fungus combinations. Additionally, virus transmission through hyphal anastomosis is not suitable since various cytoplasmic factors can be inherited making it difficult to distinguish whether any phenotypic changes are caused by inherited cytological factors, mycoviruses or even both (Meyling & Eilenberg, 2007). Consequently, for the reasons explained above creating isogenic lines that are either virus-free (VF) or virus-infected (VI) is not easy however with the help of certain chemicals that can interfere with transcription and translation this task can be made easier.

Cycloheximide is a protein synthesis inhibitor, produced by the bacterium *Streptomyces griseus* which has been used successfully to cure several mycoviruses infecting fungi (Yamada *et al.*, 2004) and is the most reliable and common method used. Ribavirin, which is a synthetic guanosine analogue, interferes with RNA metabolism and is used to treat RSV and hepatitis C infection, is also used for curing mycovirus infections. Cycloheximide and Ribavirin treatment is often accompanied by single conidia isolation of the fungi to assist virus eradication (Aoki *et al.*, 2009; Marzano *et al.*, 2015).

Producing isogenic lines of VF and VI isolates with the same genetic background is important in terms of studying morphological characteristics as well as fungal growth rate. Previously the only way of checking if the curing procedure was successful or not was by dsRNA extraction followed by agarose gel electrophoresis. However, this method is unreliable because in some cases the targeted sample might contain small amounts of dsRNA below the levels of detection in stained gels. For this reason, a more sensitive and effective technique such as RT-PCR amplification is preferable for use to confirm the presence or absence of dsRNA. This method was first described by Park *et al.* (2006), where it was used to confirm eradication of

*Chalara elegans* mitovirus (CeMV) from the fungus.

#### **4.1.2 Cycloheximide curing of BbPmV-3 from the *B. bassiana* ATHUM 4946 isolate**

Attempts were made to cure the *B. bassiana* ATHUM 4946 isolate from dsRNA infection using a variety of concentrations (0-1000 µg/mL) of cycloheximide on solid MEA and SDA.

Higher concentrations of cycloheximide >1000 µg/mL were toxic for the fungus and could not be used. All cycloheximide solutions were filter sterilised before incorporation into the growth media at ~50°C. All inoculated plates were incubated at 25°C for twenty days. In order to determine if the cycloheximide treatment was successful or not and if the mycovirus had been successfully eradicated (completely or partially) or not. The E.Z.N.A Fungal RNA kit (OMEGA) was used to extract RNA from fungal mycelia (Section 2.11) for analysis. After extraction of RNA, RT-PCR amplification assays were performed as described (Section 2.8.1) using sequence specific oligonucleotide primers (Table 4.1a) designed to generate amplicons representing a fragment of the coding region of the RdRP gene.

As seen in Figure 4.1a, successful eradication of the dsRNA elements was confirmed by RT-PCR. A band representing the region of the RdRP (699 bp, Table 4.1a), is clearly visible when RNA extracts from the PmV-3.I isolate were used, whereas with RNA extracts of the PmV-3.F isolate no amplicons were observed. This is a strong indication that mycoviral infection was successfully eradicated and the next step was to confirm that the isogenic lines of PmV-3.F and PmV-3.I isolates were indeed isolates of *B. bassiana*.

The internal transcribed spacer (ITS) sequence on genomic DNA has been used as a molecular marker for species-level identification in ecological and taxonomic studies of fungi since the early 1990s. Fungi are extremely diverse and almost ubiquitous group of heterotrophic eukaryotes with an estimated population of 1.6 million species (Moreau *et al.*, 2006). Identification of a particular fungal species is now possible with ITS amplification using a

simple PCR-based method by amplifying a region that lies between the 18S and 28S rRNA genes, rather than just relying on morphological differences in their sexual or asexual reproductive structures. Moreover, this region also contains two variable noncoding spacers and the extremely conserved 5.8S rRNA gene (Kõljalg *et al.*, 2013). Additionally, this region is composed of two extremely variable spacers ITS1 and ITS2, which often serve as species specific markers (Bengtsson-Palme *et al.*, 2013). As indicated in Appendix Part B Figure S4.1.1 amplifying the ITS region of both isolates was successful (Section 2.10). A BLAST search showed that all isolates matched, and the regions sequenced were ITS1 partial and ITS2 complete. Furthermore, multiple sequence alignment demonstrated that all isolates were 100% identical including BbPmV-3 and LmV-1 virus-infected (Appendix Part B Figure S4.1.2a) and the other BbPmV-3 and LmV-1 virus-free (Appendix Part B Figure S4.1.2b).

In order to confirm this genomic DNA extraction of the two fungal isolates were performed as detailed in Section 2.10. Following genomic DNA extraction PCR amplification was performed using ITS specific oligonucleotide primers (Table 4.1a). After molecular cloning of the amplicon samples were sequenced and analysed by BLAST searches and the sequences aligned using ClustalW2 to check for similarity between the isolates.

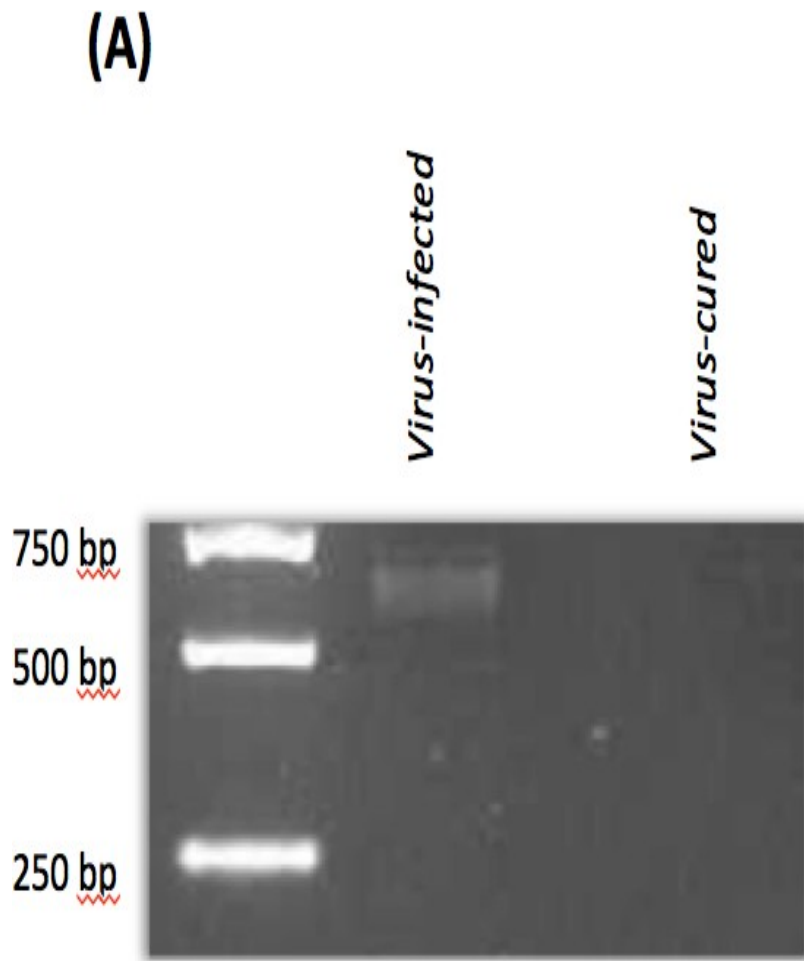


**Figure 4.1a (A)** RT-PCR amplification using sequence specific oligonucleotide primers designed to generate amplicons (**699 bp**) representing a fragment of the coding region of the BbPmV-3 RdRP present in *Beauveria bassiana* ATHUM 4946 (lane 2) but absent from a cured, virus-free isogenic line (lane 4).

Cycloheximide treatment has been used in many cases with high success rates to cure mycoviral infections from different fungal species such as, *B. bassiana* strain CG25 and *Aspergillus fumigatus* (Bergvinson & García-Lara, 2004). On the other hand, there were cases where cycloheximide treatment did not work and the curing was unsuccessful for example in *Aspergillus flavi* (Elias *et al.*, 1996), *Metarhizium anisopliae* (Martins *et al.*, 1999), *Fusarium oxysporum* (Sharzei *et al.*, 2007) and *Cytospora sacchari* (Peyambari *et al.*, 2014). Such failures might be due to high titres of dsRNA.

#### **4.1.3 Ribavirin curing of LmV-1 in *Lecanicillium muscarium* isolate 143.62**

Several attempts were made to cure mycoviral infection of *L. muscarium* isolate 143.62 using different concentrations of ribavirin. A concentration range of 40µM/mL to 100µM/mL ribavirin was investigated and 60µM/mL to 100µM/mL concentrations were successful in curing the virus. Following RNA isolation RT-PCR amplification was performed using sequence specific primers to confirm successful eradication of the dsRNA element. These primers were specifically designed to generate a 471 bp LmV-1 amplicon (Table 4.1a) representing a fragment of the coding region of the RdRP gene (Figure 4.1c) and isogenic lines were confirmed *via* ITS sequencing as described earlier.

**A)**

<b>Primers</b>	<b>Sequence</b>
BbPmV-3F	5'-GAGGAGCCGAAGCCCGCG-3'
BbPmV-3R	5'-GCGGAGGCCAACGACCTTGA-3'

**B)**

<b>Primers</b>	<b>Sequence</b>
ITS1.F	5'-CTTGGTCATTTAGAGGAAGTAA-3'
ITS4	5'-TCC TCC GCT TAT TGA TAT GC-3'

**C)**

LV.F	5'- ATGATCCGTATAAGTGTTCT - 3'
LV.R	5'- ATTGAAGTTGAAGAGCTTC - 3'

**Table 4.1a** (A) Sequence specific oligonucleotide primers used to amplify the coding region of the BbPmV-3 RdRP gene (699bp), (B) the universal primers ITS1F were used for both *Lecanicillium muscarium* and *Beauveria bassiana* ATHUM 4946 isogenic lines, and C) primers for amplifying a region of the LmV-1 RdRP sequence (471bp).

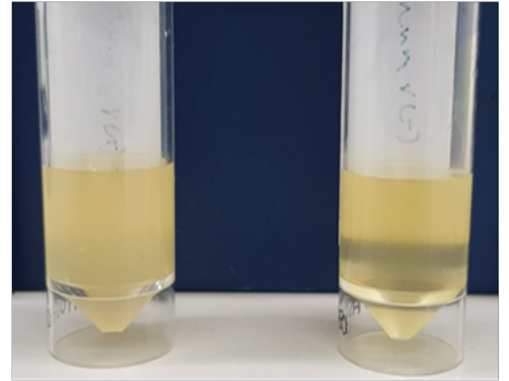
#### **4.1.4 Phenotypic differences between virus-infected and virus-free isogenic lines (symptomatic & asymptomatic)**

Thus far the only physiological differences between the VI and VF isolates concern sporulation, radial growth and pigmentation. In regards to PmV-3.I isolate, it showed increased sporulation as compared to the PmV-3.F isolate (Fig. 4.1b) following microscope spore counting using FastRead-102 disposable counting slides (Section 2.14). The PmV-3.F isolate produced on average  $1.66 \times 10^8$  spores/mL while the PmV-3.I isolate produced on average  $3.9 \times 10^8$  spores/mL. Also, the pigmentation of the isolates differs with the PmV-3.I isolate exhibiting a darker pigmentation as compared to the PmV-3.F isolate (Fig. 4.1b), suggesting that PmV-3 infection is probably symptomatic resulting in hypervirulence.

(A)



(B)



(C)

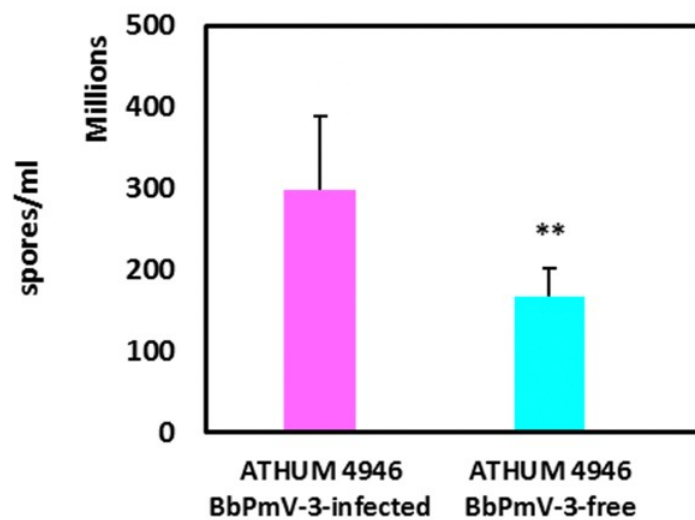


**Figure 4.1b:** (A) Cultures of PmV-3.I (left) and PmV-3.F (right) isogenic lines of ATHUM 4649 grown on PDA at 25°C for 2 weeks, showing significant differences in pigmentation. (B) Spore suspensions from PmV-3.I (left) and PmV-3.F (right) isogenic lines of ATHUM 4946 showing increased sporulation in the former as compared to the latter. (C) Differences in sporulation between the PmV-3.I and PmV-3.F isogenic lines. Student's t test: \*\* indicates P-value < 0.01. Taken from Filippou *et al.* (2021).

Similarly, sporulation and radial growth of *Lecanicillium muscarium* Virus-1.Free (LmV-1.F) and *Lecanicillium muscarium* Virus-1.Infected (LmV-1.I) isogenic lines of *L. muscarium* were also measured. No significant differences were observed between the isogenic lines in terms of sporulation, radial growth or pigmentation suggesting that LmV-1 infection is probably asymptomatic (cryptic; Figures 4.1c and 1d).

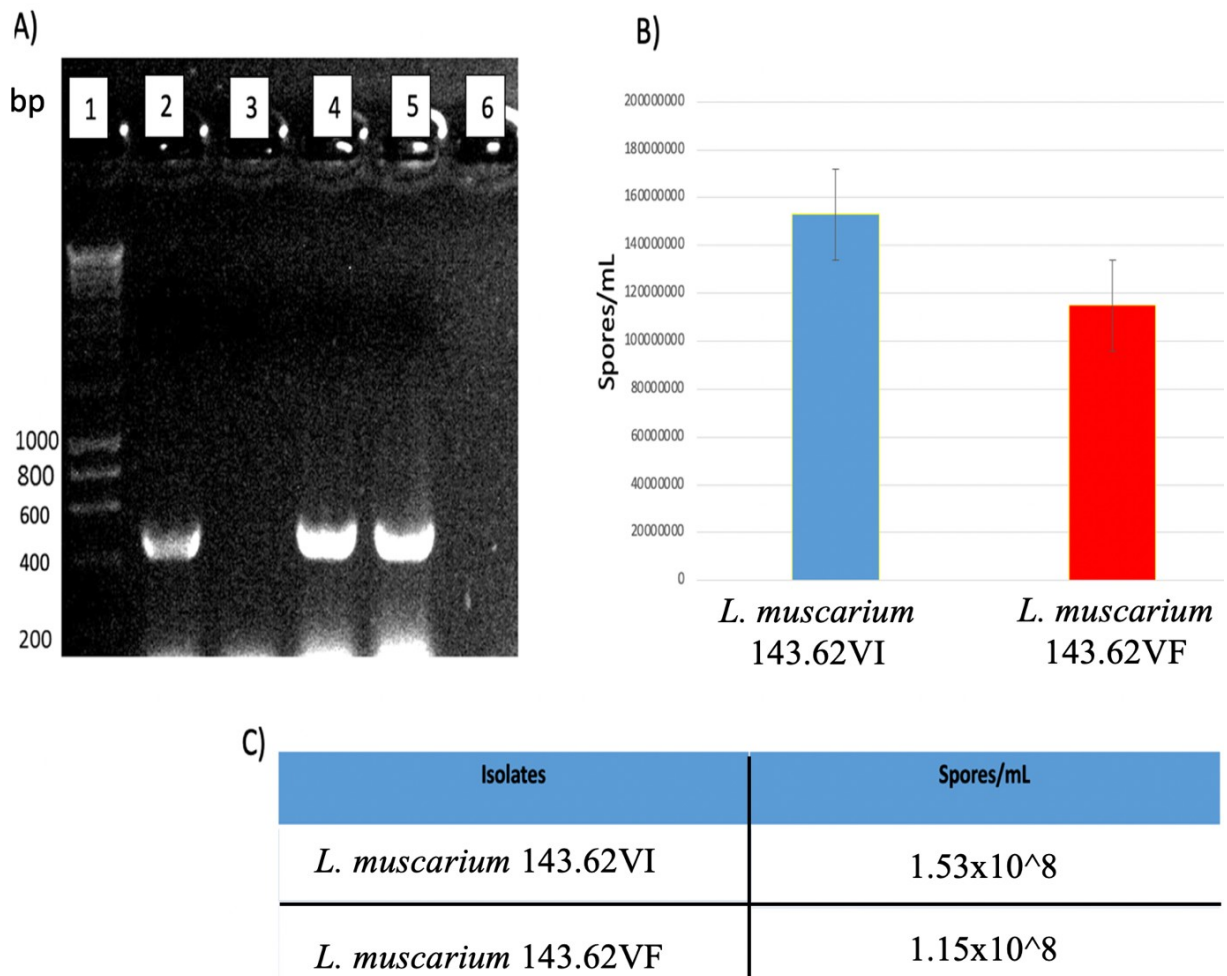


**Figure 4.1c:** **A)** Agarose gel electrophoresis showing attempted eradication of LmV-1 from *Lecanicillium muscarium* isolates using ribavirin. Lane 2; wild type LmV-1.I isolate 143.62; lane 3; LmV-1.F isolate 143.62; lane 4; wild type LmV-1.I, isolate 102071; lane 5 isolate LmV-1.I 102071 unsuccessfully freed of virus infection; lane 6 negative control. LmV-1 presence was shown by RT-PCR amplification of a virus-specific 471 bp amplicon. **B)** Difference in sporulation between LmV-1.I and V LmV-1.F isogenic lines of *Lecanicillium muscarium*. **C)** Average spore count of LmV-1.I and LmV-1.F isogenic lines of *Lecanicillium muscarium* (P – value < 0.005).

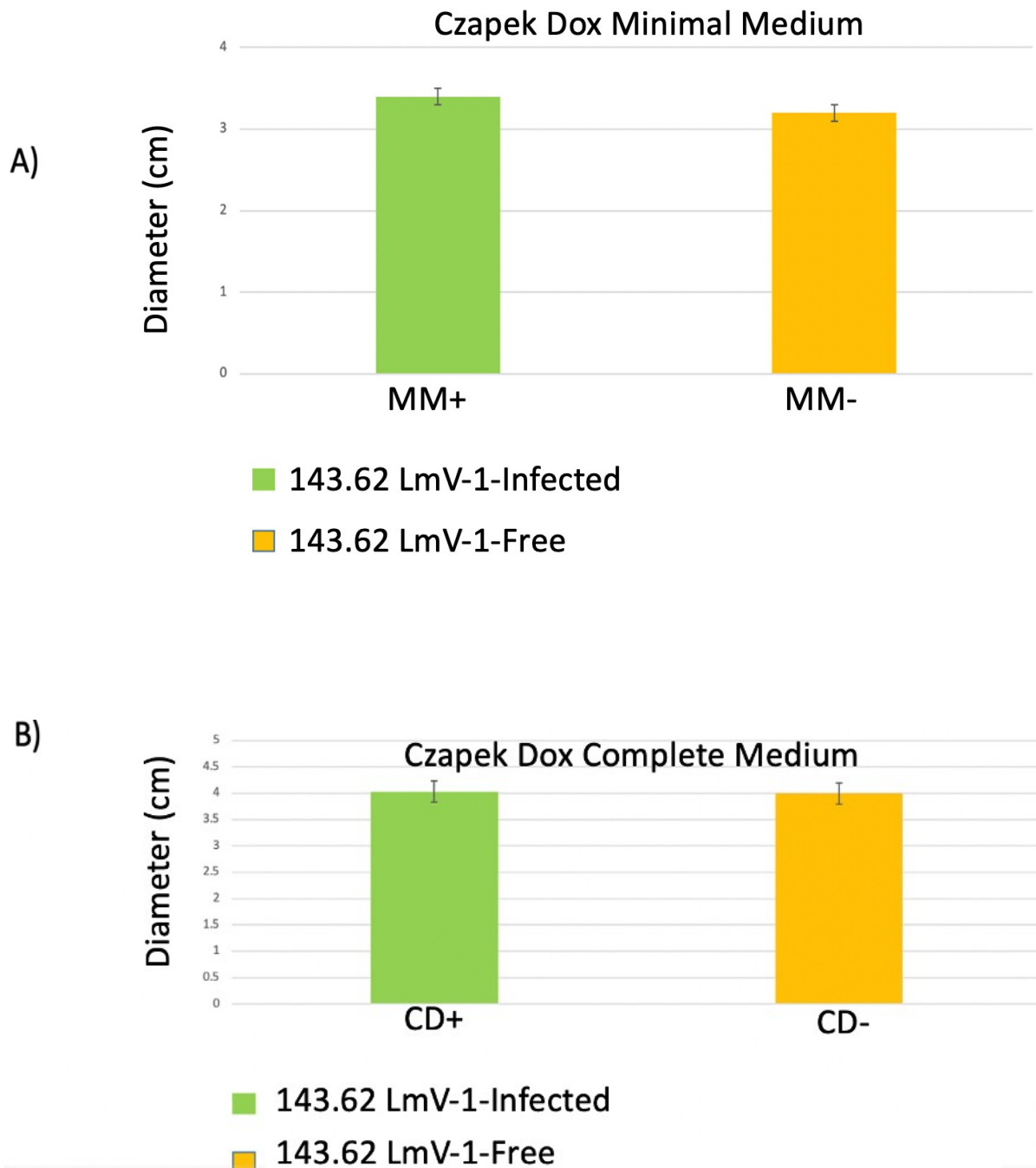


**Figure 4.1d:** Radial growth of LmV-1.I and LmV-1.F *Lecanicillium muscarium* isolate 143.62 after 18 days Petri plate culture on (A) Czapek-Dox MM; and (B) Czapek-Dox CM (P – value < 0.005).

#### **4.1.5 Vegetative growth of virus-infected and virus-free isogenic lines of *Beauveria bassiana* isolates EABb 92/11-Dm and ATHUM 4946 on media containing different carbon and nitrogen sources**

Knowledge of the nutritional requirements for the culture of any particular microorganism is crucial for virulence assays. Proteins, lipids and carbohydrates are comprised of macro elements including hydrogen, nitrogen, carbon, phosphorus and sulphur are all involved in several mechanisms such as host pathogen interactions and self defence mechanisms.

This *in vitro* study of the mycelial growth of VI and VF isogenic lines of *B. bassiana* isolates EABb 92/11-Dm and ATHUM 4946 concerned the effects of different carbon and nitrogen sources incorporated into Czapek-Dox media (Appendix Part B Table S4.1.5). All isogenic lines grew more prolifically on all nitrogen supplemented media as compared to growth on Czapek-Dox basal medium. The nitrogen sources investigated include ammonium nitrate, potassium nitrate and sodium nitrite (Appendix Part B Figure S4.1.5c) and after 18 days culture VF isolates grew significantly faster than VI isolates (Figure 4.1f). However, in similar experiments using carbon supplementation of Czapek-Dox media growth patterns varied between different incorporated carbohydrates (Appendix Part B S4.1.5b). For example, after 18 days culture VI isolates grew significantly faster than VF isolates on media supplemented with sucrose, glucose, trehalose, glycerol, and lactose but the opposite result was found for fructose and maltose (P-value < 0.05; Figure 4.1e).

For entomopathogenic fungi, such as *B. bassiana*, assimilation of alpha-glucosides, in particular, trehalose, the major carbohydrate constituent of the insect haemolymph, has been theorised to represent an essential factor for infectious growth within the insect hemocoel (Pendland *et al.*, 1993). Trehalose [alpha-D-glucopyranosyl-(1,1)-alpha-D-glucopyranoside], the non-reducing disaccharide of glucose, is the principal circulating hemolymph sugar of most insects (Thompson, 2003), therefore trehalose utilization is an essential element during fungal

infection of insects (Xia *et al.*, 2002a). There are two mechanisms for trehalose utilization in fungi. The first mechanism is the secretion of trehalase enzymes to hydrolyze extracellular trehalose into glucose, followed by uptake and assimilation of the resultant glucose. Another method is by the direct uptake of trehalose *via* active transport and the subsequent intracellular catabolism of the carbohydrate. Homologs of a glucoside transporter found in *Saccharomyces cerevisiae* called AGT1 are encoded in *B. bassiana*, it is involved in growth and development on a variety of alpha-glucosides including sucrose, trehalose, and maltose (Wang *et al.*, 2013). Gene disruption of *B. bassiana* AGT1 resulted in a strain with reduced growth and development. Furthermore, *BbAGT1* is involved in germination, vegetative growth and conidial yield on various carbohydrate carbon sources. The  $\Delta BbAGT1$  strain displayed reduced virulence in both topical and intrahemocoel injection insect bioassays, which suggests that it is involved in cuticle penetration events and assimilation of nutrients from the host (Xia *et al.*, 2002b). Growth of VI isolates on trehalose and sucrose was significantly higher than the VF isolates (Figure 4.1e) which might indicate mycoviral infection of both EABb 92/11-Dm and ATHUM 4946 isolates may upregulate the of *BbAGT1* gene enabling the maximum utilization of trehalose and sucrose. On the other hand, fructose, where increased growth of VF isolates was observed, is not considered as a substrate for Agt1p transporters.

Varga *et al.* (2003) showed that 7 dpi *B. bassiana* isolates exhibited highest spore yields in media containing 36 gL<sup>-1</sup> carbohydrate and a carbon/nitrogen ratio of 10:1. Additionally, these fungi produce a collection of hydrolytic enzymes used in cuticle penetration (Charnley & St. Leger, 1991). Proteolytic enzymes together with lipases and chitinases are key elements for entomopathogenic fungi growth (Samuels & Paterson, 1995). A serine protease called Pr1 has a major role in insect penetration and subsequent pathogenicity (St. Leger *et al.*, 1996). The factors responsible for protease expression in *B. bassiana* are still unknown (Urtz & Rice, 2000), the carbon and/or nitrogen source may be involved in the expression of the *pr1* gene

inconidia. Vegetative growth on different carbon-based sources of both isolates appears to be relatively higher as compared to nitrogen-based sources with the majority of instances of increased growth of VI isolates, whereas vegetative growth on nitrogen-based sources indicates lower growth as compared to carbon-based sources. The VF isolates exhibited increased growth on nitrogen-based sources as compared to the VI isogenic lines which exhibit a characteristic slower growth pattern.

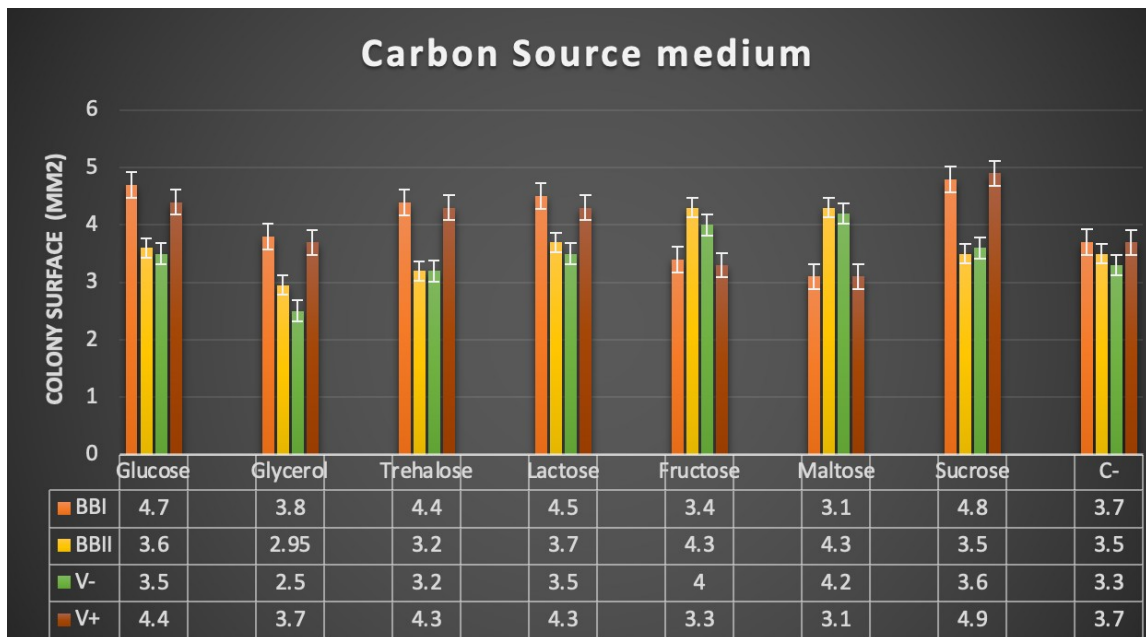


**Figure 4.1e** Growth of *Beauveria bassiana* isolates EABb 92/11-Dm PmV-1.I (BBI) and PmV-1.F (BBII) and ATHUM 4946 PmV-3.F (V-) and PmV-3.I (V+) isogenic lines after 18 days of incubation on Czapek-Dox media containing different carbohydrates. 2-way ANOVA; indicates P-value < 0.0001. Taken from Filippou *et al.* (2021).

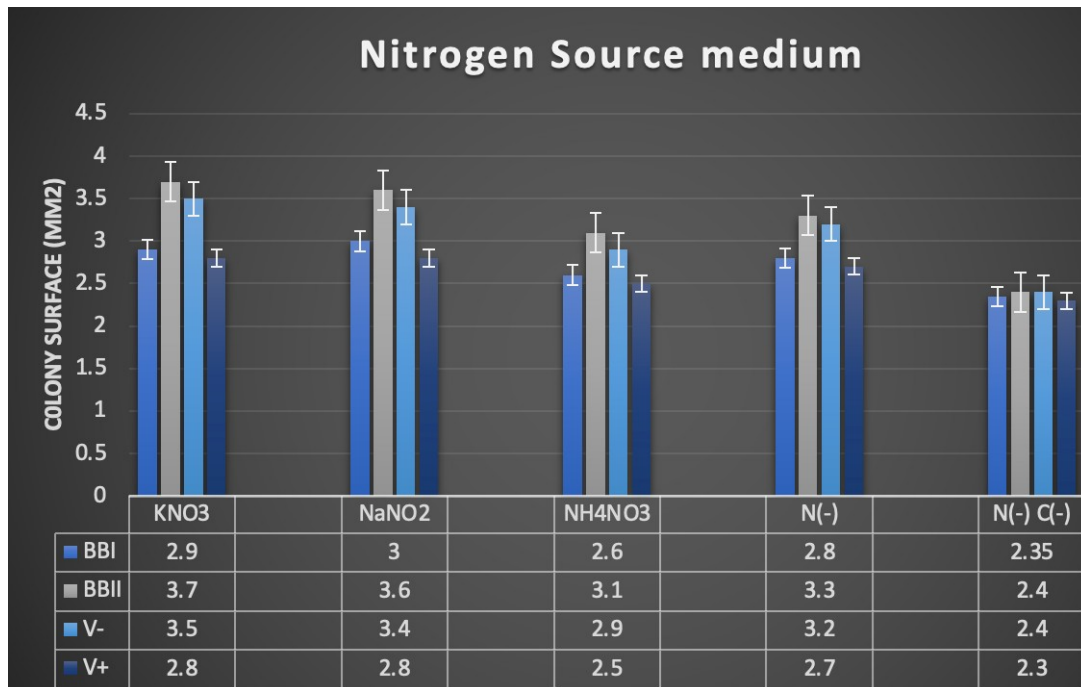


**Figure 4.1f** Growth of *Beauveria bassiana* isolates EABb 92/11-Dm PmV-1.I (BBI) and PmV-1.F (BBII) and ATHUM 4946 PmV-3.F (V-) and PmV-3.I (V+) isogenic lines after 18 days of incubation on Czapek Dox media containing different nitrogen-based source. 2-way ANOVA; indicates P-value < 0.0001. Taken from Filippou *et al.* (2021).

To summarize, the opposite phenotype in the case of maltose and fructose is due to both a significant (P-value < 0.0001) growth increase of the VF strains and a significant (P-value < 0.001) growth decrease of the VI isogenic lines. This may be attributed to potential effects of polmycoviruses on the metabolic pathway prior to the conversion of these sugars to glucose, such as the alpha/beta-glycosidase encoded by the *agdC* gene that cleave the alpha (1,4) glycosidic bond of maltose to yield glucose molecules. Since glucose is a direct substrate for glycolysis, the first step of respiration, and all other sugars need to be catabolised and/or modified to be utilised, it is possible that polmycoviruses affect a metabolic process downstream of glycolysis.

By contrast, the VI isogenic lines grow consistently slower (P-value < 0.0001) on any nitrogen source other than sodium nitrate. Nitrate is converted to nitrite and then to ammonia/ammonium, which can be used for amino acid biosynthesis. Therefore, it is likely that polmycoviruses specifically affect the uptake and/or the assimilation of sodium nitrate.

## **4.2 Investigation of *Beauveria bassiana* isolates pathogenicity against live insects**

### **4.2.1 *Tenebrio molitor* (army mealworm beetle) larvae**

The *Tenebrio molitor* (army mealworm beetle, Figure 4.2a) model was used in order to compare the virulence of isogenic lines of *Beauveria bassiana* EABb 92/11-Dm (PmV-1.I) and EABb 92/11-Dm (PmV-1.F), *Beauveria bassiana* strain ATCC 74040, also known as Naturalis and *Beauveria bassiana* strain GHA also known as BotaniGard.

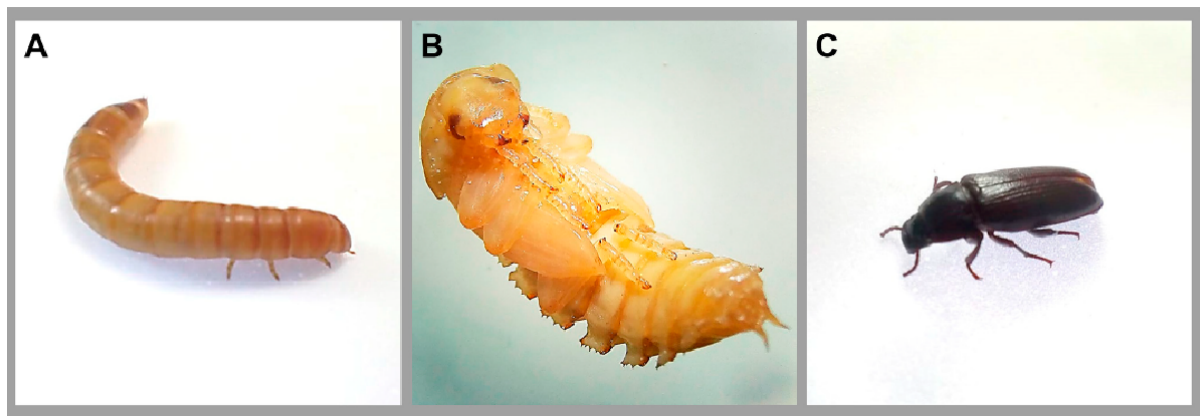


**Figure 4.2a** Lifecycle of the beetle *Tenebrio molitor*: (A) larval stage, (B) pupal stage, and (C) adult stage. Taken from de Souza *et al.* (2015).

*Tenebrio molitor* larvae in the final instar stage were obtained from BioSupplies (Australia) and stored prior to use in wood shavings in the dark to prevent pupation. Only yellow-coloured larvae were chosen for experiments and were used within 5 days of delivery. Ten larvae weighing approximately 0.2 g each were chosen at random and all experiments were duplicated and repeated on two independent occasions.

#### **4.2.2 Injection and spray inoculation of *Tenebrio molitor***

To examine the virulence of the different fungal isolates two methods were used to infect *T. molitor* larvae: a) by injecting 5  $\mu$ L of fungal spore suspension (Figure 4.2b) by spraying a fungal spore suspension as described in detailed in Section 2.16. Prior to infection fungal spores were harvested, and the viability of the spores was checked as described in Section 2.15.



**Figure 4.2b** *Tenebrio molitor* infection model system. A) Larvae weighing *ca.* 0.2 g with clear, uniform colour. B) Inoculation was achieved by injecting the inoculum into the hemocoel, at the second visible sternite above the larval legs, in the ventral portion. C) Black arrows indicate dead larvae with characteristic melanization. Taken from de Souza *et al.* (2015).

### 4.2.3 Survival assay

As different *B. bassiana* strains have different growth and sporulation rates resulting in differences in virulence preliminary experiments were designed to determine the optimal spore concentrations to facilitate clear observations of the pathogenicity of the PmV-1.I, PmV-1.F, Naturalis and BotaniGard isolates (Section 2.14).

With this aim, mealworm larvae were injected and sprayed with serially diluted spore suspensions ranging in concentration from  $1 \times 10^4$  to  $1 \times 10^7$  spores. Two isolates were examined the PmV-1.I isolate, which has increased sporulation and growth as compared to the PmV-1.F isolate which exhibited similar sporulation and growth rate to the Naturalis and BotaniGard isolates (Appendix Part B Figure S6.1a and Figure S6.1b). An infectious dose of  $1 \times 10^7$  spores/larva resulted in 100% mortality within six days after spray inoculation and 48 h after injection with the PmV-1.I (also known as BBI) isolate whilst a dose of  $1 \times 10^4$  spores/larva was uninfecious. A concentration of  $1 \times 10^5$  spores/larva was chosen as optimal for larval injection since its intermediate pathogenicity level facilitated determining differences in virulence between the different isolates, whilst a concentration of  $1 \times 10^7$  spores/larva was chosen as optimal for spraying (Section 2.16).

Infected larvae were incubated in Petri dishes in the dark at 25 °C for 10 days and mortality was recorded daily together with observations on melanisation and lack of motility. Likewise, after larval death mycosis were recorded daily (Figure 4.2c). Survival curves were plotted and statistically analysed according to Kaplan-Meier estimation using the GraphPad Prism 8.0 software and *P* values were estimated using R studio Welch's t-test. Moreover, there were statistically significant differences in the survival rates of PmV-1.I compared to the other isolates (Figure 4.2d). As observed, PmV-1.I demonstrated significantly (*P*-value < 0.05) increased mortality when compared to

BotaniGard, to Naturalis (P-value < 0.022) and to PmV-1.F (P-value < 0.045) by spraying.

Similar increased mortality was observed using the injection method, PmV-1.I compared to BotaniGard (P-value < 0.05), Naturalis (P-value < 0.04) and PmV-1.F (P-value < 0.06). This suggested that the PmV-1.I isolate was more virulent than the other three isolates in *T. molitor*.

Lethal time (LT<sub>50</sub>) is a statistically calculated average time interval during which 50% of a given population may be expected to die following acute administration of an agent, in this case a spore suspension from *B. bassiana*, at a given concentration. Subsequently, R statistical software was used to perform a logistic regression to determine the correct LT<sub>50</sub> in controlling *T. molitor* larvae. For spray assay PmV-1.I had the smallest LT<sub>50</sub> of 4.5 days compared to BotaniGard 5.1 days, Naturalis 5.3 days and VF 5.7 days (Appendix Part B Table S4.2.2a). The differences in LT<sub>50</sub> between isogenic lines PmV-1.I and PmV-1.F is evident with a difference of 1.2 days demonstrating once more the hypervirulence caused by the presence of BbPmV-1. Likewise, for the injection assay PmV-1.I again had the smallest LT<sub>50</sub> of 3.5 days, BotaniGard 3.8 days, PmV-1.F 3.9 days, and Naturalis 4.7 days (Appendix Part B Table S4.2.2b). Similarly, isogenic lines demonstrate different values of LT<sub>50</sub> with PmV-1.I exhibiting the smallest, however the difference between them is not as high as the one above. More specifically the difference in LT<sub>50</sub> between all isolates is not dissimilar to that observed in the spray method. This observation might indicate the difference in pathogenicity of each isolate and how quick they can establish infection. Additionally, LT<sub>50</sub> of PmV-1.I following injection has a difference of 24 h as compared to PmV-1.I using the spray method demonstrating once more the time needed for entomopathogenic fungi to penetrate the insect cuticle and establish infection. Furthermore, as anticipated the PmV-1.I strain had the smallest LT<sub>50</sub> as compared to the

other isolates in both assays. The smaller the LT50 value the better, indicating that the time needed to kill *T. molitor* larvae is shorter.

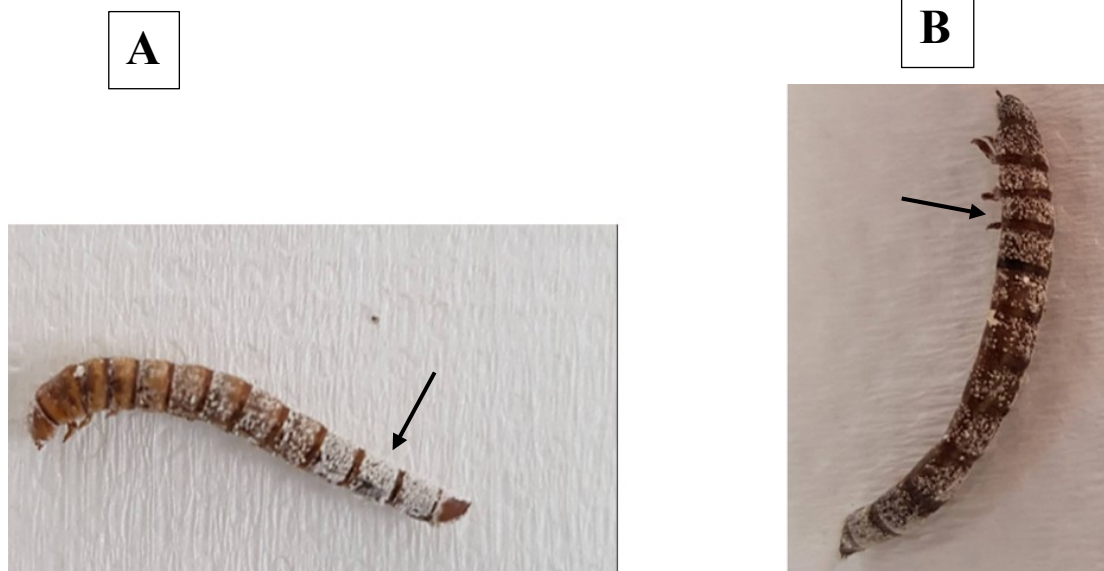
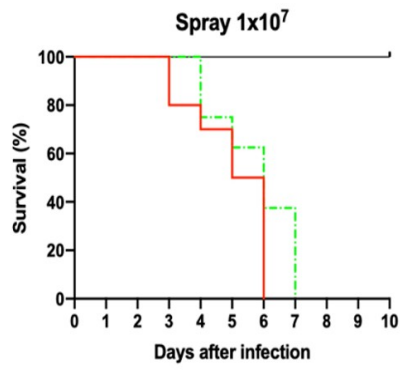


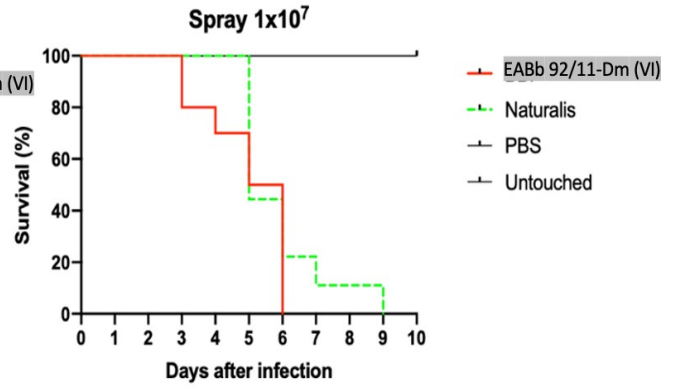
**Figure 4.2c** Mycosis (black arrows) was observed on the majority of the infected insects 72 h post-mortem. **A)** *Tenebrio molitor* inoculated with *Beauveria bassiana* EABb 92/11-Dm PmV-1.I isolate *via* injection of spore inoculation. **B)** *Tenebrio molitor* inoculated with *Beauveria bassiana* EABb 92/11-Dm PmV-1.I isolate *via* spray of spore inoculation.

(A)

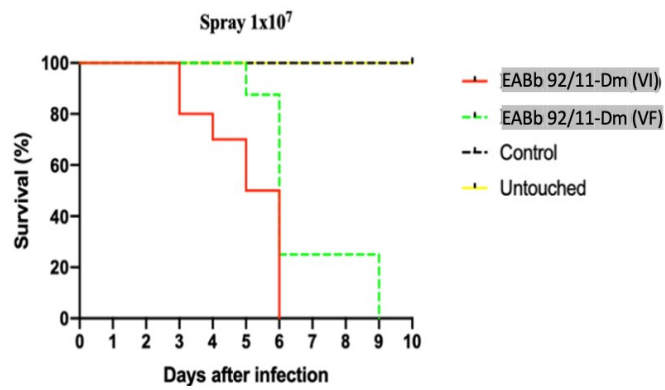
(I)



(II)

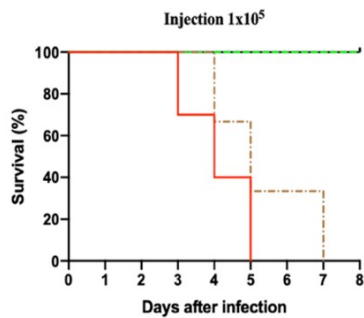


(III)

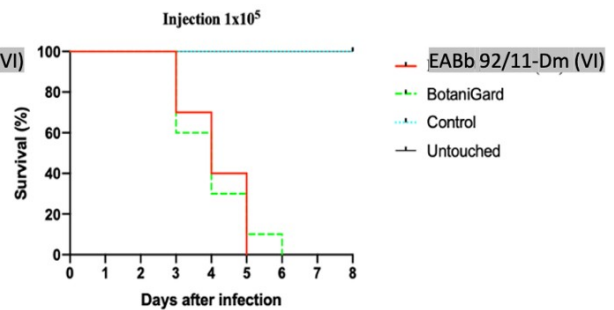


(B)

(I)



(II)



(III)

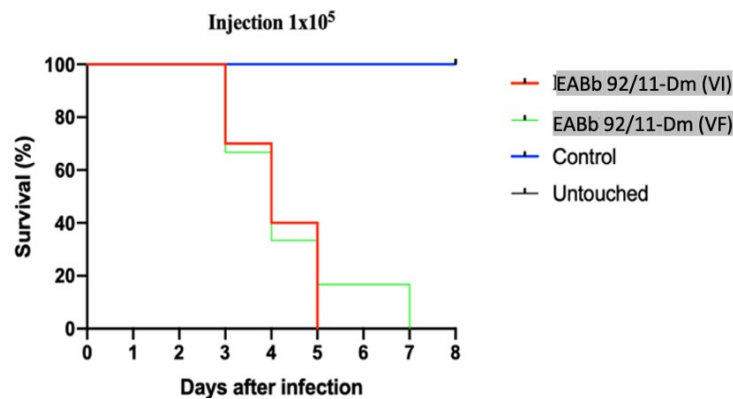


**Figure 4.2d** Survival curves of *Tenebrio molitor* larvae infected with four isolates of *Beauveria bassiana* following spray inoculation with  $10^7$  spores/larvae (A) or direct injection with  $10^5$  spores /larva(B). Infections with PmV-1.I and PmV-1.F isogenic lines of *Beauveria bassiana* isolate respectively EABb 92/11-DM (VI) and EABb 92/11-DM (VF) plus two commercial isolates Naturalis and BotaniGard were compared with PBS and untouched (insects were neither sprayed nor injected) controls. Survival curves were plotted using mean survival of *Tenebrio molitor* larvae over an 8-day incubation period. Survival curves were plotted and statistically analysed according to Kaplan-Meier estimation using the GraphPad Prism 8.0 software and P values were estimated using R studio Welch's t-test.

The results obtained clearly exhibit the crucial role of mycovirus, especially BbPmV-1, infection in mediating *B. bassiana* hypervirulence against live insects and suggest that exploiting polmycoviruses could be potentially a game changer in the pesticide industry.

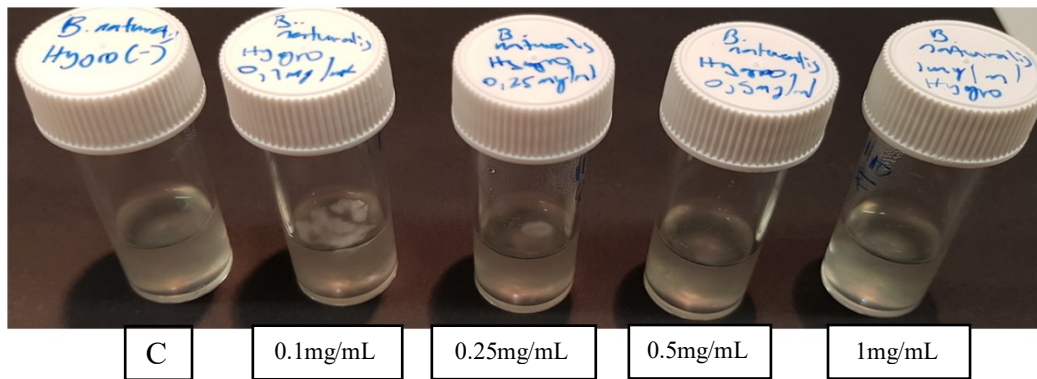
### **4.3 Evaluation of fungicides used as selection markers**

#### **4.3.1 Hygromycin B susceptibility of *Beauveria bassiana* strains**

Hygromycin is an aminoglycosidic antibiotic that targets protein synthesis in prokaryotes and eukaryotes and interferes with peptidyl-tRNA translocation (Gonzalez *et al.*, 1978; Punt *et al.*, 1987). The genes that confer resistance to HmB have been successfully isolated and characterised from *Streptomyces hygroscopicus* and *E. coli*. These genes inactivate the antibiotic through phosphorylation by HmB phosphotransferase (Malpartida *et al.*, 1983; Punt *et al.*, 1987). Based on the *E. coli hph* gene, cloning vectors conferring resistance to HmB have been constructed as selectable markers in fungi following protoplast transfection. In the majority of cases filamentous fungi are resistant to a wide range of antibiotics including some isolates of *B. bassiana*. Preliminary experiments performed by John Daudu showed that some isolates of *B. bassiana* are sensitive to HmB. It is planned to transform protoplasts of two commercial isolates of *B. bassiana*, Naturalis and Botanigard, with mycoviruses which will hopefully cause mild hypervirulence and enhanced entomopathogenic effects as determined previously for another virus-infected isolate (Punt *et al.*, 1987). To efficiently screen potential transformants it is intended to use a co-transformed selectable marker consisting of a plasmid expressing antibiotic resistance to hygromycin. The feasibility of this approach was investigated using diluted spore suspensions of fungi plated on solidified CM growth media containing 0-1000 µg/mL HmB (0 µM (control plate), 100 µM, 250 µM, 500 µM, and 1000 µM). By doing this, differences in resistance level can be observed and recorded between Naturalis and Botanigard isolates. Growth of wild type fungal colonies of both isolates was

observed in the presence of all concentrations of hygromycin after three days incubation at 25 °C indicating innate resistance to HmB (Figure 4.3a). Further experiments were performed using the overlay method to assess antibiotic sensitivity as described previously (Punt *et al.*, 1987). Spores ( $1 \times 10^7$ ) of each isolate were plated on agar plates containing CM and different concentrations of HmB (Section 2.19). After 16-20 h incubation at 25 °C the plates were overlaid with an equal volume of CM agar containing a range of concentrations of HmB as above (Section 2.19). However, growth of both Naturalis and BotaniGard isolates was observed after 3-4 days of incubation at 25 °C (Figure 4.3b) confirming innate resistance to the antibiotic. Some isolates of *B. bassiana* are known to be sensitive to HmB whilst others, such as those investigated here, are resistant. Therefore, a search for other suitable selection markers for use in protoplast transfection experiments was made which included a *Magnaporthe grisea sur* gene cassette that confers resistance to the antibiotic sulfonylurea which inhibits the acetolactate synthase enzyme is responsible for the synthesis of the amino acids isoleucine and valine (Zhang *et al.*, 2010). The potential of using the fungicide Benomyl as a selectable marker was also explored.

(A)



(B)

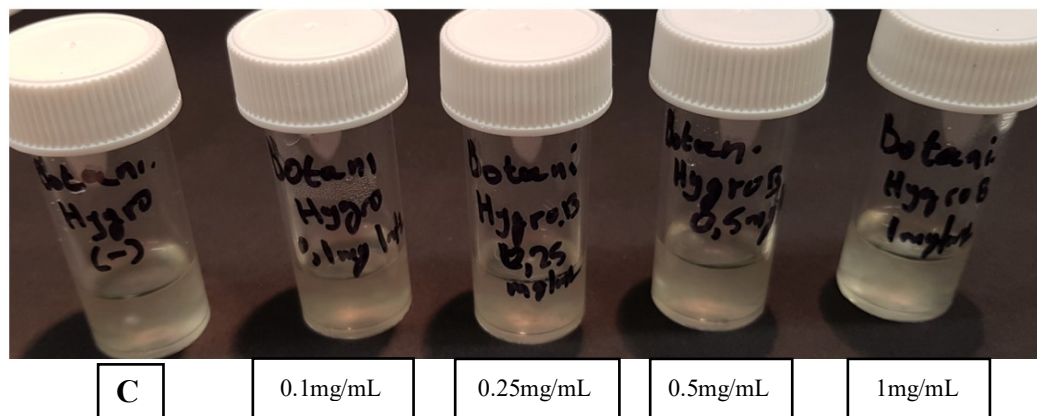


**Figure 4.3a** HmB susceptibility test of *Beauveria bassiana* Naturalis and BotaniGard isolates spore suspension ( $1 \times 10^7$ ) in liquid Czapek-Dox CM containing increasing concentrations of HmB. Both (A) Naturalis and (B) Botanigard growth are unaffected by the presence of the HmB.

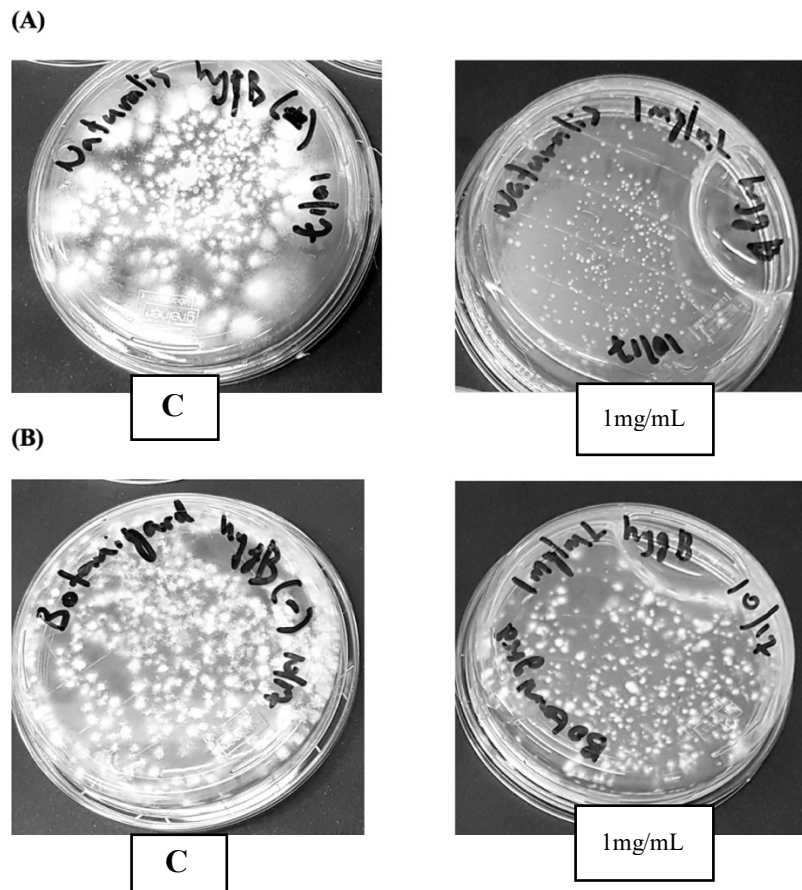


**Figure 4.3b** Overlay method; (A) A sparse growth of *Naturalis* in 1 mg/mL concentration of HmB; (B) No effect on the growth and sporulation of *Botanigard*.

Isolates	0	0.1	0.25	0.5	1	mg/mL
<i>Naturalis</i>	+	+	+	+	±	
<i>Botanigard</i>	+	+	+	+	+	

**Table 4.3a** Spore suspensions of *Beuaveria bassiana* *Naturalis* and *Botanigard* were plated on solid CM media containing 0-1 mg/mL<sup>-1</sup> HmB: The (+) sign specifies significant growth and sporulation of the fungus isolate, while (±) sign specifies sparse fungal growth.

### **4.3.2 Sulfonylurea and Benomyl susceptibility of *Beauveria bassiana* strains**

The effect of sulfonylurea and Benomyl on the growth of *B. bassiana* isolates ATCC 704040 Naturalis and GHA BotaniGard were examined. Fresh spore suspensions of  $1 \times 10^7$  conidia  $\text{mL}^{-1}$  were inoculated onto Czapek-Dox agar plates containing different concentrations of both fungicides. Benomyl at concentrations 0, 5, 7.5 and 50  $\mu\text{g/mL}$  and sulfonylurea at concentrations 0, 100, 250  $\mu\text{g/mL}$  and 1  $\text{mg/mL}$  were investigated. Both isolates grow normally on Czapek-Dox plates and in liquid media without fungicides. However, the growth of both isolates was completely inhibited by Benomyl at concentrations as low as 5  $\mu\text{g/mL}$  (Figure 4.3c). Both isolates were resistant to HmB (Figures 4.3b) and the GHA isolate was resistant to sulfonylurea both in liquid and on solid media whereas ATCC 704040 Naturalis was sensitive, and no growth was observed (Figure 4.3d). Following these observations Benomyl was chosen for use as a selection marker in future experiments.

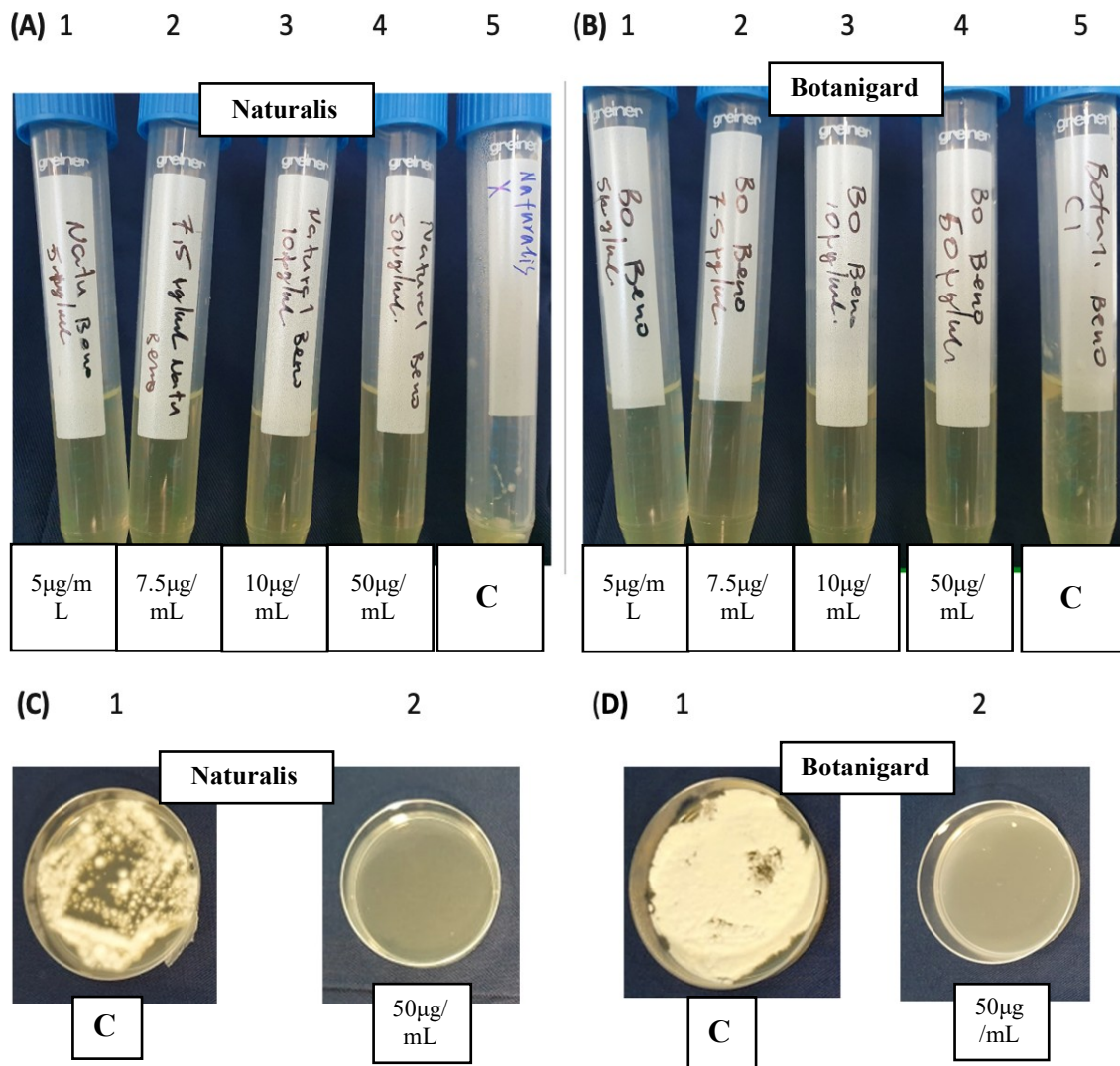


**Figure 4.3c** Benomyl sensitivity of *Beauveria bassiana* isolates ATCC 704040 Naturalis and GHA BotaniGard; A and B respectively (first panels) grown in liquid Czapek-Dox media. *B. bassiana* isolates ATCC 704040 Naturalis and GHA BotaniGard; C and D respectively (second panels) grown in solid Czapek-Dox media. Cultures were grown at 24 °C from spore suspensions ( $1 \times 10^7$ ) in liquid (A and B) and solid (C and D) Czapek-Dox media in the presence of Benomyl at concentrations of A and B): 1-5: 0, 5, 7.5, 10, and 50 µg/mL; C and D): 1-2: 0 and 50 µg/mL).

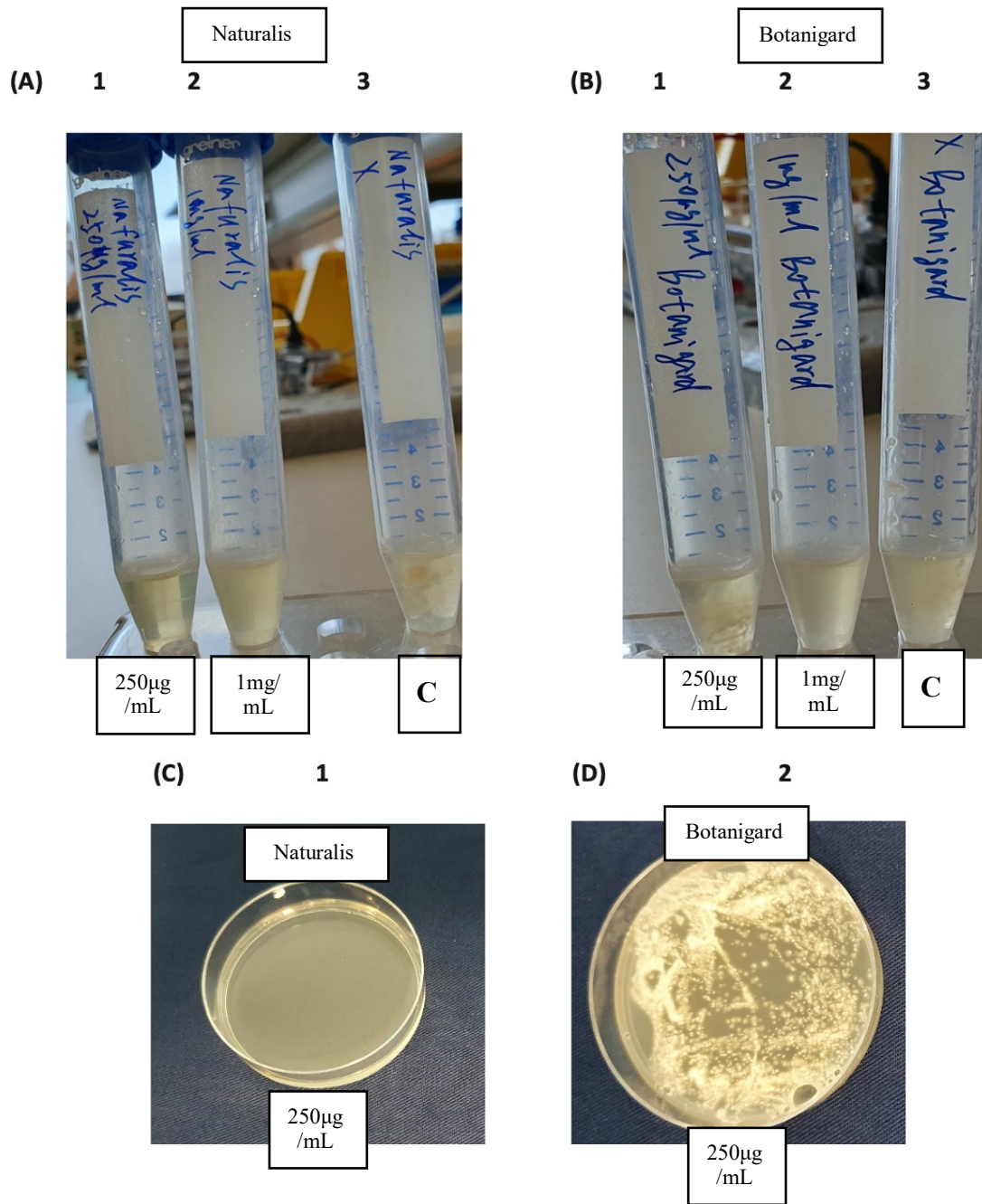


**Figure 4.3d** Sulfonylurea sensitivity of *Beauveria bassiana* isolate ATCC 704040 (Naturalis; A and C) and GHA (Botanigard; B and D). Cultures were grown at 24 °C from spore suspensions ( $1 \times 10^7 \text{ mL}^{-1}$ ) in liquid (A, B) and on solid Czapek-Dox media (C, D) in the presence of sulfonylurea in tubes 1-3 at concentrations of 0, 100, 250 µg/mL and 1 mg/mL in A and B respectively and on plates 1-2 at concentrations of 250 µg/mL in C and D, respectively. Naturalis exhibits sensitivity to Sulfonylurea in solid cultures while BotaniGard exhibits resistance.

### **4.3.3 GFP expression in *Beauveria bassiana* to study mycovirus replication and localization**

Mycoviruses are widespread in almost all major groups of fungi and most cause no obvious effects on their hosts, but some do cause obvious symptoms. The lack of knowledge and data relating to mycovirus replication and localization might be overcome by the use of protoplasts for reverse genetics investigations. In order to achieve these goals a scorable marker of successful protoplast transfection is essential and with this in mind the potential of using green fluorescent protein (GFP) as a scorable marker for gene expression was explored with *B. bassiana*. To achieve this, fungal protoplasts were transformed using pCAMsgfp plasmid (Appendix Part B Figure S4.3.3a) containing the GFP gene as well as Hygromycin B and Kanamycin A resistance cassettes, and the resultant mycelia and spores were examined by fluorescence UV microscopy. Protoplasts were isolated from *B. bassiana* ATCC 74040 and *B. bassiana* GHA BotaniGard and transfected with plasmid carrying GFP using the procedure described in section 2.17. Transfected protoplasts were then transferred onto Czapek-Dox media containing D-glucose and the cultures incubated for 14 days at 25°C in the dark. Regenerated cultures of both isolates of *B. bassiana* were spread on Czapek-Dox plates and individual colonies were selected, regrown on fresh media and the resultant cultures examined for GFP expression.

### **4.3.4 GFP expression in transformed *Beauveria bassiana***

To evaluate the expression of GFP in transformed *B. bassiana* isolates fluorescence microscopy of the transformants was performed. Fluorescence microscopy clearly showed significant expression of GFP in the hyphae and mycelia of both transformed isolates of *B. bassiana* (Figures 4.3e). No fluorescence was found in untransformed cultures of either isolate grown under identical conditions. Furthermore, fluorescence microscopy clearly demonstrated

the expression of GFP at different stages of fungal development including hyphae, mycelia, and spores (Figures 4.3e, 4.3f). These results suggest that GFP labelling will be a useful tool not only for assessing transfection efficiency but also to investigate replication and localisation of mycoviruses.

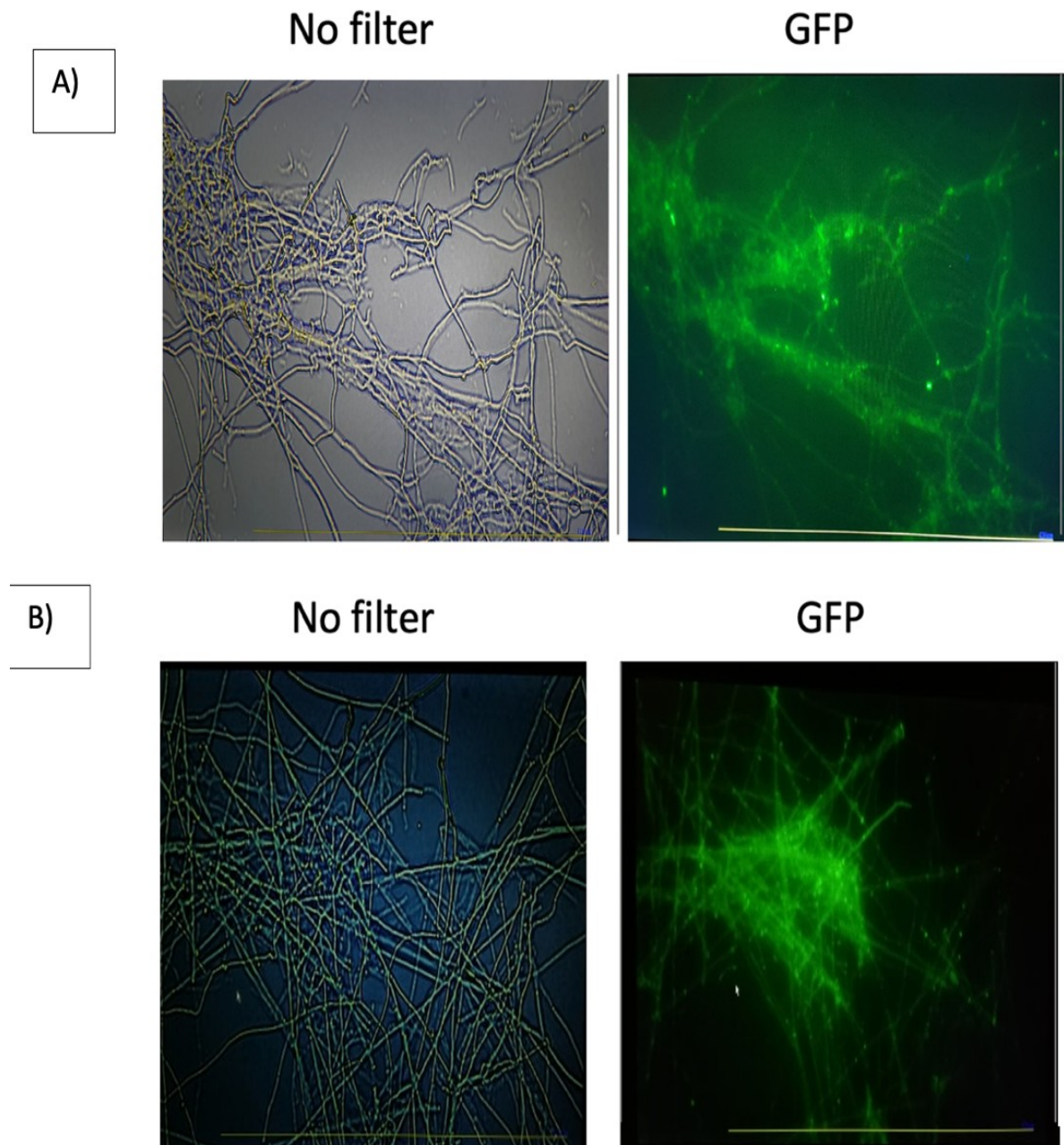


**Figure 4.3e** **A)** Fluorescence micrographs of *Beauveria bassiana* ATCC 704040 showing GFP labelled mycelia and hyphae following transfection of protoplasts using pCAMsgfp plasmid and fungus regeneration. **B)** Fluorescence micrographs of *Beauveria bassiana* GHA BotaniGard showing GFP labelled mycelia and hyphae following transfection of protoplasts with plasmid carrying GFP and fungus regeneration (400x magnification).

**No Filter**



**GFP**

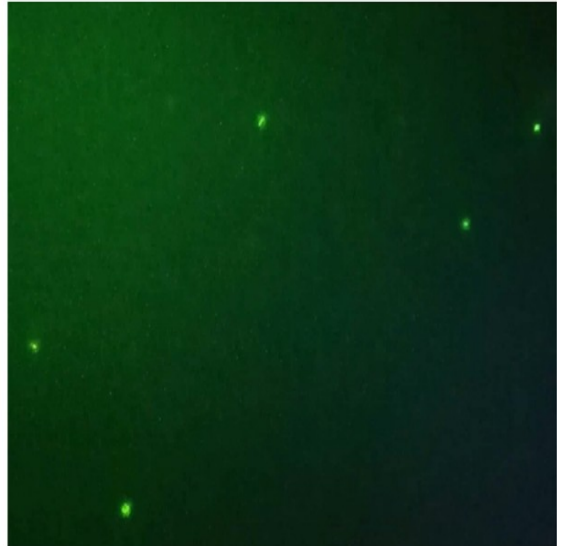
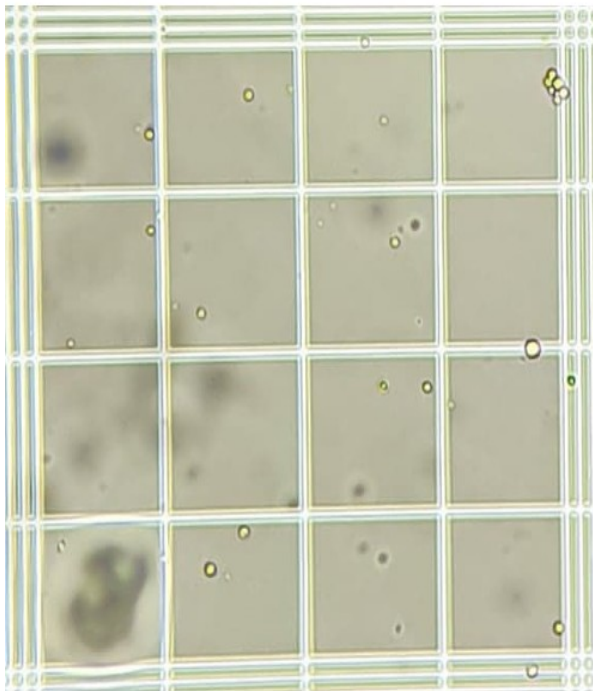


**Figure 4.3f** Fluorescence micrographs of *Beuaveria bassiana* ATCC 704040 showing GFP labelled conidiospores following transfection of protoplasts plasmid carrying GFP and fungus regeneration (400x magnification).

**(A)**



**(B)**

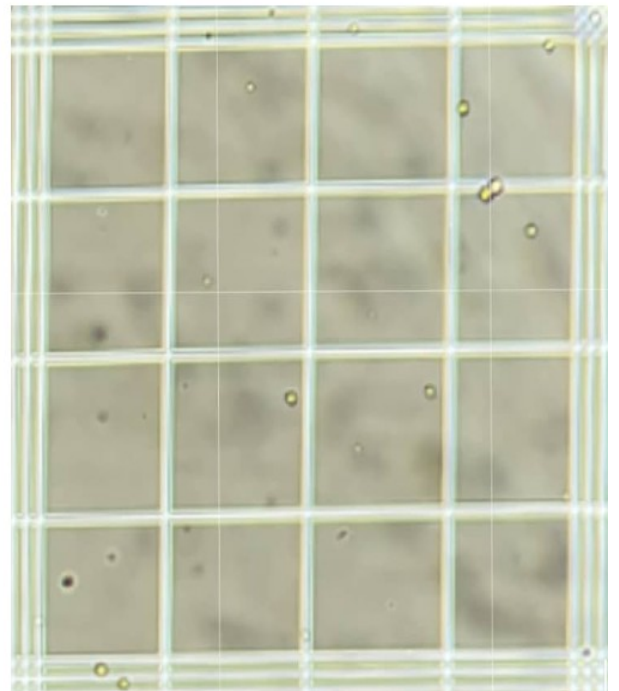


**Figure 4.3g** Protoplasts freshly isolated from *Beauveria bassiana* Naturalis (A) and BotaniGard (B) viewed in a haemocytometer with a light microscope using 400x magnification.

#### **4.3.5 Isolation of protoplasts for virus transfection and GFP expression**

To optimise the conditions for protoplast transfection attempts were initially made to introduce purified *Leptosphaeria biglobosa* quadrivirus-1 (LbQV-1) into protoplasts from a virus-free isogenic line of *Leptosphaeria biglobosa* (Section 2.17). These experiments were successful, and the presence of LbQV-1 was confirmed by RT-PCR (Figure 4.3h; Table 4.3b).

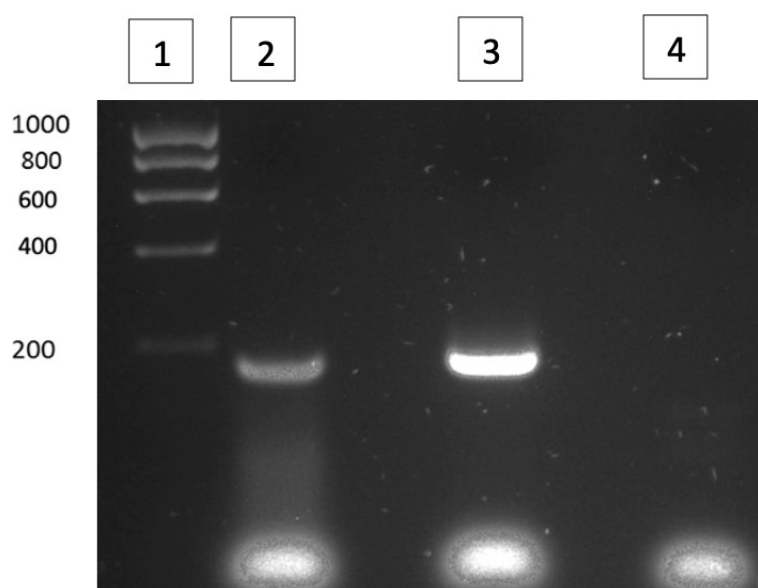


**Figure 4.3h** RT-PCR amplification of a *ca.* 180 bp amplicon from the LbQV-1 RNA genome using extracts of cultured mycelia recovered from *Leptosphaeria biglobosa* protoplasts transfected with LbQV-1 (lane 2); Lane 1, 1 kb Hyperladder marker; Lane 3, amplicon generated from a positive control of purified LbQV-1; Lane 4 water control.

**Table 4.3b:** Primer pair used for detecting the LbQV-1 in *Leptosphaeria biglobosa* transfected protoplasts.

Primer name	Primer Sequence	dsRNA	Amplicon	Organism
qPCR.LbQV1.R	5'-GCCTTGTCGTGAGTACACCA-3'	dsRNA1	183bp	<i>L. biglobosa</i>
qPCR.LbQV1.F	5'-CACCAGCATACTGCAGGGAA-3'	dsRNA1	183bp	<i>L. biglobosa</i>

Attempts were made to transfect protoplasts, isolated from the virus-free *B. bassiana* isolates ATCC 704040 and GHA, with BbPmV-1 and BbPmV-3. These transfections were performed in an attempt to make both fungal isolates hypervirulent for insect pests. Protoplasts ( $10^6$  and  $10^7$  mL<sup>-1</sup>) of both *B. bassiana* isolates were isolated from hyphal mycelia and transfected with polynucoviruses as described (Section 2.17). The optimal incubation time for isolation of viable protoplasts was established as 36 h at 25°C in the dark with shaking at 180 rpm. Cell walls of fresh mycelia were digested using 3.2% (w/v) *Trichoderma harzianum* lysing enzyme (Glucanex), the protoplasts were washed several times in isotonic buffer and examined prior to transfection to check integrity and concentration (Figure 4.3g). Polynucovirus (10 µl at 100 ng/µL per  $10^7$  protoplasts) was inoculated using PEG-mediated transfection. Transfected protoplasts were rescued, and cultures regenerated on 1% (w/v) D-glucose-enriched Czapek-Dox agar plates where they formed a lawn. Transfected fungal colonies were collected, and the mycelia subcultured. All transfectants were passaged at least 3 times and left to incubate for 15 days or until the entire Petri dish was covered with mycelia. This facilitates virus movement, subsequent infection of growing mycelia and increased virus titre in transfected cells. Transfection was confirmed following total RNA extraction from the cultures using the RNeasy Plant Mini Kit (Qiagen) and RT-PCR amplification of virus-specific amplicons ~ 850 bp in size using gene-specific primer pairs designed from the sequence of BbPmV-1. The three isolates examined here *B. bassiana* ATCC 74040 (Naturalis), *B. bassiana* GHA (Botanigard) and EABb 92/11-Dm virus-free isolate were all apparently infected with BbPmV-1 as all produced amplicons of the same expected size following RT-PCR amplification and agarose gel electrophoresis (Appendix Part B Figure S4.3.5a).

In conclusion mycoviral infections can either be symptomatic (hypervirulent or hypovirulent) or asymptomatic (cryptic). In this chapter both symptomatic and asymptomatic cases of mycoviral infections were discussed. BbPmV-1 and BbPmV-3 induced mild hypervirulence in

its fungal host in terms of conidiation, radial growth and pathogenicity, whereas no symptoms were observed with LmV-1 infected *L. muscarium* 143.62. It is not known what effects AfuPV-1A has on the phenotype and pathogenicity of its host, but it is assumed that they will be similar to those described previously by Bhatti *et al.* (2011) for AfuPV-1 where an abnormal colony phenotype, slow growth and lighter than normal pigmentation was observed.

The potential use of benomyl and GFP as scorable, selection markers for successful transfection of *B. bassiana* protoplasts with polymycoviruses is promising. Further attempts to transfect commercially available strains of the fungus to increase virulence will be attempted in the future using these selectable markers.

# **Chapter 5**

**Comparative transcriptomic analysis of the virus-free and the BbPmV-1- infected *Beauveria bassiana***

**EABb 92/11-Dm isolate**

Entomopathogenic fungi such as *B. bassiana* are promising biopesticides for the control of a wide range of insect pests. Indeed, infection with *B. bassiana* reduces the lifespan of different insect pests in the laboratory as well as in the field. Studies have demonstrated that wild type *B. bassiana* isolates can show up to 10-fold differences in virulence between the most and the least virulent isolates (Brownbridge *et al.* 2001). Entomopathogenic fungi have great potential as biological control agents of insect pests as well as for vector-borne diseases. They offer significant advantages as compared to classic chemical approaches to control insect populations: besides excellent cost-benefits, they also infect immediately following direct contact with the insect cuticle, are considered environmentally friendly and are extremely effective in insecticide-resistance or integrated vector management programs. The time required to kill any particular insect varies greatly and may range from days to weeks; it is affected by several factors, including the large variability in the pathogenicity of different fungal isolates (Figure 4.2d). This variability may be due to the fungal genome and/or the presence of extrachromosomal elements such as mycoviruses that potentially modulate fungal virulence as demonstrated in Chapter 4 (Figure 4.2d). In this study, using transcriptomics we explored the extremes of low/high virulence of three isolates of *B. bassiana*, two of which are commercially available (Naturalis and BotaniGard) and the isogenic lines of EABb 92/11-Dm PmV-1.F and PmV-1.I. The larval form of the mealworm beetle (*Tenebrio molitor*) was used as an infection model to assess the impact of polymycoviruses on the fungal host, by sequencing messenger (m) RNA 3'-termini and applying a genome comparison approach to uncover genetic mechanisms underpinning virulence.

### **Aims and scope**

The aim of this chapter is to study the effects of BbPmV-1 on the virulence of the entomopathogenic fungus EABb 92/11-Dm at the molecular level. Assessment of virulence in the presence and absence of polymycoviruses in *B. bassiana* is crucial to understanding its

pathogenicity. Total RNA of EABb 92/11-Dm PmV-1.I (BBI) and EABb 92/11-Dm PmV-1.F (BBII) isogenic lines of *B. bassiana* was extracted and used to build libraries for RNA-seq. Analysis of the results will clarify as to how BbPmV-1 affects and mediates mild hypervirulence in the *B. bassiana* EABb92/11-Dm isolate.

### **5.1 Harvesting mycelia from PmV-1.F and PmV-1.I isogenic lines at different time points**

To investigate the effects of the viral infection on the EABb 92/11-Dm isolate, mycelia from PmV-1.I and PmV-1.F isogenic lines were grown on solid PDA plates and individual samples harvested at 4, 7, 10, 14, and 21 dpi. Total RNA extraction, library construction and paired end Illumina sequencing were performed. The quality of the sequencing data was assessed using FASTQC (Section 2.18.1.1) and improved by clipping residual adapters and trimming low quality bases using Trimmomatic (Section 2.18.1.2).

#### **5.1.2 Analysis of NGS of RNA isolated from *Beauveria bassiana* infected *Tenebrio molitor***

*Tenebrio molitor* larvae were inoculated with PmV-1.I and PmV-1.F isogenic lines of *B. bassiana* EABb 92/11-Dm and *B. bassiana* isolates Naturalis and BotaniGard. Forty-eight hours post infection three sample larvae were randomly selected from inoculations with each fungal isolate and subjected to total RNA extraction. Thereafter library construction and paired end Illumina sequencing were performed as in Section 2.12. Likewise, the quality of the sequencing data was assessed and improved as in Section 2.18.

### **5.2 Genome structural annotation of EABb 92/11-Dm**

The first step before annotating the genomic data is quality control: I used Kraken to determine the microbial composition and determine if there was any evidence for any contamination. For PmV-1.I and PmV-1.F isolates grown on PDA in a time course alignment of the RNA-seq

reads with the *B. bassiana* (ASM28067) genome using Bowtie2 revealed that >90% of the reads were derived from *B. bassiana*. However, some reads aligned with other fungi most probably because of conserved regions in fungal genomes (Appendix Part B Table S5.2a and S5.2b). Likewise, alignment of the reads with the *T. molitor* genome revealed that >90% of the reads were derived from the insect while the remaining reads mostly aligned with *B. bassiana*. However, some reads were aligned to other fungi such as *Aspergillus flavus*, probably either these alignments might be due to conserved regions or this is a case of competition for space between pathogens (Appendix Part B Table S5.2c and Table S5.2d). Last but not least, several reads from 21 dpi time point aligned with a viral sequence identified as *Beauveria bassiana* RNA non-segmented virus 1 (BbNV-1), which was first isolated from *B. bassiana* isolate EABb 92/11-Dm (Appendix Part B Figure S5.2) by Kotta-Loizou *et al.* (2015). It is known that this *B. bassiana* isolate is also infected with a polymycovirus Kotta-Loizou *et al.* (2015) but no reads matching a second virus were identified in this study.

High-throughput sequencing of genomes (DNA-seq) and transcriptomes (RNA-seq) allows us to study the genetic and functional information within an organism. For instance, RNA-seq facilitates the investigation of transcript structure (e.g., alternative splicing), and allelic information (e.g., SNPs) (Hass *et al.*, 2013).

Genome alignment and *de novo* assembly steps involved at first, the reads alignment to the genome, and next the *de novo* assembling of the read sequences into transcripts. The resulting transcripts are then aligned to the genome using a cDNA alignment tool, and finally PASA is used for assembling any overlapping alignments and obtaining gene structure annotations (Trapnell *et al.* 2010).

In summary the crucial first step of a successful annotation of any genome is identifying whether its assembly is ready for annotation or not. To achieve this there are few useful summary statistics one can use such as the average gap size of a scaffold, the average number

of gaps per scaffold or N50 which indicate the completeness and contiguity of a genome assembly (Trapnell *et al.* 2010).

### **5.2.1 Counting, normalisation and differential expression**

There are many steps involved in analysing RNA-Seq data. Hence, the first step in the differential expression (DE) analysis workflow is count normalisation, which is necessary to make accurate comparisons of gene expression between samples. The counts of mapped reads for each gene are proportional to the expression of RNA (“interesting”) in addition to many other factors (“uninteresting”) as defined by Robinson and Oshlack (2010). Normalisation is the process of scaling raw count values to account for the “uninteresting” factors. In this way, the expression levels are more comparable between and/or within samples.

In this study, we have begun the analysis with the processing of the raw reads (FASTQ files) using a general fastq quality control tool (FastQC) to examine the quality of the sequencing run (Section 2. 18.1.1). Next, we have aligned the reads to eleven reference genomes (Table S5.2.1a). Then the reads were mapped to each gene using Bowtie and BWA and next the mapped reads were counted using HTSeq. This has resulted in a table of counts, which is what we performed statistical analysis to determine differentially expressed genes. It is important to mention the significance of pinpointing the exact 3’ end through manual curation (Figure 5.2a) for analysing our data due to the use of the 3’ Lexogen gene expression quantification (Haas *et al.* 2013).

The next important step before DE analysis was to normalise for library size and then normalise with TMM (Trimmed Mean of  $M$  -values). Raw counts mapped to a given gene cannot be compared between samples; similar rules apply for raw counts of different genes within one sample. Since some transcripts will be longer, more reads will be mapped to them compared with shorter transcripts. Therefore, the first step we followed before the DE analysis was to

normalise the counts using normalise expression unit TPM (Transcripts Per Million), which is important in removing technical biases such as erasing information about library size. Multiple biases can be encountered in RNA-seq experiments such as library size, which is a well-known bias, and gene length (is necessary for comparing expression between different genes within the same sample). Further TMM normalisation to remove the batch effects was performed before conversion to TPM via software called DEW (<https://github.com/alpapan/DEW>).

So, in few words, we use TMM normalisation through the Trinity pipeline as part of the DE analysis with edgeR, where it has been applied to count the data. Later on, separately, we used it to normalise the TPM values to be used for making the expression box plots (Haas *et al.* 2013). The rescaled TPM values are no longer proper TPM values (they do not sum to one million per sample) but continue to be treated as relative expression values (Zhao & Stanton, 2020). The resulting “normalised expression values” were used for DE analysis.

#### Definitions:

- **TPM** (transcripts per kilobase million; counts per length of transcript (kb) per million reads mapped). Accounted factors; sequencing depth and gene length. Recommendations for use; gene count comparisons within a sample or between samples of the same sample group (Zhao & Stanton, 2020).
- EdgeR’s trimmed mean of  $M$  -values (**TMM**; uses a weighted trimmed mean of the log expression ratios between samples). Accounted factors; sequencing depth, RNA composition, and gene length. Recommendations for use; gene count comparisons between and within samples and for DE analysis (Zhao & Stanton, 2020).

### **5.2.2 Manual curation of structural annotation**

Computer algorithms—such as Augustus, and GeneMark search for patterns in DNA sequence that define a gene, including a start codon, amino acid codons, intron/exon boundaries, and a stop codon (Hoff *et al.*, 2016). Homology-based programs look for similarities between the genome sequence and independent RNA and protein evidence from the organism under study and from related organisms (Keilwagen *et al.*, 2018). Trustworthy curation relies on data input from other scientists who discovered discrepancies in the specific genes.

Manual curation for genes of interest, was performed after genome annotation, evaluating one gene at a time, adding information and making corrections, which would eventually provide us with high quality genome data. Notably, during this study eleven *B. bassiana* genomes underwent a round of manual annotations using Apollon (a desktop graphical annotation system). Genes of interest were manually curated to detect UTRs, introns-exons, start and stop codons, and alternative splicing. Some of the manually curated genes are shown below. Due to the use of the 3' Lexogen gene expression quantification, it was important to accurately detect the UTRs in order to check if the reads were assigned correctly, which that will provide as with an accurate expression profile of each gene individually (Figure 5.2a).

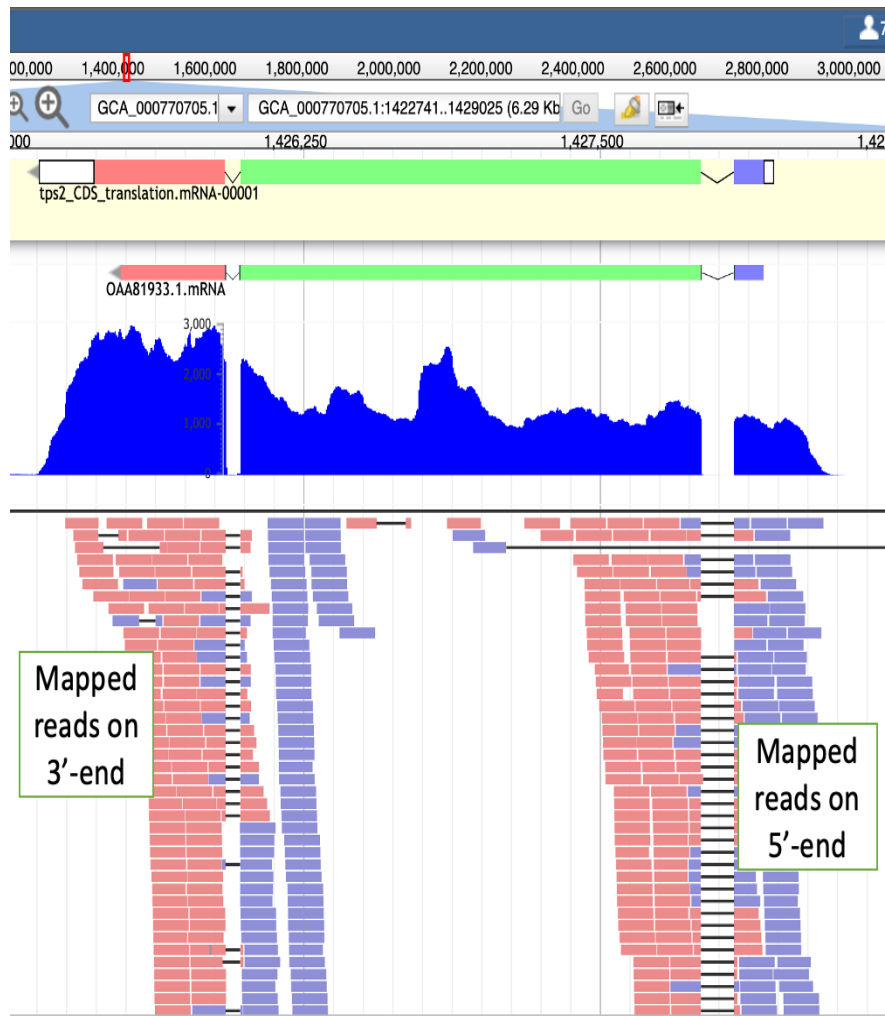


**Figure 5.2a** TPS2 gene, white regions are the UTRs that were allocated using evidence such as “Public RNA coverage” and “intron/exon junction reads”. Link access to the WebApollo curation site:

([https://curations.stressedfruitfly.com/apollo/77156/jbrowse/index.html?loc=GCA\\_000770705.1:1424586..1429497&tracks=VirulenceFactors,JunctionReads,Public%20RNASeq%20coverage](https://curations.stressedfruitfly.com/apollo/77156/jbrowse/index.html?loc=GCA_000770705.1:1424586..1429497&tracks=VirulenceFactors,JunctionReads,Public%20RNASeq%20coverage))

Bbatg1 gene, an  $\alpha$ -glucose transporter, responsible for fungal virulence, host colonization, germination and conidial yield (Wang *et al.*, 2013) after curation was found to be an alternative spliced isoform (Figure 5.2b). Alternative splicing allows multiple proteins to be expressed from a single gene and is important for numerous biological processes (McGuire *et al.*, 2008). It is unknown what the exact function of the alternative spliced Bbatg1 gene would be, but it is assumed that will be similar to Bbatg1.

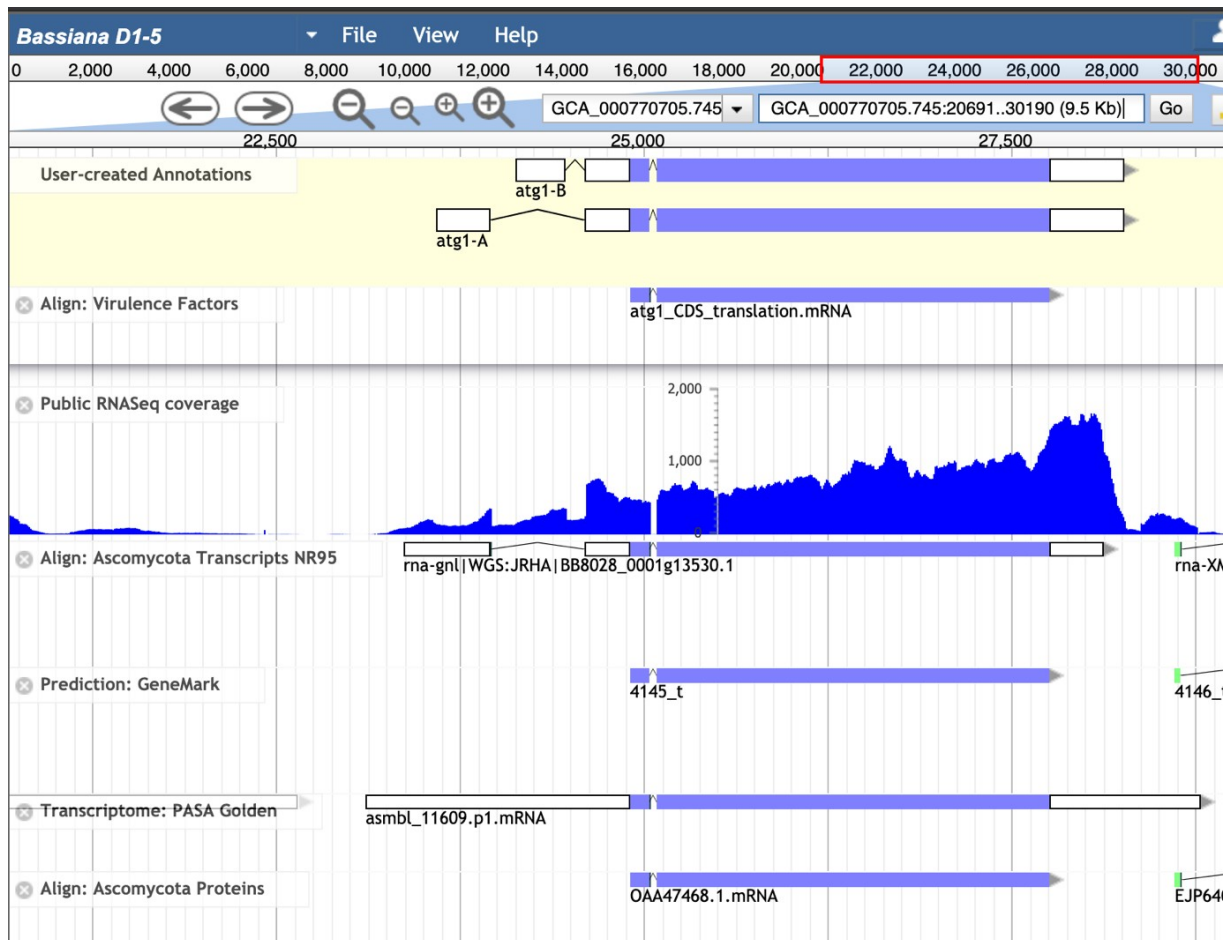


**Figure 5.2b** Curation of an alternative spliced isoform in the ATG1 gene. The Apollo editing window shows a “User-created annotation” at the top, followed by incorrect atg1\_CDS\_translation.mRNA (“Virulence Factors”). Public RNASeq coverage shows the RNA coverage, which was used to allocate the UTRs, followed by other gene prediction software such as GeneMark, Augustus, and PASA and interestingly none of these managed to suggest the alternative spliced isoform. Link access to the WebApollo/JBrowse curation site: ([https://curations.stressedfruitfly.com/apollo/77156/jbrowse/index.html?loc=GCA\\_000770705.745:20690..30190&tracks=AscomycotaProteins,VirulenceFactors,JunctionReads,Public%20RNASeq%20coverage,AscomycotaTranscriptsNr95,GeneMarkPred,PASAGOLDEN](https://curations.stressedfruitfly.com/apollo/77156/jbrowse/index.html?loc=GCA_000770705.745:20690..30190&tracks=AscomycotaProteins,VirulenceFactors,JunctionReads,Public%20RNASeq%20coverage,AscomycotaTranscriptsNr95,GeneMarkPred,PASAGOLDEN)).

Since genome annotation provides the first insight into each organism's collection of genes, properly annotating these transcript variants and their encoded proteins is essential to producing a complete catalogue of predicted transcripts.

Another issue encountered during manual curation was that some genes appeared as single exons but RNA-seq coverage plus intron/exon junction reads evidence proved otherwise. Cdep1 gene, a subtilisin-like protease, responsible for cuticle degradation, hyphal extrusion and conidiation (Fang *et al.*, 2002) appeared as a single exon based on prediction from other organisms. However, based on RNA-seq coverage and junction reads three introns and three exons were missing. Therefore, following the evidence the gene was curated adding the UTRs as well (Figure 5.2c). Then this was cross referenced with "PASA Golden", and "Gene Mark", demonstrating that manual curation is more accurate than gene prediction software.

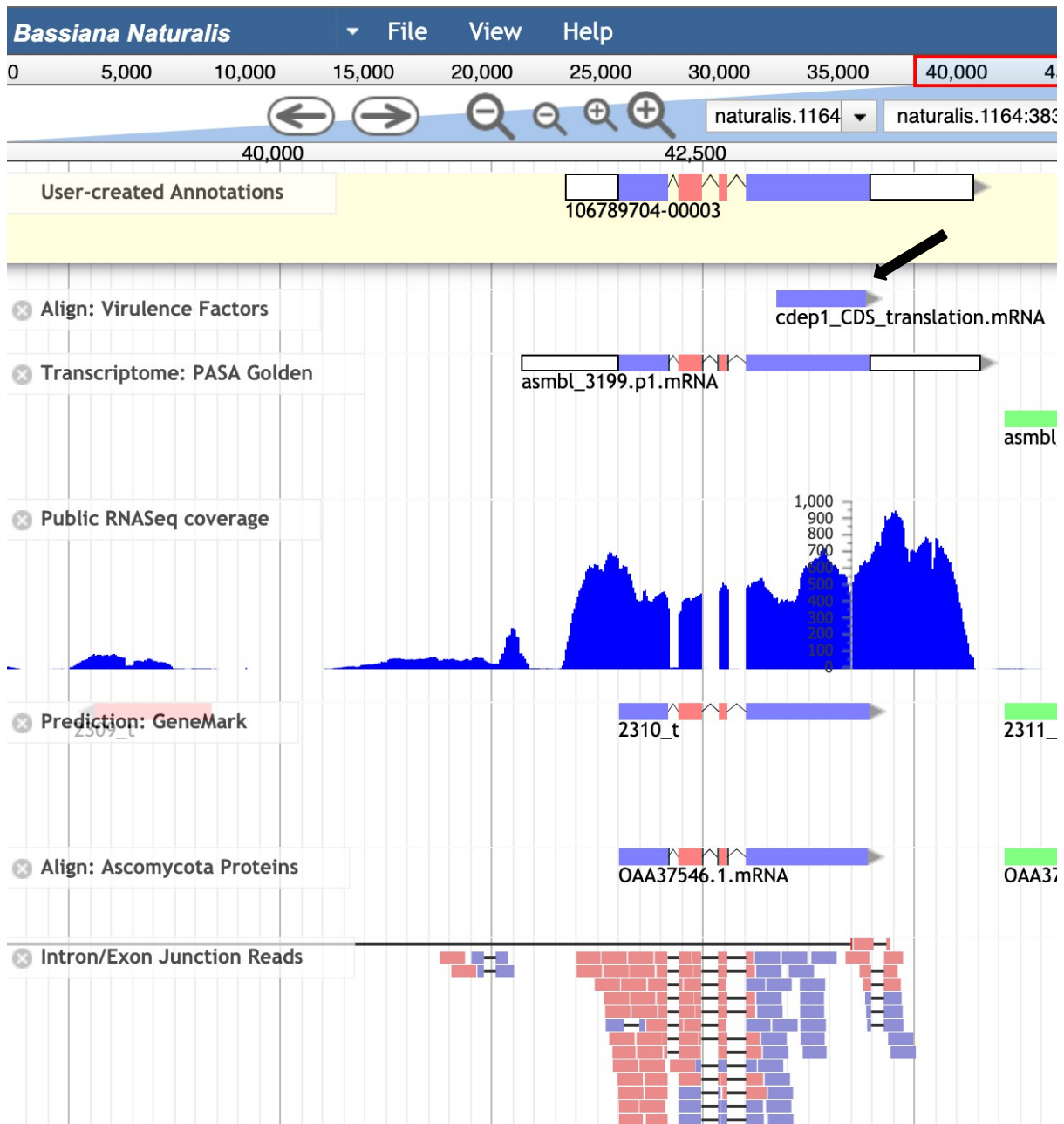


**Figure 5.2c** The Cdep1 gene first appeared as a single exon (“Virulence factors”) before manual curation (black arrow). Following the evidence provided from “Public RNA coverage”, and intron/exon junction reads it was possible to create the correct final annotation indicated as (“User created annotations”).

### 5.2.3 Program to Assemble Spliced Alignments (PASA)

PASA software is capable of incorporating expressed transcript alignments into existing eukaryotic gene structure annotations. Additionally, it can add UTR annotations to existing gene structure predictions (Haas *et al.*, 2003).

In this study, PASA was used to refine the Trinity transcripts into more complete gene models including UTRs and alternative spliced isoforms. Next, GMAP (Genome Mapping and Alignment Program) and BLAST were used to align the transcripts to their respective genomes. “PASA Golden” is the term used for the PASA assembled transcripts after updating with existing annotation. The *Bbcyp52x1* gene, a cytochrome P450 monooxygenase is implicated in fatty acid assimilation (Zhang, *et al.*, 2012), where the “PASA Golden” version was compared to the manual curated version of *Bbcyp52x1* gene and exhibited similar results. In addition, PASA was also able to predict UTRs with extreme accuracy. This is a convincing example where PASA proved to be extremely accurate when the correct evidence and correct training using pre-existing gene structures is provided (Figure 5.2d).

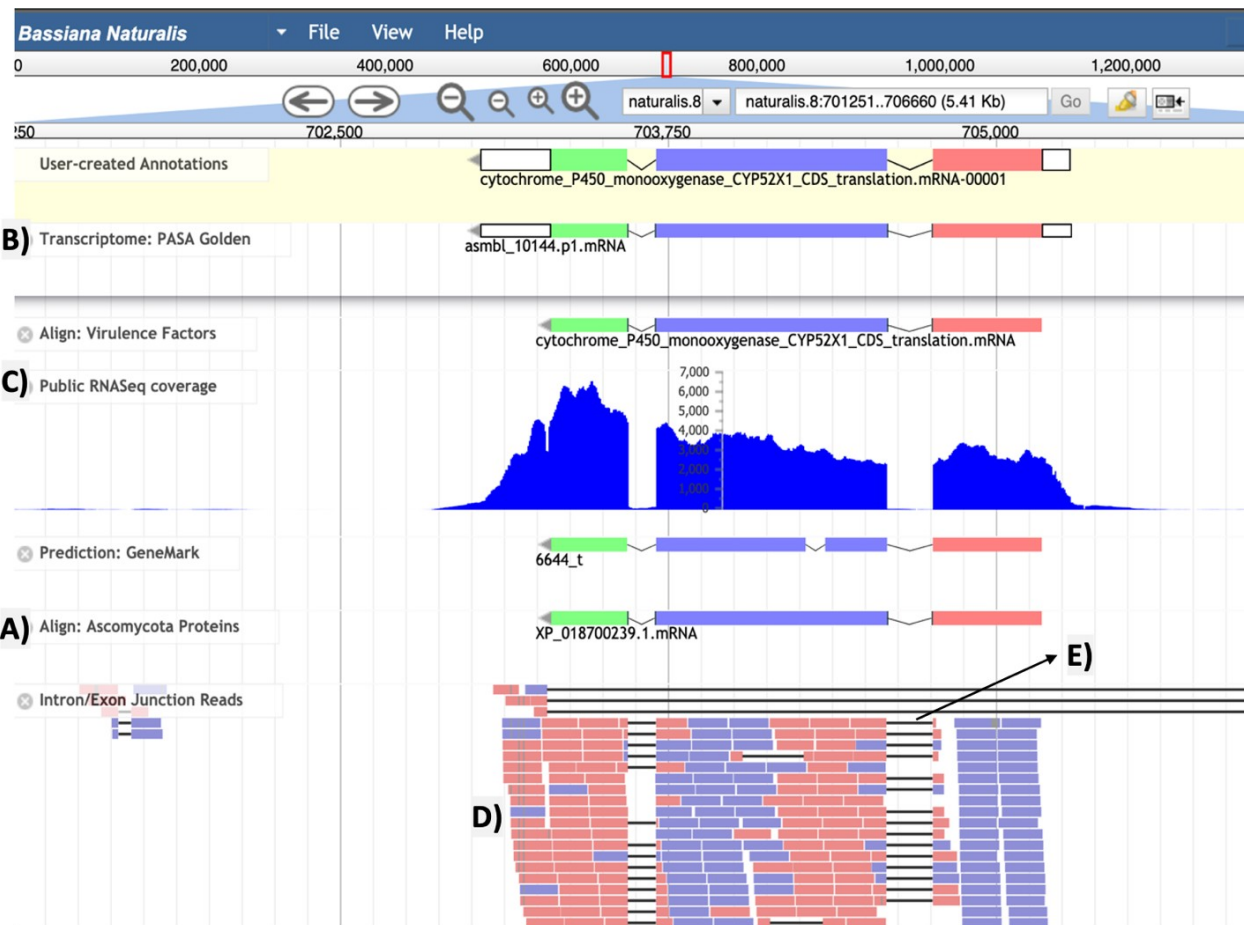


**Figure 5.2d** Examples of updated curation in *Beauveria bassiana* isolate Naturalis. Panels A-E compare the curated gene model (A) to Ascomycota Proteins (B), PASA Golden refinement (C), Public coverage (D), and pile-up of aligned reads. (E) Intronic regions are shown by lines and white boxes represent UTRs. Link access to the WebApollo/JBrowser curation site: ([https://curations.stressedfruitfly.com/apollo/77156/jbrowse/index.html?loc=GCA\\_000770705.8:664543..667106&tracks=VirulenceFactors,JunctionReads,Public%20RNASeq%20coverage](https://curations.stressedfruitfly.com/apollo/77156/jbrowse/index.html?loc=GCA_000770705.8:664543..667106&tracks=VirulenceFactors,JunctionReads,Public%20RNASeq%20coverage))

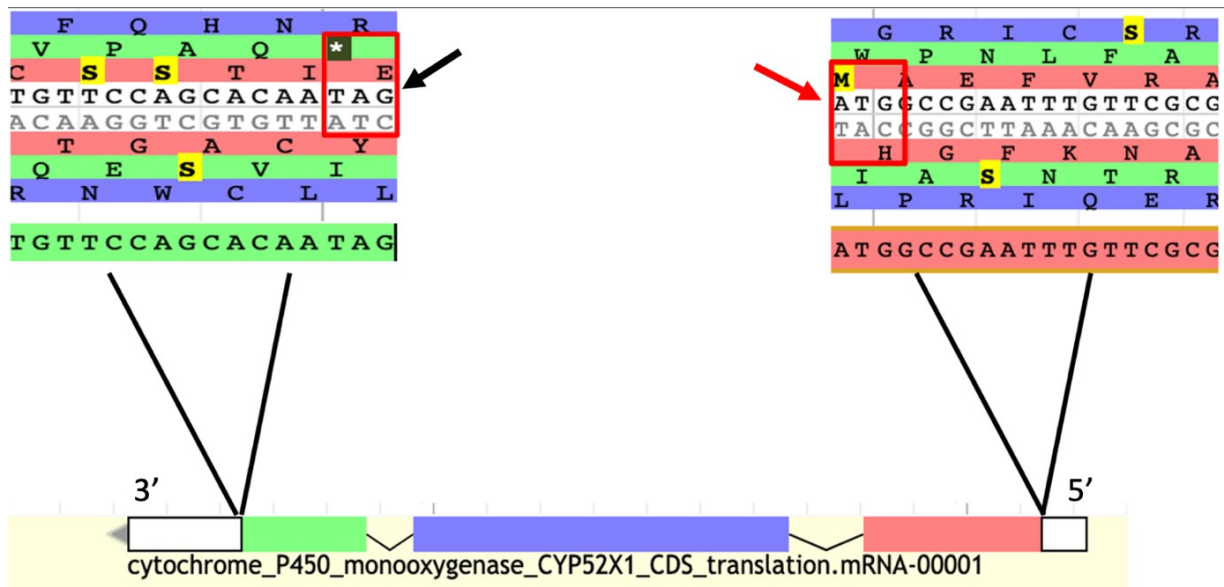


**Figure 5.2e** Cytochrome P450 subfamily CYP52X1 gene translated from the right to the left  
 Graphical representation of start (ATG; Methionine; **red arrow**) and stop (TAG; **black arrow**)  
 codons exhibiting start point and stop point of translation.

Combining different methodologies, a more complete description of the transcriptome for all the eleven *B. bassiana* isolates is now available. Still, this is not the final product, further curations were performed to improve the annotations. Therefore the 3' UTRs were subject to further manipulation by cross checking them against the read alignments (Figure 5.2f).

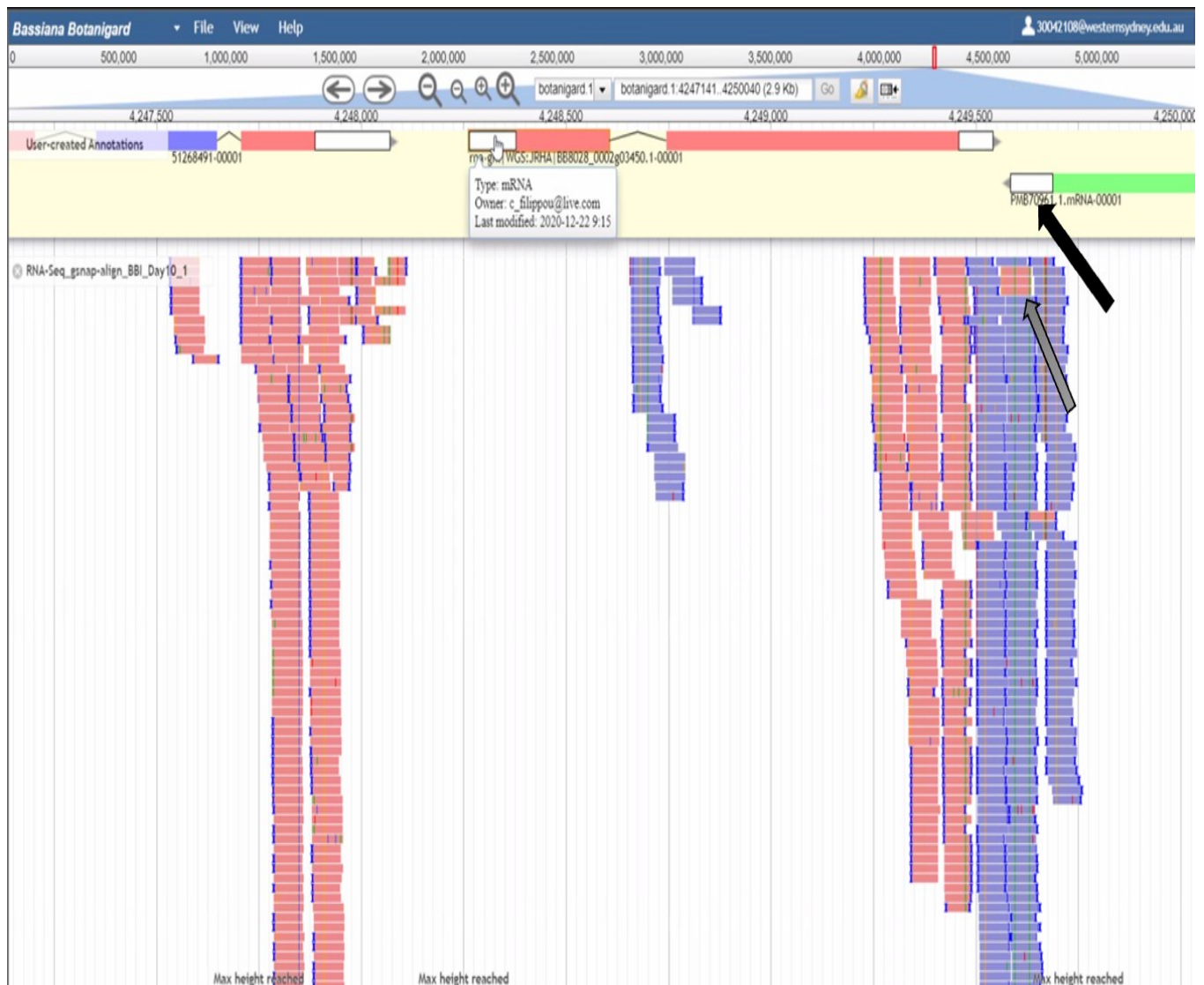


**Figure 5.2f** Black arrow indicates incorrect coverage of the 3' UTR after final curation. Grey arrow indicates spurious alignments (the reads are outside the predicted 3' UTR coverage).

The correct read alignments for the gene are shown in the top left corner of Figure 5.2f with a direction from the 5'- end to the 3'- end and are shown in red illustrating that these reads are in reverse. The reason for this is that the protocol used for library preparation sequences initiating from the 3' UTRs direction in reverse. Hence, the reads will cover a space of a maximum of 600 bases including the 3'- UTR. This read alignment indicates that the data almost certainly is representative for the specific gene that they were aligned to.

Furthermore, the blue reads in the middle of the gene do not belong to the specific gene because 1) they are not in the opposite orientation of the gene, as the gene direction is from left to right, the 3' UTR reads are expected to align in the opposite direction to the gene. 2) The reads, which are in the opposite direction, are not within the necessary 600 bases of the 3' UTR and are too distant to be acceptable. Consequently, these reads might belong to a small gene that is expressed in the opposite direction, or could be a misalignment, or they could be repeats or possible spurious alignment. Examples of spurious alignments are also shown below (Figure 5.2g). GSNAP alignment allowed for large gaps of up to 70kb on the righthand side of the 5' UTR (Figure 5.2g and 5.2h). These alignments were incorrect and cannot be used for the statistical analysis, therefore the Burrows-Wheeler Aligner (BWA) was used which is a fast short read aligner for mapping low-divergent sequences (100 bp reads) against large reference genomes (e.g., fungi, bacteria, human).

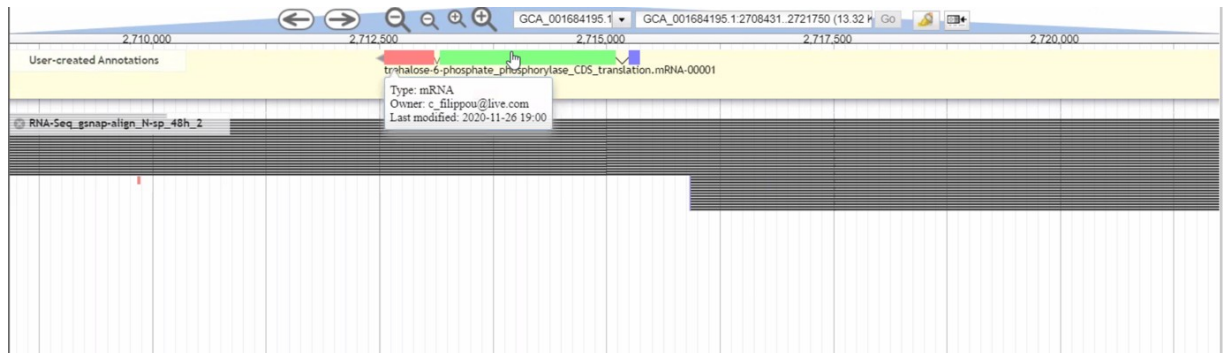


**Figure 5.2g** Spurious alignments before Burrows-Wheeler Aligner (BWA) mapping-alignment.

In summary, in order to resolve which reads belong to which gene two approaches were adopted: 1) Check the 3' UTR direction, and 2) the orientation of the reads, which have to be opposite to the direction of the gene. For example, the red colour reads (reverse) are aligned to the genes with a direction from the 5' terminus to the 3' terminus whereas the blue reads (forward) are aligned to the genes with a direction from the 3' terminus to the 5' terminus (Figure 5.2h). Therefore, it is important to manually check if all the reads have the correct orientation and that they are aligned over the full length of the 3' UTR, because the script run to count the reads is incapable of counting reads outside the 3'UTR. An excellent example of such a situation is the gene at the top right corner before final curation (Figure 5.2f) and after final curation (Figure 5.2h).

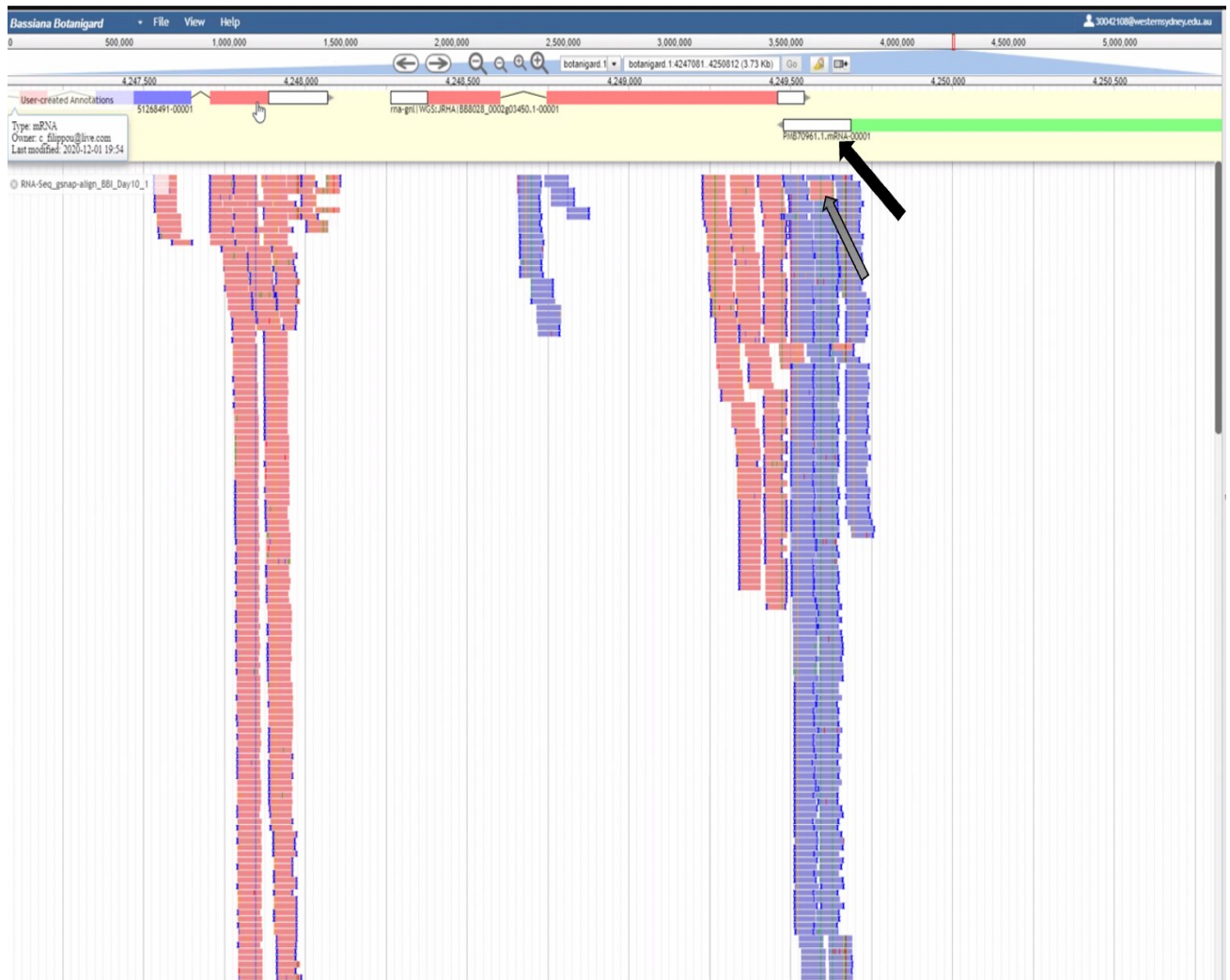


**Figure 5.2h** The black arrow indicates the correct coverage of the 3' UTR after final curation. The grey arrow indicates spurious alignments (the reads are outside the predicted 3' UTR coverage).

Additionally, the 3' UTR library protocol is not supposed to cover the entire gene but only the 3' UTR. If full mRNA sequencing had been employed instead of 3'UTR sequencing the reads would have covered the entire gene. Consequently, when the number of reads is divided by the covered length (in this case the entire mRNA) the number will be much lower as compared to the number taken from the 3'UTR division result. Also, in order to understand how the experiment works it is important to check all the available information before statistical analysis, otherwise this will result in a large volume of numbers without knowing how to extract results from them.

Therefore, a preliminary comparison of libraries was performed to ensure that all reads are correct and are correctly aligned before running a script to finalise the results. From the figures below it is clear that a repeat library, in this case BBI\_Day\_10\_2, shows no reads aligned to the genes and only spurious alignments were found (Figure 5.2i) when compared to the BBI\_Day\_10\_1 repeat and the BBI\_Day\_10\_3 repeat where highly conserved read alignment reveals three overexpressed genes (Figure 5.2j).



**Figure 5.2i** A) Library “BBI\_Day\_10\_2” repeat showing spurious alignments with no reads aligned to the 3’UTR. B) Library “BBI\_Day\_10\_1” repeat demonstrating read alignments covering the entire 3’UTR.



**Figure 5.2j** Libraries “BBI\_Day\_10\_1” and BBI\_Day\_10\_3” repeats demonstrating three highly expressed genes.

To reveal over expression data in greater clarity a script was used to count the reads across all genes of interest involved in nutrition uptake and transportation, pathogenesis and environmental stress tolerance.

### 5.3 Using gene expression box plots to derive functional annotations for key genes

To examine the expression levels of each gene, horizontal boxplots were used. Each boxplot represent the normalised (TMM and library size) expression profiles of all genes for that particular library (i.e. treatment or time) and denotes (red dot) the expression profile of a specific gene; this allows for comparison of a gene's expression simultaneously between and within libraries. For zero expression values, the red dot appears at the far left of the X axis. A boxplot is a standardised way of displaying the distribution of data based on the four quartiles 1<sup>st</sup>, 2<sup>nd</sup>, 3<sup>rd</sup>, and 4<sup>th</sup> which can be used to compare gene expression levels based on the position of the red dot. Thus, the boxplot represents the global gene expression of that specific library and the red dot is the expression value of that specific gene in that specific library. For example, in Figure 5.3a we are examining the expression profiles of adhesion proteins in PmV-1.I and PmV-1.F. Following the position of the red dot we can see that all adhesion proteins are upregulated in PmV-1.I compared to PmV-1.F, and based on the position of the red dot (on the far-right end of the 4<sup>th</sup> quartile), all three genes coding for the adhesion proteins are highly expressed at 10 dpi for both isogenic lines. Both traditional F tests and Mann-Whitney tests can be conducted to assess the significance of any pairwise expression differences or ranks, respectively, between libraries. However, statistical p-values are not useful for determining high priority candidates for downstream work as they fail to capture the metadata, use replicate averages with a standard deviation from all three samples, and do not consider the variability may have biological origin: simply put, they gloss valuable details away. Rather, an approach driven by candidate-pathways and careful qualitative analysis is however more likely to provide insights for future experiments. For example, Figure 5.3f (D) examines the expression profiles of calcium binding and transport proteins. Calcipressin (*Rcn1*) is significantly upregulated in PmV-1.I (D1, D2 and D3), however, in PmV-1.I is only expressed at 21 dpi in replicate 1 (R1). If we had estimated a p-value for that timepoint, the average would likely fail

to make this gene appear in a high priority list for further investigation. Consequently, in this case I argue that this is actually an artefact, which for some reason is expressed early on in one replicate (not knowing the reason behind that) but in the other time points is not expressed at all and only expressed in PmV-1.I. Larger sample sizes (probably a minimum of 12, i.e. significantly higher experimental costs) would alleviate this issue but this was not feasible here. Rather, using the qualitative approach to prioritise qPCR tests across larger sample sizes is an effective way to avoid false positives and false negative.

### **5.3.1 *Beauveria bassiana* virulence factors**

Virulence is a term often connected with pathogenicity and denotes the degree of pathology caused by one organism to another. Moreover, virulence is considered to be the quantifiable feature of pathogenicity reflecting the ability of a pathogenic organism to cause disease using lethal dose (LD) and lethal time (LT) as methods to measure virulence. Describing a gene as important for virulence for a pathogen we have to consider that loss of that gene will affect LT and/or LD values of the pathogen. Regarding *B. bassiana* virulence factors we need to take into consideration the strategy this fungus employs when infecting hosts and the gene families that will contribute during infection. For a pathogenic organism to cause a disease it must successfully achieve five steps of pathogenesis: i) contact, ii) adhesion, iii) colonization, iv) immune response evasion and v) infection (toxin secretion). Activation of several genes responsible for the successful completion of each step is required. In case of *B. bassiana* numerous genes of this type have been discovered and described. Targeted gene knockouts demonstrated reduced virulence of the fungus.

Mycoviruses exhibit a symbiotic relationship with their host but as mentioned above their effect is poorly understood. Therefore, it is important to understand the role of mycoviruses infecting entomopathogenic fungi and in turn their role during insect infection prior to their use as biological control tools. Expression levels of genes involved in virulence as well as in

metabolic pathways were examined in both PmV-1.I and PmV-1.F. Genes that are involved in carbohydrate assimilation and transportation, {such as ABC and carboxylic acid transporter as well as alpha-glucoside permease (ATG1), mannitol 1- phosphate dehydrogenase (Mpd), mannitol dehydrogenase (Mtd) and Trehalose-6-phosphate synthase (TPS1 and 2)}, appear to be overexpressed in PmV-1.I isolate. Interestingly, genes responsible for Ca<sup>2+</sup> binding such as {Calreticulin (*cne1*), and calcium sensor acidification (*BbCsa1*)} are overexpressed in PmV-1.F isolate. However, Ca<sup>2+</sup> transporters such as {calcium ion transporter (VCX1), Calcium-transporting ATPase 1 (PmR1), as well as calcipressin (*rcn1*) a modulator of calcineurin} were overexpressed in PmV-1.I. Furthermore, genes responsible for the biosynthesis of secondary metabolites such as tenellin (*tenS*), beauvericin (*Bbbeas*) and bassianolide (*Bbsls*) were also found to be significantly overexpressed in PmV-1.I. Last but not least, genes involved in multidrug resistance efflux pumps (*Mrp1*), thaumatin like proteins (TLPs), stress tolerance (HSP30 and HSP70), cuticle adherence (*hyd1* and *hyd2*, *Mad1*), cuticle penetration (*Chit1*, *CYP52X1*, and *Pr1*), and nitrate assimilation (*nirA*) were also significantly overexpressed in PmV-1.I. To accurately examine the expression levels of each one of these genes individually horizontal boxplots were used. These boxplots represent the actual expression of each gene at that specific time. In this section will discuss genes vital for *B. bassiana* virulence and insect pathogenicity together with environmental survival of the fungus.

### **5.3.2 Transcriptomic analysis of genes involved in *Beauveria bassiana* virulence**

#### **5.3.2.1 Host adherence**

*B. bassiana* spores are considered to be the main infectious form, and they are also capable of resisting environmental stress to a greater extent rather than hyphae and blastospores, similar to the situation for bacterial spores and the encysted forms of certain types of parasite. These spores are hydrophobic in nature and bind to similarly hydrophobic insect epicuticles (Holder

& Keyhani, 2005). Spore attachment to the insect epicuticle appears to be a challenging process. It has been demonstrated that at least two hydrophobic proteins, Hyd1 and Hyd2 are involved in the process (Cho *et al.*, 2007; Kirkland & Keyhani, 2011; Zhang *et al.*, 2011). According to Zhang *et al.* (2011) Hyd1 is present on the surface of aerial and submerged conidia and Hyd2 was also found on the surface of the aerial conidia and at the base of the germinating conidia. Additionally, both Hyd1 and Hyd2 were absent from hyphae or hyphal bodies (Zhang *et al.*, 2011). Knockout of in  $\Delta BbHyd1$  resulted in decreased fungal virulence while loss of Hyd2 in  $\Delta BbHyd2$  no effect on the fungus. However, double knockout mutants of  $\Delta BbHyd1\Delta BbHyd2$  exhibited an obvious reduction in both adhesion and virulence (Zhang *et al.*, 2011). Furthermore, homologs of adhesin like protein MAD1, originally described in *Metarhizium anisopliae*, have been found in *B. bassiana* (Xiao *et al.*, 2012). MAD1 is found on the surface of fungal spores and is a crucial component for fungal adhesion to insect cuticles. Additionally, MAD1 influences germination, blastospore formation and, ultimately, virulence (Wang & St. Leger, 2007).

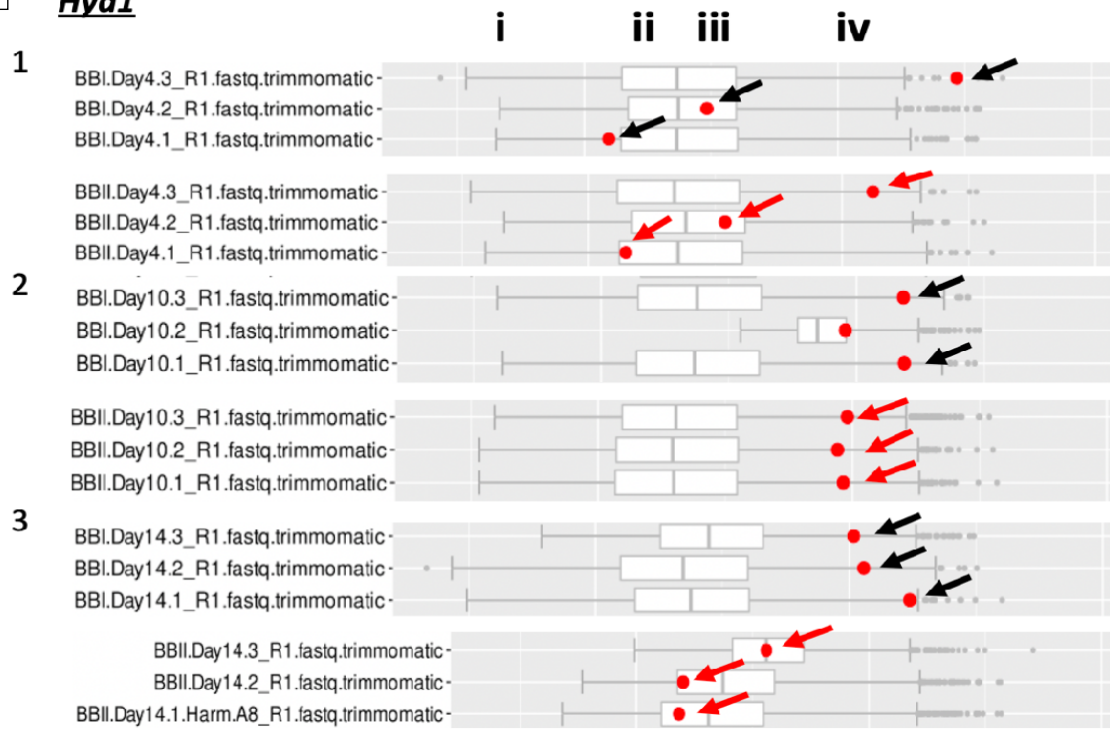
Examining the results below it is clear that the genes responsible for the expression of Hyd1, Hyd2 and MAD1 are all upregulated in PmV-1.I as compared to PmV-1.F. Generally, these genes do not appear to be highly expressed 4 dpi but are highly expressed 10 and 14 dpi (Figure 5.3a). This pattern is only observed in Hyd1 and Hyd2, whereas MAD1 expression appears to be constant across all libraries. As with all organisms, that can be grown on artificial media, *B. bassiana* biomass and sporulation is greatly affected by the depletion of nutrients, pH changes, water availability and toxic environments. *B. bassiana* cells tend to produce spores when nutrients are depleted (Liu *et al.*, 2015). Consequently, at 4 dpi the media is still rich in nutrients and probably the fungus sporulates less, whereas the opposite is true 10 and 14 dpi, where the nutrients are depleted, probably leading to increase sporulation. As mentioned previously Hyd1 and Hyd2 are found in conidia and not in hyphal bodies, therefore this might explain why at 10

and 14 dpi overexpression of these two hydrophobin proteins is observed. On the other hand, MAD1 expression levels are similar across all libraries, and this might be due to the fact that MAD1 is also found on the surface of fungal spores, but it can influence germination too. In conclusion adhesion proteins (Hyd1, Hyd2, MAD1) are crucial for the virulence of *B. bassiana* and as shown below these proteins are significantly overexpressed in PmV-1.I isogenic line as compared to PmV-1.F isogenic line 10 and 14 dpi.

Based on the results presented here overexpression of Hyd1, Hyd2, and MAD1 genes was observed 10 dpi are closely similar but not identical to the results discussed previously in Chapter 4 by Varga *et al.* (2003).

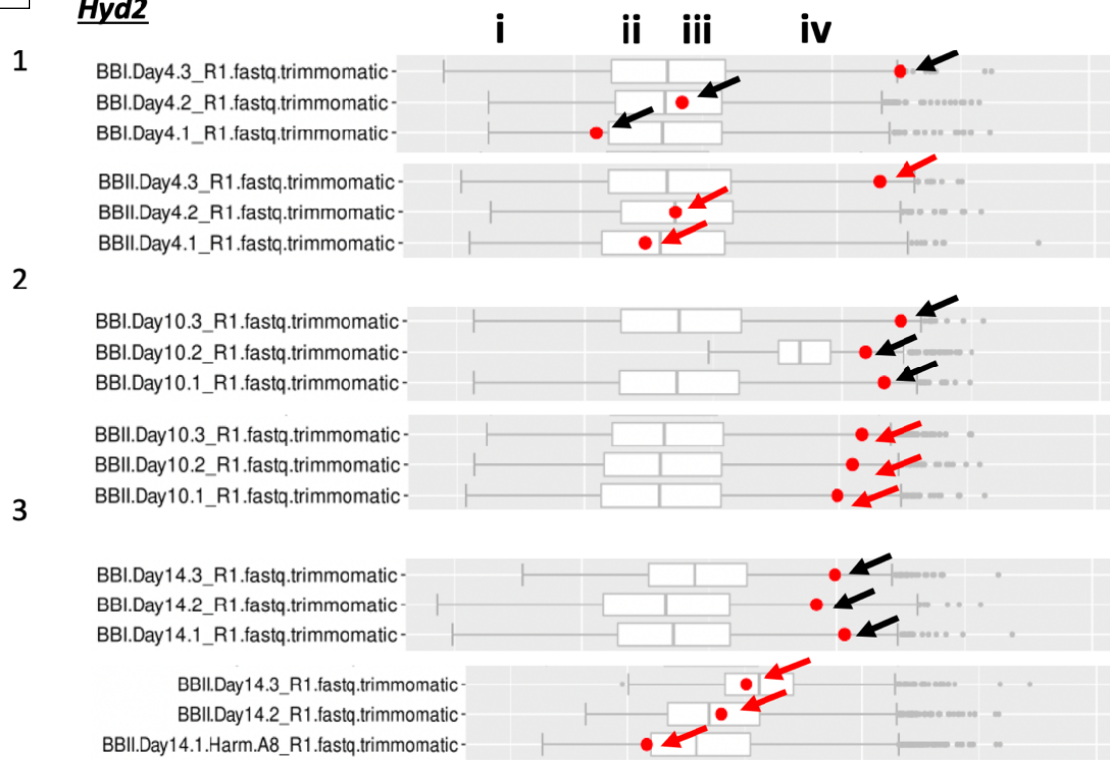
A

***Hyd1***



B

***Hyd2***



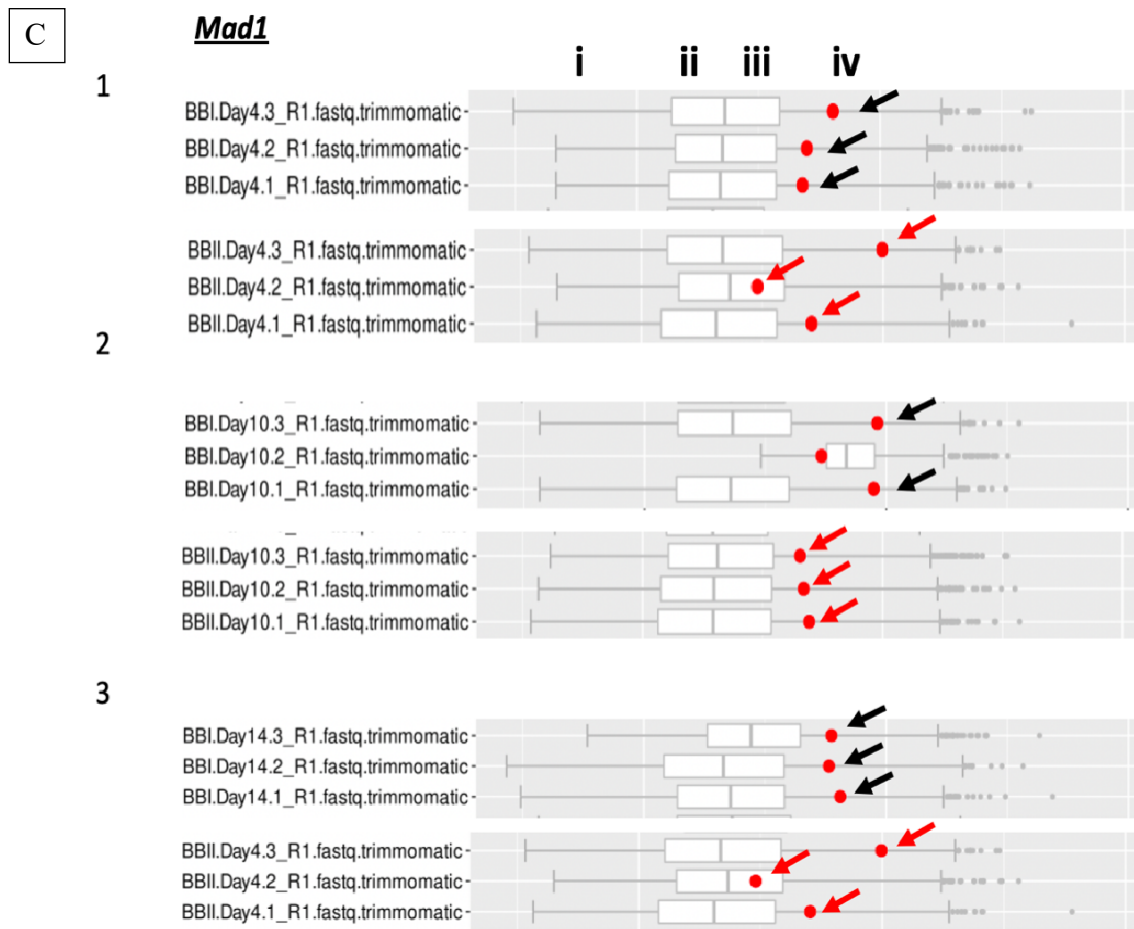


**Figure 5.3a**

Boxplots demonstrating the expression profiles of adhesion proteins. Black arrows indicate expression in PmV-1.I, and red arrows indicate expression in PmV-1.F. The four quartiles are indicated as i (first quartile), ii (second quartile), iii (third quartile), and iv (fourth quartile). A); Hyd1 is slightly upregulated in PmV-1.I at 4 and 10 dpi and significantly upregulated at 14 dpi. B); Similar expression profile of Hyd1 is observed for Hyd2 which is upregulated in PmV-1.I when they both compared to PmV-1.I C); MAD1 is upregulated slightly in PmV-1.I at 4, 10, and 14 dpi when was compared to PmV-1.F.

### 5.3.2.2 Cuticle penetration

Fungal cytochrome P450 monooxygenases are crucial for many essential processes particularly cell survival and growth. A new member of Cytochrome P450 subfamily, termed CYP52X1, was found to be involved in hydrocarbon assimilation and insect cuticle degradation and plays a crucial role in *B. bassiana* (Zhang *et al.*, 2012). Knockout of the CYP52X1 gene in the  $\Delta cyp521x1$  mutant decreased virulence for the greater wax moth, *Galleria mellonella*, when applied topically but not when injected directly into the hemocoel (Zhang *et al.*, 2012). Topical application closely resembles the natural route of infection. Similarly, when the wild type was tested with the  $\Delta cyp521x1$  mutant strain using grasshopper wing germination assays the wild type of strain exhibited germination rate differences as compared to the mutant strain (Zhang *et al.*, 2012).

Additionally in *B. bassiana* overproduction of another cuticle-degrading enzyme, chitinase (*Bbchit1*), results in faster cuticle penetration and rate of insect death representing increased infection efficiency. Knockout mutants of chitin genes have not yet been reported, but chitinase overexpression demonstrated more virulent strains (Fang *et al.*, 2005). Fungal proteases also have a crucial role in cuticle penetration and a large family of cuticle degrading enzymes known as Pr1 proteases are the best known. Pr1 protease is also considered to be a *B. bassiana* virulence factor based on the observation that Pr1 knockout mutants demonstrated a decreased virulence against grasshoppers *Melanoplus sanguinipes* (Bidochka & Khachatourians, 1990). Conversely, overexpression of Pr1 proteases resulted in increased fungal virulence (Fang *et al.*, 2005).

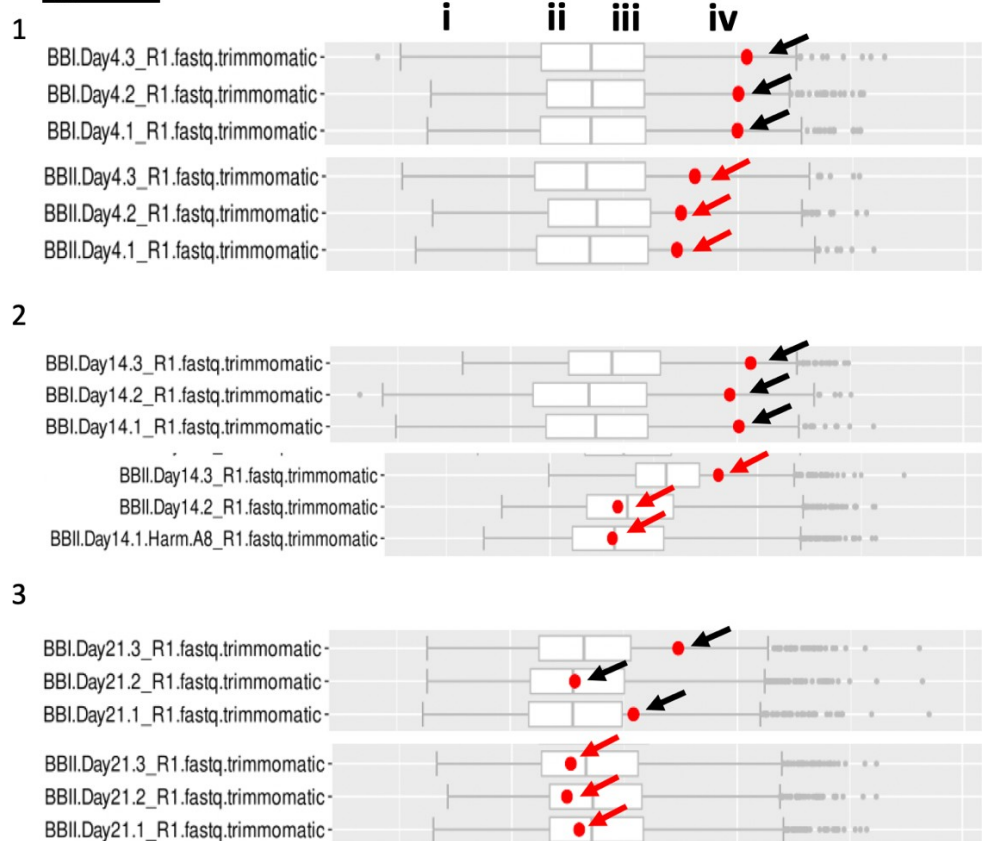
From the results obtained from the RNA-seq it is evident that CYP52X1 is significantly overexpressed in PmV-1.I across all time points (Figure 5.3b). Interestingly, this gene is also highly expressed in both PmV-1.I and PmV-1.F during early fungal growth (4 dpi). On the contrary, during late growth (14 and 21 dpi) a significant drop in expression of this gene is

observed in PmV-1.F, while in PmV-1.I there is no significant change between 4 and 14 dpi, but when compared to 21 dpi a significant drop of expression is also observed. Nutrient depletion maybe the reason behind these CPY52X1 expression pattern.

Chitinases are divided into two groups, endo- and exo-chitinases, and recently are gaining much attention due to their many potential applications in health care and agriculture (Hamid *et al.*, 2013). Chitinase 1 (Chit1) is an endo-chitinase vital for fungal virulence against insect pathogens, and it is observed to be overexpressed in PmV-1.I at 14 dpi, whereas at 7 dpi overexpression of this gene is observed in PmV-1.F. Interestingly, this gene is switched off at 21 dpi in both PmV-1.I and PmV-1.F and it appears that only in library 3, in both PmV-1.I and PmV-1.F, is being expressed with overexpression of the gene in the PmV-1.I isolate. On the other hand, Pr1 is significantly overexpressed in PmV-1.I across all time points as compared to BBII, with the latter been switched off in PmV-1.F library C3-(2). In summary, the expression patterns for these genes indicate a link between their up-regulation and the presence of BbPmV-1.

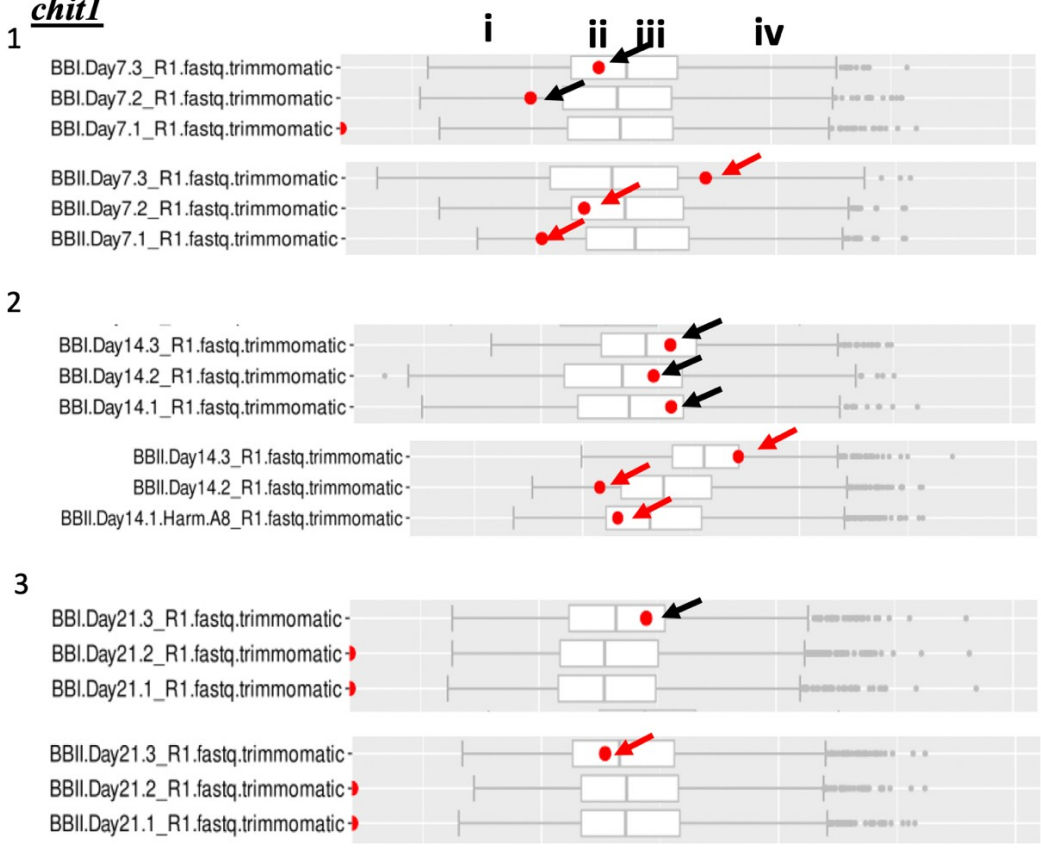
A

***cyp52x1***



B

***chit1***



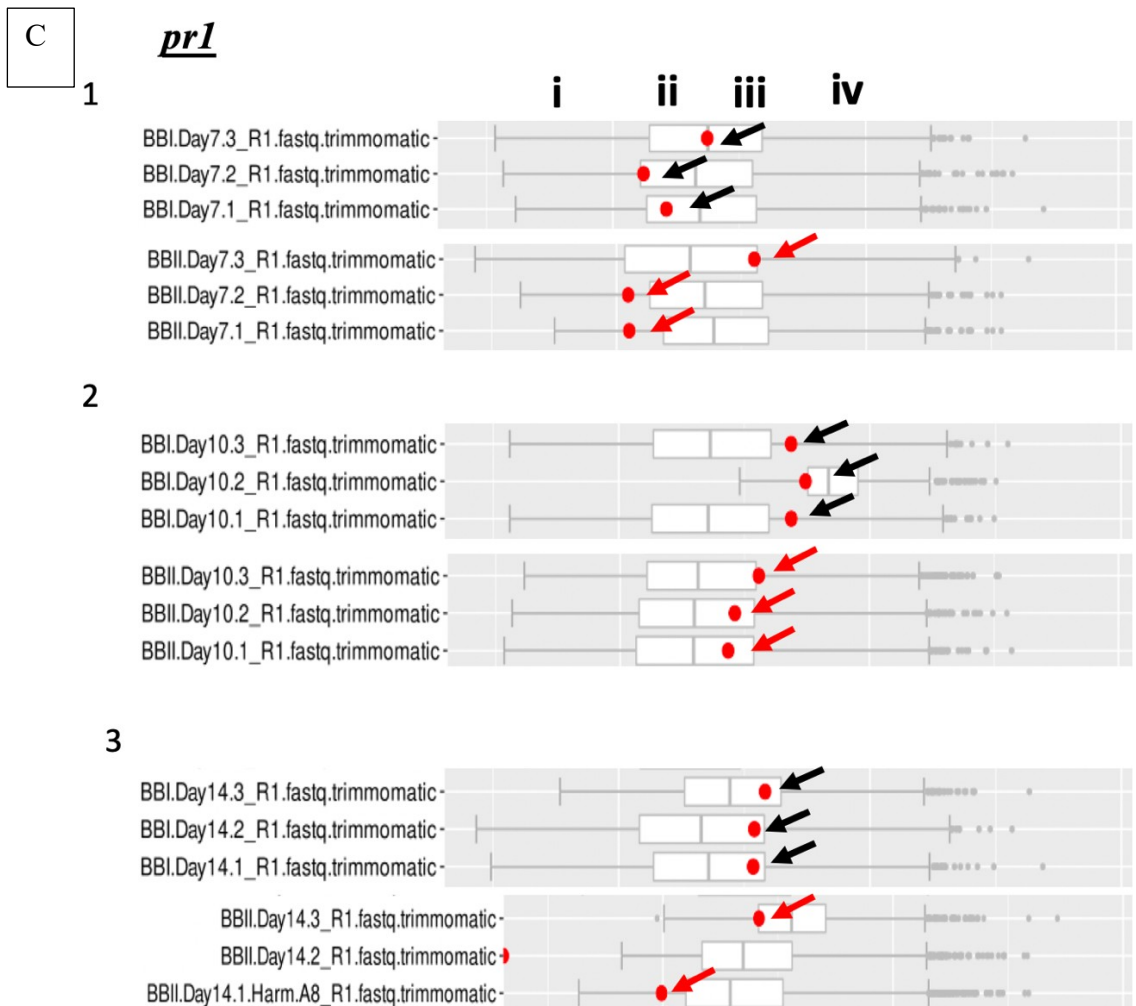


**Figure 5.3b**

Boxplots demonstrating the expression profiles of cuticle degrading proteins. Black arrows indicate expression in PmV-1.I, and red arrows indicate expression in PmV-1.F. The four quartiles are indicated as i (first quartile), ii (second quartile), iii (third quartile), and iv (fourth quartile). A) *cyp52x1* gene is significantly upregulated in PmV-1.I at 4, 14, and 21 dpi. Dots are cluster in the iv quartile for *cyp52x1* indicating that is a highly expressed when compared to the other two genes *cht1* and *pr1*. B) *Chit1* is upregulated in PmV-1.F at 7 dpi (B1), while at 14 and 21 dpi (B2 and 3) is upregulated in PmV-1.I; *Chit1* is switched off in both isolates at 21 dpi (B3; libraries 1 and 2). C) *pr1* gene also upregulated in PmV-1.I at 7, 10 and 14 dpi.

### 5.3.2.3 Carbohydrate transporters in *Beauveria bassiana*

Nutrients important for cell growth and replication are absorbed from the environment through outer membrane transporters. Likewise, these transporters are also important for the export of toxic molecules, a mechanism of great importance for the cells in terms of (multi-) drug resistance. Trehalose, as mentioned previously is the main carbohydrate found in insect hemolymph, but also is an important carbohydrate used by many organisms for buffering against osmotic shock. The ability of *B. bassiana* to utilize trehalose is an important factor for the fungus to grow within the insect hemocoel. *BbAgt1* mentioned above encodes for an  $\alpha$ -glucoside transporter, important for trehalose uptake. Increased fungal growth was observed in minimal Czapek-Dox media containing trehalose as sole carbohydrate source (Filippou *et al.*, 2021). However, deletion of this gene displayed a decreased growth in media containing different carbohydrate substrates, reduced production of conidia, and reduced virulence against insects when applied topically and also when injected into the insect hemocoel (Wang, Ji, *et al.*, 2013).

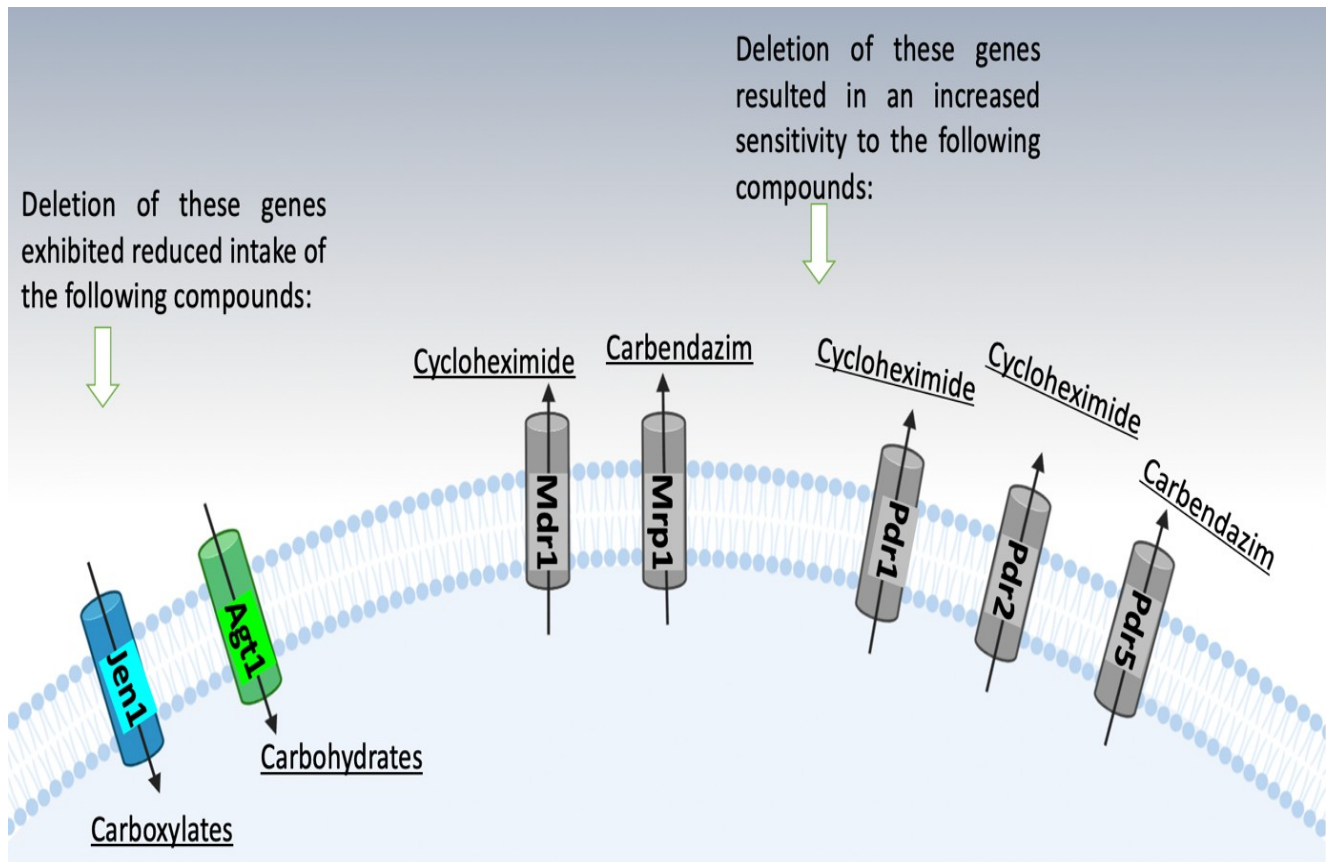


**Figure 5.3c** Overview of select *Beauveria bassiana* transporters. Jen1 (light blue), carboxylic acid transporter, Agt1 (light green), carbohydrate transporter, Mdr1, Mrp1, Pdr1, Pdr2, and Pdr5 (gray), ABC-type (multidrug) transporters. (Modified from Ortiz-Urquiza *et al.* 2016).

The ABC transporter proteins are a large family of proteins and include ABC-A, ABC-B, ABC-C and ABC-G and can catalyse the transport of several compounds across the membrane *via* ATP hydrolysis. Different transporters can transport different compounds, ABC-B (Mdr1), ABC-C (Mrp1) and ABC-G (Pdr1, Pdr2, and Pdr5) though are implicated in multidrug resistance which involves an active drug efflux of antibiotics to reduce intracellular drug accumulation (Sharom *et al.* 2011).

Single deletion of any of the transporters results in increased susceptibility to different fungicides depending on the transporter. Deletion of transporter pairs; Mdr1 and Pdr2, Mrp1 and Pdr5, results in sensitivity to several fungicide including cycloheximide, azoxystrobin, and ethirimol. The JEN1 transporter has been identified in the import of lactate or some short chain monocarboxylates across the plasma membrane into cells. Knockout of the *jen1* gene in the *ΔBbjen1* mutant gene resulted in significant reduction in the virulence of *B. bassiana* against aphids, however conidial numbers were significantly decreased in strains overexpressing the gene (Jin *et al.* 2010). These results suggest that *Bbjen1* disruption results in defective carboxylate transport into the cell, which in turn affects conidial yield through nutritional alteration (Jin *et al.*, 2010).

Both the BpbPmV-1 and BbPmV-3 virus-infected isogenic lines grew significantly faster on various carbohydrate sources as compared to the respective virus-free isogenic lines isolate (Filippou *et al.*, 2021). Increased growth in the virus-infected lines might be attributed to upregulation of the *Bbagt1* gene enabling maximum trehalose utilization (Appendix Part B; Figure S4.1.5b). Examination of the gene expression levels of different carbohydrate transporters including BbJen1, ABC-B (Mdr1), ABC-C (Mrp1), and BbAGT1 revealed significant upregulation in PmV-1.I lines confirming previous observations on the metabolism and faster growth in carbohydrates as compared to nitrogenous substrates. The expression profile of *nirA* gene responsible for nitrate assimilation was examined. This gene acts as a

positive regulator for nitrate reductase which catalyses nitrate to nitrite. Polymycoviruses appear to affect uptake and/or assimilation of sodium nitrate when compared to other nitrogen sources as mentioned in Chapter 4 and this has been confirmed here following gene expression profiling of the *nirA* gene. As shown in Figure 5.3d *nirA* is slightly upregulated at 14 dpi (F2) in PmV-1.I, while is upregulated in PmV-1.F at 21 dpi (F3).

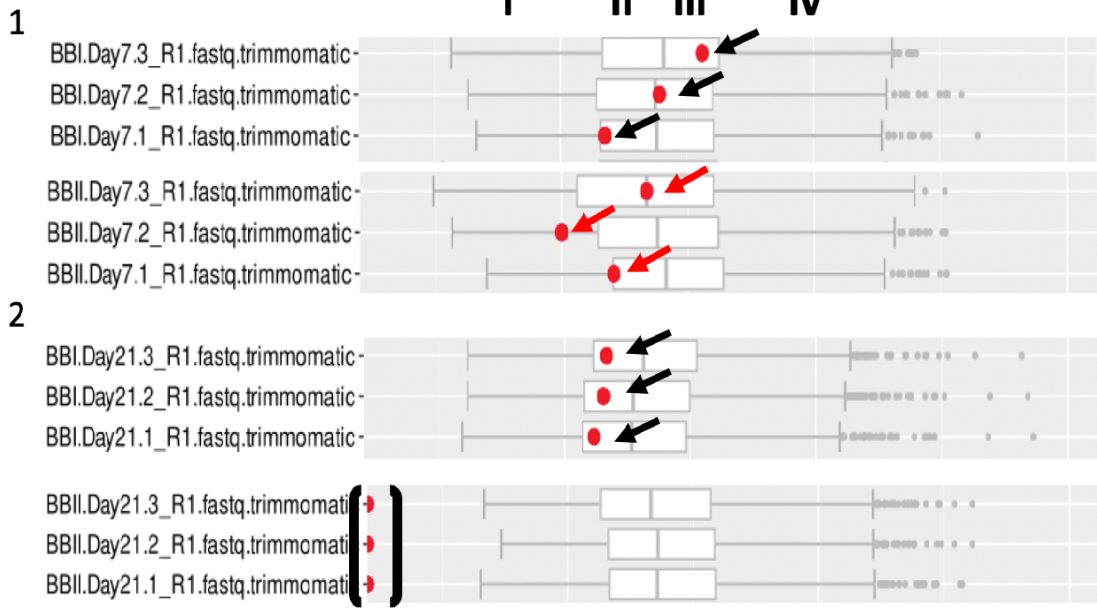
Interestingly, all genes are highly expressed 7-10 dpi, and more specifically *Bbjen1* and *nirA* are highly expressed at 10 dpi and upregulation of those genes was observed in PmV-1.I, while *BbAGT1*, *Mdr1* and *Mrp1* are highly expressed at 7 dpi and again upregulation of these genes was observed in PmV-1.I. *BbAGT1* is switched off in PmV-1.F at 21 dpi (Figure 5.3d-A2), *BbJen1* is switched off at 14 dpi in PmV-1.F and at 21 dpi in all PmV-1.F libraries and two of the libraries in PmV-1.I (Figure 5.3d-D2 & 3).

Expression levels of a putative transcription factor (TF) *nosA* were also examined since this gene has been linked to carbon starvation, late asexual development and conidiation (Vienken *et al.*, 2006). This has relevance for *B. bassiana* which tends to sporulate readily under stressful conditions including virus infection. Indeed, gene profiling of *nosA* confirms this observation as significant upregulation at 21 dpi was observed (Figure 5.3d-E4) in PmV-1.I. Furthermore, *nosA* was significantly upregulated in PmV-1.I across all timepoints, whereas in PmV-1.F was switched off 21dpi.

These results indicate that *B. bassiana* is highly active during late timepoints and that upregulation of certain genes in PmV-1.I contribute to the better assimilation of both carbohydrate and nitrogen sources (Filippou *et al.*, 2021).

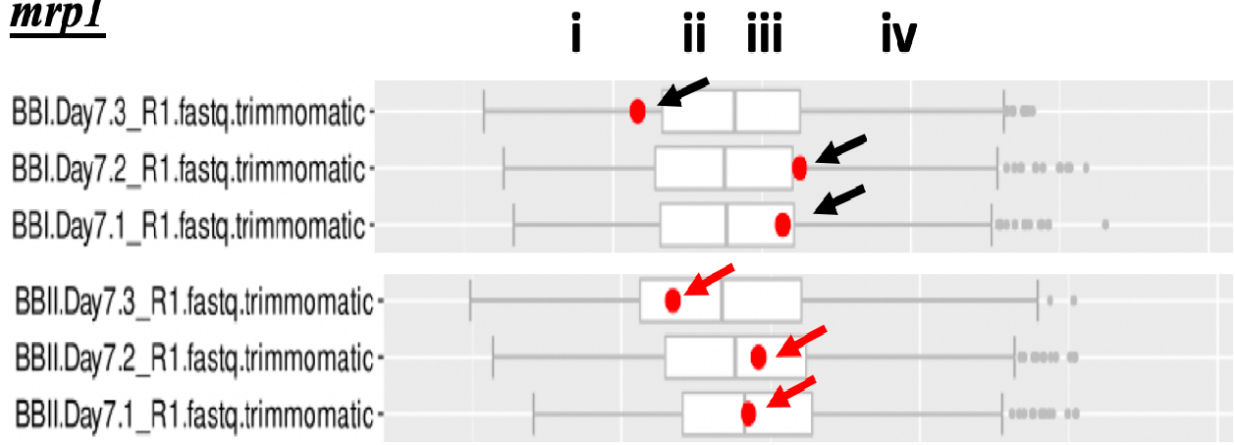
A

***Bbagt1***



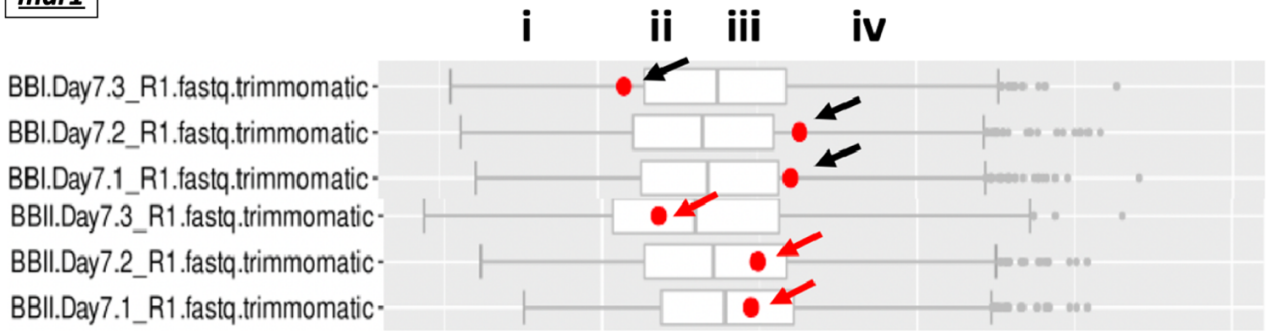
B

***mrp1***



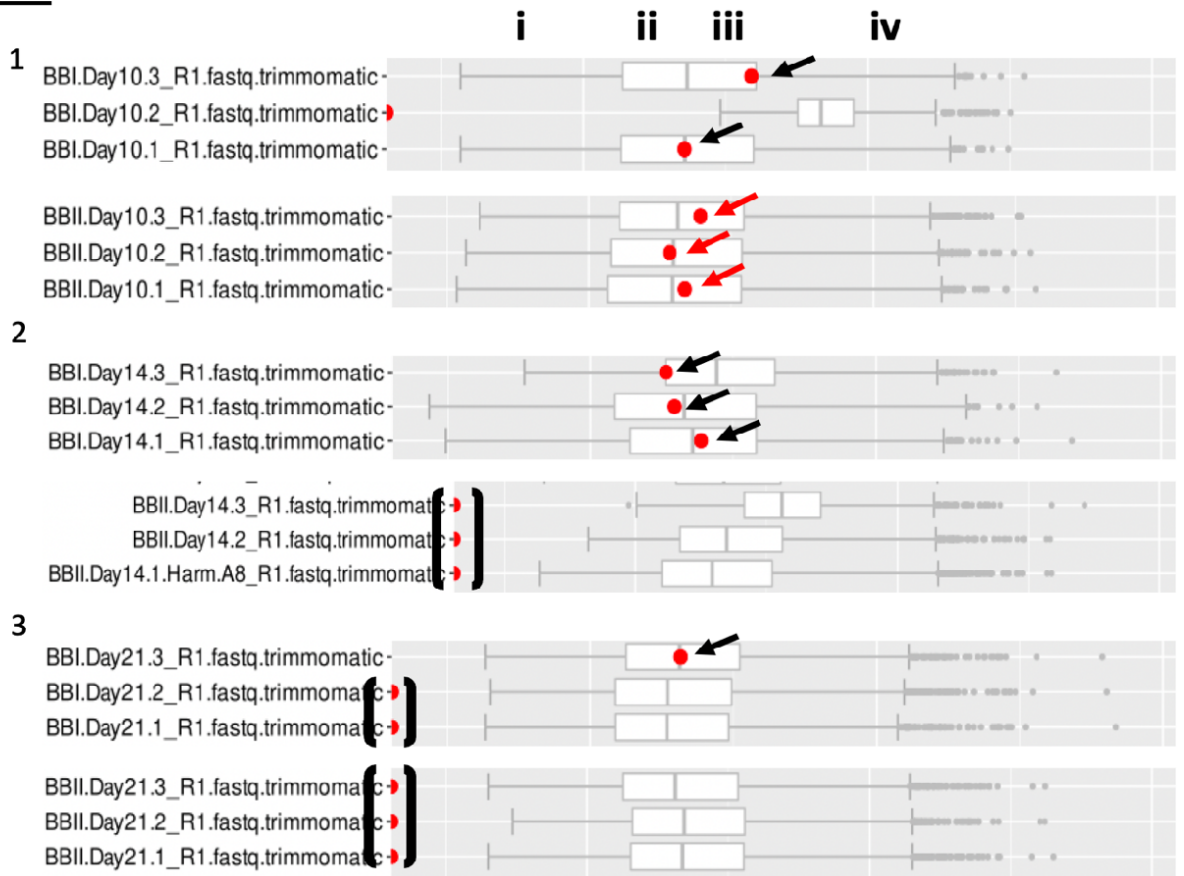
C

***mdr1***

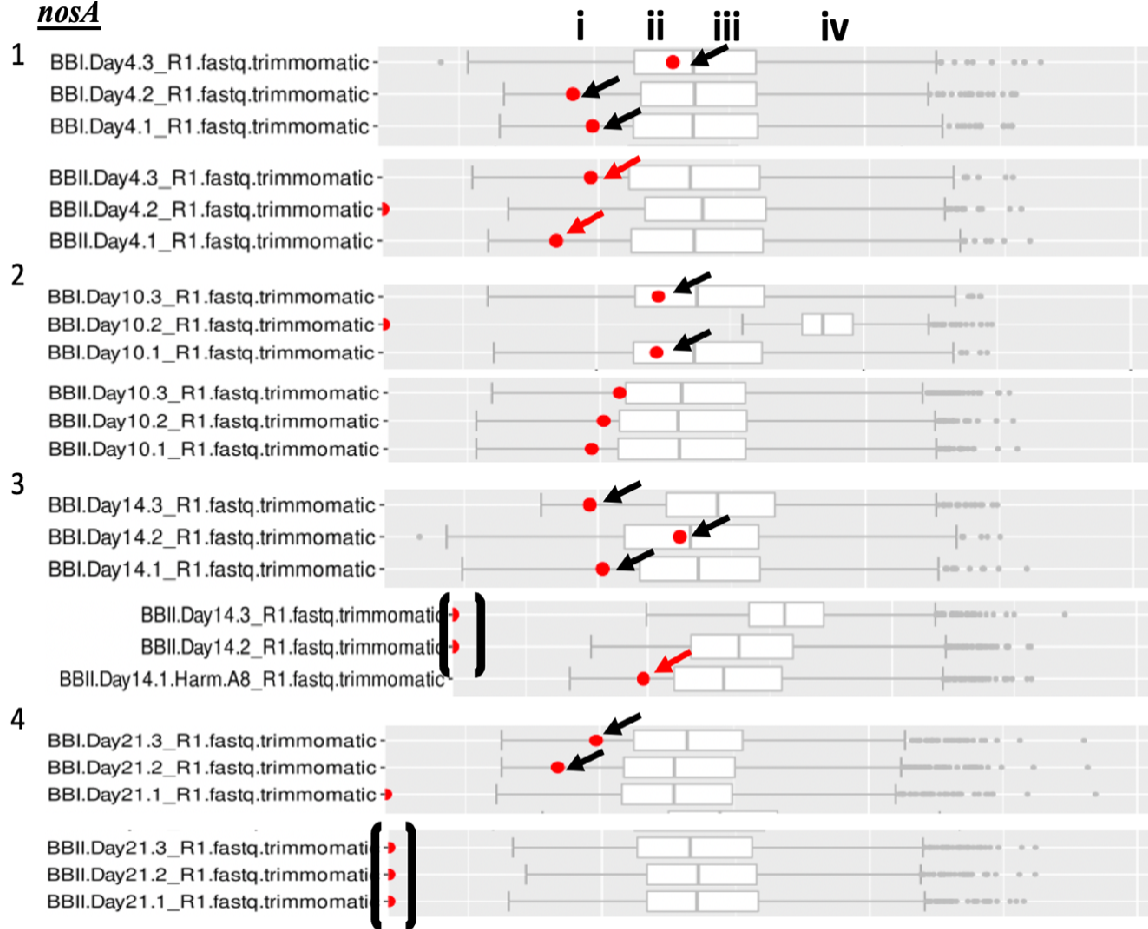


D

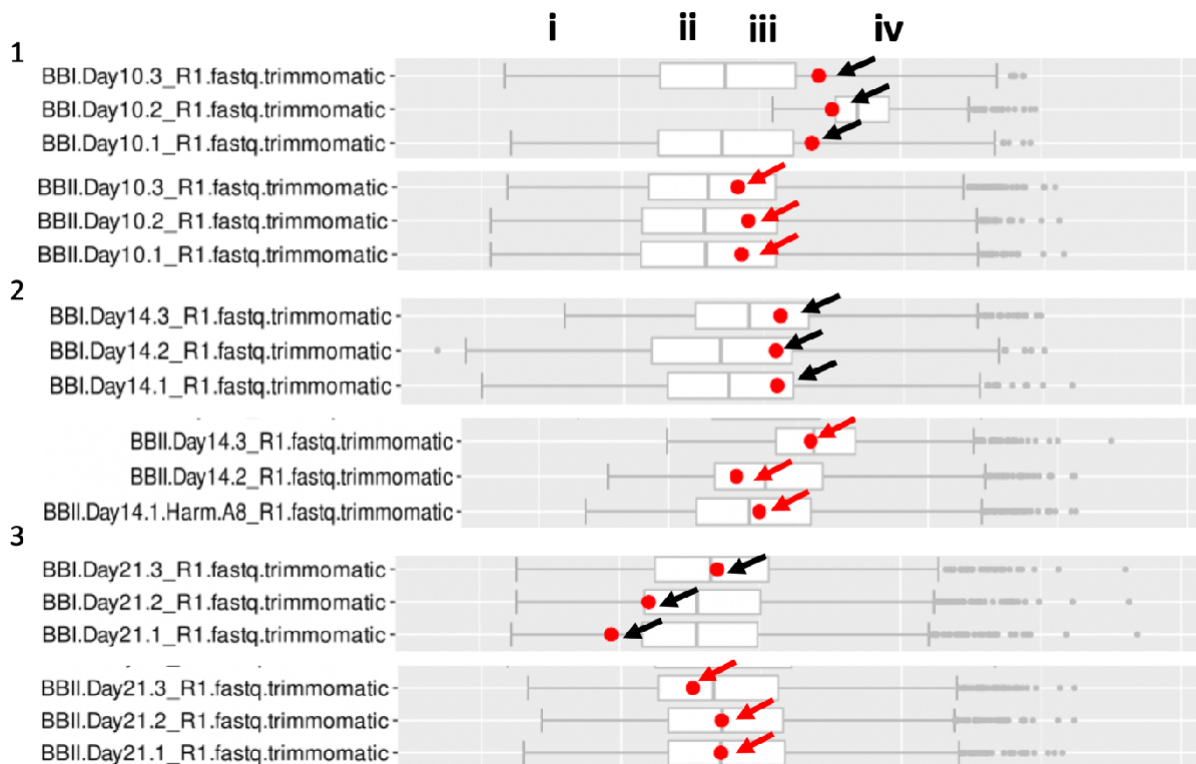
***Bbjen1***



E

*nosA*

F

*nirA*

### Figure 5.3d

Boxplots demonstrating the expression profiles of carbohydrate transport proteins, *nirA* and *nosA*. Black arrows indicate expression in PmV-1.I, and red arrows indicate expression in PmV-1.F. The four quartiles are indicated as i (first quartile), ii (second quartile), iii (third quartile), and iv (fourth quartile). A) *Bbagt1* significantly upregulated in PmV-1.I at 7 and 21 dpi, while in PmV-1.F is switched off at 21 dpi (A2). B) *mrp1* and C) *mdr1* are slightly upregulated in PmV-1.I at 7dpi. D) *Bbjen1* is significantly upregulated in PmV-1.I (D1, D2 and D3), while it is switched off in PmV-1.F at 14 and 21 dpi (D2 and D3). E) *nosA* is significantly upregulated in PmV-1.I (E1, E2, E3 and E4), while is switched off in PmV-1.F at 14 and 21 dpi (E3 and E4) as indicated by the brackets. F) *nirA* is significantly upregulated in PmV-1.I at 10 dpi (F1), slightly upregulated at 14 dpi (F2), while is upregulated in PmV-1.F at 21 dpi (F3).

#### 5.3.2.4 Calcium signaling and transport

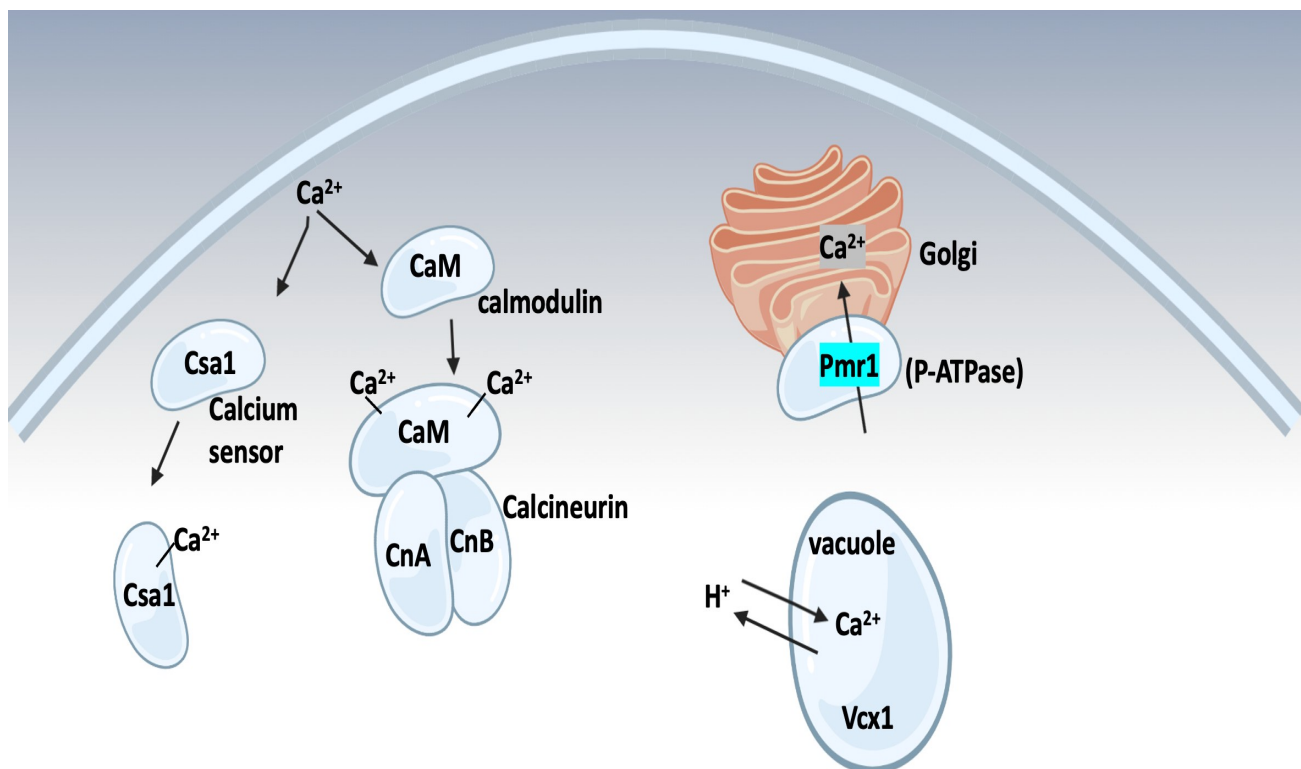
In eukaryotic organisms including fungi the intracellular calcium concentration affects different signal transduction cascades and it has been demonstrated that it is tightly regulated. Calcium ions are crucial for fungi because they are involved in the maintenance of cell structure, sporulation, and fruiting body development. For this reason, calcium transport was studied for the development of antifungal drugs, and a number of calcium-binding proteins have been isolated and described (Ortiz-Urquiza, & Keyhani 2016; Jimenez, 2016).

In filamentous fungi one of the most studied calcium pathways is the calmodulin (CaM) pathway, where activation of several downstream targets depends on  $\text{Ca}^{2+}$  binding to CaM and to calcineurin A and B subunits (CnA-CnB) forming a complex (Li *et al.*, 2015). CnA is the catalytic subunit that possesses  $\text{Ca}^{2+}$ -CaM, whereas CnB is known as the regulatory subunit as it controls the activity of the complex. Moreover, calcipressin (*Rcn1*) a regulator of

calcineurin was found to be important for fungal growth, conidiation, and virulence when a mutant strain was compared against the wild-type (Harren *et al.*, 2012). The *B. bassiana* calcium sensor acidification (*BbCsa1*) gene, is a homologue of Neuronal calcium sensor protein (NCS). Gene knockout of *BbCsa1* demonstrated significant alterations in the production of organic acids (such as oxalate, citrate and lactate), and downregulation of the membrane H<sup>+</sup> pump/ATPase (Fan *et al.* 2012). Furthermore, when applied topically the mutant strain  $\Delta$ *BbCsa1* showed a decreased virulence against *G. mellonella*, whereas when directly injected into the insect there was no significant change in virulence observed indicating the participation of *BbCsa1* during early penetration but is dispensable once the fungus is inside the hemocoel (Fan *et al.* 2012).

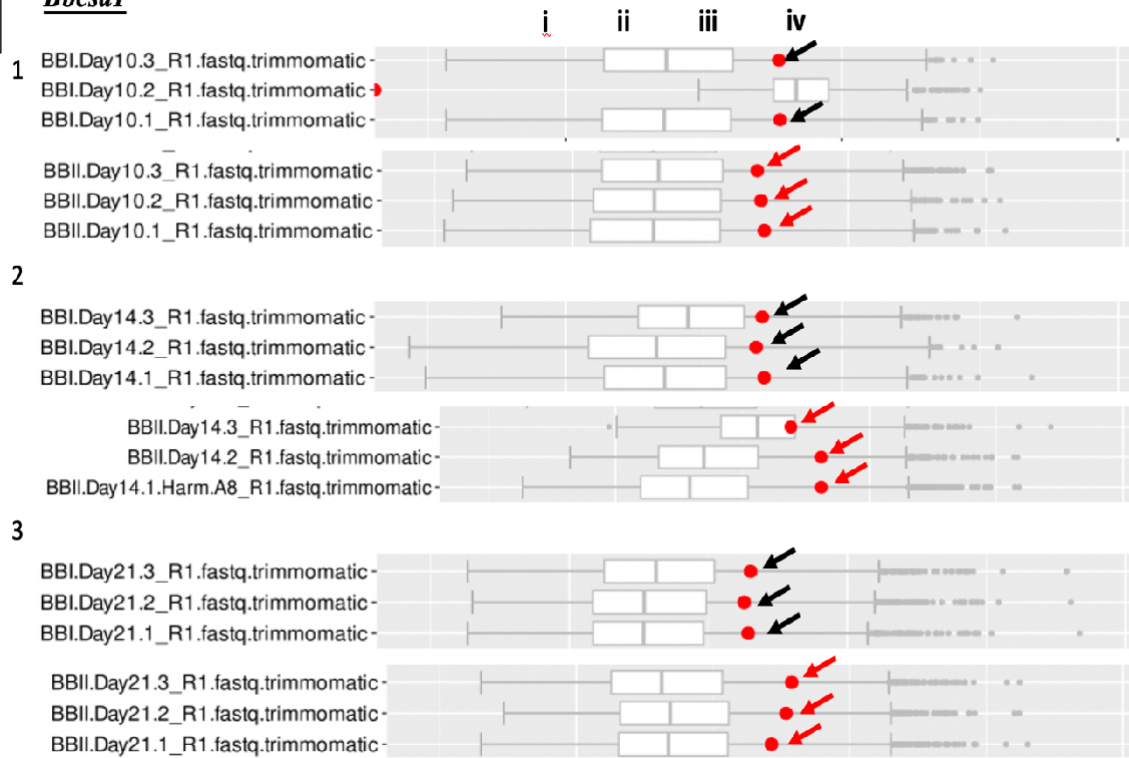
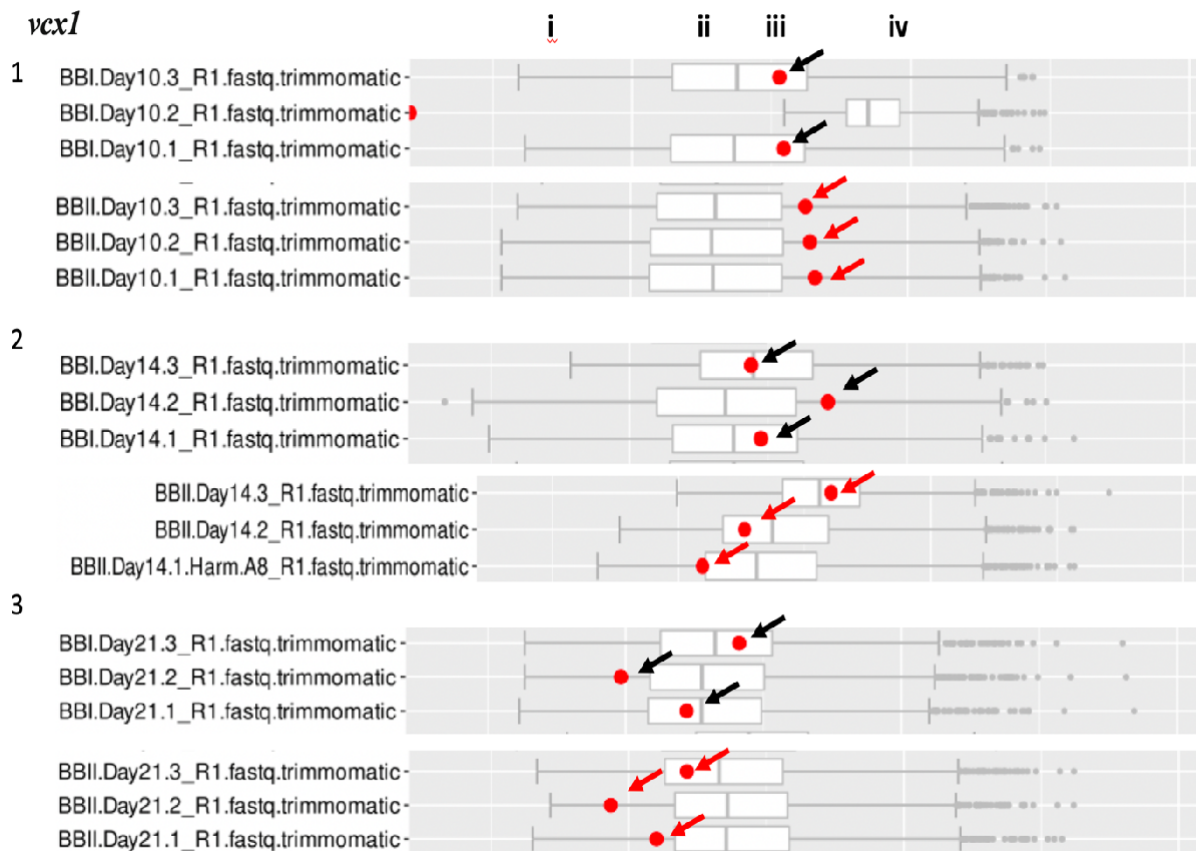
In *B. bassiana*, vacuolar calcium ion transporter complex (*BbVcx1*) is responsible for controlling Ca<sup>2+</sup> homeostasis by transporting cytosolic Ca<sup>2+</sup> into vacuoles, and at the same time contributing to stress tolerance and virulence. Inactivation of calcineurin resulted in a minor decrease in fungal growth demonstrating a close relationship between *BbVcx1* and calcineurin. Furthermore, mutant strains lacking the *BbVcx1* gene exhibited a decrease in stress tolerance and more specifically  $\Delta$ *Bbvex1* mutants were more sensitive to dithiothreitol, Congo red dye, menadione (damaging mitochondria) and hydrogen peroxide (H<sub>2</sub>O<sub>2</sub>). Moreover, when mutant strains were topically applied they demonstrated decreased virulence against *G. mellonella* demonstrating the contribution of *BbVcx1* in multi-stress responses and virulence (Hu *et al.*, 2014).

A Golgi localised Ca<sup>2+</sup> transporter/ATPase has also been identified in *B. bassiana* (*BbPmr1*) contributing to conidia growth and stress tolerance. Knockout *BbPmr1* mutant strains exhibited a significant sensitivity to UVB, osmotic, cell wall and oxidative stress as well as decreased virulence against insects when applied topically (Antebi & Fink, 1992).

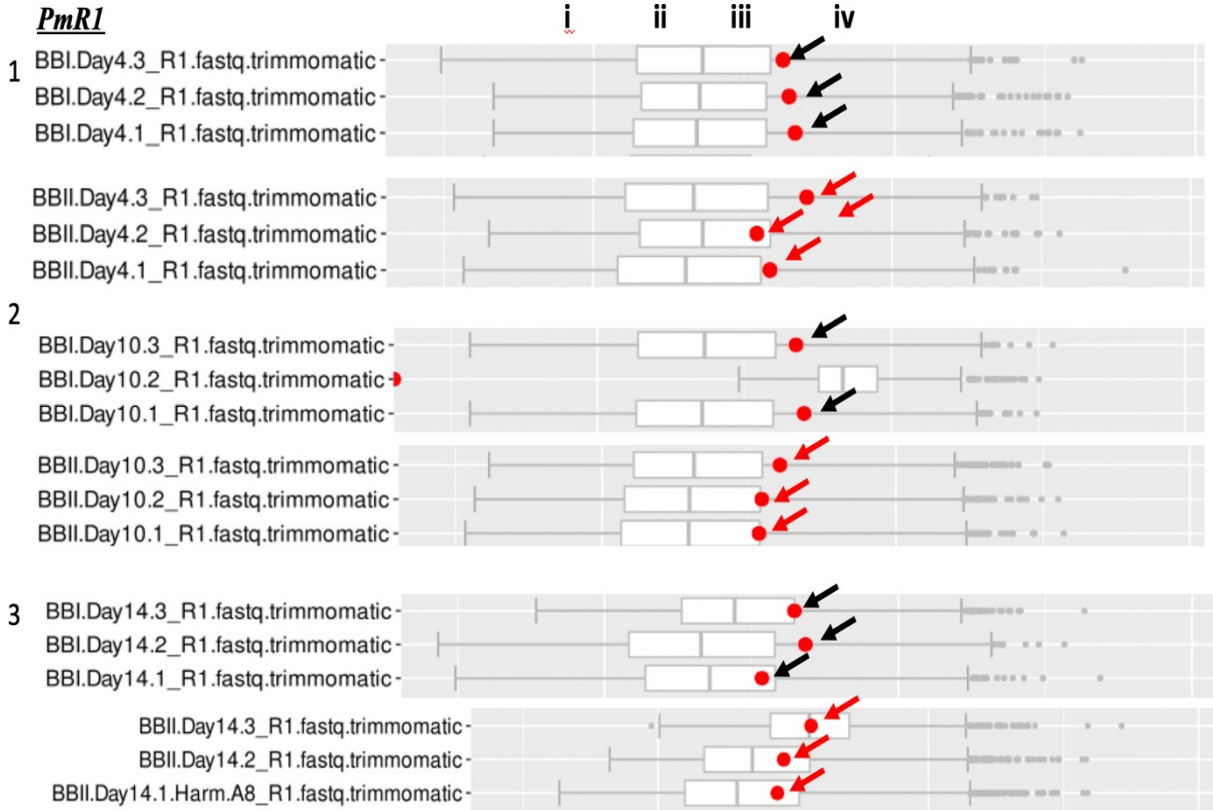


**Figure 5.3e**

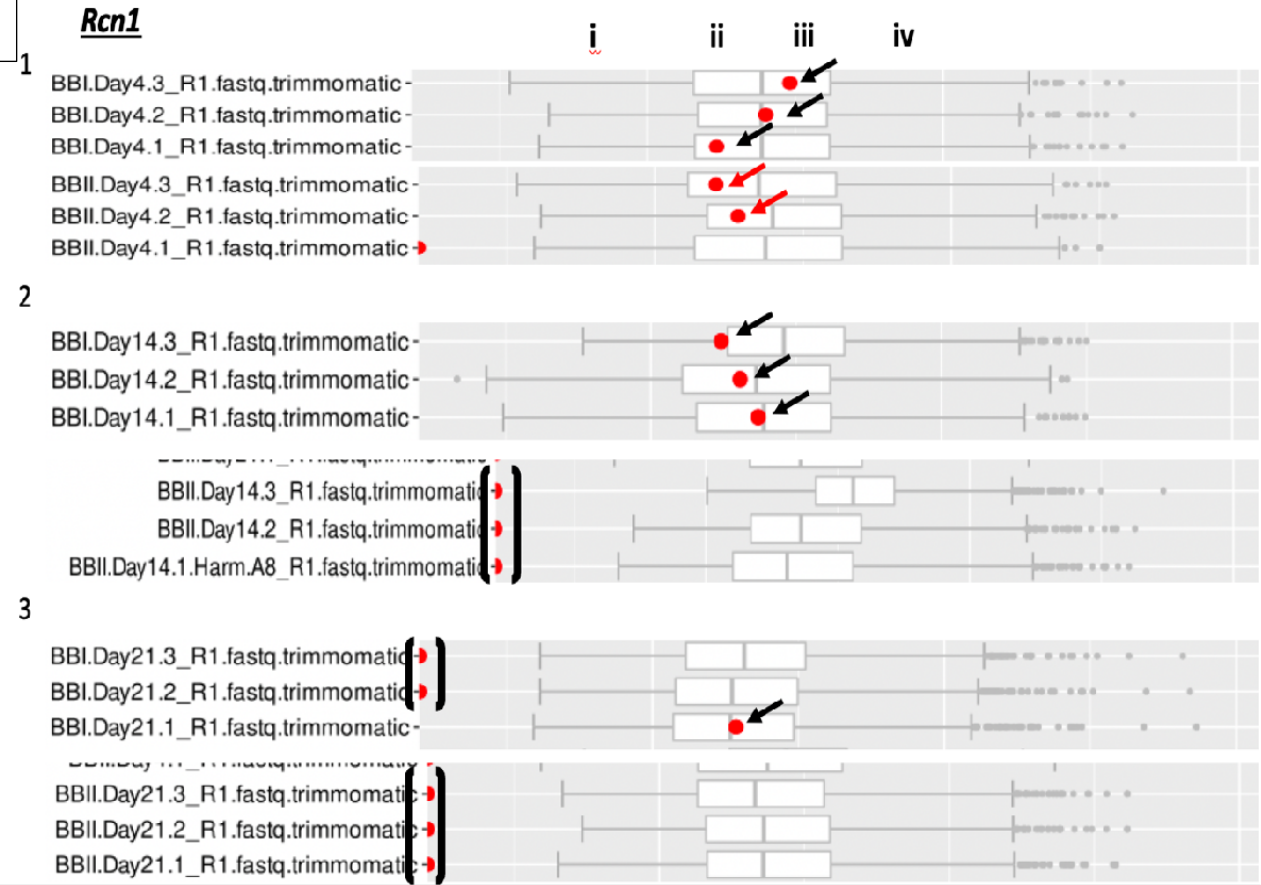
Summary of *Beauveria bassiana* genes involved in calcium signaling and transport. *Csa1*, calcium sensor acidification; *CnA/B*, calcineurin catalytic and regulatory subunits; *Vcx1*, vacuolar; *Pmr1*, are analysed in detail. (Modified from Ortiz-Urquiza *et al.*, 2016)

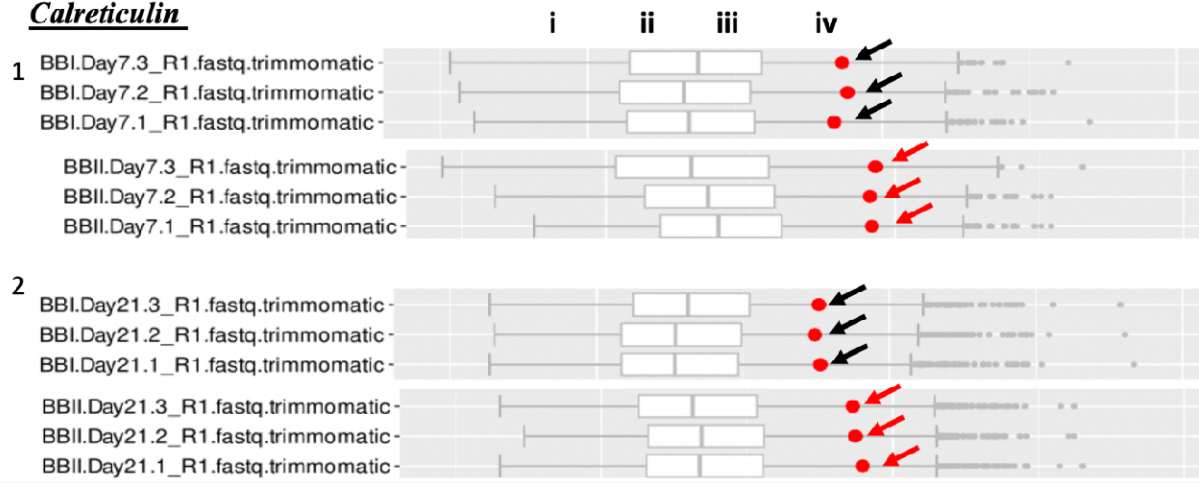
**A*****Bbcsa1*****B*****vex1***

**C**



**D**



**E****Calreticulin****Figure 5.3f**

Boxplots demonstrating the expression profiles of calcium binding and transport proteins. Black arrows indicate expression in PmV-1.I, and red arrows indicate expression in PmV-1.F. The four quartiles are indicated as i (first quartile), ii (second quartile), iii (third quartile), and iv (fourth quartile). A) *Bbcsa1* is slightly upregulated in PmV-1.F as indicated by the red arrows, upregulation of this gene is also observed at 14 and 21 dpi (A2 and A3) when compared against other timepoints. B) *vcx1* and C) *pmr1* are slightly overexpressed in PmV-1.I, however at 10 dpi *vcx1* is upregulated in PmV-1.F. D) *rcn1* is significantly upregulated in PmV-1.I (D1, D2 and D3), while it is switched off in PmV-1.F at 14 and 21 dpi (D2 and D3; indicated by the brackets). E) *cne1* is upregulated in PmV-1.I (E1 and E2) as indicated by the red arrows. *Bbcsa1*, *vcx1*, and *pmr1* are highly expressed at 10 dpi (A1, B1, and C2), *rcn1* switched off at 14 and 21 dpi (D2 and D3).

The gene profiles of proteins involved in Ca<sup>2+</sup> binding and transportation were examined in *B. bassiana* isolates VI and VF EABb 92/11-Dm. One feature is that genes responsible for Ca<sup>2+</sup> binding are upregulated in PmV-1.F, while Ca<sup>2+</sup> transporter are upregulated in PmV-1.I. In fungi Ca<sup>2+</sup> transporters such as BbVxc1 and BbPmR1 are responsible for controlling Ca<sup>2+</sup> homeostasis and stress tolerance. Both genes are upregulated in PmV-1.I across all timepoints. However, at 10 dpi BbPmr1 is upregulated in PmV-1.I and Bbvxc1 is upregulated in PmV-1.F (Figure 5.3f). Furthermore, gene expression of both transporters remains relatively high (BbPmr1 in particular) across all time points exhibiting a similar expression profile to other genes investigated including *hsp*, *mdp* and *mtd*. These observations might reflect a generalised fungal stress response.

Regulators for calcineurin proteins (RCAN) are conserved in fungi and humans and are crucial for normal calcineurin signaling (Li *et al.*, 2011). The precise role of Rcn1 is not well understood, but it exhibits both negative and positive contributions to calcineurin signaling as demonstrated in a yeast mutant lacking Rcn1 where calcineurin signaling was sufficiently reduced (Kingsbury *et al.*, 2000). Phosphorylated Rcn1 is itself a substrate of calcineurin (Hilioti *et al.*, 2004). Gene profiling of BbRcn1 displays upregulation in PmV-1.I across all timepoints with high expression 4 dpi. Furthermore, this gene is switched off in PmV-1.F at 14 and 21 dpi (Figure 5.3f-D2 & 3), while is switched on in PmV-1.I. Both Ca<sup>2+</sup> binding Bbcsa1 genes investigated demonstrated similar expression patterns and were highly expressed 14 dpi and *cne1* highly expressed 21 dpi. Calcineurin is crucial for calcium homeostasis, as it controls calcium transporters on the plasma membrane (Groppi *et al.*, 2011; Muller *et al.*, 2001). Furthermore, calcineurin inhibits BbVcx1 activity and stimulates the expression of numerous genes (Stathopoulos *et al.*, 1997) including not only BbPmr1 (Halachmi *et al.*, 1996), but also genes encoding for a  $\beta$ -1,3 glucan synthetase involved in cell-wall synthesis (Zhao *et al.*, 1998). In filamentous fungi, calcineurin is also crucial for cell cycle progression, hyphal branching,

stress adaptation and localizes at both hyphal tips and septa (Juvvadi *et al.*, 2011). Unfortunately, calcineurin was not included in this study but its regulator calcipressin was. Genes involved in calcium homeostasis (BbRcn1 and BbVcx1) and transportation (BbPmr1) are upregulated in PmV-1.I illustrating those interactions between BbPmV-1 and the fungus are not diminishing fungal viability rather improving growth under certain conditions.

#### **5.3.2.5 *Beauveria bassiana* secondary metabolites (mycotoxin)**

Mycotoxins are secondary metabolites secreted by certain pathogenic fungi which can cause disease and death to animals, insect, and sometimes, humans. Some of these molecules are used as antibiotics because of their ability to control growth of other microorganisms. *B. bassiana* produces secondary metabolites which facilitate the early stages of insect infection. Following entry of *B. bassiana* into the hemocoel the fungus needs to evade or suppress the insect's immune system, and/or inhibit growth of competing microbes. To achieve this *B. bassiana* synthesise and secretes secondary metabolite mycotoxins which include oosporein, bassianolide, beauvericin, and tenellin of some of which contribute to pathogenicity (Hof, 2008).

##### **5.3.2.5.1 Tenellin**

Tenellin a yellow pigment isolated from *B. bassiana* mycelia, is synthesised *via* a fused type I PKS-NRPS termed *TenS* whose structure contains a 2-pyridone residue (Eley *et al.*, 2007). Tenellin is toxic for mammalian erythrocytes (Jeffs & Khachatourians, 1997) but not for *Galleria mellonella* larvae following a comparison between a wild-type tenellin producing isolate and a mutant strain (Eley *et al.*, 2007). Tenellin also can act as an iron-chelator preventing iron-induced oxidative stress (Jirakkakul *et al.*, 2015). In iron-replete condition when ferricrocin-deficient (iron-chelating compound) mutants and wild-type isolates were

compared a surprising relationship between tenellin biosynthesis and ferricrocin was discovered. More specifically in iron-replete conditions a significant accumulation of iron–tenellin complex was observed in mutant strains, whereas only ferricrocin was observed in wild-type strains (Jirakkakul *et al.*, 2015). Tenellin also contains a metal binding agent called hydroxamic acid which is believed to be the main factor enabling tenellin to bind with iron (Farkas *et al.*, 2007; Williams & Sit 1982). Therefore, deficiency of the *B. bassiana* intracellular siderophore, ferricrocin, stimulates the production of tenellin which has the property of an iron-chelator protecting the cell from oxidative stress caused by increased levels of iron (Jirakkakul *et al.*, 2015).

#### **5.3.3.5.2 Beauvericin**

Beauvericin is a cyclo oligomer depsipeptide exhibiting insecticidal as well as antibiotic activity. Furthermore, beauvericin is considered to be an ionophore able of transporting monovalent cations (e.g., Na<sup>+</sup> and Cl<sup>-</sup>) across membranes resulting in uncoupling of oxidative phosphorylation (Steinrauf 1985). The *B. bassiana* gene *Beas* encodes BbBeas which is a non-ribosomal peptide synthetase responsible for beauvericin biosynthesis. Disruption of the gene in a deletion mutant  $\Delta BbBeas$  demonstrated a significant reduction in beauvericin biosynthesis (Xu *et al.*, 2008). Beauvericin exhibits increased toxicity for a variety of insect pests including the Colorado potato beetle larvae and mosquitoes but no significant toxicity was observed for the corn earworm (Champlin & Grula 1979). Beauvericin is also toxic for brine shrimp (*Artemia salina*) and moderate toxicity for Gram-positive bacteria and several other filamentous fungi (Hamill *et al.*, 1969). Beauvericin exhibits a broad-spectrum of antiproliferative activity against an array of human cancerous cells using inactivation of Ca-sensitive apoptotic pathways, and inhibition of haptotaxis (directional motility) which is important for angiogenesis, invasion and metastasis of cancer cell (Zhan *et al.*, 2007;

Carmeliet, 2003). Gene knockout of BbBeas was performed and virulence of this *B. bassiana* mutant strain was compared against the wild-type using *Galleria mellonella*, *Helicoverpa zea*, and *Spodoptera exigua* as insect bioassays. The mutant *B. bassiana* strain showed significantly low-level toxicity for insects apart from *Helicoverpa zea* even at high spore concentrations as compared to the wild-type (Xu *et al.*, 2008). These results indicate a significant contribution of beauvericin to *B. bassiana* virulence against a variety of insect hosts.

#### **5.3.2.5.3 Bassianolide**

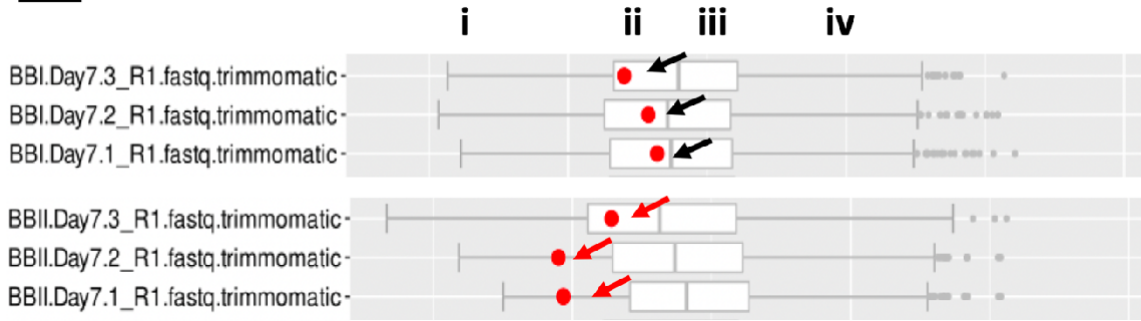
Bassianolide is a second cyclo oligomer depsipeptide which, together with beauvericin, was first detected in silkworm larvae cadavers killed by *B. bassiana* (Kwon *et al.*, 2000), highlighting the importance of these metabolites in insect pathogenesis. Purified bassianolide is toxic for *Helicoverpa zea*, which is resistant to beauvericin, and has cytotoxic activity against Apicomplexan parasites (in the genus *Plasmodium*) and demonstrates anti-mycobacterial activity *in vitro* (Jirakkakul *et al.*, 2008). A *B. bassiana* gene for a non-ribosomal peptide synthetase (NRPS), BbBsIs, has been characterised and knockout studies performed to evaluate the contribution of bassianolide to toxicity. The results obtained for the BbBsIs mutant were similar to those obtained for beauvericin and indicated reduced toxicity for the three target insects tested as compared to the wild-type (Xu *et al.*, 2009).

Generally, *B. bassiana* has the ability, to produce important secondary metabolites with both cytotoxic and antibiotic activity.

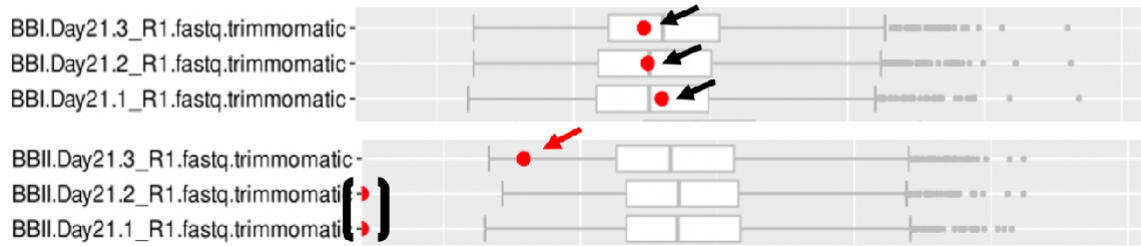
**A**

***tenS***

1



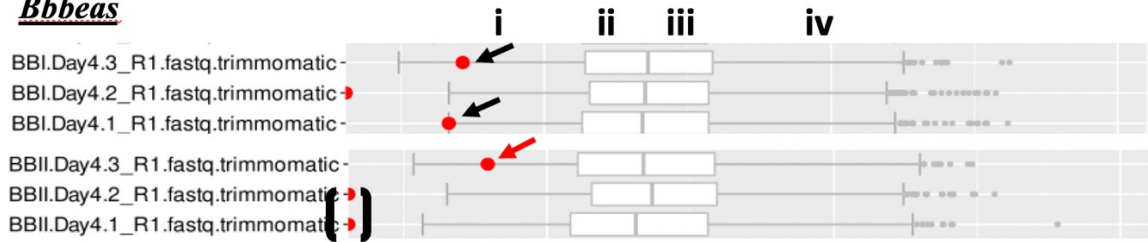
2



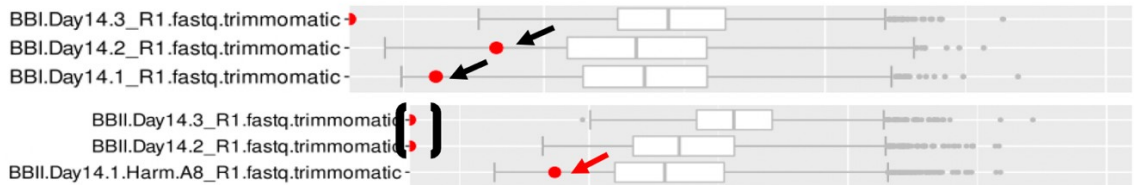
**B**

***Bbbeas***

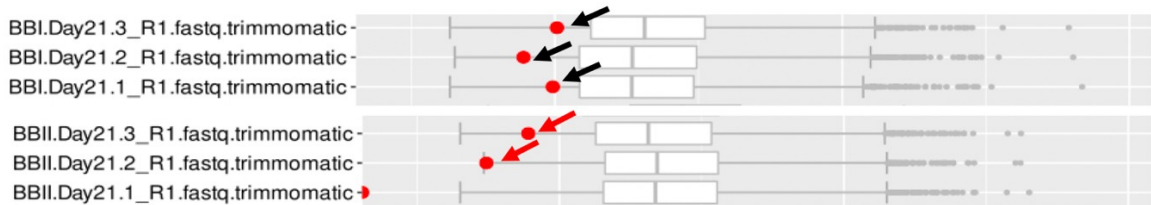
1



2



3



C

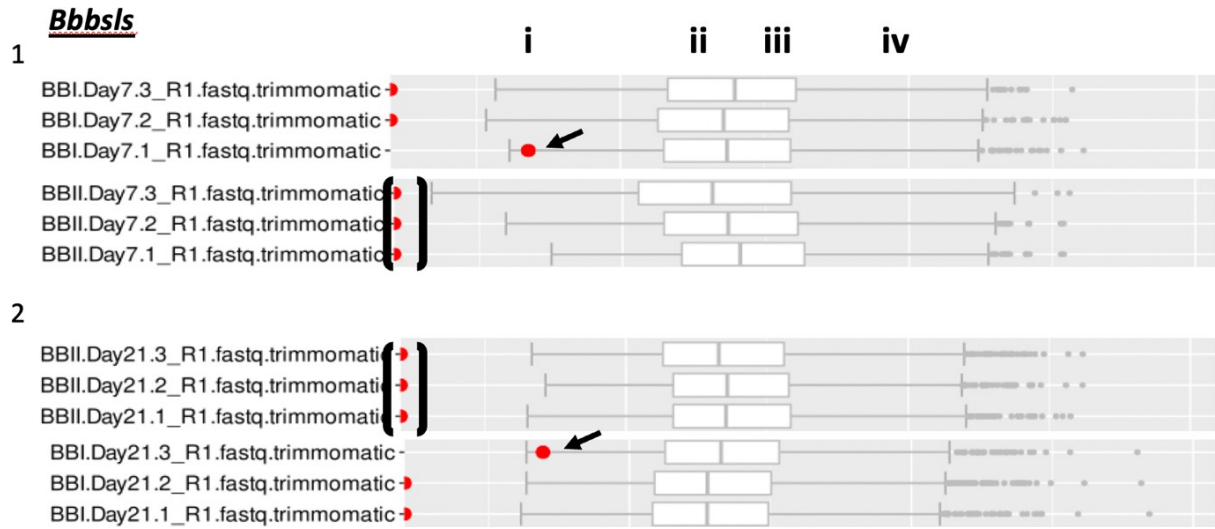


**Figure 5.3g**

Boxplots demonstrating the expression profiles of secondary metabolites. Black arrows indicate expression in PmV-1.I, and red arrows indicate expression in PmV-1.F. The four quartiles are indicated as i (first quartile), ii (second quartile), iii (third quartile), and iv (fourth quartile). A) *tenS* is significantly upregulated in PmV-1.I, while in PmV-1.F it is switched off at 21 dpi (A2). B) *BbBeas* is significantly overexpressed in PmV-1.I, while it is switched off in PmV-1.F at 14 and 21 dpi (B2 and B3). C) *BbBsIs* is switched off at 7 and 21 dpi for PmV-1.F (indicated by the brackets), while only one library is expressed in PmV-1.I (C1 library 7.1, C2 library 21.3). As indicated by the position of the dot clusters *tenS* is highly expressed as compared to the other two mycotoxins.

Gene expression profiling of *tenS* demonstrates a significant upregulation of tenellin synthesis in PmV-1.I across all timepoints. Interestingly, at 7 and 21 dpi *tenS* is highly expressed as compared to the other timepoints (Figure 5.3g-A1 & 2). Similarly at 21 dpi *tenS* is significantly upregulated in PmV-1.I, whereas in PmV-1.F it is switched off. Unlike tenellin, the gene for beauvericin (BbBeas) was not as highly expressed across the different timepoints. Gene profiling reveals an upregulation across all timepoints in PmV-1.I, while in PmV-1.F it is switched off at 4 and 14 dpi. Lastly, at 21 dpi BbBeas is significantly overexpressed as was the case with tenellin. Conversely, bassianolide is switched off across all timepoints in both PmV-1.I and PmV-1.F, however, in two libraries, one at 7 dpi and one at 21 dpi, the gene expressing bassianolide synthesis is switched on in PmV-1.I only. It is possible that these two genes are not essential when the fungus is growing in a controlled environment, hence, they are either switched off (Bassianolide; Figure 5.3g-C1 & 2) or down-regulated (Beauvericin; Figure 5.3g-B). However, tenellin, which acts as an iron-chelator and prevents iron-induced, oxidative stress appears useful for fungal survival, hence, expression across all timepoints. These results confirm and extend previous observations made by Xu *et al.*, (2008) and demonstrate that bassianolide and beauvericin are essential for toxic virulence against insects.

### **5.3.2.6 Metabolic pathways and other genes examined**

Both mannitol and trehalose are connected with spore viability, germination and stress tolerance. The two enzymes, mannitol-1-phosphate dehydrogenase (Mpd) and mannitol dehydrogenase (Mtd) are involved in mannitol biosynthesis and are necessary for full virulence of *B. bassiana*. Reduced growth and reduced tolerance to oxidative, osmotic, heat and UVB stress were recorded for gene knockouts of either Mpd or Mtd mutant's grown on several different carbohydrate sources. However, a decrease in conidia production was only observed in the  $\Delta BbMpd$  mutant with a slight decrease in virulence for both mutants' (Wang *et al.*, 2012).

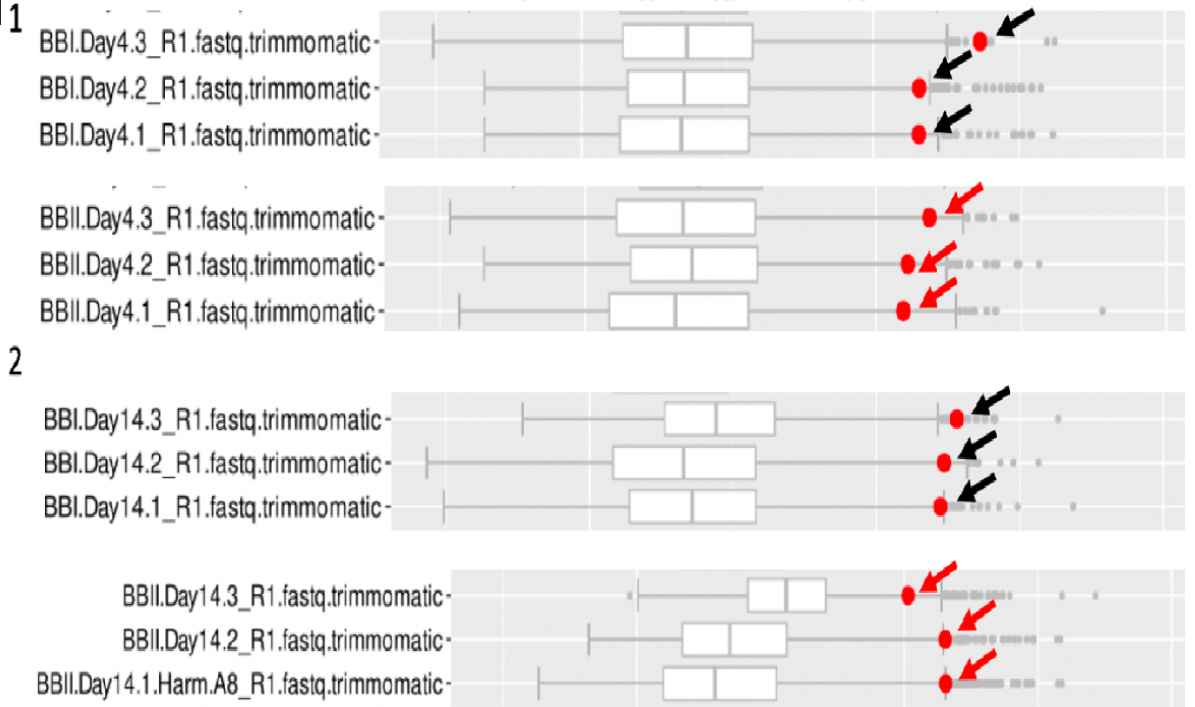
Mtd plays a crucial role in interactions between the host and pathogen and hence the decrease in virulence in the mutant strain. Gene expression profiling indicated that the *mtd* gene is similarly highly expressed across all timepoints in both PmV-1.I and PmV-1.F, however, at 10 dpi a slight overexpression is observed in PmV-1.I. A similar gene expression pattern was observed with Mpd, however, slight upregulation was observed in PmV-1.I at 4 and 14 dpi while at 21 dpi upregulation of the gene was observed in PmV-1.F. The highest upregulated expression levels were observed at 14 dpi for Mpd and at 10 dpi for Mtd, in the presence of BbPmV-1 (Figure 5.3h). Mannitol is important in protecting fungal spores against harmful factors including high temperature, drying, or increasing stress conditions. Furthermore, mannitol is responsible for controlling the cytoplasmic pH as well as acting as an antioxidant agent protecting fungal cells from reactive oxygen species (ROS) generated as a result of excessive fungal growth (Williamson *et al.*, 1995; Zamski *et al.*, 2001; Jennings *et al.*, 2002). These results highlight the importance of mannitol metabolism with respect to the ability of *B. bassiana* to resist stress tolerance and survival in toxic environments. Trehalose also plays a crucial role in cellular function, not only in carbon metabolism but also in other cellular responses such as high osmolarity, abiotic stress, nutrition starvation and dehydration (Ocón *et al.*, 2007). Trehalose is a major sugar component in insects where it circulates in the hemocoel. Trehalose synthesis involves two steps; the first step is catalysed by trehalose-6-phosphate synthase, (Tps1) and the second step by trehalose-6-phosphatase (Tps2; Wang *et al.*, 2017). Gene expression of both Tps1 and Tps2 appear to be slightly upregulated in PmV-1.I, with the highest expression levels of both genes observed to be at 7 dpi. Tps1 and Tps2 are important for normal growth, conidiation, antioxidant response and pathogenicity of the fungus (Al-Bader *et al.*, 2010). Interestingly, when Tps1 and Tps2 expression levels were compared to Mpd and Mtd overexpression of the latter were found indicating the importance of mannitol in stress tolerance. Finally, the expression levels of *agdC* gene were significant up-regulated in PmV-

1.F 4, 7 and 21 dpi as indicated by the position of the red dots in the box plots (Figure 5.3h). This gene is involved in the metabolic pathway of carbohydrates and encodes for alpha/beta-glycosidase which cleaves the alpha (1,4) glycosidic bond of disaccharides (maltose) to glucose. These findings correlate with our previous conclusions in Chapter 4 suggesting that polmycoviruses affect the metabolic pathway prior to the conversion of maltose and fructose to glucose.

In conclusion it is evident that BbPmV-1 replication does not burden the fungus, on the contrary it seems that it acts as an extrachromosomal element in a symbiotic relationship.

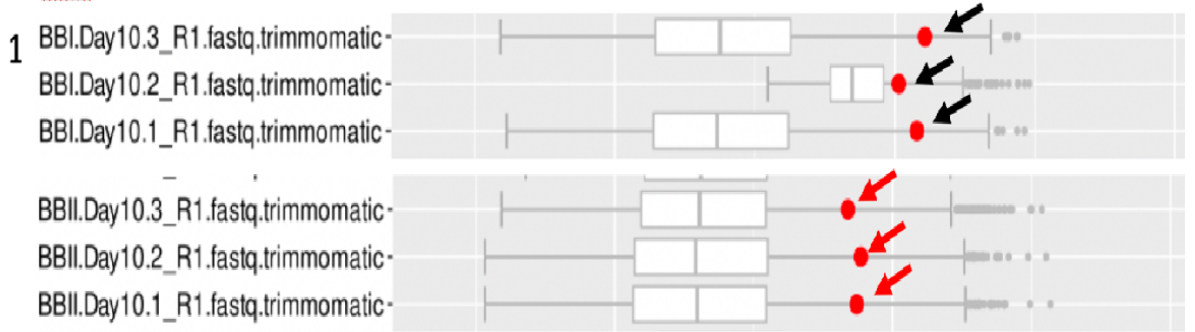
A

*mpd*

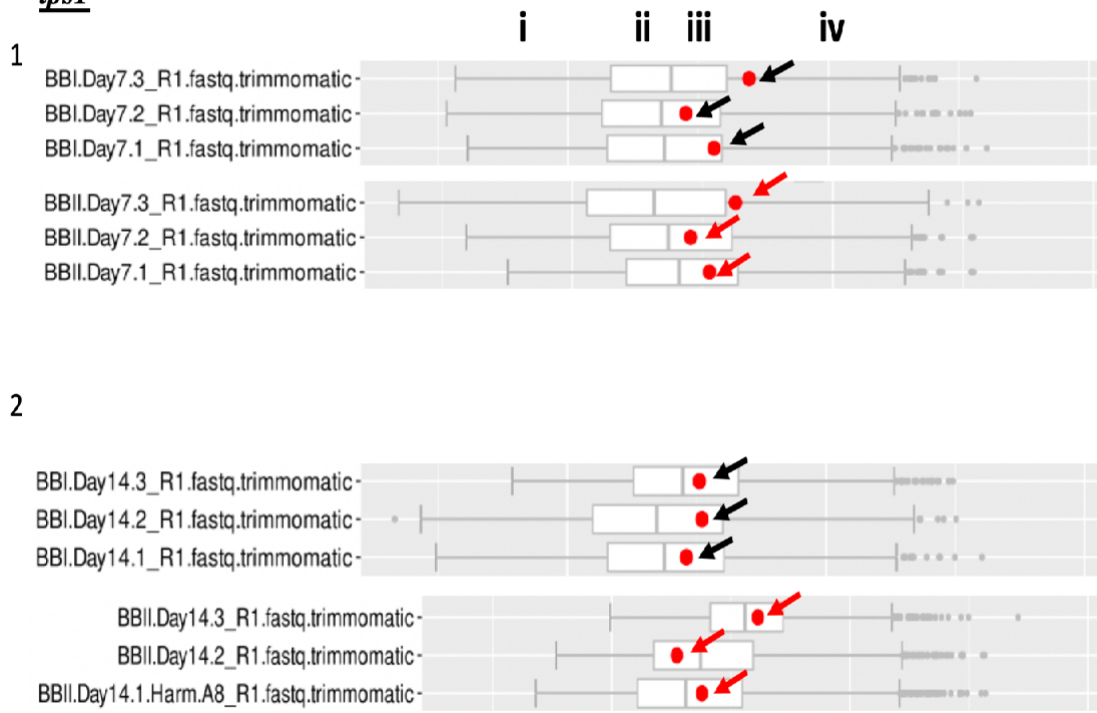


B

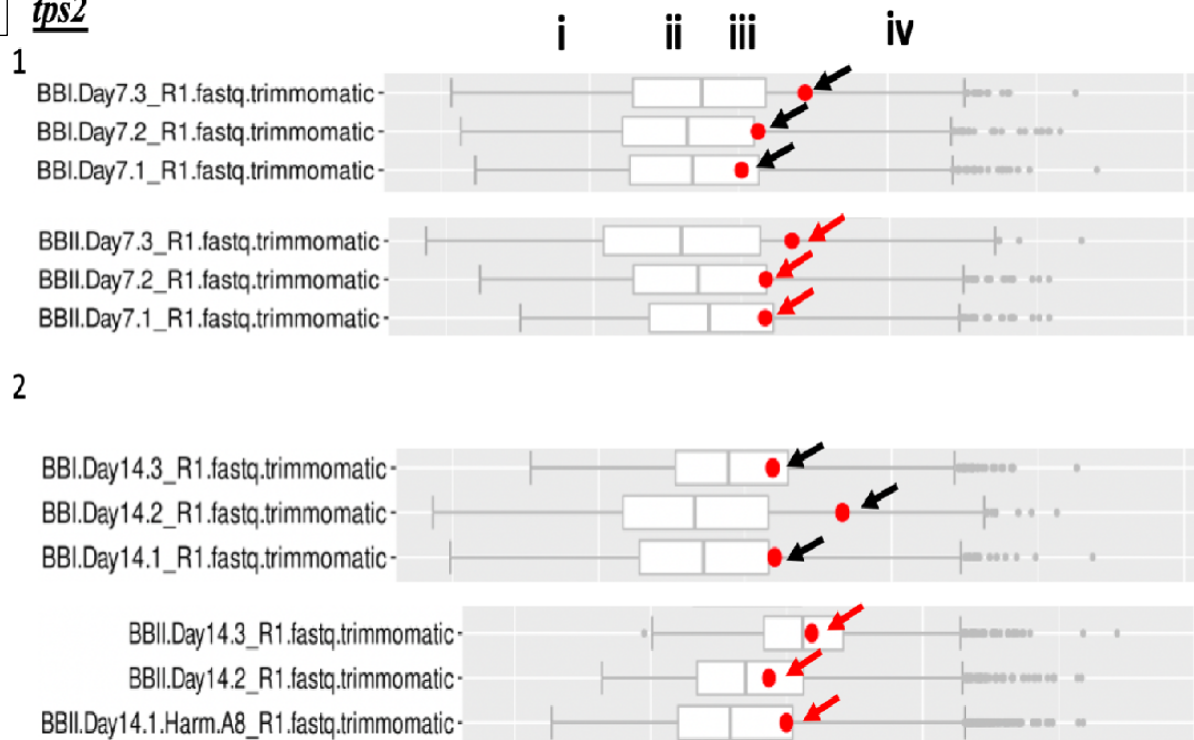
*mtd*



**C** *tps1*



**D** *tps2*



E

***agdC***

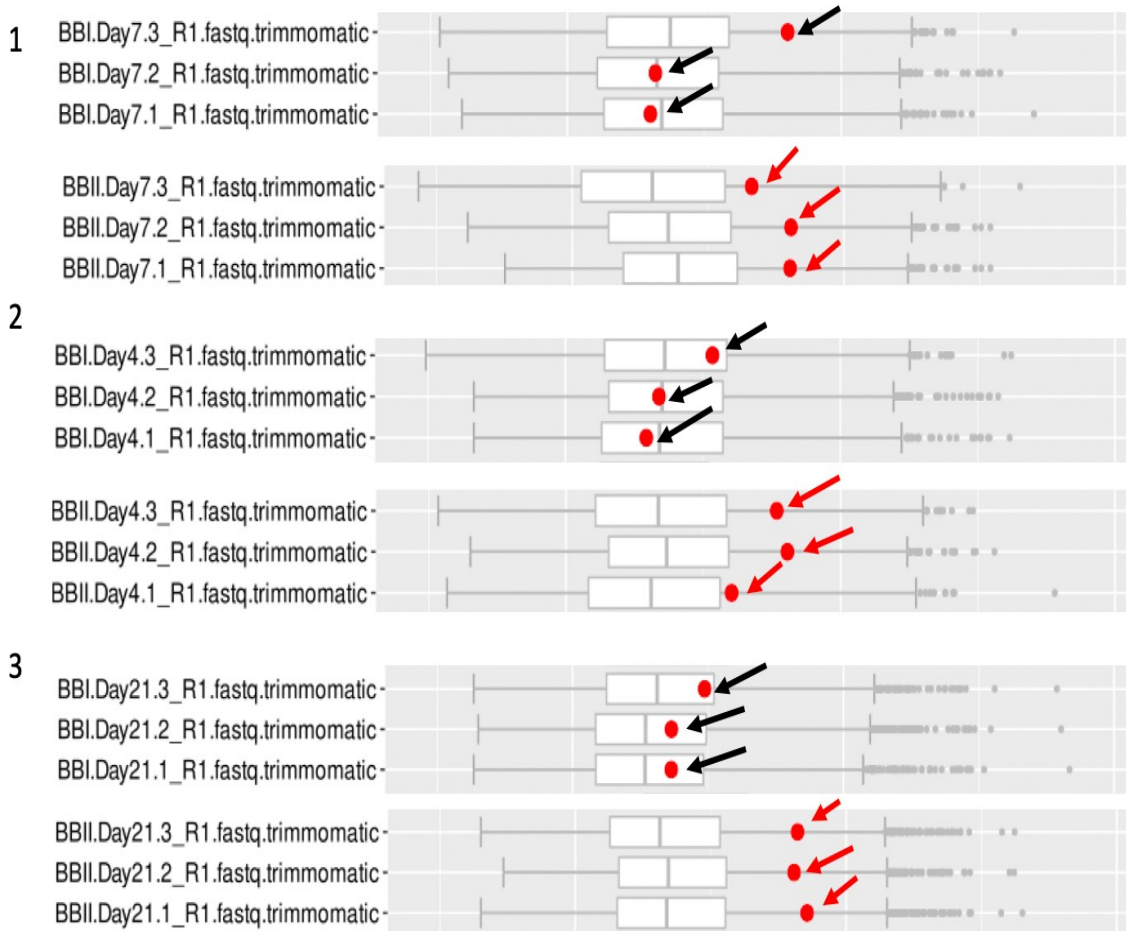


**Figure 5.3h**

Boxplots demonstrating the expression profiles of genes involved in metabolic pathways. Black arrows indicate expression in PmV-1.I, and red arrows indicate expression in PmV-1.F. The four quartiles are indicated as i (first quartile), ii (second quartile), iii (third quartile), and iv (fourth quartile). A) *mpd* and B) *mtd* exhibit similar gene expression patterns, both are upregulated in PmV-1.I and highly expressed (as indicated by the dot clusters positioned at the far-right end of the iv quartile). C) *tps1* and D) *tps2* also express similar gene expression patterns, both are upregulated in PmV-1.I, although they are not as highly expressed as *mpd* and *mtd* (the dot clusters positioned at the iii quartile). E) *agdC* is significantly upregulated at 4, 7 and 21 dpi in PmV-1.F compare to PmV-1.I.

### 5.3.2.7 Heat shock proteins (Hsp30, Hsp70, Hsp90)

Heat shock proteins are molecular chaperones and are involved in a wide range of physiological functions in fungal cells and other eukaryotes. The heat shock protein (hsp) family represents a large group of evolutionary conserved proteins which are classified based on their molecular sizes of >30 to ~100 kDa. Within the HSP family Hsp70 (~70kDa) and Hsp90 (~90kDa) both require ATP for normal function and are very important for protein quality control (Verghese *et al.*, 2012). Hsp90 interacts or activates the MAPK pathway *via* induction of a Hsf1 transcription factor (Truman *et al.*, 2007) together with orchestrating communication between the MAPK Slt2 and Hog1 pathways (Leach *et al.*, 2012). Also, Hsp70 has a significant role in growth, conidiation, pathogenicity and maintenance of cell wall integrity (Yang *et al.*, 2018), while Hsp30 is involved in conidial thermotolerance (Lee *et al.*, 2018).

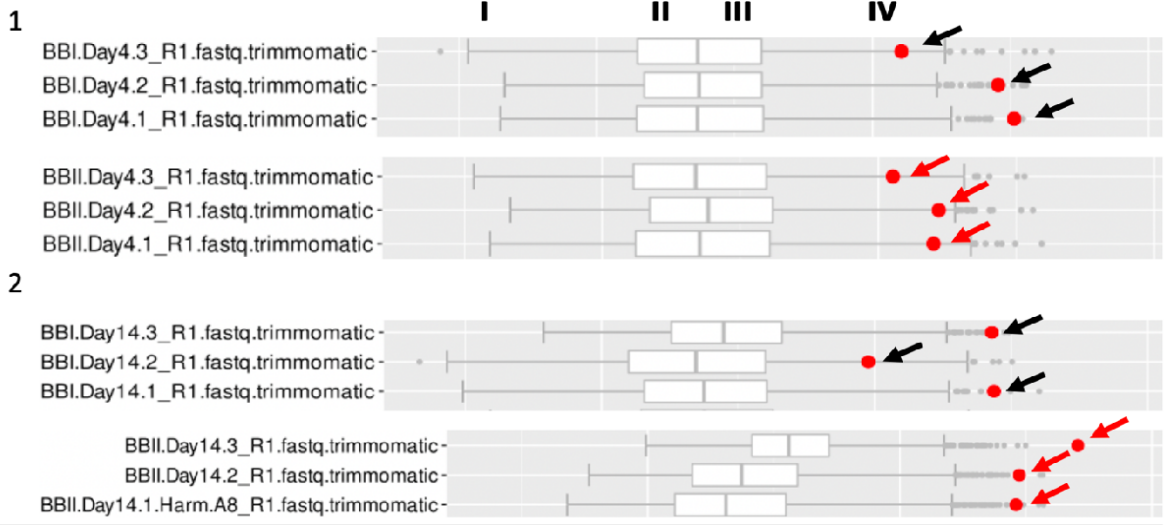
Knockout of *hsp* genes resulted in significant different defects when the fungus was exposed to environmental stresses, including reduced growth, conidiation, cell wall integrity, heat and pH reduced tolerance. Interestingly, Lamoth and colleagues tried to generate a  $\Delta hsp90$  mutant strain in *A. fumigatus* and failed demonstrating the importance of this protein for fungal survival (Lamoth *et al.*, 2012). However, genetic repression of Hsp90 revealed a significant reduction in spore viability, decreased hyphal growth, germination and conidiation all of which are linked with the downregulation of *brlA*, *wetA*, and *abaA*, all specific transcription factors involved in conidiation (Lamoth *et al.*, 2012).

In PmV-1.F overexpression of the Hsp90 gene was observed across all timepoints. Both Hsp30 and Hsp70 are overexpressed in PmV-1.I across all time points. All three heat shock proteins were highly expressed across all timepoints, but at 14 and 21 dpi their expression levels were at the highest (Figure 5.3j). It is conceivable that within those timepoints the fungus is under significant environmental stress due to a lack of nutrient and/or toxic waste accumulation

during growth. These results demonstrate that the Hsp proteins are essential for fungal survival and stress tolerance.

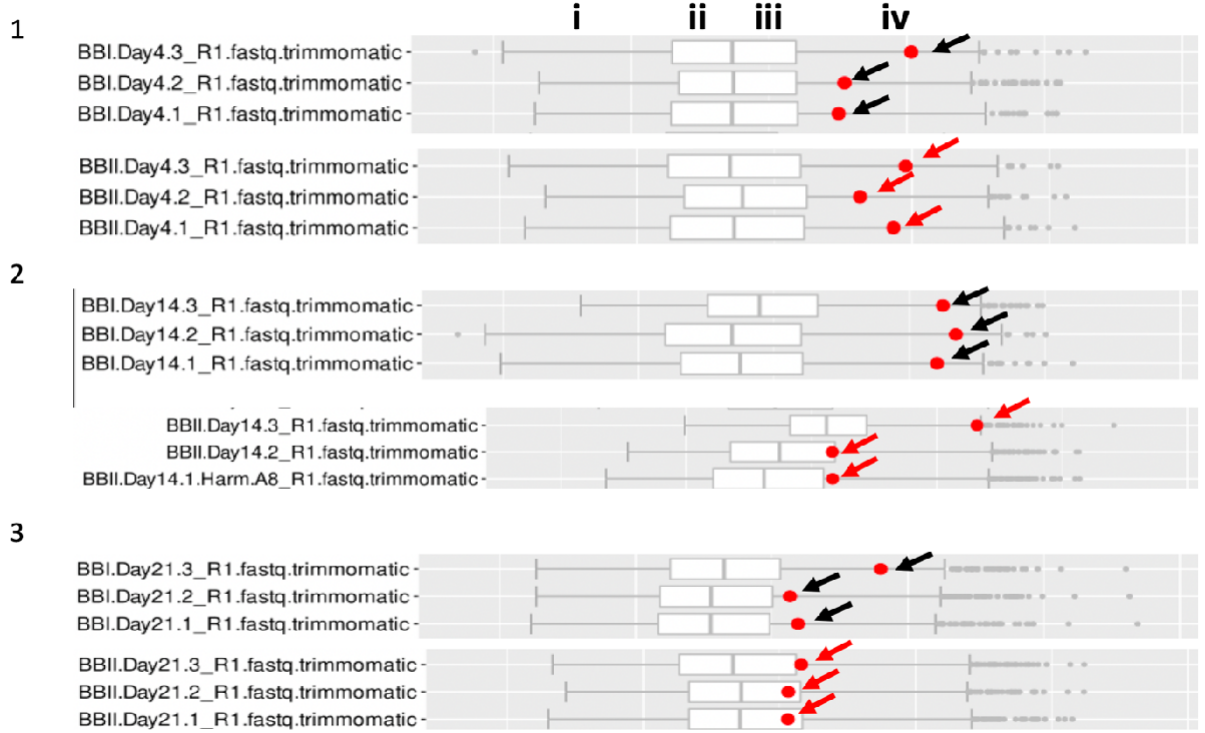
A

***hsp30***



B

***hsp70***



C

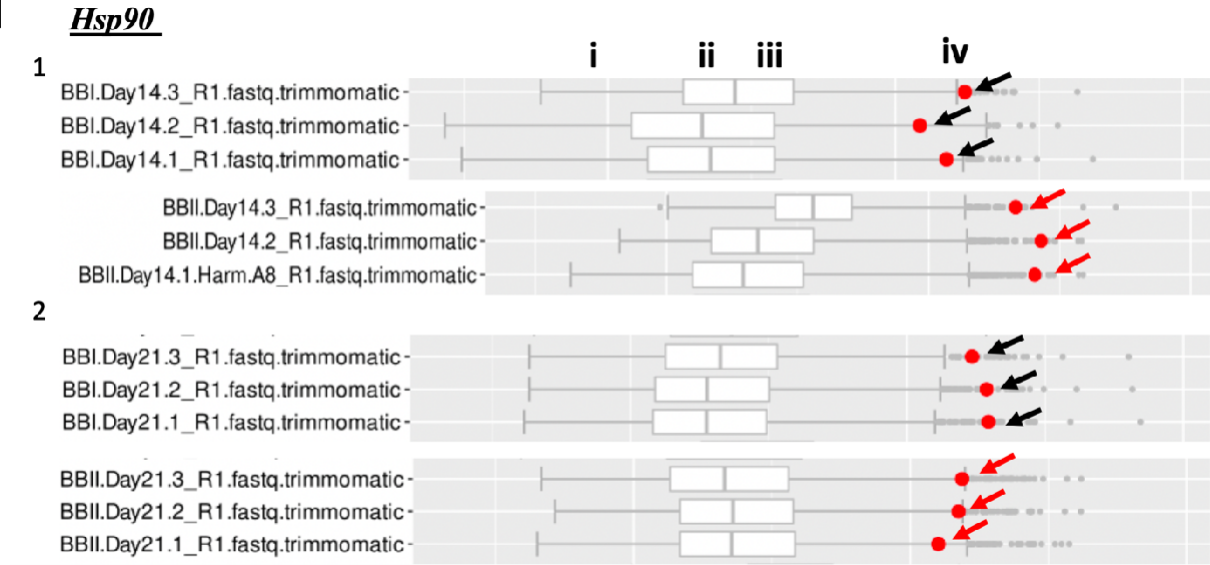


**Figure 5.3i**

Boxplots demonstrating the expression profile of heat shock protein genes. Black arrows indicate expression in PmV-1.I, and red arrows indicate expression in PmV-1.F. The four quartiles are indicated as i (first quartile), ii (second quartile), iii (third quartile), and iv (fourth quartile). **A)** *hsp30* and **B)** *hsp70* are significantly upregulated in PmV-1.I as indicated on the positions of the dots in each library, while **C)** *hsp90* is upregulated in PmV-1.F. *hsp30* and *hsp90* are both highly expressed in both PmV-1.I and PmV-1.F (as indicated by the dot clusters positioned at the far-right end of the iv quartile), while *hsp70* is less expressed but still dot clusters are positioned at the iv quartile.

### 5.3.2.8 Thaumatin-like proteins

Thaumatin-like proteins (TLPs) are a family of proteins found in plants, animals and fungi and are linked with host defence. TLPs have antifreeze, and antifungal properties (Yun *et al.*, 1998) and can bind to and hydrolyse  $\beta$ -1,3-glucan which is a common component of fungal cell walls leading to cell lysis (Grenier *et al.*, 1999). TLPs are present in plant pathogenic fungi such as *Rhizoctonia solani* as well as in saprophytes such as *Aspergillus nidulans* but their role in fungal metabolism is unclear (Greenstein *et al.*, 2006).

*T. molitor* produces numerous antimicrobial defence peptides including tenecins 1-3 which are active against entomopathogenic fungi too (Johnston *et al.*, 2014). Tenecin 3 is a TLP and is constitutively expressed during infection with *T. molitor* by *B. bassiana* where it inhibits infection and contributes to insect survival. In plants TLPs are secreted and protect them against infection with pathogenic fungi or insects. Grapevines inoculated with endophytic *B. bassiana* and were successfully protected from infection by possibly through TLP activity *Plasmopara viticola* (Rondot & Reineke, 2019). Protective mechanisms offered by *B. bassiana* acting as an endophyte, are likely to include antibiosis, competition for space and nutrients, parasitism, and induction of plant defence (Rondot & Reineke, 2019).

## Thaumatococcus-like protein

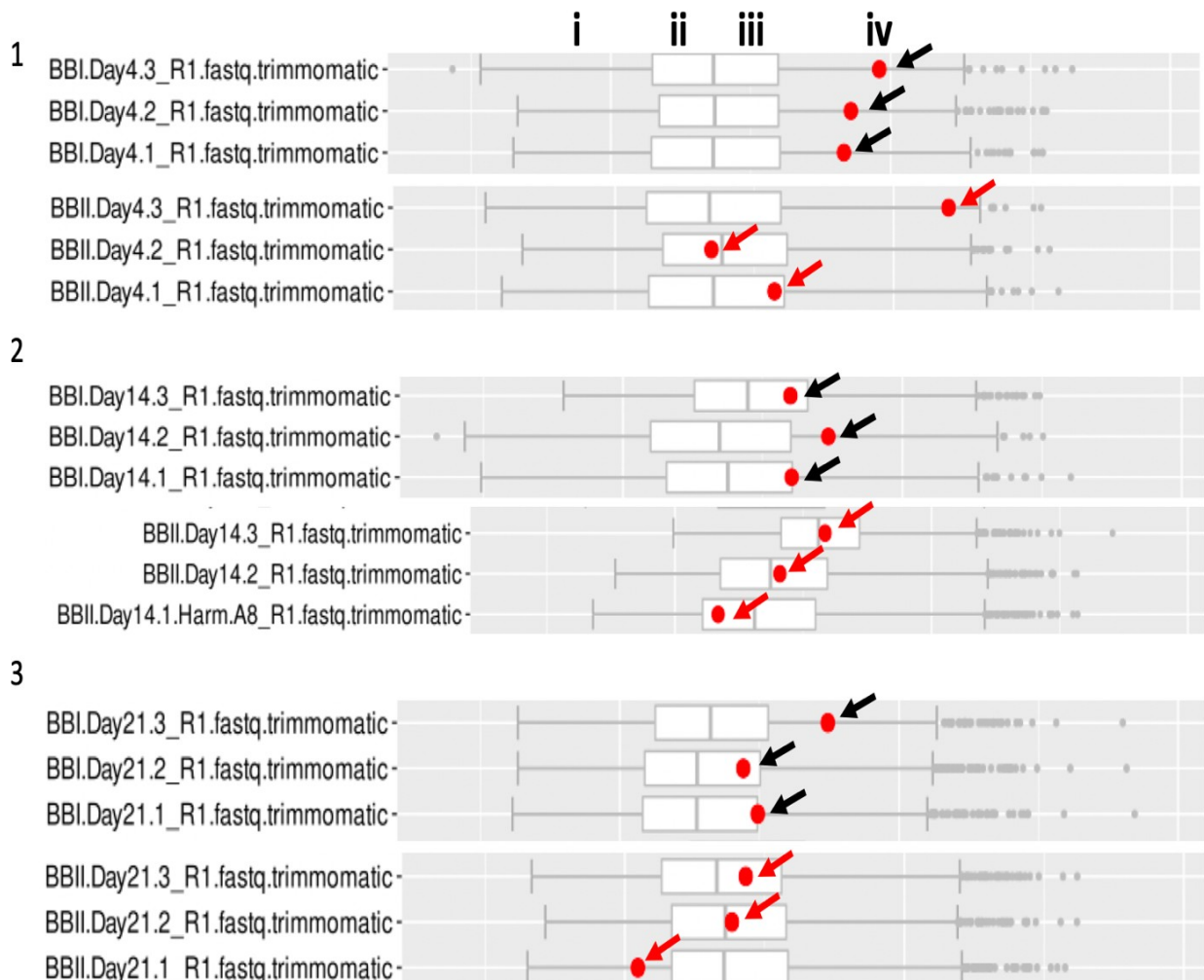


**Figure 5.3j**

Boxplots demonstrating the expression profile of thaumatin-like protein. Black arrows indicate expression in PmV-1.I, and red arrows indicate expression in PmV-1.F. The four quartiles are indicated as i (first quartile), ii (second quartile), iii (third quartile), and iv (fourth quartile). TLP is significantly upregulated in PmV-1.I as indicated on the positions of the dots in each library. TLP is highly expressed in PmV-1.I at 4 dpi as (as indicated by the dot clusters positioned at the far-right end of the iv quartile).

The gene expression levels of TLPs were significant up-regulated in PmV-1.I 4 dpi, whereas at 21 dpi expression levels were slightly lower (Figure 5.3j). The role and function of TLPs in fungi is poorly understood but is likely that they protect endophytes during colonization particularly regarding competition for space and nutrients.

To conclude, it is evident that BbPmV-1 displays a symbiotic relationship with its fungal host. Genes involved in virulence, conidiation, hyphal growth and stress tolerance (*Mtd*, *mdp*, *nosA*, *tps1*, *tps2*, *hsp* etc.) were found to be upregulated in PmV-1.I compared to PmV-1.F. Exposure of the fungus to different environmental stresses are harmful either when it is found on the soil, during insect infection (adherence, evading immune responses, competition for space) or even as an endophyte (fungicides being applied, competition for space) may affect their field stability and efficacy as a pesticide. For this reason, efficacy and stability of these biocontrol agents can be greatly improved by exploring and understanding molecular mechanisms. This study is unique as it has provided evidence for polynucoviruses acting as extrachromosomal genetic material providing new traits to PmV-1.I making it more virulent and probably able to tolerate stress better than its virus-free counterpart PmV-1.F.

# **Chapter 6**

## **General Discussion**

## 6.1 General Aims

The aim of this thesis is to identify mycovirus-induced hypervirulence in entomopathogenic fungi and how we can exploit it to improve their field stability and efficacy as pesticides. To achieve this goal, the work was divided into four main steps. The first step was to isolate entomopathogenic fungal strains including, *Beuaveria bassiana*, *Purpureocillium*, *Metarhizium*, *Isaria*, *Lecanicillium*, and *Paecilomyces*, and screen them for the presence of mycoviruses. The next step was to cure the mycoviruses from the infected isolates to eventually create virus- infected and virus-free isogenic lines. Eradication of these viruses would allow a direct comparison of their effects on fungal virulence and pathogenicity in terms of their growth, morphology in solid culture, and against live insects. Finally, using next generation sequencing (NGS), specifically RNA-seq, allowed the examination of mycovirus infection at a molecular level by studying the expression profiles of genes responsible for fungal virulence. Specifically, this thesis addresses the scenario that, in at least one instance, mycoviral infection could cause hypervirulence and can result in more effective pest biocontrol agents. Only entomopathogenic fungi (*B. bassiana*) are considered here but this research can be transferred to viruses infecting human pathogenic fungi (for example *Aspergillus* spp).

### 6.1.2 Brief outline of thesis

The main research aim of this work is to use mycovirus-mediated hypervirulence to enhance commercially available mycopesticides. The work presented in this thesis comprises of three main chapters. The results of two of these chapters have been published in leading journals of the field.

In chapter 3, the objective was to screen a large batch of entomopathogenic fungi, received from different parts of Europe, and document the presence and diversity of any mycoviruses. Furthermore, this chapter describes completing the full sequences of the viral genomes of three

viruses discovered in *B. bassiana* (BbPmV-3), *L. muscarium* (LmV-1) and, *A. fumigatus* (AfuPV-1A). Data analysis and sequencing of the mycoviruses provided us with useful information about population structure and dynamics, transmission, and pathogenicity.

Chapter 4 describes the eradication of mycoviral infections from *B. bassiana* ATHUM 4946 and *L. muscarium* 143.62 using cycloheximide and Ribavirin respectively. It focuses on the effects of mycoviral infection on fungal growth, conidiation, morphology, and pathogenicity against live insects. Furthermore, it investigated which fungicides could be used as selective markers for future experiments. Both symptomatic (hypervirulence caused by BbPmV-1 and BbPmV-3) and asymptomatic (LmV-1 infection) cases of mycoviral infections were demonstrated. Both BbPmV-1 and BbPmV-3 infections exhibited similar hypervirulent results such as increased conidiation, increased pathogenicity against insects, and increased growth when grown on various media (Czapek Dox, MEA, PDA and Czapek Dox containing different carbon sources). After investigating sensitivity of *B. bassiana* against several fungicides, I concluded that using benomyl as a potential selection marker would be helpful for any future transfection experiments.

Chapter 5 focuses on the effects of BbPmV-1 on the virulence of the entomopathogenic fungus EABb 92/11-Dm at a molecular level. Total RNA of PmV-1.I and PmV-1.F isogenic lines of *B. bassiana* EABb 92/11-Dm was extracted and sequenced using RNA-seq. Analysis of the results revealed a symbiotic relationship between virus and fungus. The results indicate that the virus acts as an extrachromosomal genetic material causing a hypervirulent effect on PmV-1.I, reminiscent of the lysogenic replication cycle in bacteriophages.

## **6.2 General Discussion**

There is a significant interest in employing entomopathogenic fungi as biocontrol agents, an alternative means to chemical pesticides (Chandler *et al.* 2011). Entomopathogenic fungi from

the genera *Beauveria*, *Metarhizium*, *Isaria*, and *Lecanicillium* within the phylum Ascomycota and order Hypocreales are used as biopesticides with more than 150 commercially available products (de Faria, & Wraight, 2007; Lacey *et al.* 2015). *B. bassiana*, discovered by Agostino Bassi in 1835, is the anamorph (i.e. asexual form) of *Cordyceps* responsible for the white muscardine disease in insects. It can be found in soil (Garrido-Jurado *et al.*, 2015) and as an endophyte (McKinnon *et al.*, 2017). Furthermore, its potential to infect a wide range of arthropod pathogens and disease vectors is not overlooked (de Faria, & Wraight, 2007). This is topical as vector control programmes are currently being threatened by increasing insecticide resistance (Ranson *et al.*, 2011; Yewhalaw *et al.*, 2011; Asidi *et al.*, 2012; Badolo *et al.*, 2012). Mosquitos, a major vector of human viral diseases (dengue and yellow fever, Zika and West Nile) and parasitic (malaria) is one such insect host of *B. bassiana*. A promising method, that would not involve any genetic modification or genome editing techniques, is the use of *B. bassiana* for controlling mosquito population and ultimately prevent the spread of these pathogenic organisms (Heinig & Thomas, 2015; Lee *et al.*, 2019). Indeed, using *B. bassiana*, and other entomopathogens, in crop protection is currently being explored as the increase of pesticide resistance in insect populations present in crops is alarming (Food and Agriculture Organization [FAO] 2012). Importantly, this approach is compatible with modern integrated pest management (IPM) paradigms. Further, compatibility of *B. bassiana* with some of the existing insecticides would improve IPM effectiveness (Islam & Omar, 2012). However, it is important to consider the interaction between chemical insecticides and *B. bassiana* before application. Sometimes these interactions could result in a detrimental, antagonistic effect (Purwar, & Sachan, 2005). An avenue of expanding interest is its endophytic ability: it could be exploited to bypass known environmental factors limiting its effectiveness such as UV radiation, desiccation, and extreme temperatures. Presently, there are three *B. bassiana* commercial products registered for agriculture: Naturalis-L (ATCC 74040 strain), Botanigard,

and the Botanigard 22 WP (GHA strain) in Spain. Although these fungi are considered not harmful to the environment and humans, they are not as efficient as chemical insecticides. Therefore, it is essential to enhance efficiency and reliability (Leger & Wang, 2010).

Mycoviruses are a diverse taxon which is only recently being explored. Mycoviruses in general (Herrero *et al.*, 2012; Kotta-Loizou *et al.*, 2015; Koloniuk *et al.*, 2015; Gilbert *et al.*, 2019), and especially polymycoviruses (Kotta-Loizou and Coutts, 2017; Filippou *et al.*, 2018 and 2021), have been shown to infect entomopathogenic fungi, in some cases increasing their growth and virulence. In some cases, other mycoviruses were observed to cause the exact opposite effects resulting in decreased virulence, slow growth rate, and poor sporulation (Bhatti *et al.*, 2011; Kotta-Loizou & Coutts 2017). Mycoviruses are increasingly being reported in a wide range of major fungal groups, including animal and plant pathogens (van Diepeningen *et al.*, 2008). Currently they are classified in seventeen taxa: sixteen families and one genus that does not belong to a family ([https://talk.ictvonline.org/ictv-reports/ictv\\_online\\_report](https://talk.ictvonline.org/ictv-reports/ictv_online_report)). In this study, a collection of more than 200 isolates of *Metarhizium* sp., *B. bassiana*, *L. muscarium*, *Isaria*, *Purpureocillium* sp., *Paecilomyces*, and *A. fumigatus* were screened for the presence of dsRNA elements (Filippou *et al.* 2018 and 2020). Screening revealed a total of fourteen putative mycoviruses out of two hundred fungal isolates (7%; Appendix Part B Table S6.1a), a low percentage and yet indicative of their sporadic appearance. From the fungal isolates acquired from Spain, it was observed that one isolate harboured a member of the family of *Partitiviridae*, three isolates found to harbour a member of the family of *Totiviridae*, while a member of the novel *Polymycoviridae* family was observed in three isolates. The remaining five exhibited a mixed infection with all three viruses. Likewise, in the Portuguese isolates it was observed that at least one isolate harboured a member of the family *Partitiviridae*, which was termed AfuPV-1A. Examination of the dsRNA profile of AfuPV-1A revealed 99% similarity to AfuPV-1. However, AfuPV-1A supports the replication of a third genomic component. The reason why

some members of the family *Partitiviridae* appear to possess a bipartite genome while others appear to be tripartite is not yet known. Initially, dsRNA3 element of AfuPV-1A was not isolated in our screens, but this is not uncommon. Disappearance of mycovirus elements could be related to fungal growth conditions and virus distribution in mycelia. The role of AfuPV-1A dsRNA3, and similar dsRNAs in other partitiviruses, in virus replication cycle remains unknown. What is known is that mycoviruses allocated to *Partitiviridae* family have two segmented dsRNA strands and in some instances have three. One encodes the RdRP and the other encodes the CP that forms icosahedral virions. The *Totiviridae* family usually possesses one linear non-segmented dsRNA strand encoding the RdRP but dsRNA segments of mycoviruses assigned to the novel family of *Polymycoviridae* range from four to eleven (please see [https://talk.ictvonline.org/ictv-reports/ictv\\_online\\_report](https://talk.ictvonline.org/ictv-reports/ictv_online_report) for more information).

In this work, screening of eleven isolates of *L. muscarium* allowed for the discovery of a novel mycovirus. Perhaps unexpectedly, online search using public databases revealed no match to any known protein available on the database, indicating that this virus could be novel. Resistance to DNase 1 and to RNase A treatment confirmed its dsRNA nature, while Northern blots verified the authenticity of the cDNA clones. To determine its polarity, RT-qPCR revealed a positive-sense dsRNA genome (Figure 3.3e). Likewise, time course study demonstrated that LmV-1 dsRNA copy number appears to be extremely high during the early time points of fungal growth, whilst *L. muscarium* biomass is significantly lower. However, a steady decrease of LmV-1 copy numbers is observed as the fungal biomass increases during the late time points (Figure 3.3f). The underlying mechanism was not determined here, but it appears that this pattern has been observed before in unencapsidated viruses (Kotta-Loizou *et al.* 2017). To verify this hypothesis and prove that LmV-1 is an actual virus and not a satellite, future investigations employing electron microscopy would provide crucial data regarding its

morphology, size, and shape. Unfortunately, due to the SARS-CoV-2 pandemic, this could not be undertaken in this work.

Beyond replication, a pathogen's infectivity depends also to its transmission. To date, dsRNA mycoviruses are incapable of extracellular transmission but they can be transmitted horizontally from one fungal strain to another either via anastomosis, or vertically during the formation of sexual or asexual spores. To examine transmission of mycoviruses and to determine evolutionary relationships, I performed a phylogenetic analysis where I demonstrated that the mycoviruses in fungal isolates with triple infections (BbVV-1, BbPV-2 and BbPmV-1) form clusters. These are more closely related to each other than to any of the other quasispecies investigated (Filippou *et al.* 2018). My collaborators and I hypothesised that these mycoviruses are transmitted as a complex, vertically or horizontally. After constructing the phylogenetic tree using ITS sequences, however, I discovered that the isolates harbouring the triple infections do not cluster together, suggesting rather that at least one past horizontal transmission event between more distantly related isolates. Conversely, vertical transmission seems to be the most likely explanation between closely related isolates (Filippou *et al.* 2018). This inability of extracellular transmission is a major limitation to the transmissibility and infectivity of mycoviruses and thus their use as pesticides, rather they would be reliant on the host's own movement and dispersal.

Moreover, in this study I have worked on a polymycovirus that was isolated from *B. bassiana* ATHUM 4649 and found it possesses a six segmented, non-conventionally encapsidated, positive-sense dsRNA genome, named BbPmV-3. The first polymycovirus discovered was isolated from *A. fumigatus* and was initially termed *Aspergillus fumigatus* tetramycovirus-1 (AfuTmV-1) and has a four segmented dsRNA genome (Kanhayuwa *et al.*, 2015). Consequently, related viruses with five (*Botryosphaeria dothidea* RNA virus 1; Zhai *et al.*, 2016), six (BbPmV 3; Kotta-Loizou & Coutts, 2017; Filippou *et al.*, 2021), seven (BbPmV

2; Kotta-Loizou & Coutts, 2017), eight (*Colletotrichum camelliae* filamentous virus 1; Jia *et al.*, 2017; *Fusarium redolens* polymycovirus 1; Mahillon *et al.*, 2019) and eleven (Hadaka virus; Sato *et al.*, 2020) genomic segments were discovered. Characterisation of BbPmV-3 demonstrated a close relationship to BbPmV-2 when both RdRP's run on BLASTX (Filippou *et al.*, 2021). Similar results were observed between BbPmV-3 dsRNA5 and BbPmV-2 dsRNA6, and BbPmV-3 dsRNA6 and BbPmV-2 dsRNA7 indicating that the close relationship these two polymycoviruses exhibit might be due to the evolutionary mutation of a common ancestor. Additionally, like in all known polymycoviruses, the highly conserved GDD motif was replaced in BbPmV-3 RdRP by the GDNQ motif; this is characteristic of negative-sense ssRNA viruses. The second dsRNA segment encodes a protein of unknown properties, however, the conserved N-terminus, cysteine-rich, zinc finger-like motif and arginine repeats. This suggests a close association with endoplasmic reticulum (ER) retention signals. The third component, dsRNA3, codes for methyl transferase which is involved in the viral mRNA capping process. Most of the cellular RNA capping takes place in the nucleus. Viruses that replicate in the cytoplasm are, however, required to generate their own by using the host's own machinery, a process also known as the "cap snatching mechanism". Mycoviruses with dsRNA genomes are not capped so they use cap snatching mechanisms to generate their own (Fujimura & Esteban 2011). Cap snatching is best described in influenza viruses, especially influenza A, and the Zikka virus where it is essential for viral replication and immune evasion (Ramanathan & Chan, 2016; Coutard *et al.*, 2017). The fourth segment, dsRNA 4, codes for a proline-alanine-serine-rich protein (PASrp) believed to coat the viral genome in an unconventional manner. It is considered that the PAS-rich protein is encoded by other capsidless viruses, including phlegiviruses (Kozlakidis *et al.*, 2009). This demonstrates how important these PASrp may be for genome protection. Meanwhile, the function of both dsRNA5 and dsRNA6 still eludes us.

An association between the presence of dsRNA and hypervirulence has been documented for some *B. bassiana* isolates (ATHUM 4946 and EABb 92/11-dm), whereas asymptomatic infection was documented for *L. muscarium* 143.62. It also has been shown that phenotypic alterations such as growth rate (Appendix Part B Figure S6.1b), sporulation and sometimes pigmentation in *B. bassiana* can be the result of hypervirulence as mentioned before (Chapter 4). Increased production of asexual conidia enhances the potential of the fungus and therefore of the polymycovirus to disperse (Appendix Part B Figure S6.1a). Producing isogenic lines of virus-free and virus-infected isolates (i.e. lines with the same genetic background) is crucial for studying morphological characteristics and estimating growth rates. Therefore, to enable this work, I established one such line by successfully “curing” a *B. bassiana* isolate ATHUM 4946 from BbPmV-3 infection using the protein synthesis inhibitor cycloheximide and *L. muscarium* 143.62 from LmV-1 infection using ribavirin, a synthetic nucleoside analogue of ribofuranose.

Likewise, the effects of polymycovirus infection were examined using *T. molitor* (experiments completed during this thesis work but analysis not completed due to the SARS-CoV-2 pandemic), *Galleria mellonella* (Kotta-Loizou *et al.*, 2017), and *Ceratitis capitata* (Filippou *et al.*, 2018) as infection models demonstrating a direct association of the increased mortality and polymycoviral infection. The findings reported in this thesis generally agree with previous investigations by Kotta-Loizou & Coutts (2017). Surprisingly, when the same experiment was performed using *Anopheles coluzzii*, the malaria vector, the PmV-1.F isolate killed mosquitoes far more rapidly than the PmV-1.I isolate (Pitaluga, personal communication, 2020). While planned, further investigation could not be conducted due to the SARS-CoV-2 pandemic. The potential significance of mild hypervirulence caused by polymycovirus infection of *B. bassiana* on field pathogenicity for insects is yet to be explored. Investigations under controlled environmental conditions would be essential to explore the underlying mechanisms. It is

intended to transfect the commercialised mycopesticides *B. bassiana* ATCC 74040 and GHA protoplast using both BbPmV-1 and BbPmV-3, hence, choosing a suitable selection marker is important for screening the transfected colonies. Consequently, to discover an antibiotic that is effective against the three *B. bassiana* isolates (GHA, ATCC 704040 and EABb 92/11-Dm), their sensitivity against different antibiotics was tested. Benomyl, a systemic fungicide, at concentrations 0, 5, 7.5 and 50 µg/mL was found to be effective against all strains, while sulfonylurea and hygromycin B were unsuccessful. Therefore, through this work we have documented the intrinsic resistance of both *B. bassiana* isolates ATCC 704040 Naturalis and GHA to hygromycin B, and GHA to sulfonylurea. Consequently, Benomyl can be used as a selection marker for future transfection experiments.

Growth rate is increased in carbon-based media with polymycovirus infected isolates, whereas in nitrogen-based media growth of polymycovirus infected isolates was significantly affected indicating that there is a direct connection between the C:N ratio in growth medium and polymycoviral infection. More specifically, when I replaced sucrose with lactose, trehalose, glucose, or glycerol both BbPmV-3 and BbPmV-1 allowed for increased growth of ATHUM 4946 and EABb 92/11-Dm respectively. The opposite effect was observed on maltose and fructose. Trehalose is an excellent factor for enhancing the growth of entomopathogenic fungi such as *B. bassiana* (Pendland *et al.*, 1993). Consequently, to further understand this connection genes responsible for carbon and nitrogen assimilation were examined and it has been shown that, in the presence of BbPmV-1, genes responsible for carbon uptake (Figure 5.3.2.3) were upregulated across all timepoints in PmV-1.I. Furthermore, genes involved in carbon metabolism (Figure 5.3.2.6) were also upregulated in PmV-1.I, whereas *agdC* gene was significantly upregulated in PmV-1.F. Likewise, we have demonstrated that BbPmV-1 drives the up-regulation of *nirA* gene which is linked to nitrate uptake and/or assimilation. Therefore, according to our findings it is evident that polymycoviruses affect glycolysis process as well

as the metabolic pathway of sugars. It further appears to affect the uptake or the assimilation of sodium nitrate when compared to other sources of nitrogen I explored. Notably, the growth trends illustrated by ATHUM 4946 and EABb 92/11-Dm on the various media, as well as conidia production (Figure 4.1e & 4.1f.; Appendix Part B Figure S6.1a) appear to be similar but not identical. EABb 92/11-Dm tends to grow faster and sporulate more than ATHUM 4946, suggesting that the fungal isolates themselves differ in their genetic background. These variations may be attributed to several factors such as the polymycovirus strain (modulating their metabolic pathways in a similar but not identical way), the fungal hosts, the host–virus pairs, a co-infection of BbNV-1 in EABb 92/11-Dm (Kotta- Loizou *et al.*, 2015), and/or a combination of these factors. Our work on polymycoviruses further supports the concept of hypervirulence, indicating that BbPmV-1 and BbPmV-3 have a direct effect with essential metabolic pathways of the entomopathogenic fungi *B. bassiana*.

I postulate that mycoviruses display similar characteristics to bacteriophages. Bacteriophages are viruses that infect bacteria and like mycoviruses they are host specific. These bacteria viruses are categorised based on their life cycle, they can have a lytic replication cycle or lysogenic cycle. Temperate bacteriophages enter a lysogenic phase where they integrate their genetic material on the bacterial genome. During this process the bacteria can gain new traits such as new virulence factor (e.g toxin production; *E. coli* O157:H7 shiga like toxin) or antibiotic resistance. In this study, I demonstrated that polymycoviruses exhibit a symbiotic relationship with their host and their action resembles that of temperate bacteriophage. As mentioned, polymycoviruses affect genes involved in sporulation and radial growth. Similar results were observed with genes involved in adhesion (Figure 5.3a), cuticle degradation (Figure 5.3b), carbohydrate transport and metabolism (Figures 5.3d and 5.3h), secondary metabolite production (Figure 5.3g), calcium homeostasis (Figure 5.3f), multidrug pumps (Figure 5.3d), and biotic-stress tolerance (Figure 5.3i). All in all, these genes are responsible

for the expression of key proteins involved in the fungus pathogenicity and are upregulated only in PmV-1.I.

Understanding how the fungus host can become more tolerant of environmental stress is crucial for improving its pesticide efficacy. The avenue undertaken here was a candidate gene approach, investigating key pathways known to affect resistance to stresses. Different *Beauveria spp.* can produce organic acids during growth and in case of *B. bassiana* ormic, lactic, orotic, oxalic and citric acids are produced, which can change the pH of the growth medium creating a toxic environment similar to the situation with bacteria (Barra-Bucarei *et al.*, 2020). Increases in pH can be toxic to microorganisms causing stress and death. Genes expressing useful mechanisms that are being utilised by *B. bassiana* to tolerate such stress were discussed (Chapter 5). Mannitol plays a crucial role in stress tolerance as a scavenger of ROS as well as enhancing environmental adaptability, germination, virulence and together with trehalose are important for stress tolerance. Furthermore, TPS deletion affected trehalose biosynthesis resulting in reduced conidiation, decrease in conidial thermotolerance, UV-B resistance, increased hyphal sensitivities to chemical stresses, and attenuated virulence (Wang *et al.*, 2017). Likewise, the heat shock protein (Hsp) complex plays a vital role in fungus survival when exposed to outdoor stresses, such as high temperatures, UV-B, and agrochemicals applied to control plant diseases and weeds. *B. bassiana* also produces tenellin a secondary metabolite, which plays an important role in iron regulation that is required for normal cell growth and metabolism as well as protecting cells against cellular stress caused by iron deficiency. These genes were found to be significantly over-expressed in PmV-1.I across all time points when compared to PmV-1.F.

Further, the calcium homeostasis system consists of many calcium pumps, proteins and enzymes which are vital for maintaining optimal  $\text{Ca}^{+2}$  levels in the cell. This system is vital for fungal cell survival under environmental stress as well as for its virulence. Some key points of

the calcium homeostasis system (BbRcn1, BbVcx1, BbPmr1 and calcineurin) were discussed above and was observed that gene expression levels were upregulated in PmV-1.I. These signaling molecules are critical for mediating cellular stress response and their upregulation during late growth may be due to the stress the fungus experiences during starvation. Furthermore, the calcium homeostasis system is an excellent target for fungicide development, however, it has not been well studied (Liu *et al.*, 2015).

To conclude, for entomopathogenic fungi the “fight on the surface” is important for a successful mycosis and to achieve it an arsenal of virulence factors is employed. But then again this fight could go either way. As we extensively have discussed and proved in this work, polymycoviruses act as extrachromosomal elements improving the efficiency of these fungi by upregulating genes involved in pathogenesis. Therefore, they can provide the advantage over other entomopathogens.

### **6.3 Conclusion, overall impact, limitations, and future work**

This project delivered a paper on mycoviruses and population studies (Chapter 3), where for the first time, in my knowledge, viral quasispecies in mycoviruses were reported and discussed. This genetic variation observed in mycoviral quasispecies was due to a recombination event that was detected in BbPmV-1-like viruses. Therefore, for this recombination event to take place it means that at least two BbPmV-1-like viruses were simultaneously presented in the same fungal isolate, a process that is common in human pathogenic RNA viruses. In this paper, we demonstrated the sporadic appearance of these mycoviruses and how difficult is to find one, by pointing out the prevalence of dsRNA elements in *Metarhizium* sp. mostly from Brazil compared the lack of these elements in *Metarhizium* sp. that we have acquired from Europe. Furthermore, an additional observation directly linked to the project and to the second paper we published addresses the hypervirulence effects of BbPmV-1 on its host. More specifically,

my co-author Dr Inmaculada Garrido-Jurado demonstrated that some of the isolates harbouring three mycoviruses caused mortalities higher than 95% when tested against the *C. capitata*, the Mediterranean fruit fly, suggesting that despite the heavy viral load, hypervirulence caused by BbPmV-1 did not affect pathogenicity. These results led to the second paper from this thesis (Chapter 4). There we demonstrated that carbon and nitrogen sources available to the host fungus greatly affected polymycovirus-mediated growth. To be more specific, polymycovirus-infected isolates grew faster on carbon source media, particularly in trehalose. Likewise, the results obtained from Chapter 5 demonstrate the symbiotic relationship between mycovirus and host together with the effects on virulence and pathogenicity, I can state with some confidence that there is accumulating evidence that polymycoviruses can confer hypervirulence to their fungal hosts.

Unfortunately, due to the sudden eruption of SARS-CoV-2 pandemic, that greatly affected normal life worldwide and forced us to rapidly adapt, made it extremely difficult for me to pursuit and explore different angles I had in planned. However, these results can be used as hypothesis generator to support future research.

Therefore, regarding future experiments, I am planning to use the BSPP Junior Fellowship Fund awarded to me on 2019 to finish transfection experiments of Naturalis-L (ATCC 74040 strain) and Botanigard 22 WP (GHA strain) protoplast with polymycoviruses- BbPmV-1 and -3. Unfortunately, due to the pandemic I had to abandon the experiment (Appendix Part B S4.3.5a), which reveals that at least BbPmV-1 is compatible and can successfully infect both isolates. Next step will include confirming isogenic line of virus-transfected and Wild Type (WT), which will then allow me to start transfections using BbPmV-3. Following successful transfections of both isolates using both polymycoviruses, I will then begin experiments to determine possible hypervirulence effects using WT isolates as a positive control. These experiments will involve examining growth and germination, morphology, and pigmentation,

UV-tolerance, spore production, and pathogenicity of transfected isolates against a range of insects, which was planned to take place at the University of Cordoba in Spain under the supervision of Prof. Enrique Quesada-Moraga. Furthermore, it would be of great interest if we can compare the transfected isolates (Naturalis and BotaniGard) against ATHUM 4946 (PmV-3.I) and EABb 92/11-Dm (PmV-1.I) regarding pathogenicity and virulence and observe similarities or differences between them.

Additionally, identifying selective markers such as Benomyl (Chapter 4) can enable future research when it comes to transfecting cDNA clones arrived from *in vitro* transcription of BbPmV-1 dsRNA elements. Together with GFP-labeling (Chapter 4), these tools would allow us to determine viral localization to enable us to understand how polymycoviruses infect and replicate. It is not yet established whether dsRNA mycoviruses replicate in the cytoplasm, like most RNA viruses do, or replicate in the nucleus. Furthermore, one other topic we can focus on is the analysis of the remaining RNA-seq data of PmV-1.I, PmV-1.F, Naturalis, and BotaniGard against *T. molitor* infection model. This will allow us to compare expression patterns of genes involved in pathogenicity (i.e adhesin-like proteins; hydrophobin-like proteins; cuticle degrading; immune evasion; osmosensors; blastospores formation; nutrient uptake etc.) and probably employ gene knock out technique to examine their action in virus-infected and virus-free isogenic lines. For instance, we could target chitin (*chit1*) and cyclin-dependent kinase 1 (*cdk1*) genes as knockouts mutants have not yet been reported and examine the effects with and without the polymycovirus. Finally, yeast two-hybrid screening is a crucial tool for deciphering function. It would enable us to examine protein-protein interactions between known and unknown proteins. For example, we can use this screening system to resolve the function of dsRNA5 and 6 in BbPmV-3 and investigate how the virus interacts with the host *in vivo*.

Given the emerging resources and diversity of questions, it is a fascinating time to do research on mycoviruses. Mycoviruses have unlimited potentials and they deserve more attention. I do see potential not only in agriculture but in medicine too. For example, what captured my interest recently was the innovative thinking of a US startup (Novavax) where they created a new vaccine for use against Covid-19 using a baculovirus DNA virus that uses moths as a host. The interesting part is that they have genetically engineered this virus to produce the spike proteins of SARS-CoV-2 when infecting the moth cells. Genetically engineering and manipulate mycoviruses in a similar way would be an avenue for new treatments of pathogens. In Chapter 5 I discussed the benefits of Beauvericin to medicine and how it can be used against Gram-positive bacteria, its ability to inhibit haptotaxis was highly notable. Based on my findings, BbPmV-1 causes up-regulation of the BbBeas gene, resulting in increased production of beauvericin. If we can extract and purify beauvericin, we could fully create new - or enhance existing - pesticide formulations. Hopefully, this work has laid one more brick for the mycoviral research field and that will attract interest to further explore their potential in both agriculture and medicine. Like Albert Einstein once said “We are all very ignorant. What happens is that we do not all ignore the same thing”.

## References

1. Ahn, I.-P., & Lee, Y.-H. (2001). A viral double-stranded RNA up regulates the fungal virulence of *Nectria radicumicola*. *Molecular Plant-Microbe Interactions*, 14(4), 496-507.
2. Al-Bader, N., Vanier, G., Liu, H., Gravelat, F. N., Urb, M., Hoareau, C. M.-Q., Campoli, P., Chabot, J., Filler, S. G., & Sheppard, D. C. (2010). Role of trehalose biosynthesis in *Aspergillus fumigatus* development, stress response, and virulence. *Infection and Immunity*, 78(7), 3007-3018.
3. Andino, R., & Domingo, E. (2015). Viral quasispecies. *Virology*, 479, 46-51.
4. Antebi, A., & Fink, G. R. (1992). The yeast Ca (2+)-ATPase homologue, PMR1, is required for normal Golgi function and localizes in a novel Golgi-like distribution. *Molecular Biology of the Cell*, 3(6), 633-654.
5. Aoki, N., Moriyama, H., Kodama, M., Arie, T., Teraoka, T., & Fukuhara, T. (2009). A novel mycovirus associated with four double stranded RNAs affects host fungal growth in *Alternaria alternata*. *Virus Research*, 140(1-2), 179-187.
6. Asidi, A., N'Guessan, R., Akogbeto, M., Curtis, C., & Rowland, M. (2012). Loss of household protection from use of insecticide-treated nets against pyrethroid-resistant mosquitoes, Benin. *Emerging infectious diseases*, 18(7), 1101.
7. Askary, H., Benhamou, N., & Brodeur, J. (1999). Ultrastructural and cytochemical characterization of aphid invasion by the hyphomycete *Verticillium lecanii*. *Journal of Invertebrate Pathology*, 74(1), 1-13.
8. Badolo, A., Traore, A., Jones, C. M., Sanou, A., Flood, L., Guelbeogo, W. M., Ranson, H., & Sagnon, N. F. (2012). Three years of insecticide resistance monitoring in *Anopheles gambiae* in Burkina Faso: resistance on the rise? *Malaria journal*, 11(1), 1-11.
9. Barra-Bucarei, L., González, M. G., Iglesias, A. F., Aguayo, G. S., Peñalosa, M. G., & Vera, P. V. (2020). *Beauveria bassiana* multifunction as an endophyte: Growth promotion and biologic control of *Trialeurodes vaporariorum*, (westwood) (hemiptera: Aleyrodidae) in tomato. *Insects*, 11(9), 591.
10. Bengtsson-Palme, J., Ryberg, M., Hartmann, M., Branco, S., Wang, Z., Godhe, A., De Wit, P., Sánchez-García, M., Ebersberger, I., & de Sousa, F. (2013). Improved software detection and extraction of ITS1

and ITS 2 from ribosomal ITS sequences of fungi and other eukaryotes for analysis of environmental sequencing data. *Methods in ecology and evolution*, 4(10), 914-919.

11. Benhamou, N., & Brodeur, J. (2000). Evidence for antibiosis and induced host defense reactions in the interaction between *Verticillium lecanii* and *Penicillium digitatum*, the causal agent of green mold. *Phytopathology*, 90(9), 932-943.
12. Benhamou, N., & Brodeur, J. (2001). Pre-inoculation of Ri T-DNA transformed cucumber roots with the mycoparasite, *Verticillium lecanii*, induces host defense reactions against *Pythium ultimum* infection. *Physiological and Molecular Plant Pathology*, 58(3), 133-146.
13. Bergvinson, D., & García-Lara, S. (2004). Genetic approaches to reducing losses of stored grain to insects and diseases. *Current Opinion in Plant Biology*, 7(4), 480-485.
14. Bhatti, M. F., Bignell, E. M., & Coutts, R. H. A. (2011). Complete nucleotide sequences of two dsRNAs associated with a new partitivirus infecting *Aspergillus fumigatus*. *Archives of Virology*, 156(9), 1677-1680.
15. Bhatti, M. F., Jamal, A., Bignell, E. M., Petrou, M. A., & Coutts, R. H. A. (2012). Incidence of dsRNA mycoviruses in a collection of *Aspergillus fumigatus* isolates. *Mycopathologia*, 174(4), 323-326.
16. Bhatti, M. F., Jamal, A., Petrou, M. A., Cairns, T. C., Bignell, E. M., & Coutts, R. H. A. (2011). The effects of dsRNA mycoviruses on growth and murine virulence of *Aspergillus fumigatus*. *Fungal Genetics and Biology*, 48(11), 1071-1075.
17. Bidochka, M. J., & Khachatourians, G. G. (1990). Identification of *Beauveria bassiana* extracellular protease as a virulence factor in pathogenicity toward the migratory grasshopper, *Melanoplus sanguinipes*. *Journal of Invertebrate Pathology*, 56(3), 362-370.
18. Blanford, S., Chan, B. H., Jenkins, N., Sim, D., Turner, R. J., Read, A. F., & Thomas, M. B. (2005). Fungal pathogen reduces potential for malaria transmission. *Science*, 308(5728), 1638-1641.
19. Bodier-Montagutelli, E., Morello, E., l'Hostis, G., Guillon, A., Dalloneau, E., Respaud, R., Pallaoro, N., Blois, H., Vecellio, L., & Gabard, J. (2017). Inhaled phage therapy: a promising and challenging approach to treat bacterial respiratory infections. *Expert opinion on drug delivery*, 14(8), 959-972.
20. Boland, G. J. (1992). Hypovirulence and double-stranded RNA in *Sclerotinia sclerotiorum*. *Canadian Journal of Plant Pathology*, 14(1), 10-17.

21. Boomsma, J. J., Jensen, A. B., Meyling, N. V., & Eilenberg, J. (2014). Evolutionary interaction networks of insect pathogenic fungi. *Annual Review of Entomology*, 59, 467-485.
22. Border, D., Buck, K., Chain, E., Kempson-Jones, G., Lhoas, P., & Ratti, G. (1972). Viruses of *Penicillium* and *Aspergillus* species. *Biochemical Journal*, 127(2), 4P-6P.
23. Brownbridge, M., Costa, S., & Jaronski, S. T. (2001). Effects of *in vitro* passage of *Beauveria bassiana* on virulence to *Bemisia argentifolii*. *Journal of Invertebrate Pathology*, 77(4), 280-283.
24. Buck, K. (1986). Fungal virology-an overview. *Fungal virology*, 1, 84.
25. Buck, K. W. (1978). Semi-conservative replication of double-stranded RNA by a virion-associated RNA polymerase. *Biochemical and Biophysical Research Communications*, 84(3), 639-645.
26. Buck, K. W. (1988). From interferon induction to fungal viruses. *European Journal of Epidemiology*, 4(4), 395-399.
27. Buck, K. W. 1998. Molecular variability of viruses of fungi. *Molecular Variability of Fungal Pathogens*, 53-72.
28. Bustin, S. A., & Mueller, R. (2005). Real-time reverse transcription PCR (qRT-PCR) and its potential use in clinical diagnosis. *Clinical Science*, 109(4), 365-379.
29. Carmeliet, P. (2003). Blood vessels and nerves: common signals, pathways and diseases. *Nature Reviews Genetics*, 4(9), 710-720.
30. Carroll, K., & Wickner, R. B. (1995). Translation and M1 double-stranded RNA propagation: MAK18=RPL41B and cycloheximide curing. *Journal of Bacteriology*, 177(10), 2887-2891.
31. Castón, J. R., Trus, B. L., Booy, F. P., Wickner, R. B., Wall, J. S., & Steven, A. C. (1997). Structure of LA virus: a specialized compartment for the transcription and replication of double-stranded RNA. *The Journal of Cell Biology*, 138(5), 975-985.
32. Castro, M., Kramer, K., Valdivia, L., Ortiz, S., & Castillo, A. (2003). A double-stranded RNA mycovirus confers hypovirulence-associated traits to *Botrytis cinerea*. *FEMS Microbiology Letters*, 228(1), 87-91.
33. Champlin, F., & Grula, E. (1979). Noninvolvement of beauvericin in the entomopathogenicity of *Beauveria bassiana*. *Applied and Environmental Microbiology*, 37(6), 1122-1126.

34. Chandler, D., Bailey, A. S., Tatchell, G. M., Davidson, G., Greaves, J., & Grant, W. P. (2011). The development, regulation and use of biopesticides for integrated pest management. *Philosophical Transactions of the Royal Society B: Biological Sciences*, 366(1573), 1987-1998.
35. Chandler, D., Hay, D., & Reid, A. P. (1997). Sampling and occurrence of entomopathogenic fungi and nematodes in UK soils. *Applied Soil Ecology*, 5(2), 133-141.
36. Charnley, A. K., & Leger, R. S. (1991). The role of cuticle-degrading enzymes in fungal pathogenesis in insects. In *The fungal spore and disease initiation in plants and animals* (pp. 267-286). Springer, Boston, MA.
37. Cho, E. M., Liu, L., Farmerie, W., & Keyhani, N. O. (2006). EST analysis of cDNA libraries from the entomopathogenic fungus *Beauveria (Cordyceps) bassiana*. I. Evidence for stage-specific gene expression in aerial conidia, in vitro blastospores and submerged conidia. *Microbiology*, 152(9), 2843-2854.
38. Choi, G. H., & Nuss, D. L. (1992). Hypovirulence of chestnut blight fungus conferred by an infectious viral cDNA. *Science*, 257(5071), 800-803.
39. Claydon, N., & Grove, J. F. (1982). Insecticidal secondary metabolic products from the entomogenous fungus *Verticillium lecanii*. *Journal of Invertebrate Pathology*, 40(3), 413-418.
40. Clerk, G. C., & Madelin, M. F. (1965). The longevity of conidia of three insect-parasitizing hyphomycetes. *Transactions of the British Mycological Society*, 48(2), 193-209.
41. Coutard, B., Barral, K., Lichièrè, J., Selisko, B., Martin, B., Aouadi, W., Lombardia, M. O., Debart, F., Vasseur, J.-J., & Guillemot, J. C. (2017). Zika virus methyltransferase: structure and functions for drug design perspectives. *Journal of virology*, 91(5).
42. Coutts, R. H. A., & Livieratos, I. C. (2003). A rapid method for sequencing the 5'-and 3'-termini of double-stranded RNA viral templates using RLM-RACE. *Journal of Phytopathology*, 151(9), 525-527.
43. Coutts, R. H. A., Covelli, L., Di Serio, F., Citir, A., Açıkgöz, S., Hernandez, C., & Flores, R. (2004). Cherry chlorotic rusty spot and Amasya cherry diseases are associated with a complex pattern of mycoviral-like double-stranded RNAs. II. Characterization of a new species in the genus *Partitivirus*. *Journal of General Virology*, 85(11), 3399-3403.

44. Dalzoto, P. R., Glienke-Blanco, C., Kava-Cordeiro, V., Ribeiro, J. Z., Kitajima, E. W., & Azevedo, J. L. (2006). Horizontal transfer and hypovirulence associated with double-stranded RNA in *Beauveria bassiana*. *Mycological Research*, 110(12), 1475-1481.
45. Dawe, A. L., & Nuss, D. L. (2001). Hypoviruses and chestnut blight: exploiting viruses to understand and modulate fungal pathogenesis. *Annual Review of Genetics*, 35(1), 1-29.
46. de Faria, M. R., & Wraight, S. P. (2007). Mycoinsecticides and mycoacaricides: a comprehensive list with worldwide coverage and international classification of formulation types. *Biological Control*, 43(3), 237-256.
47. Delarue, M., Poch, O., Tordo, N., Moras, D., & Argos, P. (1990). An attempt to unify the structure of polymerases. *Protein Engineering, Design and Selection*, 3(6), 461-467.
48. Delgado-Jarana, J., Moreno-Mateos, M. A., & Benítez, T. (2003). Glucose uptake in *Trichoderma harzianum*: role of gtt1. *Eukaryotic cell*, 2(4), 708-717.
49. Dinman, J. D., Icho, T., & Wickner, R. B. (1991). A-1 ribosomal frameshift in a double-stranded RNA virus of yeast forms a gag-pol fusion protein. *Proceedings of the National Academy of Sciences, USA*, 88(1), 174-178.
50. Doffman, S. R., Agrawal, S. G., & Brown, J. S. (2005). Invasive pulmonary aspergillosis. *Expert review of anti-infective therapy*, 3(4), 613-627.
51. Domingo, E. J. J. H., & Holland, J. J. (1997). RNA virus mutations and fitness for survival. *Annual Review of Microbiology*, 51(1), 151-178.
52. Domingo, E., & Perales, C. (2018). Quasispecies and virus. *European Biophysics Journal*, 47(4), 443-457.
53. Eley, K. L., Halo, L. M., Song, Z., Powles, H., Cox, R. J., Bailey, A. M., Lazarus, C. M., & Simpson, T. J. (2007). Biosynthesis of the 2-pyridone tenellin in the insect pathogenic fungus *Beauveria bassiana*. *ChemBioChem*, 8(3), 289-297.
54. Elias, K. S., & Cotty, P. J. (1996). Incidence and stability of infection by double-stranded RNA genetic elements in *Aspergillus section flavi* and effects on aflatoxigenicity. *Canadian Journal of Botany*, 74(5), 716-725.

55. Evans, H. C. (1982). Entomogenous fungi in tropical forest ecosystems: an appraisal. *Ecological Entomology*, 7(1), 47-60.
56. Fan, Y., Ortiz-Urquiza, A., Kudia, R. A., & Keyhani, N. O. (2012). A fungal homologue of neuronal calcium sensor-1, *Bbcsa1*, regulates extracellular acidification and contributes to virulence in the entomopathogenic fungus *Beauveria bassiana*. *Microbiology*, 158(7), 1843-1851.
57. Fang, W. G., Zhang, Y. J., Yang, X. Y., Wang, Z. K., & Pei, Y. (2002). Cloning and characterization of cuticle degrading enzyme CDEP-1 from *Beauveria bassiana*. *Yi chuan xue bao= Acta genetica Sinica*, 29(3), 278-282.
58. Fang, W., Leng, B., Xiao, Y., Jin, K., Ma, J., Fan, Y., Feng, J., Yang, X., Zhang, Y., & Pei, Y. (2005). Cloning of *Beauveria bassiana* chitinase gene *Bbchit1* and its application to improve fungal strain virulence. *Applied and Environmental Microbiology*, 71(1), 363-370.
59. Farkas, E., Bátka, D., Csóka, H., & Nagy, N. V. (2007). Interaction of imidazole containing hydroxamic acids with Fe (III): hydroxamate versus imidazole coordination of the ligands. *Bioinorganic chemistry and applications*, 2007.
60. Filippou, C., Coutts, R. H., Stevens, D. A., Sabino, R., & Kotta-Loizou, I. (2020). Completion of the sequence of the *Aspergillus fumigatus* partitivirus 1 genome. *Archives of Virology*, 165(8), 1891-1894.
61. Filippou, C., Diss, R. M., Daudu, J. O., Coutts, R. H., & Kotta-Loizou, I. (2021). The polymycovirus-mediated growth enhancement of the entomopathogenic fungus *Beauveria bassiana* is dependent on carbon and nitrogen metabolism. *Frontiers in microbiology*, 12, 12.
62. Filippou, C., Garrido-Jurado, I., Meyling, N. V., Quesada-Moraga, E., Coutts, R. H., & Kotta-Loizou, I. (2018). Mycoviral population dynamics in Spanish isolates of the entomopathogenic fungus *Beauveria bassiana*. *Viruses*, 10(12), 665.
63. Food and Agriculture Organization (2012). International code of conduct for the distribution and use of pesticides, guidelines for prevention and management of pesticide resistance. Rome: *FAO.*, 1–62.
64. Froussard, P. (1992). A random-PCR method (rPCR) to construct whole cDNA library from low amounts of RNA. *Nucleic acids research*, 20(11), 2900.
65. Fujimura T, Esteban R (2011) Cap-snatching mechanism in yeast L-A double-stranded RNA virus. *Proc Natl Acad Sci USA* 108(43):17667–17671.

66. Fukuda, T., Boeckh, M., Carter, R. A., Sandmaier, B. M., Maris, M. B., Maloney, D. G., & Marr, K. A. (2003). Risks and outcomes of invasive fungal infections in recipients of allogeneic hematopoietic stem cell transplants after nonmyeloablative conditioning. *Blood*, *102*(3), 827-833.
67. Gardes, M., & Bruns, T. D. (1993). ITS primers with enhanced specificity for basidiomycetes-application to the identification of mycorrhizae and rusts. *Molecular ecology*, *2*(2), 113-118.
68. Gardes, M., & Bruns, T. D. (1996). ITS-RFLP matching for identification of fungi. In *Species Diagnostics Protocols* (pp. 177-186). Humana Press.
69. Gardner, W. A., Sutton, R. M., & Noblet, R. (1977). Persistence of *Beauveria bassiana*, *Nomuraea rileyi*, and *Nosema necatrix* on soybean foliage. *Environmental Entomology*, *6*(5), 616-618.
70. Garrido-Jurado, I., Fernández-Bravo, M., Campos, C., & Quesada-Moraga, E. (2015). Diversity of entomopathogenic Hypocreales in soil and phylloplanes of five Mediterranean cropping systems. *Journal of Invertebrate Pathology*, *130*, 97-106.
71. Ghabrial, S. A. (1980). Effects of fungal viruses on their hosts. *Annual Review of Phytopathology*, *18*(1), 441-461.
72. Ghabrial, S. A., & Nibert, M. L. (2009). *Victorivirus*, a new genus of fungal viruses in the family *Totiviridae*. *Archives of Virology*, *154*(2), 373-379.
73. Ghabrial, S. A., & Suzuki, N. (2009). Viruses of plant pathogenic fungi. *Annual Review of Phytopathology*, *47*, 353-384.
74. Ghabrial, S. A., Castón, J. R., Jiang, D., Nibert, M. L., & Suzuki, N. (2015). 50-plus years of fungal viruses. *Virology*, *479*, 356-368.
75. Gilbert, K. B., Holcomb, E. E., Allscheid, R. L., & Carrington, J. C. (2019). Hiding in plain sight: New virus genomes discovered via a systematic analysis of fungal public transcriptomes. *PLoS One*, *14*(7), e0219207.
76. Gindin, G., Barash, I., Harari, N., & Raccach, B. (1994). Effect of endotoxic compounds isolated from *Verticillium lecanii* on the sweet potato whitefly, *Bemisia tabaci*. *Phytoparasitica*, *22*(3), 189-196.
77. Glass, N. L., & Dementhon, K. (2006). Non-self recognition and programmed cell death in filamentous fungi. *Current Opinion in Microbiology*, *9*(6), 553-558.

78. Gonzalez, A., Jimenez, A., Vazquez, D., Davies, J. E., & Schindler, D. (1978). Studies on the mode of action of hygromycin B, an inhibitor of translocation in eukaryotes. *Biochimica et Biophysica Acta (BBA)-Nucleic Acids and Protein Synthesis*, 521(2), 459-469.
79. Greenstein, S., Shadkchan, Y., Jadoun, J., Sharon, C., Markovich, S., & Osherov, N. (2006). Analysis of the *Aspergillus nidulans* thaumatin-like cetA gene and evidence for transcriptional repression of pyr4 expression in the cetA-disrupted strain. *Fungal Genetics and Biology*, 43(1), 42-53.
80. Grenier, J., Potvin, C., Trudel, J., & Asselin, A. (1999). Some thaumatin-like proteins hydrolyse polymeric  $\beta$ -1, 3-glucans. *The Plant Journal*, 19(4), 473-480.
81. Groppi, S., Belotti, F., Brandão, R. L., Martegani, E., & Tisi, R. (2011). Glucose-induced calcium influx in budding yeast involves a novel calcium transport system and can activate calcineurin. *Cell calcium*, 49(6), 376-386.
82. Haas, B. J., Papanicolaou, A., Yassour, M., Grabherr, M., Blood, P. D., Bowden, J., Couger, M. B., Eccles, D., Li, B., & Lieber, M. (2013). *De novo* transcript sequence reconstruction from RNA-seq using the Trinity platform for reference generation and analysis. *Nature protocols*, 8(8), 1494-1512.
83. Halachmi, D., & Eilam, Y. (1996). Elevated cytosolic free Ca<sup>2+</sup> concentrations and massive Ca<sup>2+</sup> accumulation within vacuoles, in yeast mutant lacking PMR1, a homolog of Ca<sup>2+</sup>-ATPase. *FEBS Letters*, 392(2), 194-200.
84. Hallsworth, J. E., & Magan, N. (1999). Water and temperature relations of growth of the entomogenous fungi *Beauveria bassiana*, *Metarhizium anisopliae*, and *Paecilomyces farinosus*. *Journal of Invertebrate Pathology*, 74(3), 261-266.
85. Hamid, R., Khan, M. A., Ahmad, M., Ahmad, M. M., Abdin, M. Z., Musarrat, J., & Javed, S. (2013). Chitinases: an update. *Journal of pharmacy & bioallied sciences*, 5(1), 21.
86. Harren, K., Schumacher, J., & Tudzynski, B. (2012). The Ca<sup>2+</sup>/calcineurin-dependent signalling pathway in the gray mold *Botrytis cinerea*: the role of calcipressin in modulating calcineurin activity. *PLoS One*, 7(7), e41761.
87. Heinig, R. L., & Thomas, M. B. (2015). Interactions between a fungal entomopathogen and malaria parasites within a mosquito vector. *Malaria journal*, 14(1), 1-10.

88. Herrero, N., Dueñas, E., Quesada-Moraga, E., & Zabalgogezcoa, I. (2012). Prevalence and diversity of viruses in the entomopathogenic fungus *Beauveria bassiana*. *Applied Environmental Microbiology*, 78(24), 8523-8530.
89. Hilioti, Z., Gallagher, D. A., Low-Nam, S. T., Ramaswamy, P., Gajer, P., Kingsbury, T. J., Birchwood, C. J., Levchenko, A., & Cunningham, K. W. (2004). GSK-3 kinases enhance calcineurin signaling by phosphorylation of RCNs. *Genes & development*, 18(1), 35-47.
90. Hof, H. (2008). Mycotoxins: pathogenicity factors or virulence factors?. *Mycoses*, 51(2), 93-94.
91. Hoff, K. J., Lange, S., Lomsadze, A., Borodovsky, M., & Stanke, M. (2016). BRAKER1: unsupervised RNA-Seq-based genome annotation with GeneMark-ET and AUGUSTUS. *Bioinformatics*, 32(5), 767-769.
92. Holder, D. J., & Keyhani, N. O. (2005). Adhesion of the entomopathogenic fungus *Beauveria* (*Cordyceps*) *bassiana* to substrata. *Applied and environmental microbiology*, 71(9), 5260-5266.
93. Hollings, M. (1962). Viruses associated with a die-back disease of cultivated mushroom. *Nature*, 196(4858), 962.
94. Hu, Y., Wang, J., Ying, S. H., & Feng, M. G. (2014). Five vacuolar Ca<sup>2+</sup> exchangers play different roles in calcineurin-dependent Ca<sup>2+</sup>/Mn<sup>2+</sup> tolerance, multistress responses and virulence of a filamentous entomopathogen. *Fungal Genetics and Biology*, 73, 12-19.
95. Huang, S., & Ghabrial, S. A. (1996). Organization and expression of the double-stranded RNA genome of *Helminthosporium victoriae* 190S virus, a totivirus infecting a plant pathogenic filamentous fungus. *Proceedings of the National Academy of Sciences, USA*, 93(22), 12541-12546.
96. Ikeda, K. I., Nakamura, H., Arakawa, M., Koiwa, T., & Matsumoto, N. (2005). Dynamics of double-stranded RNA segments in a *Helicobasidium mompa* clone from a tulip tree plantation. *FEMS Microbiology Ecology*, 51(2), 293-301.
97. Islam, M. T., & Omar, D. B. (2012). Combined effect of *Beauveria bassiana* with neem on virulence of insect in case of two application approaches. *J Anim Plant Sci*, 22(1), 77-82.
98. Jablonski, S. A., & Morrow, C. D. (1995). Mutation of the aspartic acid residues of the GDD sequence motif of poliovirus RNA-dependent RNA polymerase results in enzymes with altered metal ion requirements for activity. *Journal of Virology*, 69(3), 1532-1539.

99. Jaronski, S. T., & Jackson, M. A. (2008). Efficacy of *Metarhizium anisopliae* microsclerotial granules. *Biocontrol Science and Technology*, 18(8), 849-863.
100. Jeffs, L. B., & Khachatourians, G. G. (1997). Toxic properties of *Beauveria* pigments on erythrocyte membranes. *Toxicon*, 35(8), 1351-1356
101. Jennings, D. B., Daub, M. E., Pharr, D. M., & Williamson, J. D. (2002). Constitutive expression of a celery mannitol dehydrogenase in tobacco enhances resistance to the mannitol-secreting fungal pathogen *Alternaria alternata*. *The Plant Journal*, 32(1), 41-49.
102. Jia, H., Dong, K., Zhou, L., Wang, G., Hong, N., Jiang, D., & Xu, W. (2017). A dsRNA virus with filamentous viral particles. *Nature communications*, 8(1), 1-12.
103. Jiang, D., & Ghabrial, S. A. (2004). Molecular characterization of *Penicillium chrysogenum* virus: reconsideration of the taxonomy of the genus *Chrysovirus*. *Journal of General Virology*, 85(7), 2111-2121.
104. Jiang, Y., Luo, C., Jiang, D., Li, G., & Huang, J. (2014). The complete genomic sequence of a second novel partitivirus infecting *Ustilaginoidea virens*. *Archives of virology*, 159(7), 1865-1868.
105. Jiang, Y., Wang, J., Yang, B., Wang, Q., Zhou, J., & Yu, W. (2019). Molecular characterization of a debilitation-associated partitivirus infecting the pathogenic fungus *Aspergillus flavus*. *Frontiers in microbiology*, 10, 626.
106. Jimenez, C. V. (2016). *A multidisciplinary approach to study virulence of the entomopathogenic fungus Beauveria bassiana towards malaria mosquitoes* Wageningen University].
107. Jin, K., Zhang, Y., Fang, W., Luo, Z., Zhou, Y., & Pei, Y. (2010). Carboxylate transporter gene JEN1 from the entomopathogenic fungus *Beauveria bassiana* is involved in conidiation and virulence. *Applied and Environmental Microbiology*, 76(1), 254-263.
108. Jirakkakul, J., Cheevadhanarak, S., Punya, J., Chutrakul, C., Senachak, J., Buajarern, T., Tanticharoen, M., & Amnuaykanjanasin, A. (2015). Tenellin acts as an iron chelator to prevent iron-generated reactive oxygen species toxicity in the entomopathogenic fungus *Beauveria bassiana*. *FEMS microbiology letters*, 362(2), 1-8.
109. Jirakkakul, J., Punya, J., Pongpattanakitshote, S., Paungmoung, P., Vorapreeda, N., Tachaleat, A., Klomnara, C., Tanticharoen, M., & Cheevadhanarak, S. (2008). Identification of the nonribosomal

- peptide synthetase gene responsible for bassianolide synthesis in wood-decaying fungus *Xylaria* sp. BCC1067. *Microbiology*, 154(4), 995-1006.
110. Johnston, P. R., Makarova, O., & Rolff, J. (2014). Inducible defenses stay up late: temporal patterns of immune gene expression in *Tenebrio molitor*. *G3: Genes, Genomes and Genetics*, 4(6), 947-955.
111. Juvvadi, P. R., Fortwendel, J. R., Rogg, L. E., Burns, K. A., Randell, S. H., & Steinbach, W. J. (2011). Localization and activity of the calcineurin catalytic and regulatory subunit complex at the septum is essential for hyphal elongation and proper septation in *Aspergillus fumigatus*. *Molecular Microbiology*, 82(5), 1235-1259.
112. Kabaluk, J. T., Goettel, M., Erlandson, M., Ericsson, J., Duke, G., & Vernon, R. (2005). *Metarhizium anisopliae* as a biological control for wireworms and a report of some other naturally-occurring parasites. *IOBC/wprs Bull*, 28(2), 109-115.
113. Kanematsu, S., Arakawa, M., Oikawa, Y., Onoue, M., Osaki, H., Nakamura, H., Ikeda, K., Kuga-Uetake, Y., Nitta, H., & Sasaki, A. (2004). A reovirus causes hypovirulence of *Rosellinia necatrix*. *Phytopathology*, 94(6), 561-568.
114. Kang, J. G., Wu, J. C., Bruenn, J. A., & Park, C. M. (2001). The H1 double-stranded RNA genome of *Ustilago maydis* virus-H1 encodes a polyprotein that contains structural motifs for capsid polypeptide, papain-like protease, and RNA-dependent RNA polymerase. *Virus Research*, 76(2), 183-189.
115. Keilwagen, J., Hartung, F., Paulini, M., Twardziok, S. O., & Grau, J. (2018). Combining RNA-seq data and homology-based gene prediction for plants, animals and fungi. *BMC Bioinformatics*, 19(1), 1-12.
116. Keller, S., Zimmermann, G., Wilding, N., Collins, N. M., Hammond, P. M., & Webber, J. F. (1989). Mycopathogens of soil insects. *Insect-Fungus Interactions*, 239-270.
117. Kim, J. J., Goettel, M. S., & Gillespie, D. R. (2007). Potential of *Lecanicillium* species for dual microbial control of aphids and the cucumber powdery mildew fungus, *Sphaerotheca fuliginea*. *Biological Control*, 40(3), 327-332.
118. King, A. M., Lefkowitz, E., Adams, M. J., & Carstens, E. B. (Eds.). (2011). *Virus taxonomy: ninth report of the International Committee on Taxonomy of Viruses* (Vol. 9). Elsevier.
119. Kingsbury, T. J., & Cunningham, K. W. (2000). A conserved family of calcineurin regulators. *Genes and development*, 14(13), 1595-1604.

120. Kirkland, B. H., & Keyhani, N. O. (2011). Expression and purification of a functionally active class I fungal hydrophobin from the entomopathogenic fungus *Beauveria bassiana* in *E. coli*. *Journal of Industrial Microbiology and Biotechnology*, 38(2), 327-335.
121. Kiss, L. (2003). A review of fungal antagonists of powdery mildews and their potential as biocontrol agents. *Pest Management Science: formerly Pesticide Science*, 59(4), 475-483.
122. Knowles, N. J., Hovi, T., Hyypiä, T., King, A. M. Q., Lindberg, A. M., Pallansch, M. A., & Yamashita, T. (2011). Virus taxonomy: classification and nomenclature of viruses. *Ninth Report of The International Committee on Taxonomy of Viruses*. (ed. King, A., Adams, MJ, Carstens, EB, Lefkowitz, EJ), 855-880.
123. Kõljalg, U., Nilsson, R. H., Abarenkov, K., Tedersoo, L., Taylor, A. F., Bahram, M., Bates, S. T., Bruns, T. D., Bengtsson-Palme, J., & Callaghan, T. M. (2013). Towards a unified paradigm for sequence-based identification of fungi. *Molecular Ecology*, 22(21), 5271-5277.
124. Koloniuk, I., Hrabáková, L., & Petrzik, K. (2015). Molecular characterization of a novel amalgavirus from the entomopathogenic fungus *Beauveria bassiana*. *Archives of virology*, 160(6), 1585-1588.
125. Kong, L.-A., Yang, J., Li, G.-T., Qi, L.-L., Zhang, Y.-J., Wang, C.-F., Zhao, W.-S., Xu, J.-R., & Peng, Y.-L. (2012). Different chitin synthase genes are required for various developmental and plant infection processes in the rice blast fungus *Magnaporthe oryzae*. *PLoS Pathog*, 8(2), e1002526.
126. Kotta-Loizou, I., & Coutts, R. H. A. (2017). Studies on the virome of the entomopathogenic fungus *Beauveria bassiana* reveal novel dsRNA elements and mild hypervirulence. *PLoS Pathogens*, 13(1), e1006183.
127. Kozlakidis, Z., Hacker, C. V., Bradley, D., Jamal, A., Phoon, X., Webber, J., et al. (2009). Molecular characterisation of two novel double-stranded RNA elements from *Phlebiopsis gigantea*. *Virus Genes* 39, 132–136.
128. Krieg, A., Gröner, A., Huber, J., & Zimmermann, G. (1981). Inactivation of certain insect pathogens by ultraviolet radiation. *Z. Pflanzenkr. Pflanzenschutz*, 88(1), 38-48.
129. Krogh, A., Larsson, B., von Heijne, G. & Sonnhammer, E.L. (2001). Predicting transmembrane protein topology with a hidden Markov model: application to complete genomes. *Journal of Molecular Biology*, 305(3), 567-580.

130. Kubista, M., Andrade, J. M., Bengtsson, M., Forootan, A., Jonák, J., Lind, K., & Ståhlberg, A. (2006). The real-time polymerase chain reaction. *Molecular Aspects of Medicine*, 27(2-3), 95-125.
131. Kurtti, T. J., & Keyhani, N. O. (2008). Intracellular infection of tick cell lines by the entomopathogenic fungus *Metarhizium anisopliae*. *Microbiology*, 154(6), 1700-1709.
132. Kwon, H., Bang, E., Choi, S., Lee, W., Cho, S., I-Yeon, J., Kim, S., & Lee, K. (2000). Cytotoxic Cyclodepsipetides of *Bombycis corpus* 101A. *JOURNAL-PHARMACEUTICAL SOCIETY OF KOREA*, 44(2), 115-118.
133. Lacey, L. A., Grzywacz, D., Shapiro-Ilan, D. I., Frutos, R., Brownbridge, M., & Goettel, M. S. (2015). Insect pathogens as biological control agents: back to the future. *Journal of invertebrate pathology*, 132, 1-41.
134. Lamoth, F., Juvvadi, P. R., Fortwendel, J. R., & Steinbach, W. J. (2012). Heat shock protein 90 is required for conidiation and cell wall integrity in *Aspergillus fumigatus*. *Eukaryotic Cell*, 11(11), 1324-1332.
135. Leach, M. D., Budge, S., Walker, L., Munro, C., Cowen, L. E., & Brown, A. J. (2012). Hsp90 orchestrates transcriptional regulation by Hsf1 and cell wall remodelling by MAPK signalling during thermal adaptation in a pathogenic yeast. *PLoS Pathog*, 8(12), e1003069.
136. Leal, S. C., Bertioli, D. J., Ball, B. V., & Butt, T. M. (1994). Presence of double-stranded RNAs and virus-like particles in the entomopathogenic fungus *Metarhizium anisopliae*. *Biocontrol Science and Technology*, 4(1), 89-94.
137. Lee, J. Y., Woo, R. M., Choi, C. J., Shin, T. Y., Gwak, W. S., & Woo, S. D. (2019). *Beauveria bassiana* for the simultaneous control of *Aedes albopictus* and *Culex pipiens* mosquito adults shows high conidia persistence and productivity. *AMB Express*, 9(1), 1-9.
138. Lee, L. G., Connell, C. R., & Bloch, W. (1993). Allelic discrimination by nick-translation PCR with fluorogenic probes. *Nucleic Acids Research*, 21(16), 3761-3766.
139. Lee, S. J., Lee, M. R., Kim, S., Kim, J. C., Park, S. E., Li, D., & Kim, J. S. (2018). Genomic analysis of the insect-killing fungus *Beauveria bassiana* JEF-007 as a biopesticide. *Scientific Reports*, 8(1), 1-12.
140. Leger, R. J. S., & Wang, C. (2010). Genetic engineering of fungal biocontrol agents to achieve greater efficacy against insect pests. *Applied Microbiology and Biotechnology*, 85(4), 901-907.

- 141.Leger, R. S., Goettel, M., Roberts, D. W., & Staples, R. C. (1991). Prepenetration events during infection of host cuticle by *Metarhizium anisopliae*. *Journal of Invertebrate Pathology*, 58(2), 168-179.
- 142.Lemke, P. A., & Nash, C. H. (1974). Fungal viruses. *Bacteriological Reviews*, 38(1), 29.
- 143.Lhoas, P. (1971). Transmission of double stranded RNA viruses to a strain of *Penicillium stoloniferum* through heterokaryosis. *Nature*, 230(5291), 248.
- 144.Li, F., Wang, Z. L., Zhang, L. B., Ying, S. H., & Feng, M. G. (2015). The role of three calcineurin subunits and a related transcription factor (Crz1) in conidiation, multistress tolerance and virulence in *Beauveria bassiana*. *Applied Microbiology and Biotechnology*, 99(2), 827-840.
- 145.Li, H., Havens, W. M., Nibert, M. L., & Ghabrial, S. A. (2011). RNA sequence determinants of a coupled termination-reinitiation strategy for downstream open reading frame translation in *Helminthosporium victoriae* virus 190S and other victoriviruses (Family *Totiviridae*). *Journal of Virology*, 85(14), 7343-7352.
- 146.Li, H., Rao, A., & Hogan, P. G. (2011). Interaction of calcineurin with substrates and targeting proteins. *Trends in Cell Biology*, 21(2), 91-103.
- 147.Lin, Y. H., Chiba, S., Tani, A., Kondo, H., Sasaki, A., Kanematsu, S., & Suzuki, N. (2012). A novel quadripartite dsRNA virus isolated from a phytopathogenic filamentous fungus, *Rosellinia necatrix*. *Virology*, 426(1), 42-50.
- 148.Liu, H., Zhao, X., Guo, M., Liu, H., & Zheng, Z. (2015). Growth and metabolism of *Beauveria bassiana* spores and mycelia. *BMC Microbiology*, 15(1), 1-12.
- 149.Liu, S., Hou, Y., Liu, W., Lu, C., Wang, W., & Sun, S. (2015). Components of the calcium-calcineurin signaling pathway in fungal cells and their potential as antifungal targets. *Eukaryotic Cell*, 14(4), 324-334.
- 150.Liu, W., Duns, G., & Chen, J. (2008). Genomic characterization of a novel partitivirus infecting *Aspergillus ochraceus*. *Virus Genes*, 37(3), 322-327.
- 151.Logrieco, A., Moretti, A., Castella, G., KostECKI, M., Golinski, P., Ritieni, A., & Chelkowski, J. (1998). Beauvericin production by *Fusarium* species. *Applied. Environmental Microbiology*, 64(8), 3084-3088.
- 152.Lord, J. C., Anderson, S., & Stanley, D. W. (2002). Eicosanoids mediate *Manduca sexta* cellular response to the fungal pathogen *Beauveria bassiana*: a role for the lipoxygenase pathway. *Archives of*

*Insect Biochemistry and Physiology: Published in Collaboration with the Entomological Society of America*, 51(1), 46-54.

153. Luo, X., Keyhani, N. O., Yu, X., He, Z., Luo, Z., Pei, Y., & Zhang, Y. (2012). The MAP kinase Bbslt2 controls growth, conidiation, cell wall integrity, and virulence in the insect pathogenic fungus *Beauveria bassiana*. *Fungal Genetics and Biology*, 49(7), 544-555.
154. MacDonald, W. L., & Fulbright, D. W. (1991). Biological control of chestnut blight: use and limitations of transmissible hypovirulence. *Plant Disease*, 75(7), 656-661.
155. Mahillon, M., Decroës, A., Liénard, C., Bragard, C., & Legrève, A. (2019). Full genome sequence of a new polymycovirus infecting *Fusarium redolens*. *Archives of virology*, 164(8), 2215-2219.
156. Maistrou, S., Paris, V., Jensen, A. B., Rolff, J., Meyling, N. V., & Zanchi, C. (2018). A constitutively expressed antifungal peptide protects *Tenebrio molitor* during a natural infection by the entomopathogenic fungus *Beauveria bassiana*. *Developmental & Comparative Immunology*, 86, 26-33.
157. Malpartida, F., Zalacain, M., Jimenez, A., & Davies, J. (1983). Molecular cloning and expression in *Streptomyces lividans* of a hygromycin B phosphotransferase gene from *Streptomyces hygroscopicus*. *Biochemical and Biophysical Research Communications*, 117(1), 6-12.
158. Márquez, L. M., Redman, R. S., Rodriguez, R. J., & Roossinck, M. J. (2007). A virus in a fungus in a plant: three-way symbiosis required for thermal tolerance. *Science*, 315(5811), 513-515.
159. Martins, M. K., Furlaneto, M. C., Sosa-Gomez, D. R., Faria, M. R., & Fungaro, M. H. P. (1999). Double-stranded RNA in the entomopathogenic fungus *Metarhizium flavoviride*. *Current Genetics*, 36(1-2), 94-97.
160. Marvelli, R. A., Hobbs, H. A., Li, S., McCoppin, N. K., Domier, L. L., Hartman, G. L., & Eastburn, D. M. (2014). Identification of novel double-stranded RNA mycoviruses of *Fusarium virguliforme* and evidence of their effects on virulence. *Archives of Virology*, 159(2), 349-352.
161. Marzano, S. Y. L., Hobbs, H. A., Nelson, B. D., Hartman, G. L., Eastburn, D. M., McCoppin, N. K., & Domier, L. L. (2015). Transfection of *Sclerotinia sclerotiorum* with *in vitro* transcripts of a naturally occurring interspecific recombinant of *Sclerotinia sclerotiorum* hypovirus 2 significantly reduces virulence of the fungus. *Journal of Virology*, 89(9), 5060-5071.

162. Mascarin, G. M., & Jaronski, S. T. (2016). The production and uses of *Beauveria bassiana* as a microbial insecticide. *World Journal of Microbiology and Biotechnology*, 32(11), 177.
163. McCabe, P. M., Pfeiffer, P., & Van Alfen, N. K. (1999). The influence of dsRNA viruses on the biology of plant pathogenic fungi. *Trends in Microbiology*, 7(9), 377-381.
164. McGuire, A. M., Pearson, M. D., Neafsey, D. E., & Galagan, J. E. (2008). Cross-kingdom patterns of alternative splicing and splice recognition. *Genome biology*, 9(3), 1-19.
165. McKinnon, A. C., Saari, S., Moran-Diez, M. E., Meyling, N. V., Raad, M., & Glare, T. R. (2017). *Beauveria bassiana* as an endophyte: a critical review on associated methodology and biocontrol potential. *BioControl*, 62(1), 1-17.
166. Melzer, M. J., & Bidochka, M. J. (1998). Diversity of double-stranded RNA viruses within populations of entomopathogenic fungi and potential implications for fungal growth and virulence. *Mycologia*, 90(4), 586-594.
167. Meyling, N. V., & Eilenberg, J. (2007). Ecology of the entomopathogenic fungi *Beauveria bassiana* and *Metarhizium anisopliae* in temperate agroecosystems: potential for conservation biological control. *Biological Control*, 43(2), 145-155.
168. Miller, T. C., Gubler, W. D., Laemmlen, F. F., Geng, S., & Rizzo, D. M. (2004). Potential for using *Lecanicillium lecanii* for suppression of strawberry powdery mildew. *Biocontrol Science and Technology*, 14(2), 215-220.
169. Moreau, P. A., Peintner, U., & Gardes, M. (2006). Phylogeny of the ectomycorrhizal mushroom genus *Alnicola* (Basidiomycota, Cortinariaceae) based on rDNA sequences with special emphasis on host specificity and morphological characters. *Molecular phylogenetics and evolution*, 38(3), 794-807.
170. Mu, F., Xie, J., Cheng, S., You, M. P., Barbetti, M. J., Jia, J., Wang, Q., Cheng, J., Fu, Y., & Chen, T. (2018). Virome characterization of a collection of *S. sclerotiorum* from Australia. *Frontiers in microbiology*, 8, 2540.
171. Muller, E. M., Locke, E. G., & Cunningham, K. W. (2001). Differential regulation of two Ca<sup>2+</sup> influx systems by pheromone signaling in *Saccharomyces cerevisiae*. *Genetics*, 159(4), 1527-1538.

172. Nerva, L., Forgia, M., Ciuffo, M., Chitarra, W., Chiapello, M., Vallino, M., & Turina, M. (2019). The mycovirome of a fungal collection from the sea cucumber *Holothuria polii*. *Virus Research*, 273, 197737.
173. Nuss, D. L. (2005). Hypovirulence: mycoviruses at the fungal–plant interface. *Nature Reviews Microbiology*, 3(8), 632.
174. Ocón, A., Hampp, R., & Requena, N. (2007). Trehalose turnover during abiotic stress in arbuscular mycorrhizal fungi. *New Phytologist*, 174(4), 879-891.
175. Oliveira, C. M., Auad, A. M., Mendes, S. M., & Frizzas, M. R. (2014). Crop losses and the economic impact of insect pests on Brazilian agriculture. *Crop Protection*, 56, 50-54.
176. Oppert, B., Dowd, S. E., Bouffard, P., Li, L., Conesa, A., Lorenzen, M. D., Toutges, M., Marshall, J., Huestis, D. L., & Fabrick, J. (2012). Transcriptome profiling of the intoxication response of *Tenebrio molitor* larvae to *Bacillus thuringiensis* Cry3Aa protoxin. *PloS one*, 7(4), e34624.
177. Ortiz-Urquiza, A., & Keyhani, N. (2013). Action on the surface: entomopathogenic fungi versus the insect cuticle. *Insects*, 4(3), 357-374.
178. Ortiz-Urquiza, A., & Keyhani, N. O. (2016). Molecular genetics of *Beauveria bassiana* infection of insects. *Advances in Genetics*, 94, 165-249.
179. Osmond, B. C., Specht, C. A., & Robbins, P. W. (1999). Chitin synthase III: synthetic lethal mutants and “stress related” chitin synthesis that bypasses the CSD3/CHS6 localization pathway. *Proceedings of the National Academy of Sciences, USA*, 96(20), 11206-11210.
180. Park, Y., Chen, X., & Punja, Z. K. (2006). Molecular and biological characterization of a mitovirus in *Chalara elegans* (*Thielaviopsis basicola*). *Phytopathology*, 96(5), 468-479.
181. Pascale, M., Visconti, A., Pronczuk, M., Wisniewska, H., & Chelkowski, J. (2002). Accumulation of fumonisins, beauvericin and fusaproliferin in maize hybrids inoculated under field conditions with *Fusarium proliferatum*. *Mycological Research*, 106(9), 1026-1030.
182. Pearson, M. N., Beever, R. E., Boine, B., & Arthur, K. (2009). Mycoviruses of filamentous fungi and their relevance to plant pathology. *Molecular Plant Pathology*, 10(1), 115-128.

183. Pedrini, N., Ortiz-Urquiza, A., Zhang, S., & Keyhani, N. O. (2013). Targeting of insect epicuticular lipids by the entomopathogenic fungus *Beauveria bassiana*: hydrocarbon oxidation within the context of a host-pathogen interaction. *Frontiers in Microbiology*, 4, 24.
184. Pendland, J. C., Hung, S. Y., & Boucias, D. (1993). Evasion of host defense by *in vivo*-produced protoplast-like cells of the insect mycopathogen *Beauveria bassiana*. *Journal of Bacteriology*, 175(18), 5962-5969.
185. Perinotto, W. M., Golo, P. S., Rodrigues, C. J. C., Sá, F. A., Santi, L., da Silva, W. O. B., Junges, A., Vainstein, M. H., Schrank, A., & Salles, C. M. (2014). Enzymatic activities and effects of mycovirus infection on the virulence of *Metarhizium anisopliae* in *Rhipicephalus microplus*. *Veterinary parasitology*, 203(1-2), 189-196.
186. Petersen, T. N., Brunak, S., Von Heijne, G., & Nielsen, H. (2011). SignalP 4.0: discriminating signal peptides from transmembrane regions. *Nature Methods*, 8(10), 785.
187. Peyambari, M., Habibi, M. K., Fotouhifar, K. B., Dizadji, A., & Roossinck, M. J. (2014). Molecular characterization of a novel putative partitivirus infecting *Cytospora sacchari*, a plant pathogenic fungus. *The Plant Pathology Journal*, 30(2), 151.
188. Plaskon, N. E., Adelman, Z. N., & Myles, K. M. (2009). Accurate strand-specific quantification of viral RNA. *PLoS One*, 4(10), e7468.
189. Pomerening, J. R., Ubersax, J. A., & Ferrell Jr, J. E. (2008). Rapid cycling and precocious termination of G1 phase in cells expressing CDK1AF. *Molecular Biology of the Cell*, 19(8), 3426-3441.
190. Posteraro, B., Tumbarello, M., La Sorda, M., Spanu, T., Trecarichi, E. M., De Bernardis, F., Scoppettuolo, G., Sanguinetti, M., & Fadda, G. (2006). Azole resistance of *Candida glabrata* in a case of recurrent fungemia. *Journal of clinical microbiology*, 44(8), 3046-3047.
191. Potgieter, C. A., Castillo, A., Castro, M., Cottet, L., & Morales, A. (2013). A wild-type *Botrytis cinerea* strain co-infected by double-stranded RNA mycoviruses presents hypovirulence-associated traits. *Virology Journal*, 10(1), 220.
192. Preisig, O., Moleleki, N., Smit, W. A., Wingfield, B. D., & Wingfield, M. J. (2000). A novel RNA mycovirus in a hypovirulent isolate of the plant pathogen *Diaporthe ambigua*. *Journal of General Virology*, 81(12), 3107-3114.

193. Punt, P. J., Oliver, R. P., Dingemans, M. A., Pouwels, P. H., & van den Hondel, C. A. (1987). Transformation of *Aspergillus* based on the hygromycin B resistance marker from *Escherichia coli*. *Gene*, *56*(1), 117-124.
194. Purwar, J. P., & Sachan, G. C. (2005). Compatibility of entomogenous fungus, *Beauveria bassiana* with commonly used insecticides. *Pestology*, *29*(7), 25-31.
195. Qin, Y., Ortiz-Urquiza, A., & Keyhani, N. O. (2014). A putative methyltransferase, mtrA, contributes to development, spore viability, protein secretion and virulence in the entomopathogenic fungus *Beauveria bassiana*. *Microbiology*, *160*(11), 2526-2537.
196. Qiu, D., Eisinger, V. M., Head, N. E., Pier, G. B., & Yu, H. D. (2008). ClpXP proteases positively regulate alginate overexpression and mucoid conversion in *Pseudomonas aeruginosa*. *Microbiology (Reading, England)*, *154*(Pt 7), 2119.
197. Qiu, L., Wang, J. J., Ying, S. H., & Feng, M. G. (2015). Wee1 and Cdc 25 control morphogenesis, virulence and multistress tolerance of *Beauveria bassiana* by balancing cell cycle-required cyclin-dependent kinase 1 activity. *Environmental Microbiology*, *17*(4), 1119-1133.
198. Ramanathan, A., Robb, G. B., & Chan, S. H. (2016). mRNA capping: biological functions and applications. *Nucleic acids research*, *44*(16), 7511-7526.
199. Ranson, H., N'guessan, R., Lines, J., Moiroux, N., Nkuni, Z., & Corbel, V. (2011). Pyrethroid resistance in African anopheline mosquitoes: what are the implications for malaria control?. *Trends in parasitology*, *27*(2), 91-98.
200. Rawlings, N. D., Barrett, A. J., & Bateman, A. (2011). MEROPS: the database of proteolytic enzymes, their substrates and inhibitors. *Nucleic Acids Research*, *40*(D1), D343-D350.
201. Reddy, S. G. E. (2020). *Lecanicillium* spp. for the Management of Aphids, Whiteflies, Thrips, Scales and Mealy Bugs. *Arthropods*.
202. Roberts, D. W., & St Leger, R. J. (2004). *Metarhizium* spp., cosmopolitan insect-pathogenic fungi: mycological aspects. *Advances in Applied Microbiology*, *54*(1), 1-70.
203. Robinson, H. L., & Deacon, J. W. (2002). Double-stranded RNA elements in *Rhizoctonia solani* AG 3. *Mycological Research*, *106*(1), 12-22.

204. Robinson, M. D., & Oshlack, A. (2010). A scaling normalization method for differential expression analysis of RNA-seq data. *Genome biology*, 11(3), 1-9.
205. Romaine, C. P., & Schlagnhauser, B. (1995). PCR analysis of the viral complex associated with La France disease of *Agaricus bisporus*. *Applied and environmental microbiology*, 61(6), 2322-2325.
206. Romo, M., Leuchtmann, A., García, B., & Zabalgoitia, I. (2007). A totivirus infecting the mutualistic fungal endophyte *Epichloe festucae*. *Virus Research*, 124(1-2), 38-43.
207. Rondot, Y., & Reineke, A. (2019). Endophytic *Beauveria bassiana* activates expression of defence genes in grapevine and prevents infections by grapevine downy mildew *Plasmopara viticola*. *Plant Pathology*, 68(9), 1719-1731.
208. Sabino, R., Burco, J., Valente, J., Veríssimo, C., Clemons, K. V., Stevens, D. A., & Tell, L. A. (2019). Molecular identification of clinical and environmental avian *Aspergillus* isolates. *Archives of Microbiology*, 201(2), 253-257.
209. Sabino, R., Ferreira, J. A., Moss, R. B., Valente, J., Veríssimo, C., Carolino, E., Clemons, K. V., Everson, C., Banaei, N., & Penner, J. (2015). Molecular epidemiology of *Aspergillus* collected from cystic fibrosis patients. *Journal of Cystic Fibrosis*, 14(4), 474-481.
210. Sabino, R., Veríssimo, C., Parada, H., Brandão, J., Viegas, C., Carolino, E., & Stevens, D. A. (2014). Molecular screening of 246 Portuguese *Aspergillus* isolates among different clinical and environmental sources. *Medical Mycology*, 52(5), 519-529.
211. Salaipeth, L., Chiba, S., Eusebio-Cope, A., Kanematsu, S., & Suzuki, N. (2014). Biological properties and expression strategy of Rosellinia necatrix megabirnavirus 1 analysed in an experimental host, *Cryphonectria parasitica*. *Journal of General Virology*, 95(3), 740-750.
212. Samuels, R. I., & Paterson, I. C. (1995). Cuticle degrading proteases from insect moulting fluid and culture filtrates of entomopathogenic fungi. *Comparative Biochemistry and Physiology Part B: Biochemistry and Molecular Biology*, 110(4), 661-669.
213. Sánchez-Peña, S. R., Lara, J. S. J., & Medina, R. F. (2011). Occurrence of entomopathogenic fungi from agricultural and natural ecosystems in Saltillo, Mexico, and their virulence towards thrips and whiteflies. *Journal of Insect Science*, 11(1), 1.

- 214.Santos, B., Duran, A., & Valdivieso, M. H. (1997). CHS5, a gene involved in chitin synthesis and mating in *Saccharomyces cerevisiae*. *Molecular and Cellular Biology*, 17(5), 2485-2496.
- 215.Santos, V., Mascarin, G. M., da Silva Lopes, M., Alves, M. C. D. F., Rezende, J. M., Gatti, M. S. V., Dunlap, C. A., & Júnior, Í. D. (2017). Identification of double-stranded RNA viruses in Brazilian strains of *Metarhizium anisopliae* and their effects on fungal biology and virulence. *Plant Gene*, 11, 49-58.
- 216.Saupe, S. J. (2000). Molecular genetics of heterokaryon incompatibility in filamentous ascomycetes. *Microbiology and Molecular Biology Reviews*, 64(3), 489-502.
- 217.Schäffer, A. A., Aravind, L., Madden, T. L., Shavirin, S., Spouge, J. L., Wolf, Y. I., & Altschul, S. F. (2001). Improving the accuracy of PSI-BLAST protein database searches with composition-based statistics and other refinements. *Nucleic Acids Research*, 29(14), 2994-3005.
- 218.Schnell, M. J., & Conzelmann, K. K. (1995). Polymerase activity of *in vitro* mutated rabies virus L protein. *Virology*, 214(2), 522-530.
- 219.Sharom, F. J., Klein, C., Kuchler, K., & Valachovic, M. (2011). ABC proteins in yeast and fungal pathogens. *Essays in biochemistry*, 50, 101-119.
- 220.Sharzei, A., Banihashemi, Z., and Afsharifar, A. (2007). Detection and characterization of a double-stranded RNA mycovirus in *Fusarium oxysporum* f. sp. melonis. *Iran J. Plant Path.* 43, 9–26.
- 221.Snelders, E., Van Der Lee, H. A., Kuijpers, J., Rijs, A. J. M., Varga, J., Samson, R. A., Mellado, E., Donders, A. R. T., Melchers, W. J., & Verweij, P. E. (2008). Emergence of azole resistance in *Aspergillus fumigatus* and spread of a single resistance mechanism. *PLoS Med*, 5(11), e219.
- 222.Soldevila, A. I., & Ghabrial, S. A. (2000). Expression of the totivirus *Helminthosporium victoriae* 190S virus RNA-dependent RNA polymerase from its downstream open reading frame in dicistronic constructs. *Journal of Virology*, 74(2), 997-1003.
- 223.Souza, I. E., Azevedo, M. L., Succi, R. C., Machado, D. M., & Diaz, R. S. (2000). RNA viral load test for early diagnosis of vertical transmission of HIV-1 infection. *JAIDS Journal of Acquired Immune Deficiency Syndromes*, 23(4), 358-360.
- 224.St Leger, R. J., Joshi, L., Bidochka, M. J., Rizzo, N. W., & Roberts, D. W. (1996). Biochemical characterization and ultrastructural localization of two extracellular trypsins produced by *Metarhizium anisopliae* in infected insect cuticles. *Applied and Environmental Microbiology*, 62(4), 1257-1264.

225. Stathopoulos, A. M., & Cyert, M. S. (1997). Calcineurin acts through the CRZ1/TCN1-encoded transcription factor to regulate gene expression in yeast. *Genes & development*, *11*(24), 3432-3444.
226. Steinrauf, L. K. (1985). Beauvericin and the other enniatins. *METAL IONS BIOL. SYST.* 1985.
227. Suzaki, K., Ikeda, K. I., Sasaki, A., Kanematsu, S., Matsumoto, N., & Yoshida, K. (2005). Horizontal transmission and host-virulence attenuation of totivirus in violet root rot fungus *Helicobasidium mompa*. *Journal of General Plant Pathology*, *71*(3), 161-168.
228. Tavantzis, S. (2008). Partitiviruses of fungi. In: Mahy, B.W.J., Van Regenmortel, M.H.V. (eds) *Encyclopedia of virology*, 3rd edn. Elsevier, Oxford, 63-68.
229. Thompson, S. N. (2003). Trehalose—the insect ‘blood’ sugar. *Advances in Insect Physiology*, *31*(Supplement C), 205-285.
230. Tiago, P. V., Fungaro, M. H. P., Rodrigues de Faria, M., & Furlaneto, M. C. (2004). Effects of double-stranded RNA in *Metarhizium anisopliae* var. *acidum* and *Paecilomyces fumosoroseus* on protease activities, conidia production, and virulence. *Canadian Journal of Microbiology*, *50*(5), 335-339.
231. Trapnell, C., Williams, B. A., Pertea, G., Mortazavi, A., Kwan, G., Van Baren, M. J., Salzberg, S. L., Wold, B. J., & Pachter, L. (2010). Transcript assembly and quantification by RNA-Seq reveals unannotated transcripts and isoform switching during cell differentiation. *Nature biotechnology*, *28*(5), 511-515.
232. Treton, B. Y., Le Dall, M. T., & Heslot, H. (1987). UV-induced curing of the double-stranded RNA virus of the yeast *Yarrowia lipolytica*. *Current Genetics*, *12*(1), 37-39.
233. Truman, A.W., Millson, S.H., Nuttall, J.M., Mollapour, M., Prodromou, C., Piper, P.W., 2007. In the yeast heat shock response, Hsf1-directed induction of Hsp90 facilitates the activation of the SlT2 (Mpk1) mitogen-activated protein kinase required for cell integrity. *Eukaryotic Cell*, *(6)*, 744–752.
234. Tuomivirta, T. T., & Hantula, J. (2003). Two unrelated double-stranded RNA molecule patterns in *Gremmeniella abietina* type A code for putative viruses of the families *Totiviridae* and *Partitiviridae*. *Archives of Virology*, *148*(12), 2293-2305.
235. Tuomivirta, T. T., & Hantula, J. (2005). Three unrelated viruses occur in a single isolate of *Gremmeniella abietina* var. *abietina* type A. *Virus Research*, *110*(1-2), 31-39.

236. Urtz, B. E., & Rice, W. C. (2000). Purification and characterization of a novel extracellular protease from *Beauveria bassiana*. *Mycological Research*, 104(2), 180-186.
237. Vainio, E. J., Chiba, S., Ghabrial, S. A., Maiss, E., Roossinck, M., Sabanadzovic, S., & Nibert, M. (2018). ICTV virus taxonomy profile: *Partitiviridae*. *Journal of General Virology*, 99(1), 17-18.
238. Van De Sande, W. W. J., Lo-Ten-Foe, J. R., Van Belkum, A., Netea, M. G., Kullberg, B. J., & Vonk, A. G. (2010). Mycoviruses: future therapeutic agents of invasive fungal infections in humans? *European Journal of Clinical Microbiology and Infectious Diseases*, 29(7), 755-763.
239. van Diepeningen, A. D., Debets, A. J., & Hoekstra, R. F. (2006). Dynamics of dsRNA mycoviruses in black *Aspergillus* populations. *Fungal Genetics and Biology*, 43(6), 446-452.
240. Van Regenmortel, M. H. V. (2007). Virus species and virus identification: past and current controversies. *Infection, Genetics and Evolution*, 7(1), 133-144.
241. Varga, J., Vágvölgyi, C., & Tóth, B. (2003). Recent advances in mycovirus research. *Acta Microbiologica et Immunologica Hungarica*, 50(1), 77-94.
242. Verghese, J., Abrams, J., Wang, Y., Morano, K.A., (2012). Biology of the heat shock response and protein chaperones: budding yeast (*Saccharomyces cerevisiae*) as a model system. *Microbiological Molecular Biological Reviews*, (16), 115-158.
243. Vey, A., Hoagland, R. E., & Butt, T. M. (2001). Toxic metabolites of fungal biocontrol agents. *Fungi as biocontrol agents: progress, problems and potential*, 1, 311-346.
244. Vienken, K., & Fischer, R. (2006). The Zn (II) 2Cys6 putative transcription factor NosA controls fruiting body formation in *Aspergillus nidulans*. *Molecular Microbiology*, 61(2), 544-554.
245. Vrabl, P., Schinagl, C. W., Artmann, D. J., Heiss, B., & Burgstaller, W. (2019). Fungal Growth in Batch Culture—What We Could Benefit If We Start Looking Closer. *Frontiers in microbiology*, 10, 2391.
246. Wagner, B. L., & Lewis, L. C. (2000). Colonization of corn, *Zea mays*, by the entomopathogenic fungus *Beauveria bassiana*. *Applied and Environmental Microbiology*, 66(8), 3468-3473.
247. Wang, C., & St Leger, R. J. (2007). The MAD1 adhesin of *Metarhizium anisopliae* links adhesion with blastospore production and virulence to insects, and the MAD2 adhesin enables attachment to plants. *Eukaryotic Cell*, 6(5), 808-816.

248. Wang, J. J., Cai, Q., Qiu, L., Ying, S. H., & Feng, M. G. (2017). Additive roles of two TPS genes in trehalose synthesis, conidiation, multiple stress responses and host infection of a fungal insect pathogen. *Applied Microbiology and Biotechnology*, *101*(9), 3637-3651.
249. Wang, J., Liu, J., Hu, Y., Ying, S. H., & Feng, M. G. (2013). Cytokinesis-required Cdc14 is a signaling hub of asexual development and multi-stress tolerance in *Beauveria bassiana*. *Scientific Reports*, *3*(1), 1-8.
250. Wang, X. X., He, P. H., Feng, M. G., & Ying, S. H. (2014). BbSNF1 contributes to cell differentiation, extracellular acidification, and virulence in *Beauveria bassiana*, a filamentous entomopathogenic fungus. *Applied Microbiology and Biotechnology*, *98*(20), 8657-8673.
251. Wang, X. X., Ji, X. P., Li, J. X., Keyhani, N. O., Feng, M. G., & Ying, S. H. (2013). A putative  $\alpha$ -glucoside transporter gene BbAGT1 contributes to carbohydrate utilization, growth, conidiation and virulence of filamentous entomopathogenic fungus *Beauveria bassiana*. *Research in Microbiology*, *164*(5), 480-489.
252. Wang, Z. L., Lu, J. D., & Feng, M. G. (2012). Primary roles of two dehydrogenases in the mannitol metabolism and multi-stress tolerance of entomopathogenic fungus *Beauveria bassiana*. *Environmental Microbiology*, *14*(8), 2139-2150.
253. Waterhouse, A. M., Procter, J. B., Martin, D. M., Clamp, M., & Barton, G. J. (2009). Jalview Version 2—a multiple sequence alignment editor and analysis workbench. *Bioinformatics*, *25*(9), 1189-1191.
254. Waters, E. M., Neill, D. R., Kaman, B., Sahota, J. S., Clokie, M. R., Winstanley, C., & Kadioglu, A. (2017). Phage therapy is highly effective against chronic lung infections with *Pseudomonas aeruginosa*. *Thorax*, *72*(7), 666-667.
255. Wei, C. Z., Osaki, H., Iwanami, T., Matsumoto, N., & Ohtsu, Y. (2004). Complete nucleotide sequences of genome segments 1 and 3 of Rosellinia anti-rot virus in the family *Reoviridae*. *Archives of Virology*, *149*(4), 773-777.
256. White, T. J., Bruns, T., Lee, S. J. W. T., & Taylor, J. (1990). Amplification and direct sequencing of fungal ribosomal RNA genes for phylogenetics. *PCR protocols: a guide to methods and applications*, *18*(1), 315-322.

257. Wickner, R. B. (1996). Double-stranded RNA viruses of *Saccharomyces cerevisiae*. *Microbiological Reviews*, 60(1), 250.
258. Williams, D. R., & Sit, S. Y. (1982). Synthesis of racemic tenellin. *The Journal of Organic Chemistry*, 47(15), 2846-2851.
259. Williamson, J. D., Stoop, J. M., Massel, M. O., Conkling, M. A., & Pharr, D. M. (1995). Sequence analysis of a mannitol dehydrogenase cDNA from plants reveals a function for the pathogenesis-related protein ELI3. *Proceedings of the National Academy of Sciences, USA*, 92(16), 7148-7152.
260. Wu, M., Jin, F., Zhang, J., Yang, L., Jiang, D., & Li, G. (2012). Characterization of a novel bipartite double-stranded RNA mycovirus conferring hypovirulence in the phytopathogenic fungus *Botrytis porri*. *Journal of Virology*, 86(12), 6605-6619.
261. Xia, Y., Clarkson, J. M., & Charnley, A. K. (2002a). Trehalose-hydrolysing enzymes of *Metarhizium anisopliae* and their role in pathogenesis of the tobacco hornworm, *Manduca sexta*. *Journal of invertebrate pathology*, 80(3), 139-147.
262. Xia, Y., Gao, M., Clarkson, J. M., & Charnley, A. K. (2002b). Molecular cloning, characterisation, and expression of a neutral trehalase from the insect pathogenic fungus *Metarhizium anisopliae*. *Journal of invertebrate pathology*, 80(2), 127-137.
263. Xiao, G., Ying, S.-H., Zheng, P., Wang, Z.-L., Zhang, S., Xie, X.-Q., Shang, Y., Leger, R. J. S., Zhao, G.-P., & Wang, C. (2012). Genomic perspectives on the evolution of fungal entomopathogenicity in *Beauveria bassiana*. *Scientific reports*, 2(1), 1-10.
264. Xie XQ, Li F, Ying SH, Feng MG (2012) Additive contributions of two manganese-cored superoxide dismutases (MnSODs) to antioxidation, UV tolerance and virulence of *Beauveria bassiana*. *PLoS One*, 7(1), e30298Xie.
265. Xu, Y., Orozco, R., Wijeratne, E. K., Espinosa-Artiles, P., Gunatilaka, A. L., Stock, S. P., & Molnár, I. (2009). Biosynthesis of the cyclooligomer depsipeptide bassianolide, an insecticidal virulence factor of *Beauveria bassiana*. *Fungal Genetics and Biology*, 46(5), 353-364.
266. Xu, Y., Orozco, R., Wijeratne, E. K., Gunatilaka, A. L., Stock, S. P., & Molnár, I. (2008). Biosynthesis of the cyclooligomer depsipeptide beauvericin, a virulence factor of the entomopathogenic fungus *Beauveria bassiana*. *Chemistry & Biology*, 15(9), 898-907.

267. Yamada, T., Seno, M., Shiraishi, T., Kato, H., An, C., Yoshida, T., & Oku, H. (1991). Isolation and characterization of double-stranded RNAs from the pea pathogen, *Mycosphaerella pinodes*. *Plant and Cell Physiology*, *32*(1), 65-71.
268. Yang, J., Liu, M., Liu, X., Yin, Z., Sun, Y., Zhang, H., Zheng, X., Wang, P., & Zhang, Z. (2018). Heat-shock proteins MoSsb1, MoSsz1, and MoZuo1 attenuate MoMkk1-mediated cell-wall integrity signaling and are important for growth and pathogenicity of *Magnaporthe oryzae*. *Molecular Plant-Microbe Interactions*, *31*(11), 1211-1221.
269. Yang, Y. T., Lee, M. R., Lee, S. J., Kim, S., Nai, Y. S., & Kim, J. S. (2018). *Tenebrio molitor* Gram-negative-binding protein 3 (TmGNBP3) is essential for inducing downstream antifungal Tenecin 1 gene expression against infection with *Beauveria bassiana* JEF-007. *Insect Science*, *25*(6), 969-977.
270. Yewhalaw, D., Wassie, F., Steurbaut, W., Spanoghe, P., Van Bortel, W., Denis, L., Tessema, D. A., Getachew, Y., Coosemans, M., & Duchateau, L. (2011). Multiple insecticide resistance: an impediment to insecticide-based malaria vector control program. *PloS one*, *6*(1), e16066.
271. Yu, X., Li, B., Fu, Y., Xie, J., Cheng, J., Ghabrial, S. A., Li, G., Yi, X., & Jiang, D. (2013). Extracellular transmission of a DNA mycovirus and its use as a natural fungicide. *Proceedings of the National Academy of Sciences*, *110*(4), 1452-1457.
272. Yun, D.-J., Ibeas, J. I., Lee, H., Coca, M. A., Narasimhan, M. L., Uesono, Y., Hasegawa, P. M., Pardo, J. M., & Bressan, R. A. (1998). Osmotin, a plant antifungal protein, subverts signal transduction to enhance fungal cell susceptibility. *Molecular cell*, *1*(6), 807-817.
273. Zamski, E., Guo, W. W., Yamamoto, Y. T., Pharr, D. M., & Williamson, J. D. (2001). Analysis of celery (*Apium graveolens*) mannitol dehydrogenase (Mtd) promoter regulation in Arabidopsis suggests roles for MTD in key environmental and metabolic responses. *Plant Molecular Biology*, *47*(5), 621-631.
274. Zare, R., Gams, W., & Evans, H. C. (2001). A revision of *Verticillium* section Prostrata. V. The genus *Pochonia*, with notes on Rotiferophthora. *Nova Hedwigia*, *73*(1/2), 51-86.
275. Zhai, L., Xiang, J., Zhang, M., Fu, M., Yang, Z., Hong, N., & Wang, G. (2016). Characterization of a novel double-stranded RNA mycovirus conferring hypovirulence from the phytopathogenic fungus *Botryosphaeria dothidea*. *Virology*, *493*, 75-85.

- 276.Zhan, J., Burns, A. M., Liu, M. X., Faeth, S. H., & Gunatilaka, A. L. (2007). Search for cell motility and angiogenesis inhibitors with potential anticancer activity: beauvericin and other constituents of two endophytic strains of *Fusarium oxysporum*. *Journal of natural products*, 70(2), 227-232.
- 277.Zhang, S., Fan, Y., Xia, Y. X., & Keyhani, N. O. (2010). Sulfonylurea resistance as a new selectable marker for the entomopathogenic fungus *Beauveria bassiana*. *Applied Microbiology and Biotechnology*, 87(3), 1151-1156.
- 278.Zhang, S., Widemann, E., Bernard, G., Lesot, A., Pinot, F., Pedrini, N., & Keyhani, N. O. (2012). CYP52X1, representing new cytochrome P450 subfamily, displays fatty acid hydroxylase activity and contributes to virulence and growth on insect cuticular substrates in entomopathogenic fungus *Beauveria bassiana*. *Journal of Biological Chemistry*, 287(16), 13477-13486.
- 279.Zhang, S., Xia, Y. X., Kim, B., & Keyhani, N. O. (2011). Two hydrophobins are involved in fungal spore coat rodlet layer assembly and each play distinct roles in surface interactions, development and pathogenesis in the entomopathogenic fungus, *Beauveria bassiana*. *Molecular microbiology*, 80(3), 811-826.
- 280.Zhang, T., Jiang, Y., Huang, J., & Dong, W. (2013). Genomic organization of a novel partitivirus from the phytopathogenic fungus *Ustilaginoidea virens*. *Archives of virology*, 158(11), 2415-2419.
- 281.Zhao, C., Jung, U. S., Garrett-Engle, P., Roe, T., Cyert, M. S., & Levin, D. E. (1998). Temperature-Induced Expression of YeastFKS2 Is under the Dual Control of Protein Kinase C and Calcineurin. *Molecular and cellular biology*, 18(2), 1013-1022.
- 282.Zhao, S., Ye, Z., & Stanton, R. (2020). Misuse of RPKM or TPM normalization when comparing across samples and sequencing protocols. *Rna*, 26(8), 903-909.
- 283.Zhai, L., Xiang, J., Zhang, M., Fu, M., Yang, Z., Hong, N., & Wang, G. (2016). Characterization of a novel double-stranded RNA mycovirus conferring hypovirulence from the phytopathogenic fungus *Botryosphaeria dothidea*. *Virology*, 493, 75-85.
- 284.Zimmermann, G. (2007). Review on safety of the entomopathogenic fungi *Beauveria bassiana* and *Beauveria brongniartii*. *Biocontrol Science and Technology*. 17(6), p553-596.
- 285.Zuker, M. (2003). Mfold web server for nucleic acid folding and hybridization prediction. *Nucleic Acids Research*, 31(13), 3406-3415.

# Appendices

## Part A

### 1. Antibiotics

Antibiotics were filter-sterilised, and aliquots stored at -20°C. The media were cooled below 50°C to prevent heat inactivation of antibiotics.

**Table 1** List of antibiotics and their concentrations

Antibiotic	Stock concentration	Working concentration
Streptomycin	100 mg/mL	100 µg/ mL
Ampicillin	100 mg/ mL	100 µg/ mL
Kanamycin	100 mg/ mL	100 µg/ mL

### 2. Buffers, Media and Solutions

#### 2.1 Malt extract agar (MEA)

Malt extract (Oxoid) 20 g

Technical agar no.3 (Oxoid) 15 g

Sterilised distilled water 1000 mL

#### 2.2 LBA medium

Tryptone (Oxoid) or Peptone 10 g

NaCl 10 g

Yeast extract 5 g

Technical agar no.3 (Oxoid) 12 g

Sterilised distilled water 1000 mL

### **2.3 1x LB medium**

Tryptone (Oxoid) or Peptone 10 g

NaCl 10 g

Yeast extract 5 g

Sterilised distilled water 1000 mL

### **2.4 2x LB medium**

Tryptone (Oxoid) or Peptone 20 g

NaCl 20 g

Yeast extract 10 g

Sterilised distilled water 1000 mL

### **2.5 Czapek-Dox medium (Liquid)**

Sucrose 30 g

KH<sub>2</sub>PO<sub>4</sub> 0.5 g

KCl 1 g

NaNO<sub>3</sub> 2 g

MgCl<sub>2</sub> 7H<sub>2</sub>O 0.62 g

FeSO<sub>4</sub> or FeCl<sub>3</sub> 0.01 g

Peptone 1.5 g

Yeast extract 1.5 g

Malt extract 1.5 g

Distilled water to 1000 mL Czapek-Dox agar medium was prepared to culture *B. bassiana* isolates.

## **2.6 Transformation storage solution (TSS)**

2x LB 5 mL

PEG 8000 1 g

Dimethyl sulfoxide (DMSO) 0.5 mL

MgCl<sub>2</sub> (1 M) 0.5 mL

Sterilised distilled water 3 mL

## **2.7 X-gal solution**

IPTG 10 µL

X-gal 20 µL

Sterilised distilled water 90 µL

X-gal solution is freshly prepared.

## **2.8 Extraction buffer**

EDTA (20 mM) (pH 8.0)

Tris-HCl (20 mM) (pH 7.5)

1% SDS

1% NaCl

## **2.9 TE buffer**

Tris-HCl (1 M) 50 mL

EDTA (0.5 M) 2 mL

Sterilised distilled water 948 mL

### **2.10 50x TAE buffer**

Tris base 242 g

Glacial acetic acid 57.1 mL

EDTA (0.5 M) 100 mL

Sterilised distilled water 842.9 mL

### **2.11 Maleic Acid Buffer**

0.1 M Maleic acid, 0.15 M NaCl; adjust with NaOH (solid) to pH 7.5

### **2.12 Blocking Solution**

Dilute 10× Blocking Solution (vial 6) 1:10 with maleic acid buffer

### **2.13 Washing buffer**

0.1 M Maleic acid, 0.15 M NaCl; pH 7.5; 0.3% (v/v) Tween 20

### **2.14 Detection Buffer**

0.1 M Tris-HCL, 0.1M NaCl, pH 9.5 (20°C)

### **2.15 Lysis buffers for extraction of high molecular weight DNA from fungi for long read sequencing.**

#### **1. Buffer A:**

- a. 0.35 M sorbitol
- b. 0.1 M Tris-HCL, pH 9
- c. 5 mM EDTA, pH 8
- d. Autoclave to sterilize

## 2. Buffer B:

- a. 0.2 M Tris-HCl, pH 9
- b. 50 mM EDTA, pH 8
- c. 2 M NaCl
- d. 2% [w/v] CTAB
- e. Autoclave to sterilize

## 3. Buffer C:

- a. Sarkosyl (*N*-lauroylsarcosine sodium salt)

### 2.16 Trace element solution

$\text{Na}_2\text{B}_4\text{O}_7 \cdot 10\text{H}_2\text{O}$	40 mg
$\text{CuSO}_4 \cdot 5\text{H}_2\text{O}$	400 mg
$\text{FePO}_4 \cdot 2\text{H}_2\text{O}$	800 mg
$\text{MnSO}_4 \cdot 2\text{H}_2\text{O}$	800 mg
$\text{Na}_2\text{MoO}_4 \cdot 2\text{H}_2\text{O}$	800 mg
$\text{ZnSO}_4 \cdot 7\text{H}_2\text{O}$	8 g
Sterile distilled water to	1000 ml

The solution was sterilised at 121 °C for 15 min 121 °C and kept at 4 °C. Mix before use.

### 2.17 LB plates with ampicillin

15 g of technical grade agar (Oxoid) was added to 1 litre of LB medium and then autoclaved. The medium was allowed to cool to 50°C before adding 0.1 g/mL ampicillin to a final concentration of 0.1 mg/mL. Then 30 mL of the medium was poured into Petri plates, the medium was allowed to solidify, and the plates were then stored at 4°C for up to 1 month.

### 2.18 LB plates with ampicillin/IPTG/X-Gal

The LB plates with ampicillin were made as described above. IPTG/X-Gal solution (10  $\mu$ L IPTG, 20  $\mu$ L X-Gal and 90  $\mu$ L sterile dH<sub>2</sub>O) was spread over the surface of an LB ampicillin plate and allowed to absorb for 30 min at 37°C prior to use.

### 2.19 DEPC-treated water (0.1% v/v)

Diethyl pyrocarbonate (Sigma)	1.0 mL
Distilled water to	1000 mL

The solution was shaken in a water bath at 37 °C overnight and then sterilised at 121 °C for 45 min to inactivate traces of DEPC.

### 2.20 Polyethylene Glycol (PEG) Solution, for 100 mL:

60% PEG	(60 g of PEG 4000)
50 mM CaCl <sub>2</sub>	(0.735 g of CaCl <sub>2</sub> •2H <sub>2</sub> O)
50 mM Tris-HCl, pH 7.5	(5 ml of 1 M Tris-HCl, pH 7.5 stock)

### 2.21 Solutions for DIG northern blot hybridization

Solution for gel denaturation:

0.25 N HCl;	dH <sub>2</sub> O	78.4 mL
conc. HCl (SIGMA)		26.1 mL
100 mM NaOH;	NaOH (SIGMA)	4 g
	dH <sub>2</sub> O	1 L
100 mM Tris-HCl (pH 8.0)	Tris-HCl (Trizma SIGMA)	157.6 g
	dH <sub>2</sub> O	1 L

**DIG Easy-Hyb:** Add 64 ml sterile DEPC H<sub>2</sub>O to DIG Easy-Hyb Granules. Dissolve by stirring at 37 °C for 5 min

**Washing buffer, pH 7.5:**

0.1 M maleic acid	11.607 g
0.15 M NaCl	8.766 g
0.3% (v/v) Tween 20	3 ml
DEPC-treated H <sub>2</sub> O	to 1000 ml

**Maleic acid buffer, pH 7.5:**

0.1 M maleic acid	11.607 g
0.15 M NaCl	8.766 g
DEPC-treated H <sub>2</sub> O	to 1000 ml

**Detection buffer, pH 9.5:**

0.1 M Tris-HCl	12.14 g
0.1 M NaCl	5.855 g
DEPC-treated H <sub>2</sub> O	to 1000 mL

**Blocking solution:** prepare 1x blocking solution by diluting 10x blocking solution in maleic acid buffer (1:10)

**Antibody solution:** centrifuge anti-digoxigenin-AP for 5 min at 10,000 rpm. Dilute anti-dig-AP: 1x blocking solution = 1:10,000. Keep in ice.

**2x SSC + 0.1% SDS:**

20x SSC	20 ml
10% SDS	2 ml
DEPC-treated H <sub>2</sub> O	to 200 ml

**0.1x SSC + 0.1% SDS:**

20x SSC	1 ml
10% SDS	2 ml
DEPC-treated H <sub>2</sub> O	to 200 ml

**Part B**  
**Figures and Tables**

**3.2 Identification and characterization of mycoviruses in entomopathogenic fungi.**

**Table S3.2.1** Description of mycovirus-infected *Beauveria bassiana* isolates Spanish location of isolation and viruses identified. Taken from Filippou *et al.* (2018).

<b>Species</b>	<b>Isolate</b>	<b>Habitat</b>	<b>Location</b>	<b>Mycovirus present</b>
<i>B. bassiana</i>	EABb 00/11-Su	Soil (scrubland)	Jaen	BbVV-1 + BbPV-2 + BbPmV-1
<i>B. bassiana</i>	EABb 00/13-Su	Soil (woodland)	Jaen	BbVV-1 + BbPV-2 + BbPmV-1
<i>B. bassiana</i>	EABb 01/12-Su	Soil (scrubland)	Seville	BbVV-1
<i>B. bassiana</i>	EABb 01/33-Su	Soil (olive grove)	Cadiz	BbVV-1
<i>B. bassiana</i>	EABb 01/112-Su	Soil (wheat field)	Seville	BbVV-1
<i>B. bassiana</i>	EABb 07/06-Rf	<i>Rhynchophorus ferrugineus</i>	Alicante	BbVV-1 + BbPV-2 + BbPmV-1
<i>B. bassiana</i>	EABb 09/07-Fil	Phylloplane (meadow)	Malaga	BbPV-2
<i>B. bassiana</i>	EABb 10/01-Fil	Phylloplane (olive grove)	Malaga	BbPmV-1
<i>B. bassiana</i>	EABb 10/28-Su	Soil (olive grove)	Cordoba	BbPmV-1
<i>B. bassiana</i>	EABb 10/30-Fil	Phylloplane (olive grove)	Cordoba	BbPmV-1
<i>B. bassiana</i>	EABb 10/57-Fil	Phylloplane (meadow)	Cordoba	BbVV-1 + BbPV-2 + BbPmV-1
<i>B. bassiana</i>	EABb 11/01-Mg	<i>Monochamus galloprovincialis</i>	Palencia	BbVV-1 + BbPV-2 + BbPmV-1

**Table S3.2.2:** Oligonucleotide primers used for RT-PCR amplification of *Beauveria bassiana* virus sequences. Taken from Filippou *et al.* (2018).

Name	Sequence	T <sub>m</sub>	Amplicon	Reference
BbVV1.F	5'-AGACCCGTGCAATCTTCGC-3'	60°C	BbVV-1-like RdRP; 436 bp	Kotta-Loizou and Coutts, 2017
BbVV1.R	5'-TACACATCATCACCGGTGTG-3'	58°C		Kotta-Loizou and Coutts, 2017
BbPV2.F	5'-CGTGTCTGGCGGGTCAGCG-3'	66°C	BbPV-2-like RdRP; 787 bp	this study
BbPV2.R	5'-CGCCACCTAACCACAGGCC-3'	64°C		this study
BbPmV1.F	5'-CTGAGGGGCTAGATGCGATG-3'	63°C	BbPmV-1-like RdRP; 876 bp	this study
BbPmV1.R	5'-CATGCCGACTCCGATAGAAG-3'	61°C		this study

**Table S3.2.3:** Detailed information of all *Beauveria bassiana* isolates screened for the presence of dsRNA elements. Taken from Filippou *et al.* (2018).

Isolate	Species	Year of isolation	Habitat	Location	Mycovirus
EABa 10/01-Su	<i>Beauveria amorpha</i>	2010	Soil (sunflower field)	Córdoba (Spain)	-
EABb 00/11-Su	<i>Beauveria bassiana</i>	2000	Soil (scrubland)	Jaén (Spain)	+
EABb 00/13-Su	<i>Beauveria bassiana</i>	2000	Soil (woodland)	Jaén (Spain)	+
EABb 00/23-Su	<i>Beauveria bassiana</i>	2000	Soil (meadow)	Tenerife (Spain)	-
EABb 00/26-Su	<i>Beauveria bassiana</i>	2000	Soil (meadow)	Badajoz (Spain)	-
EABb 01/110-Su	<i>Beauveria bassiana</i>	2001	Soil (oak grove)	Sevilla (Spain)	-
EABb 01/112- Su	<i>Beauveria bassiana</i>	2001	Soil (wheat field)	Sevilla (Spain)	+
EABb 01/12-Su	<i>Beauveria bassiana</i>	2001	Soil (scrubland)	Sevilla (Spain)	+
EABb 01/171-Su	<i>Beauveria bassiana</i>	2001	Soil (cotton field)	Huelva (Spain)	-
EABb 01/33-Su	<i>Beauveria bassiana</i>	2001	Soil (olive grove)	Cadiz (Spain)	+
EABb 04/01-Tip	<i>Beauveria bassiana</i>	2004	<i>Iraella luteipes</i> (Himenoptera: Cinipidae)	Sevilla (Spain)	-
EABb 04/04-Su	<i>Beauveria bassiana</i>	2004	Soil (grassland)	Madrid (Spain)	-
EABb 07/06-Rf	<i>Beauveria bassiana</i>	2007	<i>Rhynchophorus ferrugineus</i> (Coleoptera: Curculionidae)	Alicante (Spain)	+
EABb 09/04-Su	<i>Beauveria bassiana</i>	2009	Soil (oak grove)	Ciudad Real (Spain)	-
EABb 09/06-Su	<i>Beauveria bassiana</i>	2009	Soil (eucalyptus grove)	Ciudad Real (Spain)	-
EABb 09/07-Fil	<i>Beauveria bassiana</i>	2009	Phylloplane (meadow)	Málaga (Spain)	+
EABb 09/11-Su	<i>Beauveria bassiana</i>	2009	Soil (olive grove)	Málaga (Spain)	-
EABb 09/16-Su	<i>Beauveria bassiana</i>	2009	Soil (olive grove)	Málaga (Spain)	-
EABb 09/31-Fil	<i>Beauveria bassiana</i>	2009	Phylloplane (oak grove)	Sevilla (Spain)	-
EABb 09/42-Fil	<i>Beauveria bassiana</i>	2009	Phylloplane (oak grove)	Sevilla (Spain)	-
EABb 10/01-Fil	<i>Beauveria bassiana</i>	2010	Phylloplane (olive grove)	Málaga (Spain)	+
EABb 10/103-Fil	<i>Beauveria bassiana</i>	2010	Phylloplane (olive grove)	Córdoba (Spain)	-
EABb 10/108-Su	<i>Beauveria bassiana</i>	2010	Soil (olive grove)	Córdoba (Spain)	-
EABb 10/111-Fil	<i>Beauveria bassiana</i>	2010	Phylloplane (meadow)	Málaga (Spain)	-
EABb 10/118-Fil	<i>Beauveria bassiana</i>	2010	Phylloplane (meadow)	Córdoba (Spain)	-
EABb 10/147-Fil	<i>Beauveria bassiana</i>	2010	Phylloplane (meadow)	Sevilla (Spain)	-
EABb 10/18-Su	<i>Beauveria bassiana</i>	2010	Soil (olive grove)	Córdoba (Spain)	-
EABb 10/27-Fil	<i>Beauveria bassiana</i>	2010	Phylloplane (meadow)	Málaga (Spain)	-
EABb 10/28-Su	<i>Beauveria bassiana</i>	2010	Soil (olive grove)	Córdoba (Spain)	+
EABb 10/30-Fil	<i>Beauveria bassiana</i>	2010	Phylloplane (olive grove)	Córdoba (Spain)	+
EABb 10/57-Fil	<i>Beauveria bassiana</i>	2010	Phylloplane (meadow)	Córdoba (Spain)	+
EABb 10/67-Fil	<i>Beauveria bassiana</i>	2010	Phylloplane (sunflower field)	Córdoba (Spain)	-
EABb 10/78-Fil	<i>Beauveria bassiana</i>	2010	Phylloplane (sunflower field)	Córdoba (Spain)	-
EABb 10/79-Fil	<i>Beauveria bassiana</i>	2010	Phylloplane (meadow)	Córdoba (Spain)	-
EABb 10/80-Fil	<i>Beauveria bassiana</i>	2010	Phylloplane (meadow)	Málaga (Spain)	-
EABpb 10/83-Fil	<i>Beauveria pseudobassiana</i>	2010	Phylloplane (meadow)	Málaga (Spain)	-
EABb 11/01-Mg	<i>Beauveria bassiana</i>	2011	<i>Monochamus galloprovincialis</i> (Coleoptera: Cerambycidae)	Palencia (Spain)	+
EABb 12/03-Pa	<i>Beauveria bassiana</i>	2012	<i>Paysandisia archon</i> (Lepidoptera: Castniidae)	Montpellier (France)	-
EABb 90/2-Dm	<i>Beauveria bassiana</i>	1990	<i>Doclostaurus maroccanus</i> (Orthoptera: Acrididae)	unknown	-

EABb 91/6-Ci	<i>Beauveria bassiana</i>	1991	<i>Calliptamus italicus</i> (Orthoptera: Acridide)	unknown	-
EABb 91/7-Dm	<i>Beauveria bassiana</i>	1991	<i>Dociostaurus maroccanus</i> (Orthoptera: Acrididae)	unknown	-
EABb 92/10-Dm	<i>Beauveria bassiana</i>	1992	<i>Dociostaurus maroccanus</i> (Orthoptera: Acrididae)	unknown	-
EABb 93/14-Tp	<i>Beauveria bassiana</i>	1993	<i>Thaumetopoea pytiocampa</i> (Lepidoptera: Notodontidae)	unknown	-
EABps 10/01-Su	<i>Beauveria pseudobassiana</i>	2010	Soil (oak grove)	Sevilla (Spain)	-
EABps 10/02-Su	<i>Beauveria pseudobassiana</i>	2010	Soil (oak grove)	Sevilla (Spain)	-
EABps 10/03-Su	<i>Beauveria pseudobassiana</i>	2010	Soil (oak grove)	Sevilla (Spain)	-
EABps 10/04-Su	<i>Beauveria pseudobassiana</i>	2010	Soil (oak grove)	Sevilla (Spain)	-
EABv 09/01-Su	<i>Beauveria varroae</i>	2009	Soil (oak grove)	Sevilla (Spain)	-
EABv 09/02-Su	<i>Beauveria varroae</i>	2009	Soil (oak grove)	Sevilla (Spain)	-
EABv 10/01-Su	<i>Beauveria varroae</i>	2010	Soil (oak grove)	Sevilla (Spain)	-
EAI f 10/01-Msp	<i>Isaria farinosa</i>	2010	<i>Monochamus sp.</i>	Palencia (Spain)	-
EALa 11/01-Msp	<i>Lecanicillium attenuatum</i>	2011	<i>Monochamus sp.</i>	Palencia (Spain)	-
EALa 12/01-Pa	<i>Lecanicillium attenuatum</i>	2012	<i>Paysandisia archon</i>	Catania (Italy)	-
EAMa 01/121-Su	<i>Metarhizium anisopliae</i>	2001	Soil (cotton field)	Sevilla (Spain)	-
EAMa 01/152-Su	<i>Metarhizium anisopliae</i>	2001	Soil (cotton field)	Sevilla (Spain)	-
EAMa 01/158-Su	<i>Metarhizium robertsii</i>	2001	Soil (olive grove)	Sevilla (Spain)	-
EAMa 01/58-Su	<i>Metarhizium brunneum</i>	2001	Soil (wheat field)	Córdoba (Spain)	-
EAMa 04/01-Ci	<i>Metarhizium anisopliae</i>	2004	<i>Calliptamus italicus</i>	Tbilisi (Georgia)	-
EAMa 06/01-Ct	<i>Metarhizium anisopliae</i>	2006	<i>Capnodis tenebrionis</i>	Apulia (Italy)	-
EAMa 08/01-Rf	<i>Metarhizium anisopliae</i>	2008	<i>Rhynchophorus ferrugineus</i>	Maglie (Italy)	-
EAMa 08/02-Rf	<i>Metarhizium anisopliae</i>	2008	<i>Rhynchophorus ferrugineus</i>	Brindisi (Italy)	-
EAMa 10/02-Fil	<i>Metarhizium anisopliae</i>	2010	Phylloplane (meadow)	Córdoba (Spain)	-
EAMa 10/05-Su	<i>Metarhizium guizhouense</i>	2010	Soil (olive grove)	Córdoba (Spain)	-
EAMa 10/06-Su	<i>Metarhizium guizhouense</i>	2010	Soil (olive grove)	Córdoba (Spain)	-
EAMb 09/01-Su	<i>Metarhizium brunneum</i>	2009	Soil (oak grove)	Sevilla (Spain)	-
EAMr 09/01-Su	<i>Metarhizium robertsii</i>	2009	Soil (oak grove)	Sevilla (Spain)	-
EAPI 10/01-Fil	<i>Purpureocillium lilacinum</i>	2010	Phylloplane (meadow)	Córdoba (Spain)	-
EAPI 10/01-Su	<i>Paecilomyces marquandii</i>	2010	Soil (olive grove)	Málaga (Spain)	-
EAPI 10/02-Fil	<i>Purpureocillium lilacinum</i>	2010	Phylloplane (meadow)	Córdoba (Spain)	-
EAPI 10/13-Su	<i>Purpureocillium lilacinum</i>	2010	Soil (olive grove)	Córdoba (Spain)	-
EAPI 10/14-Su	<i>Purpureocillium lilacinum</i>	2010	Soil (olive grove)	Córdoba (Spain)	-
EAPI 10/16-Su	<i>Purpureocillium lilacinum</i>	2010	Soil (olive grove)	Málaga (Spain)	-
EAPI 16/01-Su	<i>Purpureocillium lilacinum</i>	2016	Soil (sunflower field)	Córdoba (Spain)	-
EAPI 16/02-Su	<i>Purpureocillium lilacinum</i>	2016	Soil (sunflower field)	Cadiz (Spain)	-

EAPI 16/03-Su	<i>Purpureocillium lilacinum</i>	2016	Soil (sunflower field)	Sevilla (Spain)	-
KVL12-28	<i>Metarhizium flavoviride</i>	2009	Soil; baited with <i>Tenebrio molitor</i>	Denmark	-
KVL12-29	<i>Metarhizium majus</i>	2009	Soil; baited with <i>Tenebrio molitor</i>	Denmark	-
KVL12-30	<i>Metarhizium brunneum</i>	2009	Soil; baited with <i>Tenebrio molitor</i>	Denmark	-
KVL12-32	<i>Metarhizium robertsii</i>	2009	Soil; baited with <i>Tenebrio molitor</i>	Denmark	-
KVL12-35	<i>Metarhizium robertsii</i>	2009	Soil; baited with <i>Tenebrio molitor</i>	Denmark	-
KVL12-36	<i>Metarhizium robertsii</i>	2009	Soil; baited with <i>Tenebrio molitor</i>	Denmark	-
KVL12-37	<i>Metarhizium brunneum</i>	2009	Soil; baited with <i>Tenebrio molitor</i>	Denmark	-
KVL03-122	<i>Beauveria bassiana</i>	2002	Fly <i>Pegoplata aestiva</i> (Diptera: Anthomyiidae)	Denmark	-
KVL03-144	<i>Beauveria bassiana</i>	2002	Grass bug <i>Leptopterna dolabrata</i> (Hemiptera: Miridae)	Denmark	-

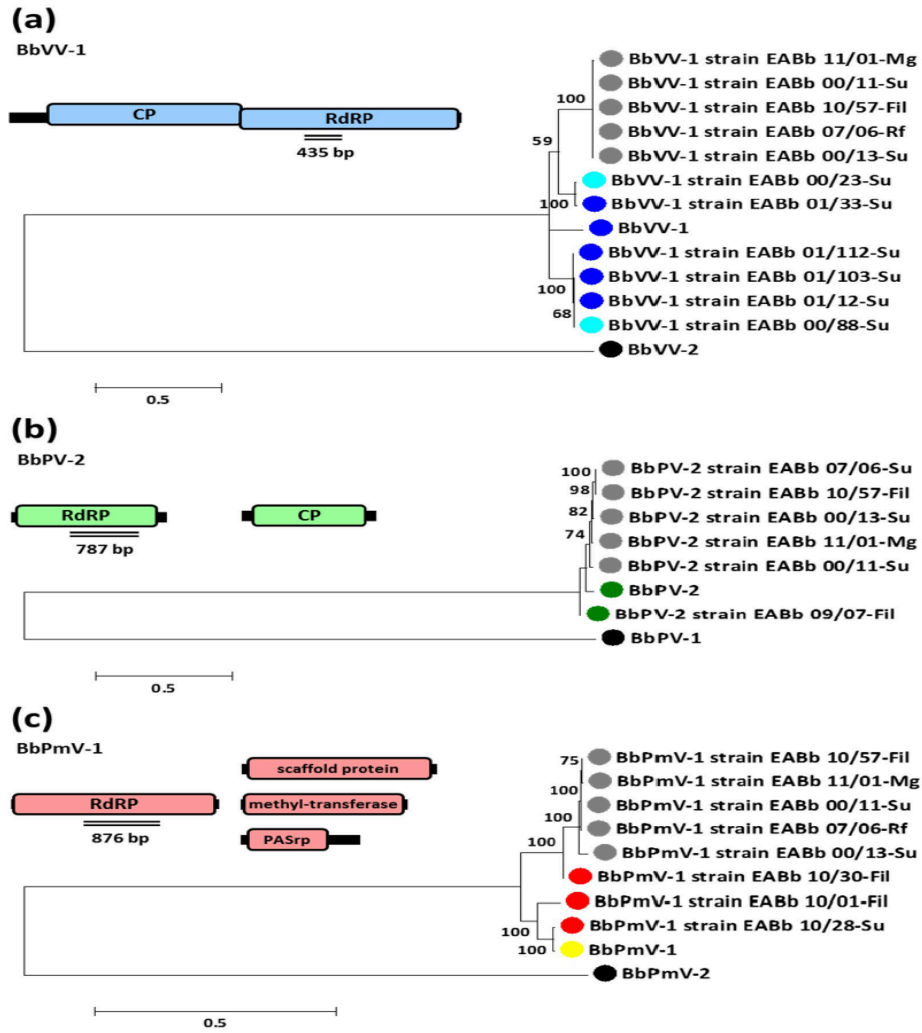


**Figure S3.2.1** Maximum likelihood phylogenetic trees created based on the alignment of RdRP sequences of (a) members of the family *Partitiviridae*, (b) members of the family *Totiviridae* and (c) the proposed family *Polymycoviridae* infecting *Beauveria bassiana*. At the end of the branches: grey circles indicate that the *Beauveria bassiana* isolate is infected with all three BbPV-2-like, BbVV-1-like, and BbPmV-1-like viruses; single infections of *Beauveria bassiana* isolate are indicated by blue circles for BbVV-1-like virus; green circles for BbPV-2-like virus; red circles for BbPmV-1-like virus; turquoise circles for BbVV-1-like virus and a partitivirus; yellow circles indicate that the *Beauveria bassiana* isolate is infected with a BbPmV-1-like virus and a unirnavirus; black circles indicate outgroups. The ORFs and predicted genomic products of representatives of each virus family are shown on the left-hand side of the figure. Taken from Filippou *et al.* (2018).

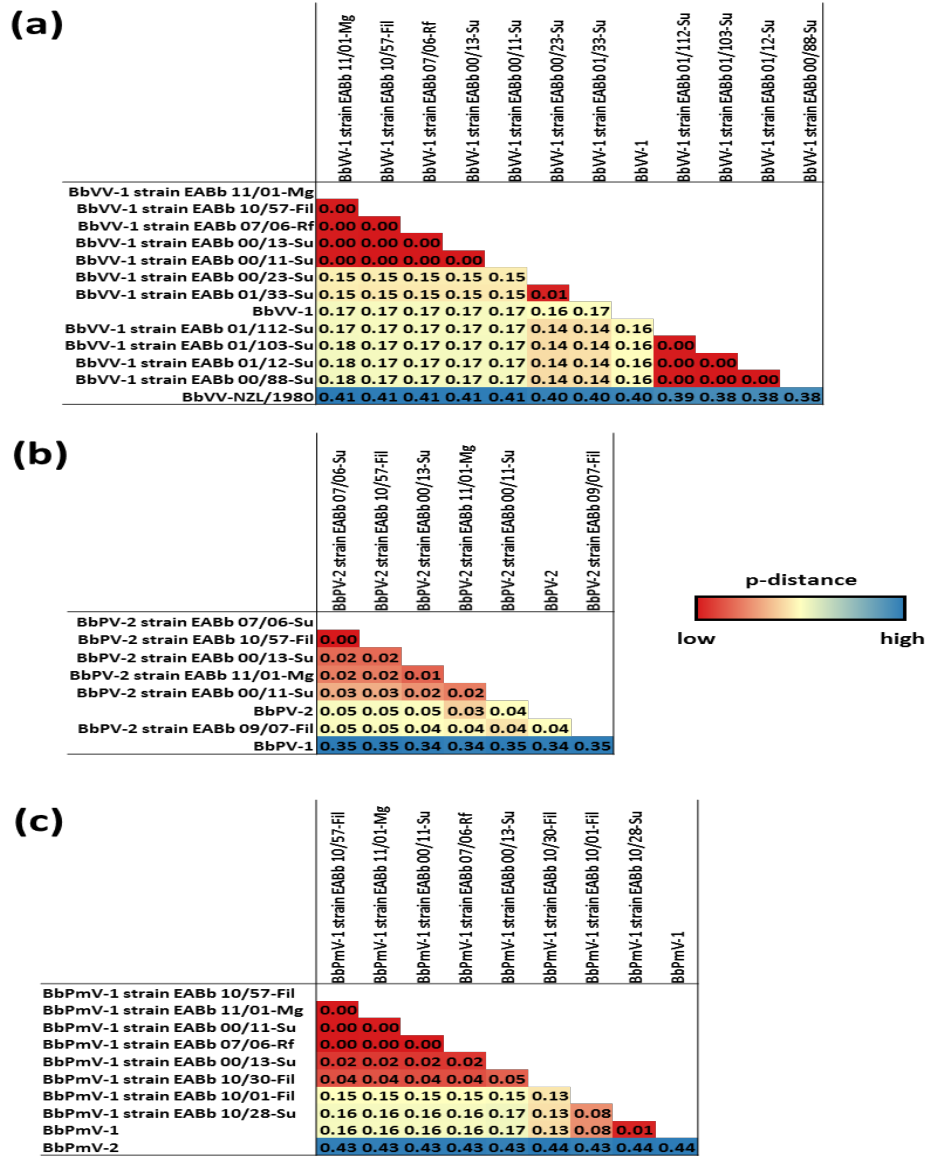


**Figure S3.2.2** Pairwise distance matrix created based on the RdRP sequences of chrysovirus and related viruses; **(a)** members of the family *Partitiviridae*, **(b)** members of the family *Totiviridae* and **(c)** members of the proposed family *Polymycoviridae* infecting *Beauveria bassiana*. Taken from Filippou *et al.* (2018).

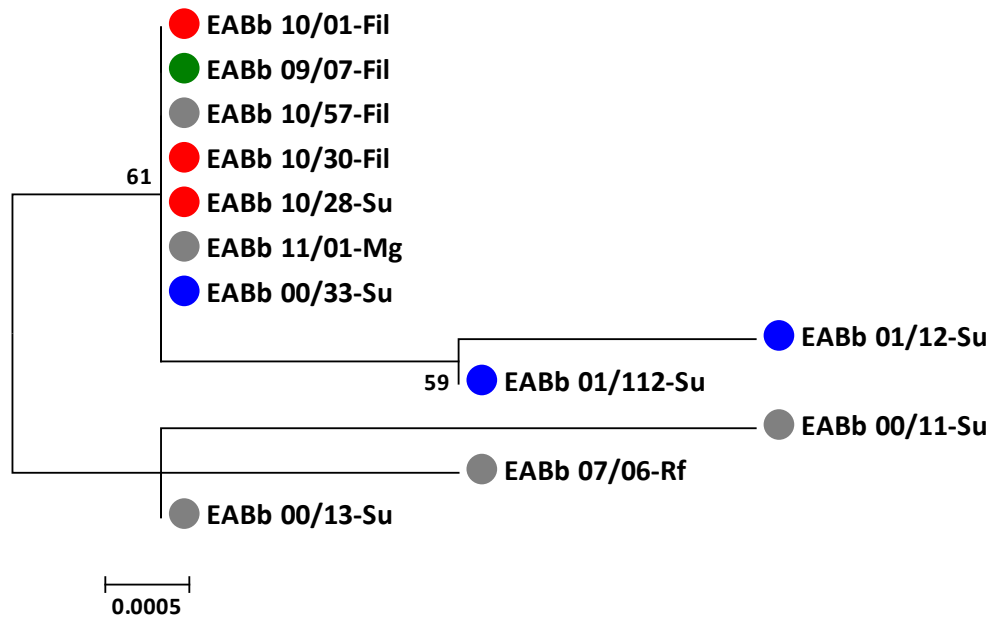


**Figure S3.2.3** Maximum likelihood phylogenetic tree created based on the alignment of ITS sequences of the twelve mycovirus infected *Beauveria bassiana* isolates. At the end of the branches: grey circles indicate that the *Beauveria bassiana* isolate is infected with all three BbPV-2-like, BbVV-1-like and BbPmV-1-like viruses; blue circles indicate that the *Beauveria bassiana* isolate is exclusively infected with a BbVV-1-like virus; green circles indicate that the *Beauveria bassiana* isolate is exclusively infected with a BbPV-2-like virus; red circles indicate that the *Beauveria bassiana* isolate is exclusively infected with a BbPmV-1-like virus. Taken from Filippou *et al.* (2018).

**Table S3.3.7** Primers used in qPCR experiments for LmV-1 together with the targeted sequence name, amplicon size, Slope, Y-intercept and Efficiency.

Primer name	Primer sequence	Target of the primer pair	Amplicon size	Slope	Y-intercept	Efficiency (Eff%)
Lbtub.F1	5'- AATTGGTGCTGCTTTCTGGC -3'	Housekeeping gene ( $\beta$ -tubulin)	231bp	-3.3595	18.488	98.5%
Lbtub.R2	5'- TTGTTGCCGGAAGCCTAGAG-3'					
*qPCR.LV.F	5'- CAATGTTTGTCCCGGATGGC-3'	<i>L. muscarium</i> Virus	155bp	-3.374	38.288	97.87%
*qPCR.LV.R	5'- CGTGAAAGGTCCCCTCGAAA-3'			-3.2983	18.366	101%

\* Primer pair used to determine the relative RNA levels of the positive and negative strands of LmV-1 as well as to determine the biomass production of *Lecanicillium muscarium* isolate 143.62 over the course of 7 days **(In white)**.

**Characterisation of *Beauveria bassiana* polymycovirus-3 dsRNA5 and dsRNA6 (RLM-RACE)**

**Table S3.4.2a:** Primers for obtaining the 5' terminal sequence of BbPmV-3 dsRNA5

BbPmV-3.R5	5'-GCATCGCGACCAACGCGCAC-3'
LIG FOR	5'-CCGCTCTAGAACTAGTTGGATC-3'

**Table S3.4.2b:** Primers for obtaining 3' terminal sequence of BbPmV-3 dsRNA5

LIG FOR	5'-CCGCTCTAGAACTAGTTGGATC-3'
BbPmV-3.F5	5'-GTGGTCCCGTCTTTGGCCGG-3'

**Table S3.4.5a:** Primers for obtaining the 5' terminal sequence of BbPmV-3 dsRNA6

BbPmV-3.R6	5'-CGCCTCGTGCGTGTCATGG-3'
LIG FOR	5'-CCGCTCTAGAACTAGTTGGATC-3'

**Table S3.4.5b:** Primers for obtaining 3' terminal sequence of BbPmV-3 dsRNA6

LIG FOR	5'-CCGCTCTAGAACTAGTTGGATC-3'
BbPmV-3.F6	5'-GTGGATGAGGCAGTGGCAAC-3'

**Figure S3.4.2** Characterisation of BbPmV-3 dsRNA5 using genome walking technique

**>dsRNA 5**

[T/C]GAACTCAAGCGTTTTTCTTCAACAAGCCGGCCCGTACGACCCGGGCTTTACGCATTAGTTACCAACGTGTCACATAAAATCAAACGA  
CGTGCACCTGATTGCGATGCCTTTCTAGGTAAGTCACTTGCCCCCTGCCGTCGCCAACGTGCGCGTTGGTCGCGATGCTCTTGCCCTTAC  
CGTTCGTCCCAATCCAGTGAGTTCACTGGTGCGAACGGCGTACCCGGGAGTGGGTGCGCGCTTGTCCCGCTGACGGTCCGTGG  
CCGGACCCGCAATTTAACCTGCGTTTTTCGGCTTACGGATTGGGCAGTCGAGCAGCTGCCTGCCGAGCAGAGAGAGATAGCGTGCGAT  
GTTGACGTGGTTTATTACCCCGTCTTCTTGGCGCTCGGGTCATACTCTGCCCTCGATCTGGGCCCGGCTTGTACTGGCTGTTTATTGAC  
GGCCTTGACCCCTGGTTATCCATCCGCGTGCACGCTGATTGACGCCGGTCTCGGCGCGGGTGCCGTTCTGTCTTCATTGACCGGGT  
GTCAGTTCGAACTGGCCCCGACCTTTACTTCTCGCTGTTGAGGCAGCTGAGTTGGGGTCCGCTGGTCCCGTCTTTGGCCGGTAACTT  
GAGTTCAGCCCCTTGTTTTGTGTTTGTGTTGAGGCGTGAACACCCCGAGGGTGGTCCGTCGTTGATGTGTTGGCTATCGAGGGC  
TGCTGCCCCGGGTTCCAGTAGTGCATAACCCGGCTCTCAGTCTACGCCAACCCAGTTACGGTTTATGCGCGTGGTTGATGCTCTG  
AGTGGTTGCTCCTCGTGTGTTGCCCCGCTGCCTAACCCGAGTATGGGATAAGCGTCACGGGCCATGAGACCGCGAAGGTGGCGTT  
GGTTTGGCGCCAGAAGCGGGGGCTCAATTTGTTCCCCCGTCCATGACTTT

**Steps:**

1. FROUSARD method yielded an amplicon between yellow highlighted sequence and green equal to 336 bp.
2. Yellow highlighted sequence was reversed complement into reverse primer and together with LIG For. were used to obtain the 5' terminal sequence of BbPmV-3 dsRNA5
3. Green highlighted sequence was used as forward primer and together with LIG For. amplified a region of 155 bp up to blue highlighted sequence.
4. Blue highlighted sequence was used as forward primer and together with LIG For. used to obtain the 3' terminal and complete the sequence of BbPmV-3 dsRNA5.

ATG codon codes for Methionine start codon and TAA codes for a stop codon.

**Figure S3.4.4** Characterisation of BbPmV-3 dsRNA6 using genome walking technique

**>dsRNA 6**

[T/C]GAAATCAAGAGTTCTTCTACGCAAGCACTGCCTTGCAGTAGGTATCTGGTACTTATTGACCATTTTTCTATTCGCAAGACCTTCTAAGCTCG  
CTAGTACTGATGTCGGAGGCATCCTCTTTTGTATGACCCGGAGCAGCAGCCGCCAGTCCAAGGGTTGCAGAGTGGGCCGCTGACGCACGCCGTG  
CGTCGGGGCCGGTCGATCGTAGTGGTATTGGTCCGGTGTGTACCCACCCAGCACCGTGGCGTCTGCTGTTCCGTGCCATGACACGCACGAG  
GCGACGCCAGTCTCCTCCTGCGACCGTCGTTGACGGTAGTGATGGTGAGGAAAGTGTTCCTGAAGACGCCGATCCCTTCCCCGTACGTTTC  
TCGGCAGGCGCTCGGCCTGGTGATAGCGTATCTCTAACGGCAATAGGCGGATGGGGTCCGCTGGGACGACCGTTCTACAGTGAGTCTCACC  
GACTCGACCGTAGACCGTTGGCCGTGCGGATCGCTGACCTAACGTTGGTCCCGCAAACCGTCGCCGTTGGTTCCCACTGTGGATGAGG  
CAGTGGCAACTACCGCGCGCCACAGGCGCCCTCGTCTGAGCTCAATCAGCGAGAGGCCGGCTGTTGGCGTGTGGCGGCTTTGGTTTTCGGGAC  
CAAGGATAGTCTACGACAAACAACGCCACGTAAGTACTGCGAGCAAGACGACGCGGGCATAGCCCGCCTTGCCTCCCTGGATGTGGGGGCCTT  
TGATGCCCATCCTAGCCATGAAGATAGTCCAACCCGGGTTTTCCCGGCCGCGGAATTTTTCTCGCTTCGGATCATGATTCTTAGTCCCTTTCC  
AGTTGAATTTT

**Steps:**

1. FROUSARD method yielded an amplicon between yellow highlighted sequence and green equal to 500 bp.
2. Blue highlighted sequence was reversed complement into reverse primer and together with LIG For. were used to obtain the 5' terminal sequence of BbPmV-3 dsRNA6.
3. Red highlighted sequence was used as forward primer and together with LIG For. used to obtain the 3' terminal and complete the sequence of BbPmV-3 dsRNA6.

ATG codon codes for Methionine start codon and TAG codes for a stop codon.

### 3.4.4 Construction of cDNA clones of BbPmV-3 dsRNA6 using rPCR amplification.

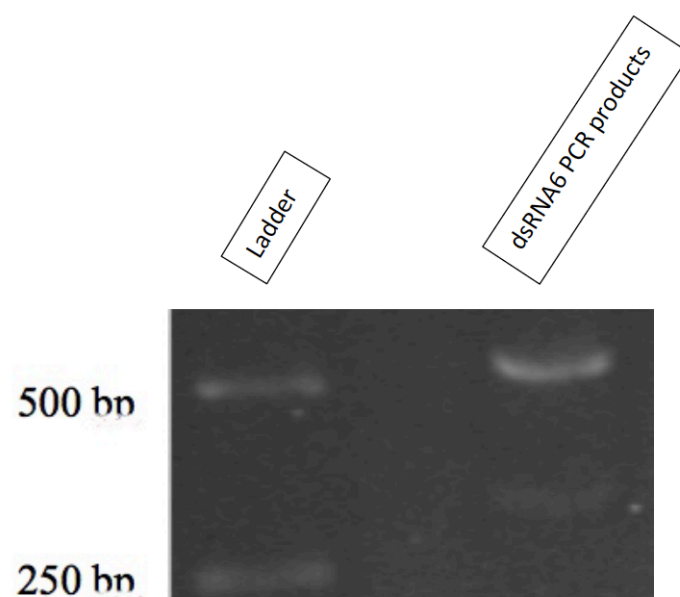


**Figure S3.4.4:** Agarose gel electrophoresis showing the PCR products generated by random primed PCR method (rPCR) with Froussard primers using BbPmV-3 dsRNA6 as a template. GeneRuler 1 kb DNA Ladder (Promega) was used as marker.

### 3.4.7 Sequence analysis of the remaining 4 dsRNAs of BbPmV-3

**Table S3.4.7:** Properties of BbPmV-3.

Segment	Length (bp)	ORF size			UTR length (bp)	
		(nt)	(aa)	(kDa)	5'-UTR	3'-UTR
dsRNA 1	2,401	2,304	767	83	26	71
dsRNA 2	2,240	2,094	697	74	70	90
dsRNA 3	1,989	1,848	615	66	51	90
dsRNA 4	1,131	807	268	29	110	214
dsRNA 5	937	513	170	18	101	323
dsRNA 6	865	618	205	22	104	143

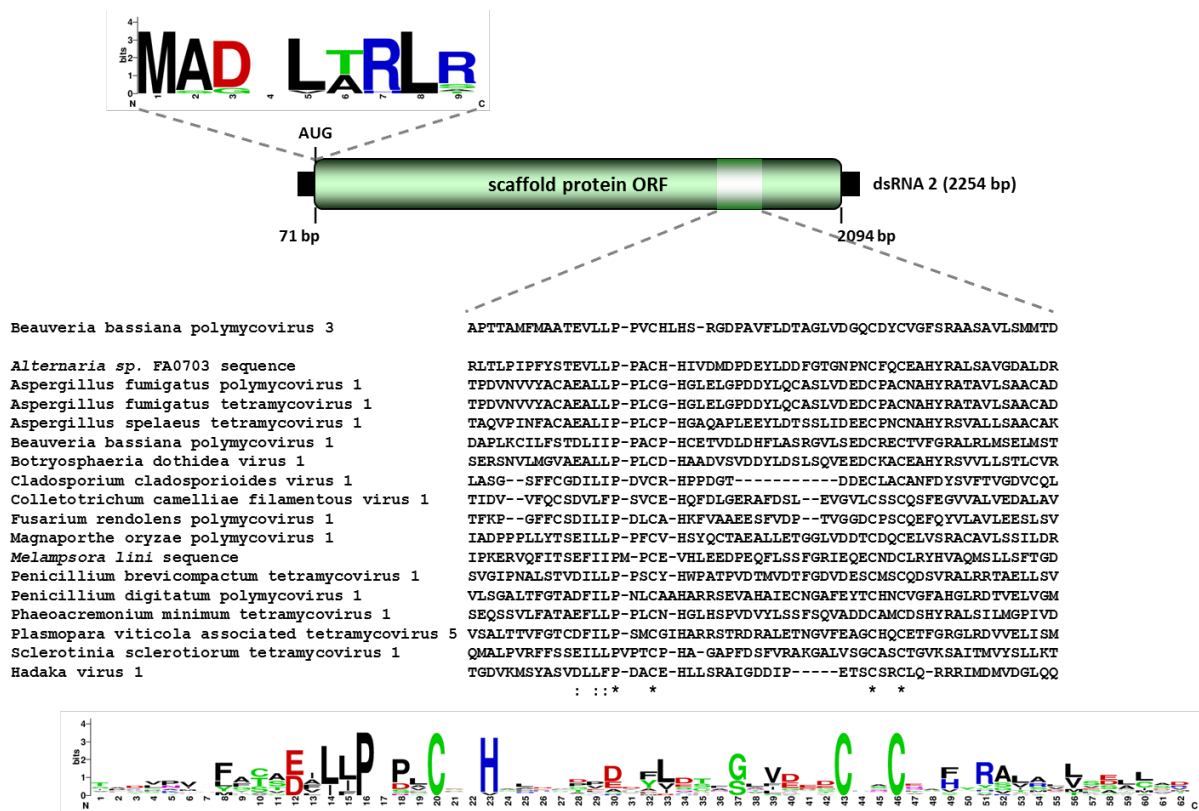


**Figure S3.4.7a** Schematic representation of BbPmV-3 dsRNA2, encoding a putative scaffold protein whose ORF (dark green coloured box) is flanked by 5'- and 3'-UTRs (black boxes). The light green coloured box represents the cysteine-rich zinc finger, and a multiple alignment of all known polmycoviruses and related viruses illustrates the conserved cysteine and proline residues. Sequence logos for the conserved N-terminus and the cysteine-rich zinc finger of the putative scaffold protein were also generated. Taken from Filippou *et al.* (2021).

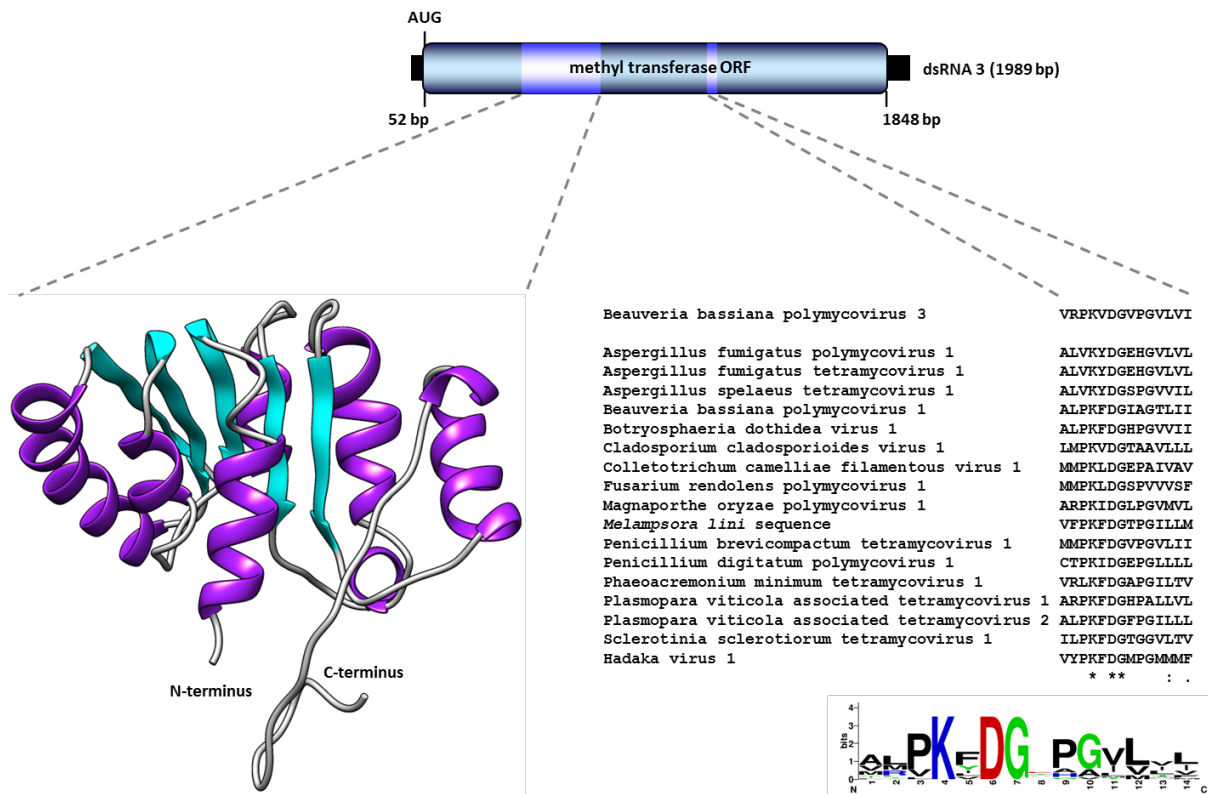


**Figure S3.4.7b:** Schematic representation of BbPmV-3 dsRNA3, encoding a methyltransferase whose ORF (dark blue coloured box) is flanked by 5'- and 3'-UTRs (black boxes). The light blue-coloured boxes represent the methyltransf\_25 protein family and the methyltransferase catalytic motif. The structure of Rossmann fold domain where the methyltransferase cofactor binds is visualised. A multiple alignment of all known polynucleotides and related viruses illustrates the conserved catalytic residues of the methyltransferase, for which a sequence logo was also generated. Taken from Filippou *et al.* (2021).

### 3.4.9 Phylogenetic analysis of the putative BbPmV-3 RdRP gene

✓ Query_10001	448	DAANSL---[2	GDDVYFGVH	TY[1]-R[1]-GEVSR	TLKTSQLRMNPI	KQS--VGHLS	TEFLRNC-SSGRATR	508
✓ Query_10002	383	VEIRNLRVL	GDDSAFRSG	DQ	FD	LDVAKGDAEPTQMLVNTD	KSG--KSKDPADFKLLG-TTYRCGR	444
✓ Query_10003	750	LYGVSVAIM[4	GDDIVLGLS	DP[1]-Y[1]-PQFLET	MSMLFKANKW	KQM--FG-VRSEFFRNT-ITDGS	SMY	814
✓ Query_10004	380	VEPKDLRVL	GDDSAFRSC	AD	LD	LGQAERDAKDVNMVLHPE	KCD--VKTDPTKMKLLG-TTYRNGH	441
✓ Query_10005	380	LEIRNLKVL	GDDSAFRST	DQ	FD	LEVAKDCVPTGMVIKPE	KCE--RTEDPNDFKLLG-TKYRDGR	441
✓ Query_10006	380	VKIPKPEVL	GDDSAFRSN	DQ	FD	LEVAKDCVPTGMVIRPE	KCE--KTEDPAEFKLLG-TKYRSGR	441
✓ Query_10007	361	VNAKNLRVL	GDDSAFMAA	ET	MD	LSVAEDAAGVMDLSDE	KSI--SVEDATELKLKLLG-VRYRDGH	422
✓ Query_10008	381	VEARGLRVL	GDDSAFRSP	VE	FS	LEQAQSDCEPTGMILKPE	KCE--KTEDPSDFKLLG-TTYRGCH	442
✓ Query_10009	380	VEIRLKVVL	GDDSAFVSG	KD	FS	FSQATADCIPTGMVLKPE	KCD--VTDNPSEFKLLG-VKYRDGR	441
✓ Query_10010	366	-NARRFRVL	GDDSSFLIP[3]SK[1]-D[1]VEISEKAWETFGFTLKL-				-KKlrIANKQQDRKFLG---YQCNA	428
✓ Query_10011	380	CEIRALRVL	GDDSAFRSC	DP	FS	LDLASHDAECVNMILHPE	KCE--KTDPAPFKLLG-TTYRNGR	441
✓ Query_10012	381	VEIRNLKVL	GDDSAFRSS	DE	FQ	LETAKLDCKPTGMVIKPE	KCE--KTADPAEFKLLG-TKYRSGH	442
✓ Query_10013	380	VEIRNLKVL	GDDSAFRAD	DS	FS	LAVAERDSSAVGMVHHPD	KCE--KTLNPSEFKLLG-TVYIDGH	441
✓ Query_10014	380	VEIRNLKVL	GDDSAFRAG	DQ	FD	LELAQTDCDVMGMVLRPE	KCD--KSKDPCDFKLLG-VKYRNGH	441
✓ Query_10015	425	PLHCIKVKQ	GDDSILRLT[5]DQ[4]MD[1]--IVRLADTYFNSIVNVK				KSE--VRNSLNGCEVLS-YRNHNGL	494
✓ Query_10016	468	IKQLLVFIM	GDDNVIFTP[6]IE[1]FD[1]--FAKYTLDRFGMVINIS				KSA--VTSIRRKIEVLG-YTNNYGF	535
✓ Query_10017	346	-PPQQCHTL	GDDSLVGDN	--[2]VN[1]-QAIIEAANKLGWHFNPD			KTQ--YSTVPEEITFLG-RTYVGG	406
✓ Query_10018	380	VEIRNLRVL	GDDSAFRSS	NQ	FD	LEVAKQDCVPTGMVIKPE	KCE--RSEDPSEFKLLG-TKYRGGH	441
✓ Query_10019	380	VEIRNLRVL	GDDSAFCSG	GQ	FD	LELAKGCENTGMVIKPE	KCE--RTKDPGEFKLLG-TTYRGGH	441
✓ Query_10020	383	VEIRNLRVL	GDDSAFRSG	DQ	FD	LDVAKGDAEPTQMLVNTD	KSG--KSKDPADFKLLG-TTYRCGR	444
✓ Query_10021	718	TRNTRTKIL[2	GDNQVLCPT[3]SP[4]EG[4]LESISRNALSIYRAIEEG[8]KKE--ETMCSYDFLIYgkTPLFRGN					801
✓ Query_10022	530	RHHIRDRL[2	GDNQLFSSA[2]KV[4]YD[1]-QKHAEFLSRFGMKLKID				ETE--VTRHIGRVRFCsrAVVMTPH	600
✓ Query_10023	515	DSLSSL---[2	GDDVYIRAN	TL[1]-D[1]-DYILNRCRDYGCRLNPA			KQS--VGYYGAEFLRVA-IRGERAY	575

**Figure S3.4.9** Amino acid sequence alignment of RdRP regions of BbPmV-3 dsRNA1 and 21 mycoviruses belonging to the families *Partitiviridae*, *Totiviridae* and *Chrysoviridae* plus the animal rabies virus. The alignment was generated using the NCBI Cobalt multiple alignment tool. The GDD motifs are highlighted and the GDNQ motif in both the rabies virus and BbPmV-3 are circled in green. Accession numbers of RNA viruses used for the multiple sequence alignment analysis above can be found in Appendix Part B Table S3.4.9.

Virus	Abbreviation	Run Accession #
Aspergillus mycovirus 178	AsV178	Query_10001
Aspergillus fumigatus Partitivirus – 1	AfuPV-1	Query_10002
Aspergillus fumigatus chrysovirus	AfuCV	Query_10003
Aspergillus ochraceus virus	AoV	Query_10004
Discula destructiva virus 1	DdV-1	Query_10005
Discula destructiva virus 1	DdV-2	Query_10006
Fusarium solani virus 1	FsV1	Query_10007
Gremmeniella abietina virus MS1	GaV-. MS1	Query_10008
Ophiostoma partitivirus-1	OPV-1	Query_10009
Penicillium stoloniferum Virus S	PsV-S	Query_10010
Penicillium stoloniferum Virus F	PsV-F	Query_10011
Botryotinia fuckeliana partitivirus 1	BfPV1	Query_10012
Beauveria bassiana Partitivirus 1	BbPV-1	Query_10013
Beauveria bassiana Partitivirus 2	BbPV-2	Query_10014
White clover cryptic virus 1	WCCV1	Query_10015
Atkinsonella hypoxylon partitivirus	AhPV	Query_10016
Penicillium chrysogenum virus -1	PcV-1	Query_10017
Ustilaginoidea virens partitivirus	UvPV	Query_10018
Verticillium dahliae partitivirus 1	VdPV-1	Query_10019
Rabies lyssavirus	RABV	Query_10020
Beuaveria bassiana Polymycovirus -3	BbPmV-3	Query_10021
Aspergillus foetidus slow virus -1	AfV-slow-1	Query_10022

**Table S3.4.9** Run Accession numbers of RNA viruses used for the multiple sequence alignment analysis in Appendix Part B Figure S3.4.9.

#### 4.1.2 Cycloheximide curing of BbPmV-3 from the *Beauveria bassiana* ATHUM 4946 isolate

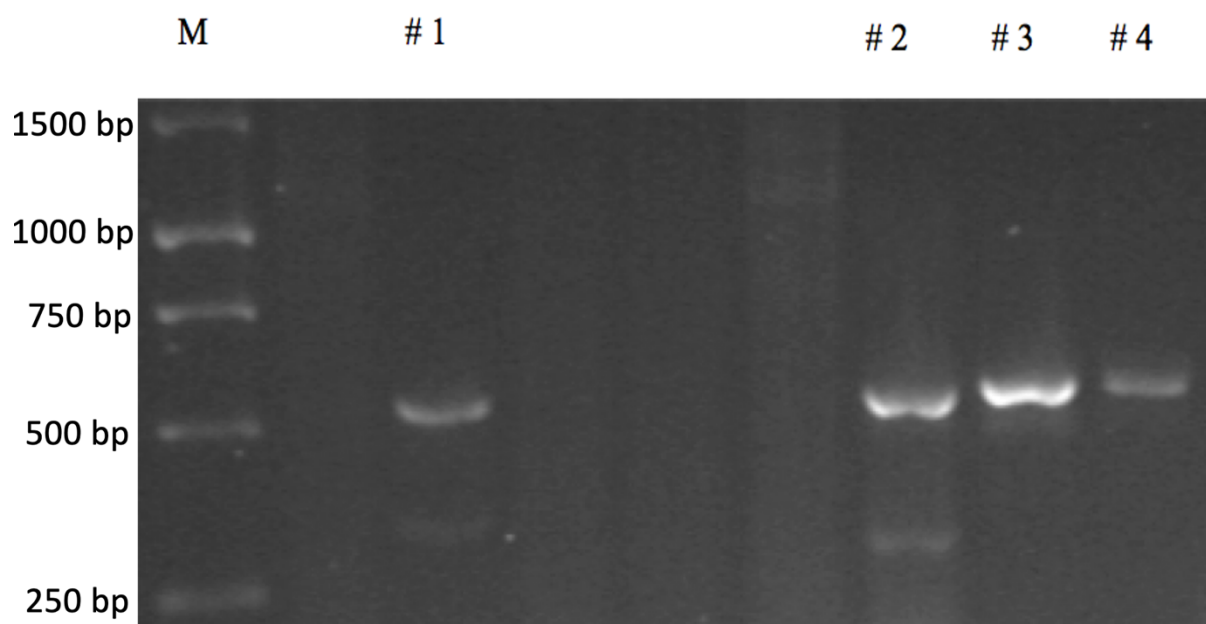


**Figure S4.1.1:** Genomic DNA extraction followed by PCR amplification of ITS (18S and 25S rRNA) sequences of *Beauveria bassiana* ATHUM 4946 virus-free (VF) and virus-infected (VI) isolates, using specific oligonucleotide primers to confirm their authenticity as isogenic lines. Lane M contains the GeneRuler 1 kb DNA Ladder (Promega), the sizes of which are shown to the left of the gel. Amplicons generated from the VI (lanes 1 and 2) and VF (lanes 3 and 4) isogenic lines of *Beauveria bassiana* ATHUM 4946 VI are shown.



Consensus	ACTCCAAACCCAAATGTGAACATACCAATCGTTGCTTCGGCGGACTCGTCCCAGCGT	60
LmusVI	ACTCCAAACCCAAATGTGAACATACCAATCGTTGCTTCGGCGGACTCGTCCCAGCGTCC	60
LmusVF	ACTCCAAACCCAAATGTGAACATACCAATCGTTGCTTCGGCGGACTCGTCCCAGCGTCC	60
Consensus	GGTGGCCTTGCGCCGCCCGGGCTGGAACAGGCGACCGCGGAGGCATTCAAAC	120
LmusVI	GGTGGCCTTGCGCCGCCCGGGCTGGAACAGGCGACCGCGGAGGCATTCAAAC	120
LmusVF	GGTGGCCTTGCGCCGCCCGGGCTGGAACAGGCGACCGCGGAGGCATTCAAAC	120
Consensus	TTTGATTACCAGTATCTTCTGAATCCGCCGAAGGCAAAACAAATGAATCAAAC	180
LmusVI	TTTGATTACCAGTATCTTCTGAATCCGCCGAAGGCAAAACAAATGAATCAAAC	180
LmusVF	TTTGATTACCAGTATCTTCTGAATCCGCCGAAGGCAAAACAAATGAATCAAAC	180
Consensus	AACAACGGATCTCTGGTCTGGCATCGATGAAGAACGACGCGAAATGCGATAAGTAA	240
LmusVI	AACAACGGATCTCTGGTCTGGCATCGATGAAGAACGACGCGAAATGCGATAAGTAA	240
LmusVF	AACAACGGATCTCTGGTCTGGCATCGATGAAGAACGACGCGAAATGCGATAAGTAA	240
Consensus	TGAATTGCAGAAATCAGTGAATCATCGAATCTTGAACGCACATTGCGCCCGCAGCA	300
LmusVI	TGAATTGCAGAAATCAGTGAATCATCGAATCTTGAACGCACATTGCGCCCGCAGCA	300
LmusVF	TGAATTGCAGAAATCAGTGAATCATCGAATCTTGAACGCACATTGCGCCCGCAGCA	300
Consensus	CTGGCGGGCATGCCTGTTGAGCGTCATTTCAACCTCGAGCTCCCCTTGGGAGCCG	360
LmusVI	CTGGCGGGCATGCCTGTTGAGCGTCATTTCAACCTCGAGCTCCCCTTGGGAGCCG	360
LmusVF	CTGGCGGGCATGCCTGTTGAGCGTCATTTCAACCTCGAGCTCCCCTTGGGAGCCG	360
Consensus	CGTTGGGACCGGCTCTACCGCCGACCCGAAATACAGTGGCGGCCCGTCAACGGGAC	420
LmusVI	CGTTGGGACCGGCTCTACCGCCGACCCGAAATACAGTGGCGGCCCGTCAACGGGAC	420
LmusVF	CGTTGGGACCGGCTCTACCGCCGACCCGAAATACAGTGGCGGCCCGTCAACGGGAC	420
Consensus	CTCTGCGTAGTAACTCAACCTCGCACCGGAAACCCGACGTGGCCACGCGTAAACAC	480
LmusVI	CTCTGCGTAGTAACTCAACCTCGCACCGGAAACCCGACGTGGCCACGCGTAAACAC	480
LmusVF	CTCTGCGTAGTAACTCAACCTCGCACCGGAAACCCGACGTGGCCACGCGTAAACAC	480
Consensus	CACTTCTGAACGTTGACCTCGGATCAGGTAGGAATACCCGCTGAACCTAAGCATATCA	540
LmusVI	CACTTCTGAACGTTGACCTCGGATCAGGTAGGAATACCCGCTGAACCTAAGCATATCA	540
LmusVF	CACTTCTGAACGTTGACCTCGGATCAGGTAGGAATACCCGCTGAACCTAAGCATATCA	540
Consensus	AAGCGGAGGAAAGAAACCAACAGGGATTGCCAGTAAACGGGAGTGAAGCGGCAAC	600
LmusVI	AAGCGGAGGAAAGAAACCAACAGGGATTGCCAGTAAACGGGAGTGAAGCGGCAAC	600
LmusVF	AAGCGGAGGAAAGAAACCAACAGGGATTGCCAGTAAACGGGAGTGAAGCGGCAAC	600
Consensus	CTCAAAATTTGAAATCTGGTCCCAGGGCCGAGTTGTAATTTGTAGAGGATGCTTTGG	660
LmusVI	CTCAAAATTTGAAATCTGGTCCCAGGGCCGAGTTGTAATTTGTAGAGGATGCTTTGG	660
LmusVF	CTCAAAATTTGAAATCTGGTCCCAGGGCCGAGTTGTAATTTGTAGAGGATGCTTTGG	660
Consensus	AAGTGCCTTCCGAGTTCCTTGAACGGGACGCCATAGAGGGTGAAGCCCGTCTGGT	720
LmusVI	AAGTGCCTTCCGAGTTCCTTGAACGGGACGCCATAGAGGGTGAAGCCCGTCTGGT	720
LmusVF	AAGTGCCTTCCGAGTTCCTTGAACGGGACGCCATAGAGGGTGAAGCCCGTCTGGT	720
Consensus	GGACCCGAGCCTCTGTAAGCTCCTTGCAGCAGTCGAGTAGTTTGGGAATGCTGCTCAA	780
LmusVI	GGACCCGAGCCTCTGTAAGCTCCTTGCAGCAGTCGAGTAGTTTGGGAATGCTGCTCAA	780
LmusVF	GGACCCGAGCCTCTGTAAGCTCCTTGCAGCAGTCGAGTAGTTTGGGAATGCTGCTCAA	780
Consensus	AATGGGAGGTATATGCTTCTAAAGCTAAATATAGGCCAGAGACCGATAGCGCACAAAG	840
LmusVI	AATGGGAGGTATATGCTTCTAAAGCTAAATATAGGCCAGAGACCGATAGCGCACAAAG	840
LmusVF	AATGGGAGGTATATGCTTCTAAAGCTAAATATAGGCCAGAGACCGATAGCGCACAAAG	840
Consensus	GAGTGATCGAAAGATGAAAAGCACTTTGAAAAGAGGGTTAAAAAGTACGTGAAATTTG	900
LmusVI	GAGTGATCGAAAGATGAAAAGCACTTTGAAAAGAGGGTTAAAAAGTACGTGAAATTTG	900
LmusVF	GAGTGATCGAAAGATGAAAAGCACTTTGAAAAGAGGGTTAAAAAGTACGTGAAATTTG	900
Consensus	AAAGGGAAGCGCCTATGACCAGACTTGAGCCGGTGAATCATCCAGCGTTCTCGCTGG	960
LmusVI	AAAGGGAAGCGCCTATGACCAGACTTGAGCCGGTGAATCATCCAGCGTTCTCGCTGG	960
LmusVF	AAAGGGAAGCGCCTATGACCAGACTTGAGCCGGTGAATCATCCAGCGTTCTCGCTGG	960
Consensus	CACTTTGCCTGGGACAGGCCAGCATCAGTTTGGCGCGGGGATAAAGGCTTTGGGAATG	1020
LmusVI	CACTTTGCCTGGGACAGGCCAGCATCAGTTTGGCGCGGGGATAAAGGCTTTGGGAATG	1020
LmusVF	CACTTTGCCTGGGACAGGCCAGCATCAGTTTGGCGCGGGGATAAAGGCTTTGGGAATG	1020
Consensus	GGCTCCCTCGGGAGTGTATAGCCATTGCGCAATACCCTGCGCCGACTGAGGTACGG	1080
LmusVI	GGCTCCCTCGGGAGTGTATAGCCATTGCGCAATACCCTGCGCCGACTGAGGTACGG	1080
LmusVF	GGCTCCCTCGGGAGTGTATAGCCATTGCGCAATACCCTGCGCCGACTGAGGTACGG	1080
Consensus	CATCGCA	1088
LmusVI	CATCGCA	1088
LmusVF	CATCGCA	1088

**Figure S4.1.2b:** Multiple sequence alignment sequence, using MAFFT alignment of the sequences of ITS amplicons generated from LmV-1 virus-free and LmV-1 virus-infected isolates showing 100% identity. Geneious version 2021.0 created by Biomatters. Available from <https://www.geneious.com>.

**4.1.5 Vegetative growth of virus-infected and virus-free isogenic lines of *Beauveria bassiana* isolates EABb 92/11-Dm and ATHUM 4946 on media containing different carbon and nitrogen sources.**

**Table S4.1.5:** Czapek-Dox MM and variations. Taken from Filippou et al. (2021).

Name	Ingredients													
	carbon source (30 g/l)							nitrogen source (3 g/l)					others	
	sucrose	fructose	glucose	lactose	maltose	trehalose	glycerol	none	NaNO <sub>3</sub>	NaNO <sub>2</sub>	KNO <sub>3</sub>	NH <sub>4</sub> NO <sub>3</sub>		none
														1.0 g/l KH <sub>2</sub> PO <sub>4</sub> 0.5 g/l KCl 0.5 g/l MgCl <sub>2</sub> 0.01 g/l FeSO <sub>4</sub>
MM	+	-	-	-	-	-	-	-	+	-	-	-	-	+
MM[fructose]	-	+	-	-	-	-	-	-	+	-	-	-	-	+
MM[glucose]	-	-	+	-	-	-	-	-	+	-	-	-	-	+
MM[lactose]	-	-	-	+	-	-	-	-	+	-	-	-	-	+
MM[maltose]	-	-	-	-	+	-	-	-	+	-	-	-	-	+
MM[trehalose]	-	-	-	-	-	+	-	-	+	-	-	-	-	+
MM[glycerol]	-	-	-	-	-	-	+	-	+	-	-	-	-	+
MM[C <sup>-</sup> ]	-	-	-	-	-	-	-	+	+	-	-	-	-	+
MM[NaNO <sub>2</sub> ]	+	-	-	-	-	-	-	-	-	+	-	-	-	+
MM[KNO <sub>3</sub> ]	+	-	-	-	-	-	-	-	-	-	+	-	-	+
MM[NH <sub>4</sub> NO <sub>3</sub> ]	+	-	-	-	-	-	-	-	-	-	-	+	-	+
MM[N <sup>-</sup> ]	+	-	-	-	-	-	-	-	-	-	-	-	+	+
MM[C <sup>-</sup> N <sup>-</sup> ]	-	-	-	-	-	-	-	+	-	-	-	-	+	+



**Figure S4.1.5a:** Cultures of ATHUM 4946 BbPmV-3–infected and –free (left) and EABb 92/11-Dm BbPmV-1–infected and –free (right) on Czapek-Dox CM; Czapek-Dox MM; Czapek-Dox MM lacking a carbon source; Czapek-Dox MM lacking a nitrogen source; Czapek-Dox MM lacking both a carbon and a nitrogen source. Taken from Filippou *et al.* (2021).



**Figure S4.1.5b:** Cultures of ATHUM 4946 BbPmV-3–infected and –free (left) and EABb 92/11-Dm BbPmV-1–infected and –free (right) on Czapek-Dox MM containing lactose as a carbon source; Czapek-Dox MM containing maltose as a carbon source; Czapek-Dox MM containing trehalose as a carbon source; Czapek-Dox MM containing fructose as a carbon source; Czapek-Dox MM containing glucose as a carbon source; Czapek-Dox MM containing glycerol as a carbon source. Taken from Filippou *et al.* (2021).

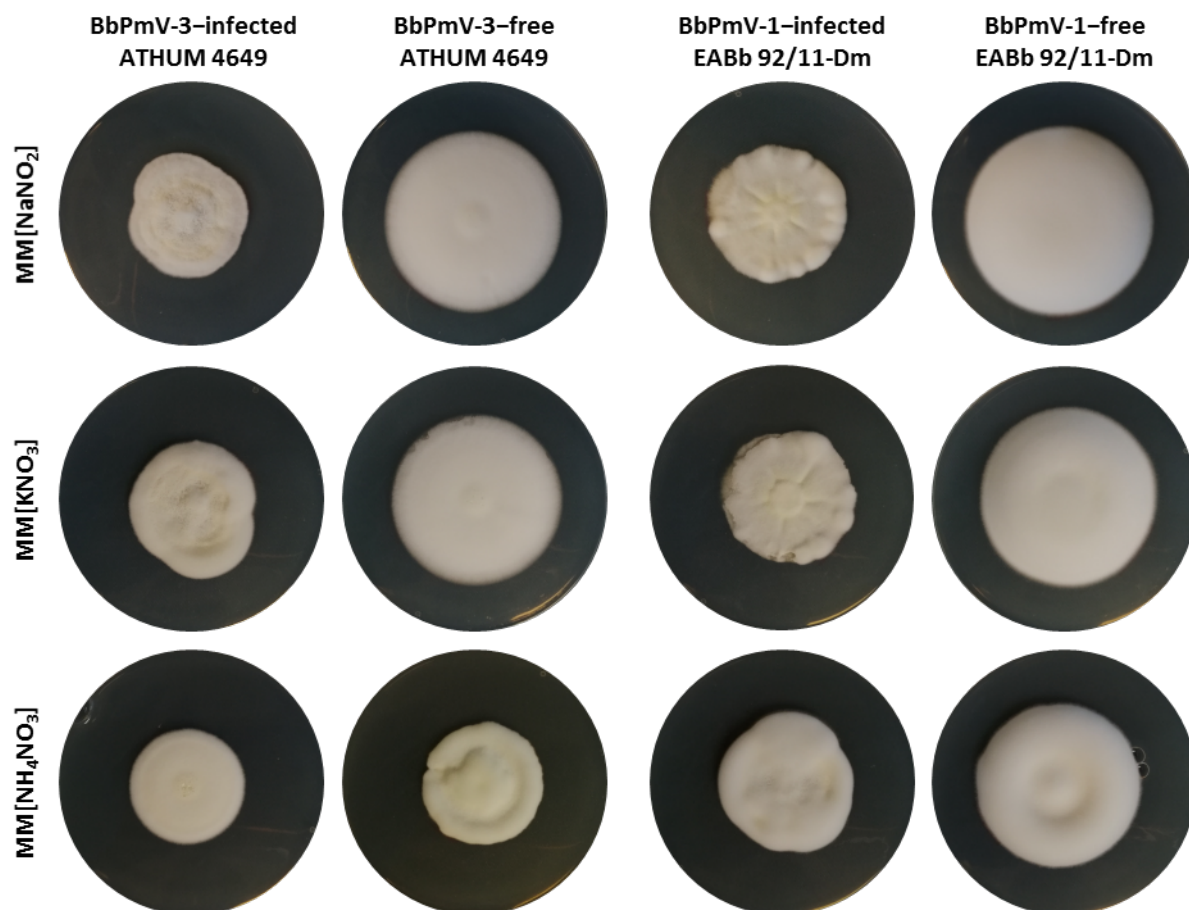


**Figure S4.1.5c:** Cultures of ATHUM 4946 BbPmV-3–infected and –free (left) and EABb 92/11-Dm BbPmV-1–infected and –free (right) on Czapek-Dox MM containing sodium nitrite as a nitrogen source; Czapek-Dox MM containing potassium nitrate as a nitrogen source; Czapek-Dox MM containing ammonium nitrate as a nitrogen source. Taken from Filippou *et al.* (2021).

#### 4.2.2 Injection and spray inoculation of *Tenebrio molitor* - Survival assay

**Table S4.2.2a:**  $LT_{50} \pm SE$  for Spray method

<b>Isolate</b>	<b><math>LT_{50} \pm SE</math></b>
PmV-1.I	4.5 days $\pm$ 0.21
PmV-1.F	5.7 days $\pm$ 0.322
Naturalis	5.3 days $\pm$ 0.26
Botanigard	5.1 days $\pm$ 0.221

**Table S4.2.2b:**  $LT_{50} \pm SE$  for injection method

<b>Isolate</b>	<b><math>LT_{50} \pm SE</math></b>
PmV-1.I	3.5 days $\pm$ 0.2
PmV-1.F	3.9 days $\pm$ 0.28
Naturalis	4.7 days $\pm$ 0.26
Botanigard	3.8 days $\pm$ 0.23

### 4.3.3 GFP expression in *Beauveria bassiana* to study mycovirus replication and localization.

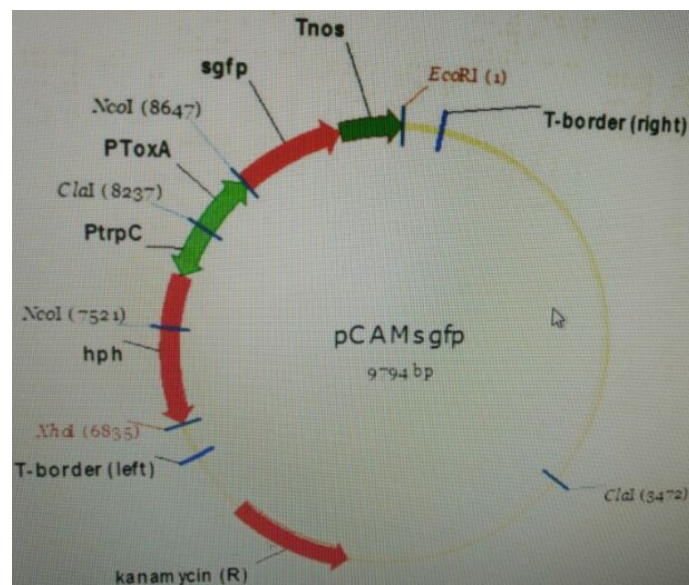


**Figure S4.3.3a:** Plasmid (pCAMsgfp) used for the GFP labeling experiments. It contains a Hygromycin B and Kanamycin A resistance cassette.

### 4.3.5 Isolation of protoplasts for virus transfection and GFP expression.

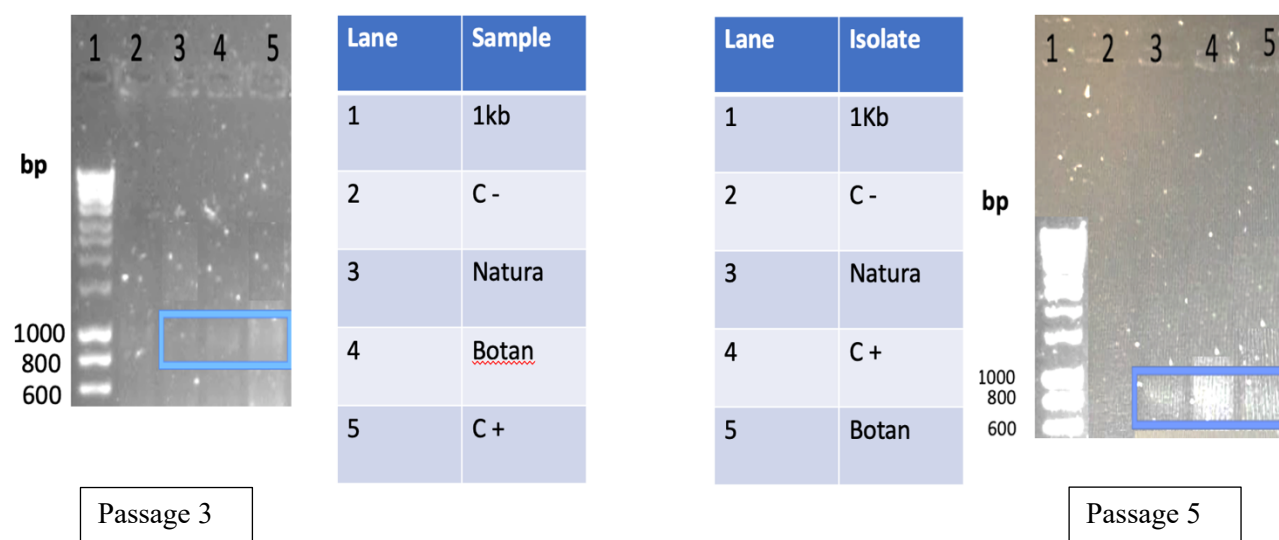


**Figure S4.3.5a:** RT-PCR amplification after transfection of *Beauveria bassiana* ATCC 74040 (Naturalis), *Beauveria bassiana* GHA (BotaniGard) and EABb 92/11-Dm VF (used as control, PmV-1.F) isolates using PmV-1. On the left is RT-PCR performed on the three isolates after passage 3 (Generation 3). On the right is RT-PCR performed on the three isolates after passage 5 (Generation 5). The difference in the PCR products between the two passages is obvious, indicating that the viral load is increasing by each passage.

## 5.2 Genome structural Annotation of EABb 92/11-Dm

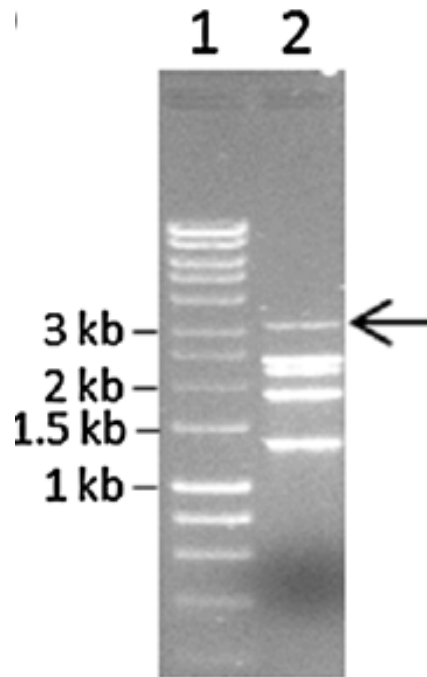


**Figure S5.2:** Agarose gel electrophoresis of viral dsRNA extracted from *Beauveria bassiana* isolate EABb 92/11-Dm (lane 2). *Beauveria bassiana* non-segmented virus-1 is shown by an arrow. Lane 1 indicates the DNA marker Hyperladder I (Bioline), the sizes of which are shown to the left of the gel. Picture was taken from Kotta-Loizou *et al.*, 2015.

SampleName	TotalReads	OverallAlignment (ASM28067) %	TotalSequencesClassifiedByKraken(%; db=fungi_refseq_latest)	TopHit (fungi_refseq_latest)	TotalSequencesClassifiedByKraken(%; db=nt)	TopHit (nt)
BBII-Day4-1	2113991	93.06	88.06	Beauveria ba	1.01	Beauveria bassiana
BBII-Day4-1	2083135	92.93	87.97	Beauveria ba	1.02	Beauveria bassiana
BBII-Day4-1	2095527	93.01	88.09	Beauveria ba	1.03	Beauveria bassiana
BBII-Day4-2	1832056	90.96	81.36	Beauveria ba	0.79	Beauveria bassiana
BBII-Day4-2	1804767	90.9	81.27	Beauveria ba	0.78	Beauveria bassiana
BBII-Day4-2	1818922	90.96	81.28	Beauveria ba	0.77	Beauveria bassiana
BBII-Day4-3	4845080	84.93	82.09	Beauveria ba	0.84	Beauveria bassiana
BBII-Day4-3	4756805	84.83	82.06	Beauveria ba	0.85	Beauveria bassiana
BBII-Day4-3	4799065	84.88	82.07	Beauveria ba	0.85	Beauveria bassiana
BBII-Day7-1	1144699	89.79	80.35	Beauveria ba	0.81	Beauveria bassiana
BBII-Day7-1	1127907	89.66	80.26	Beauveria ba	0.81	Beauveria bassiana
BBII-Day7-1	1134955	89.75	80.29	Beauveria ba	0.81	Beauveria bassiana
BBII-Day7-2	2377661	91.22	81.21	Beauveria ba	0.77	Beauveria bassiana
BBII-Day7-2	2342143	91.13	81.14	Beauveria ba	0.77	Beauveria bassiana
BBII-Day7-2	2354610	91.18	81.16	Beauveria ba	0.77	Beauveria bassiana
BBII-Day7-3	6466053	90.69	86.65	Beauveria ba	0.87	Beauveria bassiana
BBII-Day7-3	6345707	90.58	86.55	Beauveria ba	0.88	Beauveria bassiana
BBII-Day7-3	6412194	90.67	86.61	Beauveria ba	0.87	Beauveria bassiana
BBII-Day10-1	4528084	91.33	85.06	Beauveria ba	0.71	Beauveria bassiana
BBII-Day10-1	4440674	91.31	85.02	Beauveria ba	0.71	Beauveria bassiana
BBII-Day10-1	4484855	91.31	85.05	Beauveria ba	0.72	Beauveria bassiana
BBII-Day10-2	4691064	76.42	81.91	Beauveria ba	0.7	Beauveria bassiana
BBII-Day10-2	4599407	76.35	81.87	Beauveria ba	0.7	Beauveria bassiana
BBII-Day10-2	4646155	76.41	81.89	Beauveria ba	0.7	Beauveria bassiana
BBII-Day10-3	3341664	87.12	85.01	Beauveria ba	0.69	Beauveria bassiana
BBII-Day10-3	3282690	87	84.93	Beauveria ba	0.69	Beauveria bassiana
BBII-Day10-3	3312741	87.12	84.99	Beauveria ba	0.69	Beauveria bassiana
BBII-Day14-1	7846877	30.92	29.87	Beauveria ba	1.97	Helicoverpa armigera
BBII-Day14-1	7736638	30.76	29.72	Beauveria ba	1.97	Helicoverpa armigera
BBII-Day14-1	7776107	30.87	29.81	Beauveria ba	1.97	Helicoverpa armigera
BBII-Day14-2	1185242	88.47	79.03	Beauveria ba	0.47	Beauveria bassiana
BBII-Day14-2	1161899	88.37	78.87	Beauveria ba	0.49	Beauveria bassiana
BBII-Day14-2	1172460	88.45	78.95	Beauveria ba	0.49	Beauveria bassiana
BBII-Day14-3	151580	91.51	84.73	Beauveria ba	0.88	Beauveria bassiana
BBII-Day14-3	150882	91.05	84.37	Beauveria ba	0.86	Beauveria bassiana
BBII-Day14-3	150704	91.37	84.59	Beauveria ba	0.89	Beauveria bassiana
BBII-Day21-1	2322984	82.38	79.25	Beauveria ba	0.47	Beauveria bassiana
BBII-Day21-1	2275756	82.26	79.11	Beauveria ba	0.49	Beauveria bassiana
BBII-Day21-1	2297837	82.36	79.21	Beauveria ba	0.48	Beauveria bassiana
BBII-Day21-2	1650511	83.41	78.83	Beauveria ba	0.52	Beauveria bassiana
BBII-Day21-2	1624859	83.33	78.8	Beauveria ba	0.51	Beauveria bassiana
BBII-Day21-2	1633366	83.39	78.8	Beauveria ba	0.51	Beauveria bassiana
BBII-Day21-3	2993887	80.32	79.55	Beauveria ba	0.53	Beauveria bassiana
BBII-Day21-3	2934733	80.26	79.46	Beauveria ba	0.53	Beauveria bassiana
BBII-Day21-3	2960865	80.32	79.48	Beauveria ba	0.53	Beauveria bassiana

**Table S5.2a:** Alignment of reads to *Beauveria bassiana* (ASM18067) reference genome using Bowtie2 and classification of reads using Kraken of the PmV-1.F isogenic line taken from five time points. First lane represents the Sample name; second lane represents the total number of reads in fastq file; lane three represents the percentage of raw *Beauveria bassiana* reads that aligned to the refseq reference genome; fourth lane represents the percentage of the 'TotalReads' classified by Kraken when samples were run against the fungi refseq database; fifth lane represents the percentage of reads were other species were also classified; seventh lane represents the top hit organism which in this case is *Beauveria bassiana* EABb 92/11-Dm isolate.

SampleName	TotalReads	OverallAlignment (ASM28067) %	TotalSequencesClassifiedByKraken(%; db=fungi_refseq_latest)	TopHit (fungi_refseq_latest)	TotalSequencesClassifiedByKraken(%; db=nt)	TopHit (nt)
BBI-Day4-1	1562898	90.38	87.93	Beauveria ba	0.9	Beauveria bassiana
BBI-Day4-1	1541476	90.32	87.87	Beauveria ba	0.9	Beauveria bassiana
BBI-Day4-1	1546585	90.38	87.95	Beauveria ba	0.9	Beauveria bassiana
BBI-Day4-2	1382134	86.98	83.55	Beauveria ba	0.71	Beauveria bassiana
BBI-Day4-2	1364231	86.84	83.42	Beauveria ba	0.72	Beauveria bassiana
BBI-Day4-2	1364718	86.96	83.52	Beauveria ba	0.73	Beauveria bassiana
BBI-Day4-3	4625256	79.69	84.24	Beauveria ba	1.06	Beauveria bassiana
BBI-Day4-3	4546977	79.63	84.19	Beauveria ba	1.05	Beauveria bassiana
BBI-Day4-3	4583718	79.7	84.21	Beauveria ba	1.05	Beauveria bassiana
BBI-Day7-1	1620313	91.63	85.95	Beauveria ba	1.24	Beauveria bassiana
BBI-Day7-1	1598797	91.55	85.88	Beauveria ba	1.24	Beauveria bassiana
BBI-Day7-1	1611504	91.58	85.9	Beauveria ba	1.24	Beauveria bassiana
BBI-Day7-2	2422455	89.72	87.74	Beauveria ba	0.92	Beauveria bassiana
BBI-Day7-2	2386348	89.61	87.61	Beauveria ba	0.92	Beauveria bassiana
BBI-Day7-2	2403100	89.7	87.67	Beauveria ba	0.91	Beauveria bassiana
BBI-Day7-3	2821436	85.36	87.73	Beauveria ba	1.45	Beauveria bassiana
BBI-Day7-3	2773376	85.34	87.71	Beauveria ba	1.44	Beauveria bassiana
BBI-Day7-3	2803226	85.34	87.76	Beauveria ba	1.44	Beauveria bassiana
BBI-Day10_1	3038973	86.87	84.58	Beauveria ba	0.78	Beauveria bassiana
BBI-Day10_1	3076856	86.9	84.65	Beauveria ba	0.77	Beauveria bassiana
BBI-Day10-1	3048250	87.03	84.89	Beauveria ba	0.77	Beauveria bassiana
BBI-Day10-2	10106	83.58	76.37	Beauveria ba	0.94	Beauveria bassiana
BBI-Day10-2	10375	82.76	76.25	Beauveria ba	0.67	Beauveria bassiana
BBI-Day10-2	10458	83.92	76.58	Beauveria ba	0.7	Beauveria bassiana
BBI-Day10-3	4309960	87.27	85.25	Beauveria ba	0.76	Beauveria bassiana
BBI-Day10-3	4236010	87.23	85.25	Beauveria ba	0.76	Beauveria bassiana
BBI-Day10-3	4273362	87.28	85.27	Beauveria ba	0.76	Beauveria bassiana
BBI-Day14-1	4381504	82.78	82.68	Beauveria ba	0.92	Beauveria bassiana
BBI-Day14-1	4301620	82.71	82.64	Beauveria ba	0.91	Beauveria bassiana
BBI-Day14-1	4343096	82.73	82.64	Beauveria ba	0.92	Beauveria bassiana
BBI-Day14-2	12894122	79.38	87.02	Beauveria ba	0.95	Beauveria bassiana
BBI-Day14-2	12673523	79.3	86.94	Beauveria ba	0.95	Beauveria bassiana
BBI-Day14-2	12785066	79.36	86.99	Beauveria ba	0.95	Beauveria bassiana
BBI-Day14-3	866982	90.69	85.56	Beauveria ba	0.71	Beauveria bassiana
BBI-Day14-3	852196	90.58	85.36	Beauveria ba	0.73	Beauveria bassiana
BBI-Day14-3	859822	90.66	85.45	Beauveria ba	0.72	Beauveria bassiana
BBI-Day21-1	2456079	82.08	82.39	Beauveria ba	0.89	Beauveria bassiana RNA virus 1
BBI-Day21-1	2411763	82.09	82.44	Beauveria ba	0.89	Beauveria bassiana RNA virus 1
BBI-Day21-1	2432041	82.15	82.44	Beauveria ba	0.88	Beauveria bassiana RNA virus 1
BBI-Day21-2	3362255	80.99	82.56	Beauveria ba	0.89	Beauveria bassiana RNA virus 1
BBI-Day21-2	3312822	80.92	82.47	Beauveria ba	0.88	Beauveria bassiana RNA virus 1
BBI-Day21-2	3324975	80.98	82.55	Beauveria ba	0.89	Beauveria bassiana RNA virus 1
BBI-Day21-3	2285719	80.77	82.61	Beauveria ba	0.9	Beauveria bassiana RNA virus 1
BBI-Day21-3	2245819	80.69	82.57	Beauveria ba	0.92	Beauveria bassiana RNA virus 1
BBI-Day21-3	2261011	80.78	82.59	Beauveria ba	0.92	Beauveria bassiana RNA virus 1

**Table S5.2b:** Alignment of reads to *Beauveria bassiana* (ASM18067) reference genome using Bowtie2 and classification of reads using Kraken of the PmV-1.I isogenic line taken from five time points. First lane represents the Sample name; second lane represents the total number of reads in fastq file; lane three represents the percentage of raw *Beauveria bassiana* reads that aligned to the refseq reference genome; fourth lane represents the percentage of the 'TotalReads' classified by Kraken when samples were run against the fungi refseq database; fifth lane represents the percentage of reads were other species were also classified; seventh lane represents the top hit organism which in this case is *Beauveria bassiana* EABb 92/11-Dm isolate.

A

SampleName	TotalReads	OverallAlignment (ASM28067) %	TotalSequencesClassifiedByKraken(%; db=fungi_refseq_latest)	TopHit (fungi_refseq_latest)	TotalSequencesClassifiedByKraken(%; db=nt)	TopHit (nt)
024_S24	3263156	0.54	0.58	Aureobasidium	0.72	Tenebrio molitor
subset2/PAP	3269212	0.52	0.58	Aureobasidium	0.72	Tenebrio molitor
subset2/PAP	3272937	0.54	0.59	Aureobasidium	0.72	Tenebrio molitor
subset2/PAP	3267132	0.52	0.58	Aureobasidium	0.71	Tenebrio molitor
013_S13	3090306	0.57	0.69	Aureobasidium	0.74	Tenebrio molitor
subset2/PAP	3094847	0.55	0.69	Aureobasidium	0.74	Tenebrio molitor
subset2/PAP	3098373	0.55	0.7	Aureobasidium	0.74	Tenebrio molitor
subset2/PAP	3094012	0.55	0.7	Aureobasidium	0.74	Tenebrio molitor
019_S19	3040805	0.73	0.87	Aureobasidium	0.67	Tenebrio molitor
subset2/PAP	3041230	0.72	0.87	Aureobasidium	0.68	Tenebrio molitor
subset2/PAP	3049605	0.72	0.87	Aureobasidium	0.68	Tenebrio molitor
subset2/PAP	3035889	0.72	0.88	Aureobasidium	0.69	Tenebrio molitor

B

SampleName	TotalReads	OverallAlignment (ASM28067) %	TotalSequencesClassifiedByKraken(%; db=fungi_refseq_latest)	TopHit (fungi_refseq_latest)	TotalSequencesClassifiedByKraken(%; db=nt)	TopHit (nt)
015_S15	3053747	0.79	1.01	Hyphopichia	0.79	Tenebrio molitor
subset2/PAP	3012302	0.77	1.01	Hyphopichia	0.8	Tenebrio molitor
subset2/PAP	3052385	0.78	1.01	Hyphopichia	0.79	Tenebrio molitor
subset2/PAP	3000099	0.77	1.02	Hyphopichia	0.8	Tenebrio molitor
007_S7	3711585	0.84	11.37	Aspergillus fl	0.92	Tenebrio molitor
subset2/PAP	3719612	0.82	11.29	Aspergillus fl	0.92	Tenebrio molitor
subset2/PAP	3723945	0.83	11.34	Aspergillus fl	0.92	Tenebrio molitor
subset2/PAP	3713160	0.82	11.3	Aspergillus fl	0.92	Tenebrio molitor
018_S18	2953932	0.98	1.06	Hyphopichia	0.47	Tenebrio molitor
subset2/PAP	2959682	0.95	1.05	Hyphopichia	0.47	Tenebrio molitor
subset2/PAP	2964242	0.96	1.06	Hyphopichia	0.47	Tenebrio molitor
subset2/PAP	2953351	0.95	1.06	Hyphopichia	0.47	Tenebrio molitor

SampleName	TotalReads	OverallAlignment (ASM28067) %	TotalSequencesClassifiedByKraken(%; db=fungi_refseq_latest)	TopHit (fungi_refseq_latest)	TotalSequencesClassifiedByKraken(%; db=nt)	TopHit (nt)
017_S17	3487994	1.09	0.81	Aureobasidium	0.48	Tenebrio molitor
subset2/PAP	3483203	1.08	0.82	Aureobasidium	0.48	Tenebrio molitor
subset2/PAP	3490602	1.09	0.82	Aureobasidium	0.48	Tenebrio molitor
subset2/PAP	3485201	1.08	0.82	Aureobasidium	0.48	Tenebrio molitor
021_S21	3795326	1.1	1.02	Hyphopichia	0.75	Tenebrio molitor
subset2/PAP	3782853	1.08	1	Hyphopichia	0.74	Tenebrio molitor
subset2/PAP	3802962	1.09	1	Hyphopichia	0.75	Tenebrio molitor
subset2/PAP	3779694	1.09	1.01	Hyphopichia	0.74	Tenebrio molitor
022_S22	3025639	1.09	0.89	Aureobasidium	0.58	Tenebrio molitor
subset2/PAP	3043489	1.05	0.9	Aureobasidium	0.58	Tenebrio molitor
subset2/PAP	3039317	1.06	0.89	Aureobasidium	0.58	Tenebrio molitor
subset2/PAP	3035910	1.06	0.89	Aureobasidium	0.58	Tenebrio molitor

SampleName	TotalReads	OverallAlignment (ASM28067) %	TotalSequencesClassifiedByKraken(%; db=fungi_refseq_latest)	TopHit (fungi_refseq_latest)	TotalSequencesClassifiedByKraken(%; db=nt)	TopHit (nt)
026_S26	8948	1.27	2.65	Aspergillus fl	0.69	Tenebrio molitor
subset2/PAP	9049	1.12	2.33	Aspergillus fl	0.62	Tenebrio molitor
subset2/PAP	9114	1.08	2.66	Aspergillus fl	0.56	Tenebrio molitor
subset2/PAP	8981	1.05	2.59	Aspergillus fl	0.53	Tenebrio molitor
023_S23	3099310	1.32	0.9	Aureobasidium	0.6	Tenebrio molitor
subset2/PAP	3095714	1.28	0.91	Aureobasidium	0.6	Tenebrio molitor
subset2/PAP	3104476	1.31	0.9	Aureobasidium	0.61	Tenebrio molitor
subset2/PAP	3090664	1.3	0.91	Aureobasidium	0.6	Tenebrio molitor
005_S5	3415217	1.39	0.91	Aspergillus fl	1.05	Tenebrio molitor
subset2/PAP	3435983	1.38	0.89	Aspergillus fl	1.04	Tenebrio molitor
subset2/PAP	3424866	1.39	0.89	Aspergillus fl	1.04	Tenebrio molitor
subset2/PAP	3433232	1.38	0.9	Aspergillus fl	1.03	Tenebrio molitor

**Table S5.2c:** Alignment of reads to *Beauveria bassiana* (ASM18067) reference genome using Bowtie2 and classification of reads using Kraken of the four *Beauveria bassiana* isolates sprayed on *Tenebrio molitor* infection model. First lane represents the Sample name; second lane represents the total number of reads in fastq file; lane three represents the percentage of raw *Beauveria bassiana* reads that aligned to the refseq reference genome; fourth lane represents the percentage of the 'TotalReads' classified by Kraken when samples were run against the fungi refseq database; fifth lane represents the percentage of reads were other species were also classified; seventh lane represents the top hit organism which is *Tenebrio molitor*. Spore inoculation was sprayed on mealworm *Tenebrio molitor*; **Fig. (A)** PmV-1.F isolate, **Fig. (B)** Naturalis isolate, **Fig. (C)** Botanigard isolate, **Fig (D)** PmV-1.I isolate.

A							
SampleName	TotalReads	OverallAlignment (ASM28067) %	TotalSequencesClassifiedByKraken(%; db=fungi_refseq_latest)	TopHit (fungi_refseq_latest)	TotalSequencesClassifiedByKraken(%; db=nt)	TopHit (nt)	
016_S16	3058583	1.52	0.92	Aureobasidium	0.49	Tenebrio molitor	
subset2/PAP	3064533	1.49	0.93	Aureobasidium	0.49	Tenebrio molitor	
subset2/PAP	3067609	1.52	0.92	Aureobasidium	0.49	Tenebrio molitor	
subset2/PAP	3062684	1.51	0.93	Aureobasidium	0.5	Tenebrio molitor	
020_S20	3490754	1.59	1.07	Hyphopichia	0.65	Tenebrio molitor	
subset2/PAP	3490842	1.54	1.07	Hyphopichia	0.64	Tenebrio molitor	
subset2/PAP	3502381	1.57	1.07	Hyphopichia	0.65	Tenebrio molitor	
subset2/PAP	3489038	1.57	1.07	Hyphopichia	0.65	Tenebrio molitor	
006_S6	4422137	1.76	1.03	Aspergillus fl	0.97	Tenebrio molitor	
subset2/PAP	4417688	1.7	1.02	Aspergillus fl	0.98	Tenebrio molitor	
subset2/PAP	4432879	1.73	1.01	Aspergillus fl	0.98	Tenebrio molitor	
subset2/PAP	4407537	1.72	1.01	Aspergillus fl	0.97	Tenebrio molitor	

B							
SampleName	TotalReads	OverallAlignment (ASM28067) %	TotalSequencesClassifiedByKraken(%; db=fungi_refseq_latest)	TopHit (fungi_refseq_latest)	TotalSequencesClassifiedByKraken(%; db=nt)	TopHit (nt)	
001_S1	4624606	2.37	1.71	Aspergillus fl	0.79	Tenebrio molitor	
subset2/PAP	3905738	1.79	1.3	Aspergillus fl	0.39	Tenebrio molitor	
subset2/PAP	3903789	1.79	1.31	Aspergillus fl	0.39	Tenebrio molitor	
subset2/PAP	3912763	1.78	1.31	Aspergillus fl	0.38	Tenebrio molitor	
009_S9	3341616	1.99	1.48	Aspergillus fl	0.73	Tenebrio molitor	
subset2/PAP	3351835	1.97	1.47	Aspergillus fl	0.73	Tenebrio molitor	
subset2/PAP	3346560	1.98	1.46	Aspergillus fl	0.72	Tenebrio molitor	
subset2/PAP	3350214	1.96	1.45	Aspergillus fl	0.72	Tenebrio molitor	
004_S4	2971814	2.04	0.91	Aspergillus fl	0.44	Tenebrio molitor	
subset2/PAP	2979916	2.03	0.9	Aspergillus fl	0.45	Tenebrio molitor	
subset2/PAP	2979958	2.05	0.9	Aspergillus fl	0.45	Tenebrio molitor	
subset2/PAP	2975618	2.05	0.9	Aspergillus fl	0.45	Tenebrio molitor	

SampleName	TotalReads	OverallAlignment (ASM28067) %	TotalSequencesClassifiedByKraken(%; db=fungi_refseq_latest)	TopHit (fungi_refseq_latest)	TotalSequencesClassifiedByKraken(%; db=nt)	TopHit (nt)
027_S27	2776091	2.37	0.71	Aspergillus fl	0.99	Tenebrio molitor
subset2/PAP	2774603	2.33	0.7	Aspergillus fl	0.99	Tenebrio molitor
subset2/PAP	2780763	2.35	0.71	Aspergillus fl	0.99	Tenebrio molitor
subset2/PAP	2775990	2.34	0.7	Aspergillus fl	1	Tenebrio molitor
011_S11	3927284	2.98	1.29	Aspergillus fl	0.6	Tenebrio molitor
subset2/PAP	3933789	2.93	1.28	Aspergillus fl	0.6	Tenebrio molitor
subset2/PAP	3929174	2.95	1.28	Aspergillus fl	0.6	Tenebrio molitor
subset2/PAP	3933002	2.93	1.28	Aspergillus fl	0.6	Tenebrio molitor
025_S25	2885133	2.92	0.74	Aspergillus fl	0.95	Tenebrio molitor
subset2/PAP	4627607	2.41	1.71	Aspergillus fl	0.8	Tenebrio molitor
subset2/PAP	4623203	2.38	1.7	Aspergillus fl	0.79	Tenebrio molitor
subset2/PAP	4631831	2.4	1.72	Aspergillus fl	0.79	Tenebrio molitor

SampleName	TotalReads	OverallAlignment (ASM28067) %	TotalSequencesClassifiedByKraken(%; db=fungi_refseq_latest)	TopHit (fungi_refseq_latest)	TotalSequencesClassifiedByKraken(%; db=nt)	TopHit (nt)
025_S25	11535207	2.94	0.74	Aspergillus fl	0.95	Tenebrio molitor
subset1/PAP	2882313	2.98	0.73	Aspergillus fl	0.97	Tenebrio molitor
subset1/PAP	2883197	2.91	0.74	Aspergillus fl	0.95	Tenebrio molitor
subset1/PAP	2884564	2.96	0.74	Aspergillus fl	0.95	Tenebrio molitor
012_S12	3649649	3.51	1.18	Aspergillus fl	0.61	Tenebrio molitor
subset2/PAP	3652461	3.44	1.18	Aspergillus fl	0.6	Tenebrio molitor
subset2/PAP	3658863	3.46	1.17	Aspergillus fl	0.61	Tenebrio molitor
subset2/PAP	3643988	3.46	1.17	Aspergillus fl	0.6	Tenebrio molitor
subset2/PAP	3083822	5.12	3.11	Aspergillus fl	0.74	Tenebrio molitor
subset2/PAP	3088897	5	3.09	Aspergillus fl	0.75	Tenebrio molitor
subset2/PAP	3086284	5.05	3.12	Aspergillus fl	0.74	Tenebrio molitor
subset2/PAP	3088608	5.05	3.11	Aspergillus fl	0.75	Tenebrio molitor

**Table S5.2d:** Alignment of reads to *Beauveria bassiana* (ASM18067) reference genome using Bowtie2 and classification of reads using Kraken of the four *Beauveria bassiana* isolates injected on *Tenebrio molitor* infection model. First lane represents the Sample name; second lane represents the total number of reads in fastq file; lane three represents the percentage of raw *Beauveria bassiana* reads that aligned to the refseq reference genome; fourth lane represents the percentage of the 'TotalReads' classified by Kraken when samples were run against the fungi refseq database; fifth lane represents the percentage of reads were other species were also classified; seventh lane represents the top hit organism which is *Tenebrio molitor*; **Fig. (A)** Naturalis isolate, **Fig. (B)** PmV-1.F isolate, **Fig. (C)** Botanigard isolate, **Fig (D)** PmV-1.I isolate.

**Table S5.2.1a:** Fungal reference genomes used to align the reads

<b>Fungus</b>	<b>Strain</b>
<i>Beauveria bassiana</i>	ARSEF 1520
<i>Beauveria bassiana</i>	ARSEF 2597
<i>Beauveria bassiana</i>	ARSEF 4305
<i>Beauveria bassiana</i>	ARSEF 8028
<i>Beauveria bassiana</i>	BCC 2660
<i>Beauveria bassiana</i>	D1-5
<i>Beauveria bassiana</i>	Botaniquard
<i>Beauveria bassiana</i>	Naturalis
<i>Beauveria bassiana</i>	ERL836
<i>Beauveria bassiana</i>	GCA_002871155
<i>Beauveria bassiana</i>	JAU2

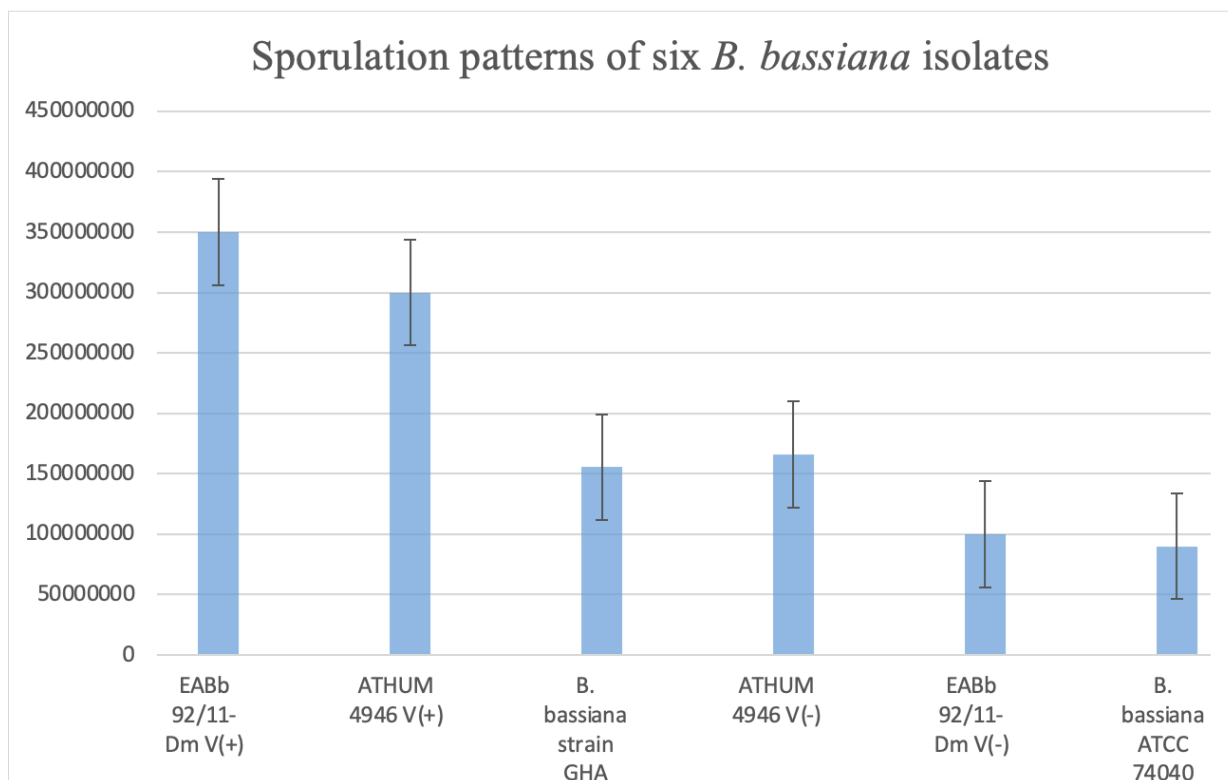


**Figure S6.1a** Histogram representation of difference in sporulation between four isolates of the entomopathogenic fungus *Beauveria bassiana*. Isolates EABb 92/11-Dm (VI) and ATHUM 4946 (VI) infected with polmycovirus 1 and 3 respectively, cured isogenic lines (VF) of the same fungi. *Beauveria bassiana* GHA (BotaniGard) and *Beauveria bassiana* ATCC 74040 (Naturalis). Difference in sporulation between virus-infected and virus-free isogenic lines. Student's t test indicates P-value < 0.01.

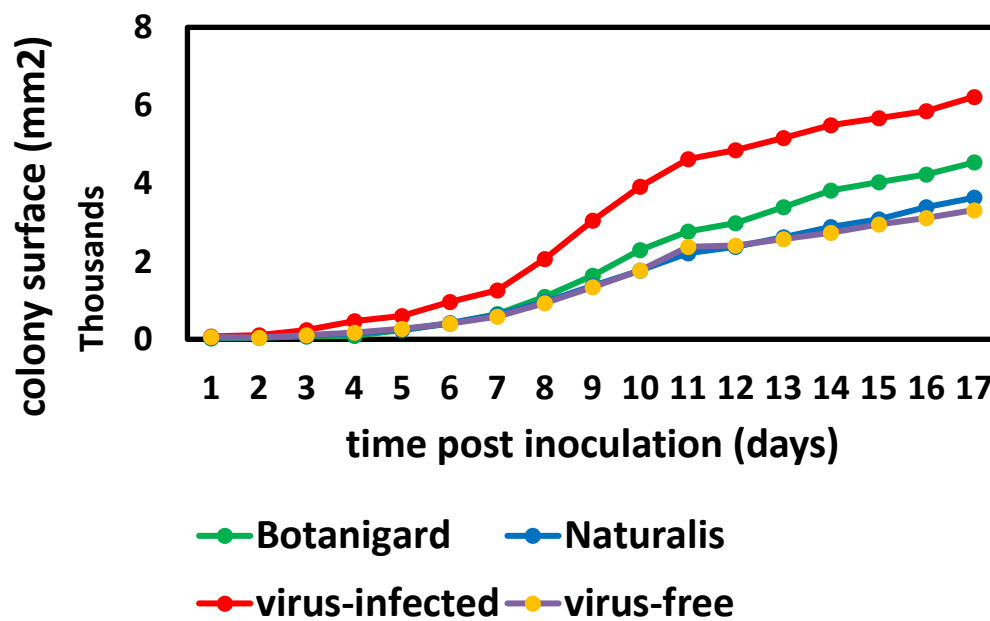


**Figure S6.1b** Schematic representation of differences in radial expansion of two commercial virus-free isolates of *Beauveria bassiana*, BotaniGard and Naturalis and PmV-1.I and PmV-1.F isogenic lines of isolate EABb 92/11-Dm (Figure courtesy of Dr Ioly Kotta-Loizou).

Species	Isolate	Location	Mycovirus
<i>B. bassiana</i>	EABb 00/11-Su	Jaen	BbVV-1 + BbPV-2 + BbPmV-1
<i>B. bassiana</i>	EABb 00/13-Su	Jaen	BbVV-1 + BbPV-2 + BbPmV-1
<i>B. bassiana</i>	EABb 01/12-Su	Seville	BbVV-1
<i>B. bassiana</i>	EABb 01/33-Su	Cadiz	BbVV-1
<i>B. bassiana</i>	EABb 01/112-Su	Seville	BbVV-1
<i>B. bassiana</i>	EABb 07/06-Rf	Alicante	BbVV-1 + BbPV-2 + BbPmV-1
<i>B. bassiana</i>	EABb 09/07-Fil	Malaga	BbPV-2
<i>B. bassiana</i>	EABb 10/01-Fil	Malaga	BbPmV-1
<i>B. bassiana</i>	EABb 10/28-Su	Cordoba	BbPmV-1
<i>B. bassiana</i>	EABb 10/30-Fil	Cordoba	BbPmV-1
<i>B. bassiana</i>	EABb 10/57-Fil	Cordoba	BbVV-1 + BbPV-2 + BbPmV-1
<i>B. bassiana</i>	EABb 11/01-Mg	Palencia	BbVV-1 + BbPV-2 + BbPmV-1
<i>A. fumigatus</i>	12/43	Portugal	AfuPV-1A
<i>L. muscarium</i>	143.62	Netherlands	LmV-1
<i>L. muscarium</i>	102071	Netherlands	LmV-1

**Table 6.1a** Mycoviruses isolated in this work from fungal isolates acquired from Spain, Portugal, and Netherlands.

## **Publications**

1. **Filippou, C.**, Garrido-Jurado, I., Meyling, N., Quesada-Moraga, E., Coutts, R. H.A., & Kotta-Loizou, I. (2018). Mycoviral population dynamics in Spanish isolates of the entomopathogenic fungus *Beauveria bassiana*. *Viruses*, *10* (12), 665-678.
2. **Filippou, C.**, Coutts, R. H., Stevens, D. A., Sabino, R., & Kotta-Loizou, I. (2020). Completion of the sequence of the *Aspergillus fumigatus* partitivirus 1 genome. *Archives of Virology*, *165*(8), 1891-1894.
3. Pitaluga, A. N., **Filippou, C.**, Blakiston, J., Coutts, R. H., Christophides, G. K., & Kotta-Loizou, I. (2020). A Mycovirus Mediates the Virulence of an Insect-Killing Fungus against the Malaria Mosquito Vector. *Multidisciplinary Digital Publishing Institute Proceedings*, *50*(1), 148.
4. **Filippou, C.**, Diss, R. M., Daudu, J. O., Coutts, R. H., & Kotta-Loizou, I. (2021). The polymycovirus-mediated growth enhancement of the entomopathogenic fungus *Beauveria bassiana* is dependent on carbon and nitrogen metabolism. *Frontiers in microbiology*, *12*, 12.